A STUDY OF LOCOMOTIVE UNDERCARRIAGE EQUIPMENT CASE DESIGN USING COMPOSITE MATERIALS AND FINITE ELEMENT ANALYSIS.

by

Carolyn Hardaker B.Sc (Hons)

A Thesis submitted in partial fulfilment of the requirements
for the award of
Master of Philosophy of the Loughborough University of Technology.

September 1990

ACKNOWLEDGEMENTS

I wish to express my thanks to Dr. P.W. Sharman of the Department of Transport Technology for the advice, direction and support he has given throughout the research.

Thanks are also due to Brush Electrical Machines Ltd. for providing sponsorship and Computing Services at Leicester Polytechnic for their help and co-operation.

Finally, I wish to thank my parents, Jen and John and friends Andy and Martin for helping in the production of this thesis.

SUMMARY

The research, commissioned by Brush Electrical Machines Ltd. of Loughborough, centres around the design of locomotive undercarriage equipment cases. These cases are generally of mild steel construction and are used to carry a wide variety of equipment from electromechanical switchgear to electronic monitoring equipment. Reviewing their design showed that they tend to be overdesigned, complex structures, with their manufacture and assembly being labour intensive and costly. In the competitive traction engineering market, with severe weight penalties featuring in all present day contracts it is important minimise weight and costs. Hence, it was proposed to investigate the possibility of redesigning a case in composite material in order to produce a light weight, less complex structure to satisfy the standard railway service loads at a reduced cost.

Finite Element Analysis was used extensively in the research, initially to evaluate the structural integrity of a typical steel case indicating the weak points of the design and providing an accurate value for the mass of the case, it was then used in the development of an equivalent composite model. However, as the Finite Element Analysis of composite structures is a relatively new field, it was necessary to perform extensive software testing as a precursor to composite case development in order to assure accuracy of results in terms of stress and displacements. Once confidence in the software had been established an experimental model was developed from uni-directional and woven cloth Glass/Epoxy composites, this was analysed and compared with the earlier analysis of the typical case.

The case developed was found to be equivalent in structural integrity to the isotropic case analysed, both were shown to have acceptable stress levels, minimal deflections and satisfactory fatigue life when subjected to the standard railway service loads. The mass of the composite model, was calculated to be approximately 72% of the equivalent isotropic case, which would save a ballpark

figure of 100kg per case, with further investigation in alternative composite materials leading to additional weight reduction. This advantage combined with a reduction in internal complexity through integral moulded equipment attachment points and a high resistance to corrosion make the proposition of a composite undercarriage equipment case viable. Hence it can be concluded that in the long term, the use of composite materials in an equipment case application would result in a reduction of both manufacturing and operational costs, although it should be noted that initial investment would be required for further development work and tooling.

The research concludes also that Finite Element Analysis is an effective tool to use in the design and development of both isotropic and composite structures, providing an accurate stress and displacement analyses, without the need for expensive prototypes.

NOTATION

M	Bending Moment
m	Moment Intensity
E_F	Young's Modulus of the Fibre
E_M	Young's Modulus of Matrix
V_F	Fibre Volume fraction
V_M	Matrix Volume fraction
E_1	Young's Modulus of the material in the fibre direction.
E_2	Young's Modulus of the material transverse to the fibre direction.
G_{12}	In - plane Shear Modulus
ϵ_1	Strain in the fibre direction.
ϵ_2	Strain of the material transverse to the fibre direction.
ψ_1	Shear Strain .
σ_1	Direct Stress in the fibre direction.
σ_2	Direct Stress in the material transverse to the fibre direction.
τ_{12}	In plane Shear Stress.

LIST OF CONTENTS

LIST OF FIGURES

Figure Number **Page**

Figure Number		**Page**

LIST OF APPENDICES

CHAPTER 1

Introduction to the Research

This research was commissioned by the Traction Division of Brush Electrical Machines Ltd., Loughborough, one of the leading Traction Engineering companies in the U.K, supplying locomotives and electromechanical equipment worldwide.

The research centres around the design of locomotive undercarriage equipment cases with the major objectives being as follows:-

i. To investigate and improve current equipment case design, by the use of Composite Materials and Finite Element Analysis.

ii. To develop expertise in the use of Finite Element Analysis for the stress analysis of isotropic and composite structures.

Undercarriage equipment cases are generally mild steel structures, carrying a large variety of electromechanical equipment suspended either directly from the case or from internal frameworks. At present cases are designed using basic stressing methods and thus tend to be overdesigned, with their manufacture and assembly being very labour intensive. This suggests the possibilities of design improvements to save weight, reduction of internal complexity and hence manufacturing costs.

To remain competitive in the world market all these considerations must be investigated in order to produce well designed lightweight structures at low cost, this philosophy applying not only to equipment cases but the total product as a whole. Weight savings are particularly important in present day locomotive engineering, with severe weight penalties clauses written into all contracts.

The research involved the extensive use of Finite Element Analysis, a powerful computer aided engineering tool used here to perform stress analyses and evaluate displacements for idealisations of structures subjected to a variety of loading conditions. The technique enables new features and design changes to be simulated without the need for expensive prototypes. The Finite Element software used throughout the research was the Pafec 75 integrated suite of software, pre and post-processing being done via PIGS, version 4.2 and the analyses performed with Pafec, version 6.2.

The initial research into equipment case design involved a survey of recent designs and the Finite Element Analysis of a typical case to evaluate structural integrity and possible design improvements. The survey established that equipment case design, although adequate could be improved and led to a feasibility study of a composite case, with the aim to develop a model which would satisfy the standard service loads and to achieve a series of design proposals for a lightweight, less complex structure.

Finite Element Analysis of composite structures is a relatively new field, hence before any case idealisation could take place, the accuracy of Pafec Orthotropic Finite Elements was investigated in terms of displacements and stress analysis, via extensive element testing. On assuring satisfactory accuracy, but limited with Pafec Orthotropic Finite Elements, work commenced on composite case design. It should be noted that this research did not investigate the intricacies of composite material design or material selection, this area to be the objective of further work.

The research introduced above involved several investigations which have been consolidated as a whole in the following report. Each part of the research has been detailed in a specific chapter which if necessary can be read independently.

CHAPTER 2

A Review of Equipment Case Design

2.1 Introduction

Undercarriage equipment cases support the control gear required for the operation of locomotive traction motors. The equipment contained within the cases varies from large masses such as chokes to smaller components of electromechanical control gear with also a vast array of electronics control and monitoring equipment. They are a self contained assembly and as their name suggests affixed to the locomotive undercarriage. The number of motors each case controls is locomotive dependent, varying from two to a maximum of eight.

An overview of case design reveals their design to be complex and manufacture highly labour intensive. In order to be competitive and adhere to the strict weight restrictions imposed in locomotive specifications, it is necessary to produce designs which are :-

i. effective in their purpose of supporting and enclosing the equipment.
ii. capable of supporting all the load cases imposed by the locomotive requirements.
iii. economical both in initial production cost and in subsequent durability and maintenance requirements.
iv. accessible for maintenance or replacement of equipment.
v. of minimum weight consistent with achieving the above four objectives.

The following chapter discusses current equipment case design, highlighting the main features and possible improvements, concluding with a series of objectives for the ensuing research.

2.2 Main features of design

2.2.1 Equipment Case Review

Equipment cases are currently individually designed to suit each new type of locomotive and as such their design varies considerably. There are however many fundamental features common to all designs. Typical examples reviewed are the equipment cases designed by Brush Electrical Machines Ltd. of Loughborough for the following vehicles:-

i. Articulated Light Rail Vehicle (ALRV) - An articulated street car.

ii. H6 Tube Stock - A London Underground locomotive.

iii. Taiwan Locomotive - A general purpose locomotive.

iv. Class 318 - A British Rail locomotive.

Sketches, photographs and fabrication drawings of these cases can be seen in figures 2.1-2.8, which on examination, the following points were noted.

2.2.2 General Layout and Construction

Equipment cases are large compartments mounted under the chassis of an electrically powered locomotive which carry all the electrical equipment associated with the traction motors. An equipment case usually weighs around 2.5 tonnes total with approximately two thirds its weight being equipment. The severe weight penalty clauses in present day contracts mean that it is imperative to keep this figure to a minimum, a typical penalty clause can charge the supplier $42/kg overweight (1990 figure) for every equipment case ordered in the contract. However, weight is not the only design consideration, there are other important factors such as to provide adequate equipment protection from the elements and to ensure ease of access for maintenance.

A typical current design of equipment case is constructed from mild steel sheet of 3-5 mm thickness and rectangular section mild steel tube, although 2-3mm Stainless Steel (Austenitic Type 304L) was used for the Taiwan locomotive.

The basic structure comprises of two end frames connected by two longitudinal beams which support both the structure and the contents of the equipment case. The structure is completed by lateral frames at appropriate positions and by sheet metal panels to increase stiffness and provide enclosure. Removable skin sections are required for access to the equipment.

In some designs there has been a limited use of composite materials in lightly loaded parts of the structure but as far as is known composite material has never been used for the main load carrying parts of the structure. A typical example of the use of composites in existing designs is a contactor housing used on the ALRV locomotive but here the composite material did not support the weight of the contactor, see figure 2.5.

The heavy bulk items of equipment carried in the equipment case such as chokes and some control gear are usually located in the space between the longitudinal beams. The heaviest item, normally the choke (1200kg) is supported by its own short cross beams which attach to the upper part of the main longitudinal beams with the choke being suspended below the beams. Lighter components, with a typical mass of 20kg are in general mounted on brackets attached to whatever part of the structure is dictated by convenience of layout. Figures 2.3 and 2.7 show the internal detail of the ALRV case, it should be noted that figure 2.7 shows the case in the process of assembly and as such is upside down.

All the electronic control and monitoring equipment is contained within the side panniers along with lighter items of control gear, figure 2.6 shows a view of a typical of pannier in the process of assembly. Again the equipment is attached either directly to the casing or to frameworks within the panniers. Detachable GRP covers are usually used to protect pannier contents from the environment.

As the cases hold a vast array of equipment, the associated wiring is complex, with cable runs and supports contributing a great deal to complexity and overall cost. The electrical power connection from the case to the motors is also complex, comprising of numerous heavy cable connections.

The whole equipment case is attached to the locomotive frame at four suspension points located at each end of the longitudinal support beams, either by vertical bolts or horizontally via a yoke fitting around the beam section.

The whole structure including mountings is designed to meet, as a minimum, vertical, longitudinal and transverse limit loading conditions specified in each individual contract. Typical values are shown in Appendix A1. Both proof load cases, in which no significant permanent distortion should result from the application of the limit loads and the fatigue case, in which no fatigue failure should occur in a specified number of fatigue cycles are considered. The typical contract load cases are are specified as 'g' loads, the actual loading thus depending on the mass and mass distribution of the structure.

The type of equipment case described above has been in service with many railway operators for a considerable time and has proved to be generally satisfactory. Thus scope for improvement by minor changes to the basic design is limited and the only possibilities for a large step improvement are either new electrical design, which could result in the use of lighter equipment or a total rethink of the structural design.

The first option is unlikely in the short term although future developments in electrical equipment will no doubt bring benefits in this area. The second option of improving the support structure is considered in the following research which together with possible improvements in equipment layout would achieve a more economic case.

2.3 Review of Possible Design Improvements

Areas where design improvements are possible can be divide into several categories such as weight reduction, reduced complexity, cost reduction, improved maintainability and customer appeal. The following sections indicate where structural improvements and better layout can contribute to a better product.

2.3.1 Weight reduction

In the early days of the railway locomotive, weight was considered to be desirable, within the limits of the supporting strength of the track, as it improved traction. Recent designs with all wheel drive and traction control make excessive weight undesirable, which combined with the strict weight penalty clauses result in a requirement to reduce structural weight.

Considering the existing component weights and layouts the typical equipment case structure is reasonably efficient within the limitations of steel construction and avoidance of expensive manufacturing techniques such as chemical etching to suit local loading conditions used widely in the aircraft industry. Thus the potential for large weight reductions in the structure is limited unless new materials are considered.

The possibilities for new construction material are in essence a light alloy option (such as aluminium and magnesium) or composite materials. This research investigates the use of composite material as these materials were considered more suitable for the application than light alloys for the following reasons.

i. High stiffness per unit weight.

ii. Good fatigue life and vibration damping qualities.

iii. Good electrical insulation properties.

iv. Non magnetic properties.

v. Chemical inertness and biocompatability ie complete resistance to corrosion.

Additional possibilities in weight reduction could come from optimum layout of equipment to reduce cable runs etc.

2.3.2 Reduced Complexity

If the electrical circuit is considered to be fixed, reductions in complexity can only be achieved by layout improvements, grouping inter connected components as closely as possible.

There are also potential improvements in the structure particularly in a composite design to make some of the many mounting brackets integral with the structural members and thus reducing the number of bolted joints. Figure 2.4 illustrates the complexity of typical mounting arrangements, with each of the mounting bolts shown is an attachment for a piece of equipment or a cable clamp.

2.3.3 Cost Reduction

Structural material costs for the typical current design are low, particularly if mild steel is used and are unlikely to be undercut by the use of an alternative material. There is however scope for reduced labour costs by reducing hand fitting work by means of more integral brackets on structural members, reduced layout complexity and shorter cable runs.

It is unlikely that any improved equipment case on the lines considered in this report would be substantially cheaper to produce, in the limited quantities required, than the current item. However, if overall costs can be kept substantially the same for a better performing product the change would be worthwhile.

2.3.4 Maintainability

Given equipment reliability, maintainability can be divided into ease of access for routine attention and component changes and the effectiveness and life of the corrosion protection system. Attention to component layout could improve access and the use of a material which did not need corrosion protection would be a considerable advantage.

2.3.5 Customer Appeal

The sale of railway locomotives is a competitive business, where the number of potential customers is limited. Thus advanced design features are a marketing advantage when comparing similar designs from competing companies. This is not an engineering reason for change but is another factor to be considered in the design strategy for a new locomotive.

2.4. Conclusions

The review of existing designs of locomotive equipment cases and the considerations of possible routes to improvement carried out in the previous sections has indicated various areas where improvements are possible.

It can be concluded that it is a worthwhile proposition to investigate the possible structural improvements which may come from a change of material from steel to glass reinforced composite material for the main case structure and produce a series of design proposals for such a case. It is also noted that further benefits could be achieved through improvements in equipment layout and by reducing the wiring complexity to save weight and cost.

Figure 2.1 A General View of a Typical Equipment Case (H6 Tube Stock)

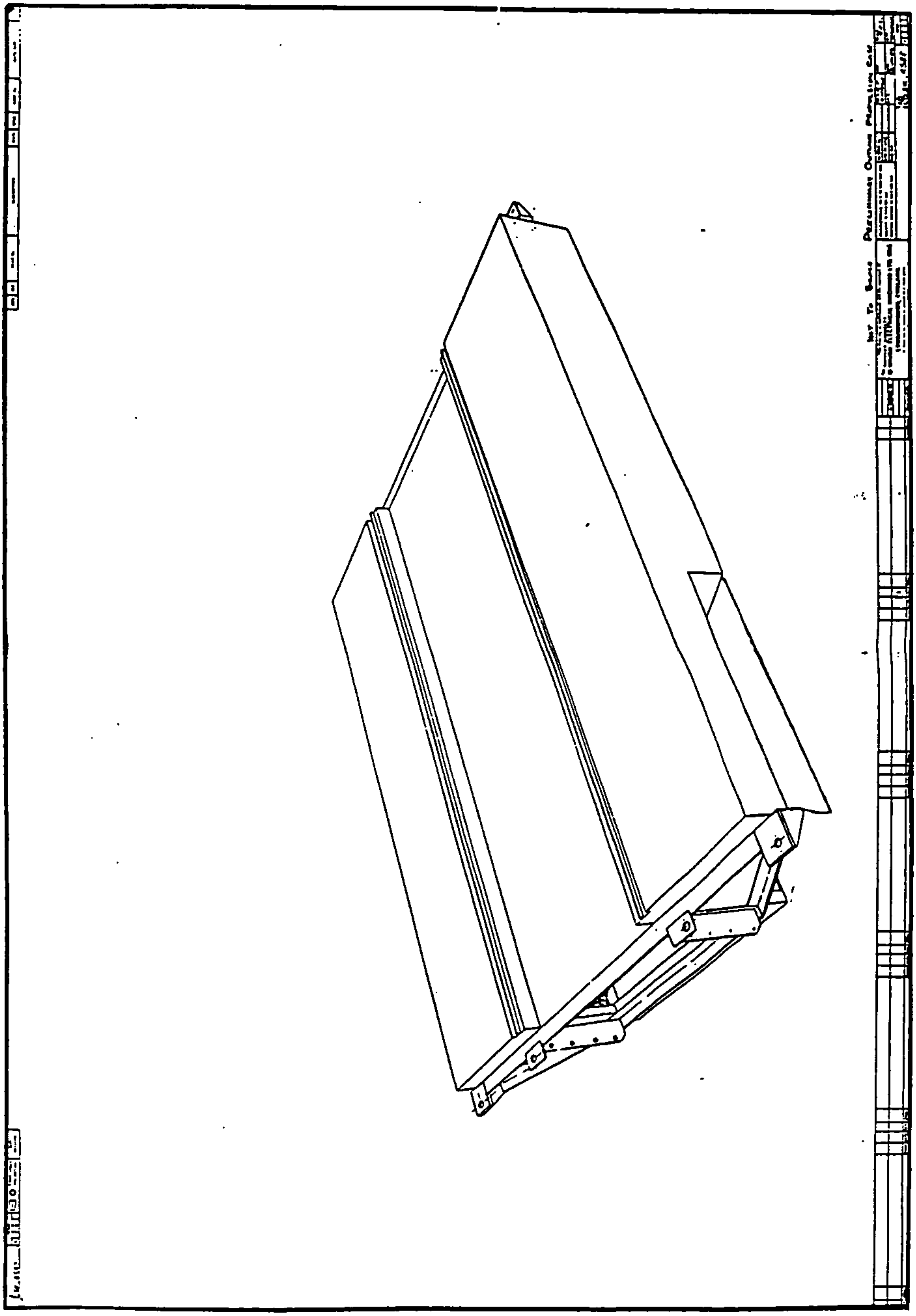

Figure 2.2 Three Views of a Typical Structure (ALRV)

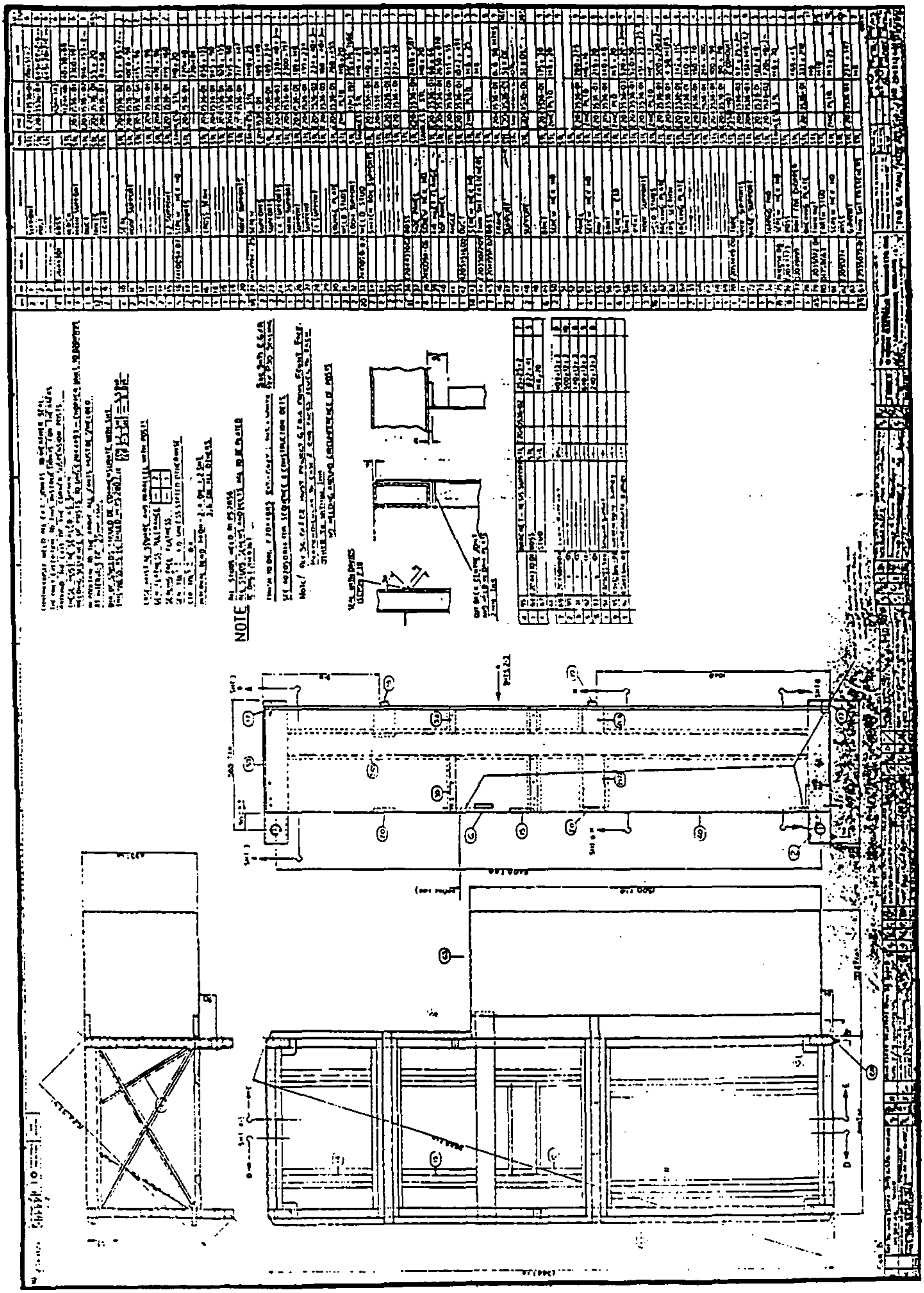

Figure 2.3 Internal Detail of the ALRV Case.

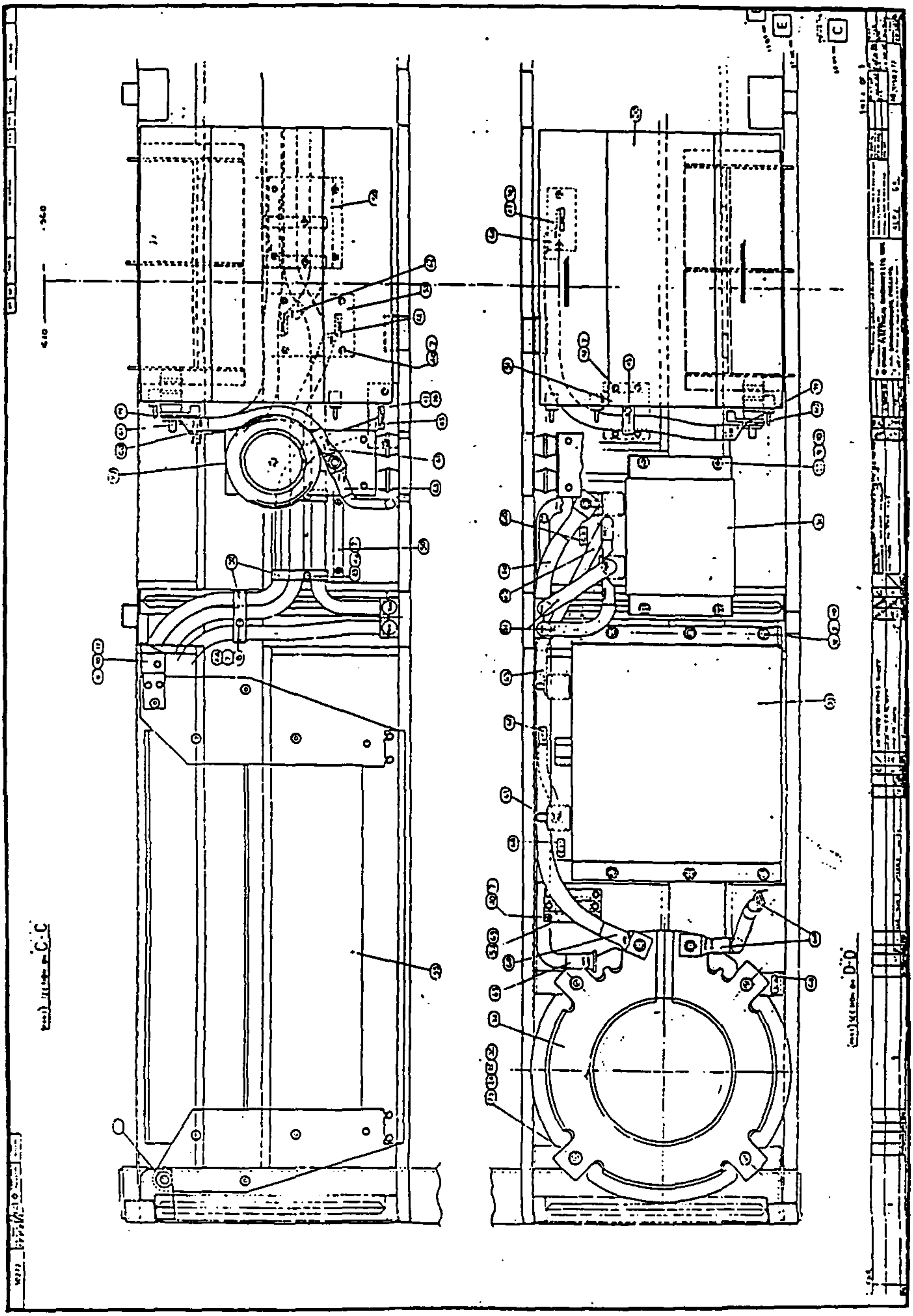

Figure 2.4 Side View of a Typical Pannier showing Internal Mounting Arrangements (Class 318)

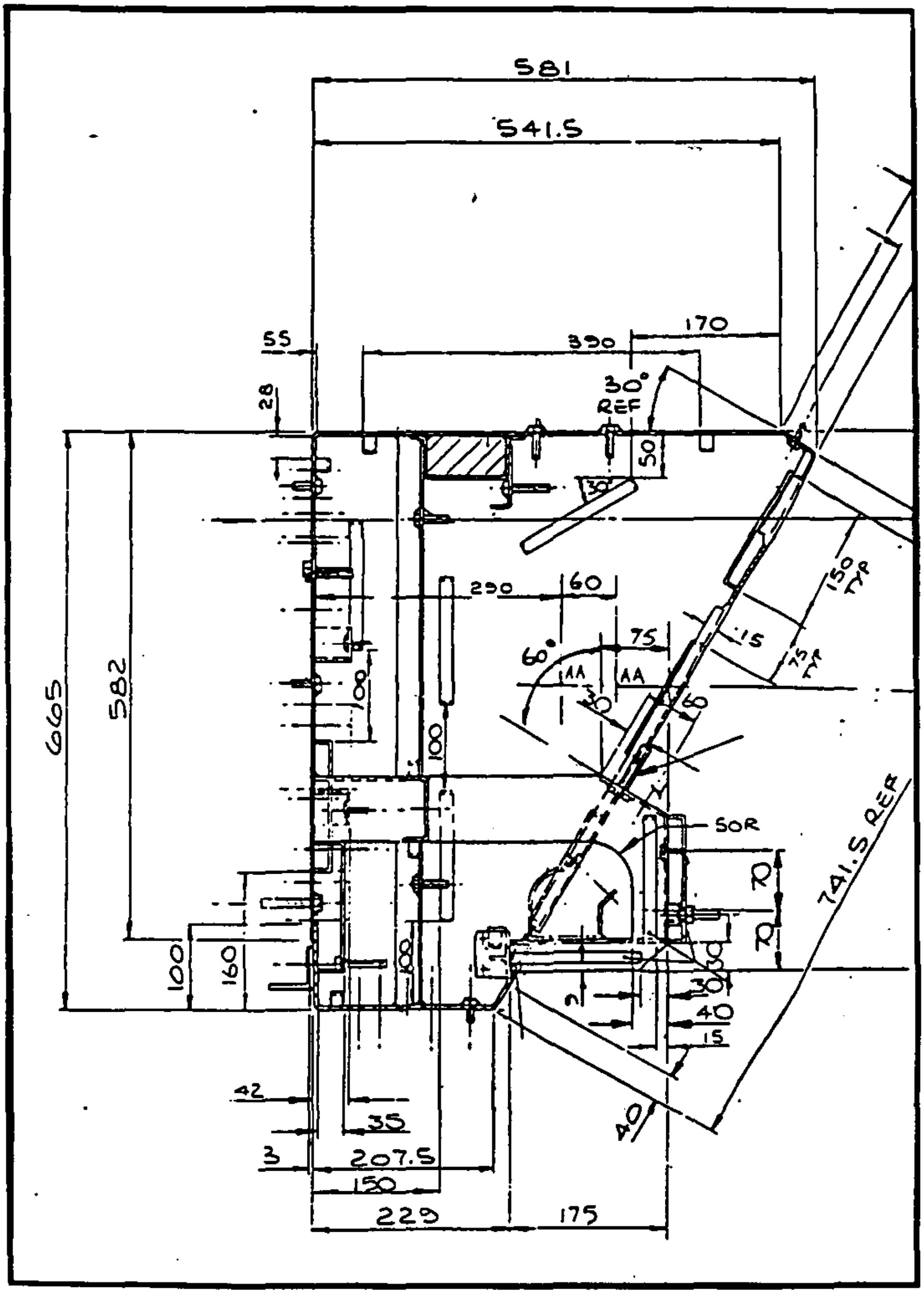

Figure 2.5 Composite Contactor Housing (ALRV)

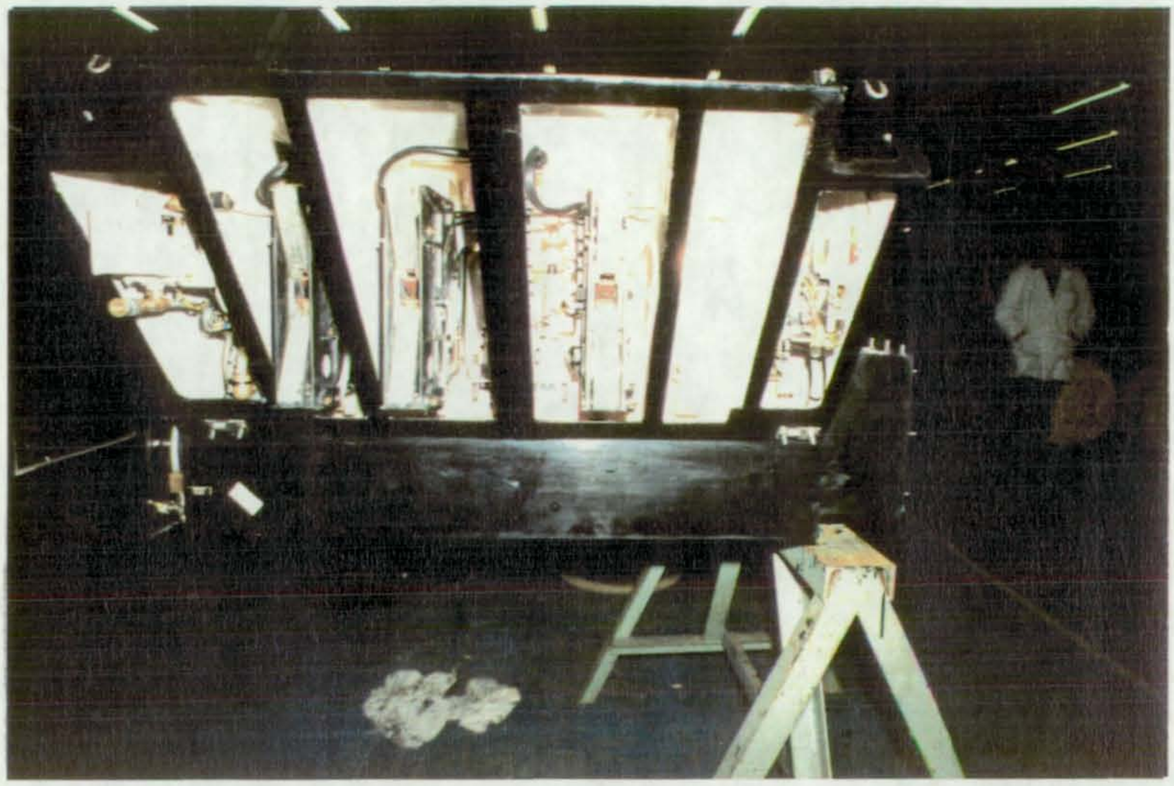

Figure 2.6 Pannier under assembly (ALRV)

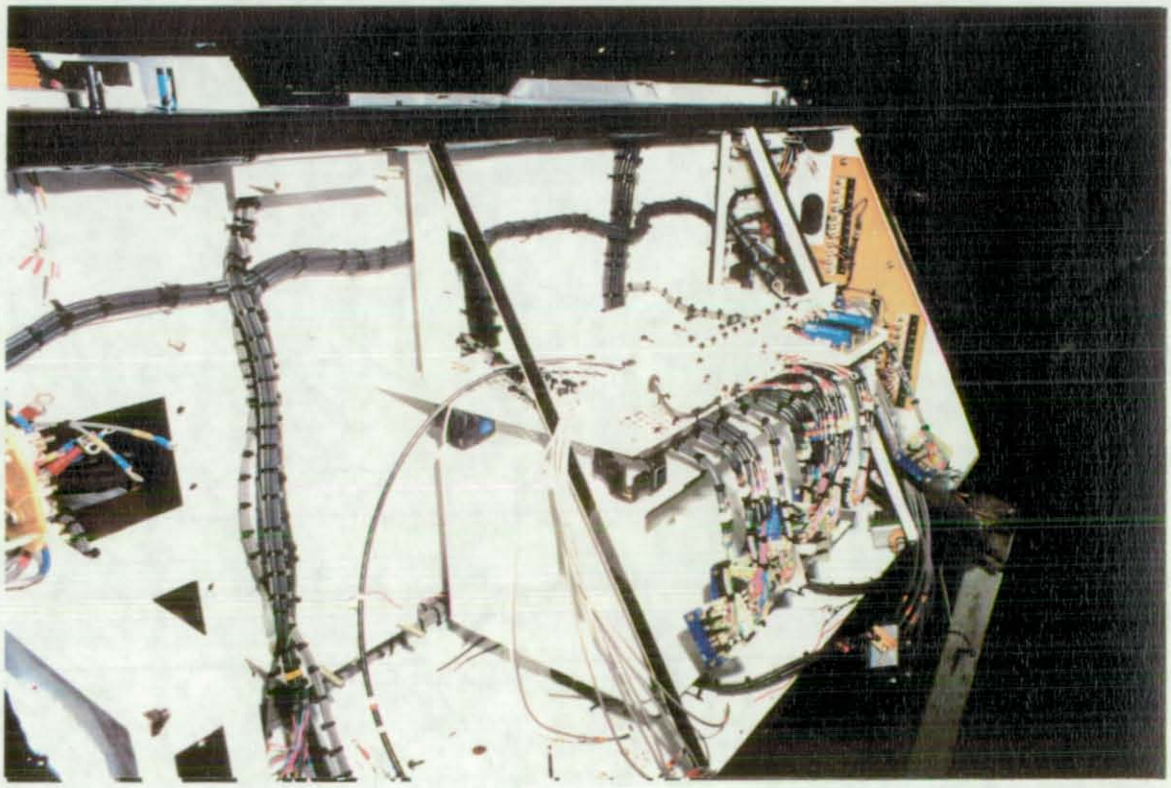

Figure 2.7 View of the internal structure of a Case (ALRV)

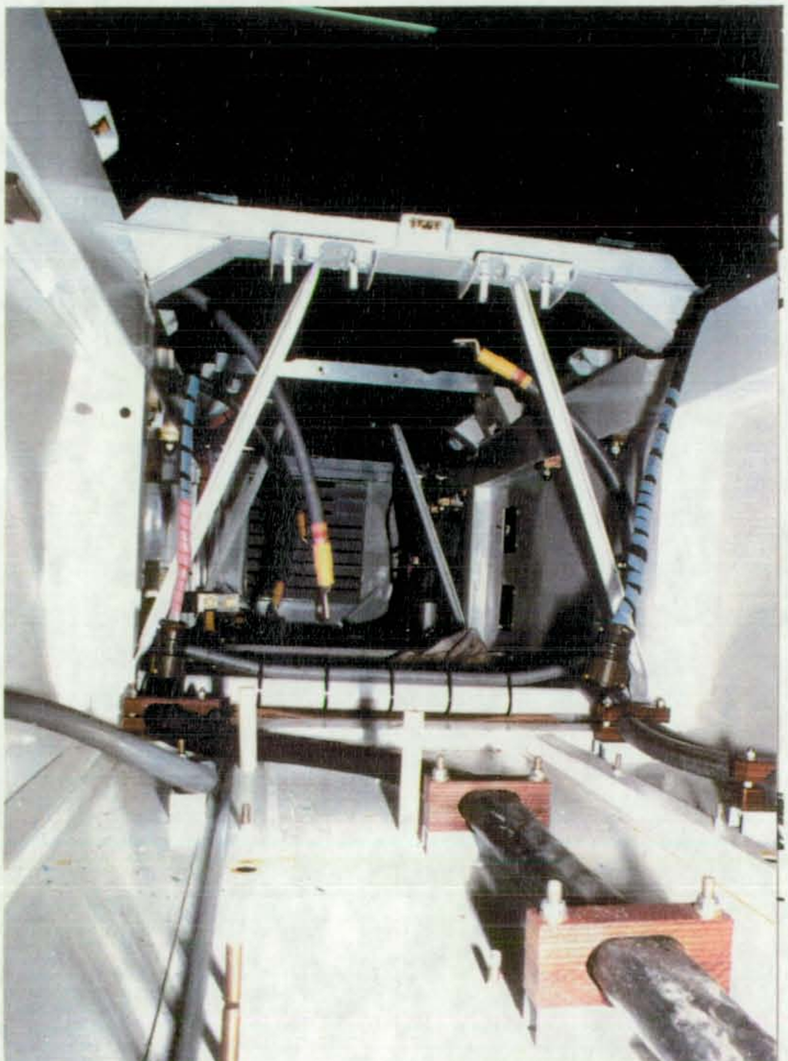

CHAPTER 3

Analysis of an Isotropic Case

3.1 Introduction

A detailed analysis of a typical isotropic equipment case was performed , in order to achieve a set of results for stresses and displacements under the defined standard service load cases. The mass of the unloaded structure was also established. These results were used to assess the efficiency of the structure with a view to improving its design , reducing weight and for comparison with future models. The investigation involved a static and elastic stress analysis of the structure using the Pafec Finite Element software. The typical Finite Element approach was adopted throughout the investigation, initially analysing a fairly coarse mesh model of the case and progressing to further enhanced models and analyses.

The chapter discusses the Finite Element idealisation of the model, the analysis technique and finally the results and conclusions.

3.2 The Equipment Case

The case to be modelled can be seen in Appendix B1. It is a hybrid case incorporating many features typical in equipment case design. The case is constructed from Austenitic Stainless Steel, Type 340L with two lateral mild steel sections for additional strength and has overall dimensions of 3.4 x 2.3 x 0.8 m. The case has of two sets of longitudinal double box section beams situated directly above each other and separated by a vertical panel. The ends of the upper beams serve as attachment points to the undercarriage of the locomotive. Equipment is supported on either side of these beams, the choke is situated between them and on either side in panniers is the switchgear and electronics. The equipment is protected from the environment by steel floor, roof, and side panels with removable covers over the panniers. These covers being generally formed in composite materials.

3.3 Finite Element Modelling

The equipment case was idealised using the PIGS pre-processor, all significant dimensions being read from the drawing in Appendix B1. The case displays two planes of symmetry, so for the symmetrical vertical load case a quarter of the case was modelled. The lateral and longitudinal load cases being antisymmetric involved using a full model which was achieved simply from the quarter model by mirror and copy commands. Initially a coarse mesh model was generated and analysed, which resulted in a series of model developments until a satisfactory analysis was achieved whose results could be viewed with confidence.

Certain simplifying assumptions were made in the modelling process:-

i. The less structurally significant stiffeners were modelled initially as tension rods and later as beams.

ii. Any filleted corners were modelled as sharp.

iii. Any welded joints between plates were represented by planes meeting at sharp edges.

The initial coarse mesh model was developed using the 'in-plane', first order quadrilateral elements, type 36200 and tension bars, type 34000, to model the less significant stiffeners, see Reference 1 for detailed information on element types. However, on mesh refinement and a change to the second order version of the quadrilateral element (36210), the results from the analysis could not be viewed with confidence in certain areas of the structure where 'out of plane' effects take place. These areas being the vertical shear panel, lower beam panel and support locations. The 'out of plane' effects caused by loads applied in these areas had not been catered for in the element type selection. A further change of element type was made to the 44210 element, a second order facet shell element and the beam element 34400, with both element types incorporating rotational degrees of freedom. The final model for a quarter case can be seen in figure 3.1 and the full model case can be seen in figure 3.2. The quarter case has 557 nodes, 233 elements , 3114 degrees of freedom, the full case has 1975 nodes, 932 elements, 6590 degrees of freedom.

3.4 Load Cases

Four proof load cases and a body fatigue load case were considered in the investigation, these load cases being taken from the standard cases featured in Appendix A1. The details of each are as follows:-

3.4.1 Proof Load Cases

The equipment mountings must be able to withstand the mass of the equipment, choke and pannier loads when subjected to the following accelerations, all loads being reacted at the support.

i. Vertical 1.0g (up)

ii. Vertical 1.5g (down)

iii. Lateral 1.1g $\pm$ 1.0g vertical (down)

iv. Longitudinal 3.0g $\pm$ 1.0g vertical (down)

3.4.2 Fatigue Load Case

All equipment mountings must be designed to have a fatigue life of not less than 10^7 cycles for the loads produced by the following accelerations acting on the mass of the equipment, ie choke and pannier loads.

i. Vertical 1.0g (down) $\pm$ 0.3g

ii. Lateral $\pm$0.3g

iii. Longitudinal $\pm$0.2g

3.5 Load Case Idealisation

The case must be self-supporting and carry the following loads:-

i. Choke, mass 1.2 tonnes applied as point load at four fixing locations .

ii. Pannier loads of 700 kg each side, distributed along the length of the case. The pannier loads were applied on both upper and lower beams to simulate equipment loadings more realistically.

3.5.1 Vertical Load Case

Since this load case has two axes of symmetry a quarter model of the equipment case was used subjected to a quarter of the total load carried The pannier loads were distributed along the upper and lower beam sections, half the load being carried by each section. The loading across these structures was applied to the nodes along the overhanging edge of the bracket section and was adjusted in the ratio of 1:4:1 across each element to obtain the second order 44210 elements. The choke load was carried by the two nodes that provided the connection points for the channel section and main case.

As only a quarter model was loaded, the boundaries along the axes of symmetry of the model had to be restrained to ensure that symmetry with the other three quadrants was preserved. Hence along the longitudinal axis of symmetry, displacements in the lateral direction and rotations around the longitudinal and vertical axes were restrained. Along the other axis of symmetry, the lateral axis, displacements in the longitudinal direction and rotations about the vertical and lateral axes were restrained.

The reaction to the applied loads was achieved by restraining all displacements at the support nodes.

3.5.2 Lateral and Longitudinal Load Cases

Both of these load cases are antisymmetric, the lateral load case is antisymmetric about the longitudinal plane and visa versa. A full case idealisation was used to model both these load cases as combinations of loadcases were required, with the loading being applied as described above for the vertical load case. Restraints were applied to the four support loactions to prevent any displacements at these points.

3.6 Results

3.6.1 Proof Load Cases

The displacement and stress contour plots obtained from the proof load analyses can be seen in figures 3.3 - 3.7. The stress contour plots are uninformative having few contours and so only one has been included as an example of the output obtained. On identification of the areas of high displacement and stress, namely the supports, beams and separating vertical shear panel, several graphs have been plotted out via the PIGS post-processor to clarify the results for each load case . The graphs of stress distribution use Von Mises equivalent stress criterion evaluated along the mid surface of the shell elements. The Von Mises stress was evaluated as the stresses are two dimensional and this criterion combines the two direct and one shear stress into a single equivalent ? ?
stress based on a shear distortion energy limit at yield, Reference 2. The resulting graphs all have sharp, jagged contours which have been smoothed out to illustrate the stress distribution more realistically. Considering each proof load case in turn:-

3.6.1.1 Vertical Load Cases

i. 1.0g Vertical up

ii. 1.5g Vertical down

The results for load case (i), as expected were found to be proportionally smaller and in the opposite ?
ii ?
direction to load case (i). The results described here are for the more severe load case (ii).

The displacement graphs, figures 3.8 - 3.10, show the vertical and lateral components of displacement experienced by the upper and lower beams and their separating shear panel, the central web. It should be noted that the graphs for this load case terminate at the centre of the case, due to the symmetrical nature of the load case. It can be seen that the vertical displacements are negative throughout, they have a maximum value at the ends of the beams and a minimum value at the centre, the actual value being very small, in the order of 10^{-1}mm . The maximum vertical displacement occurs at the centre of the lower beam, magnitude 2.0mm.

Lateral displacements are again very small, in the order of 10^{-1}mm and are positive throughout showing that the right hand side of the case tends to bow outwards, in the positive x direction. Along the upper beam the lateral displacements are virtually constant and negligble at 0.003mm, however along the central web and lower beam they are at a minimum at the ends rising sharply to a maximum at the centre, the maximum displacement being 2.2mm at the centre of the central web. Longitudinal displacements throughout were in the order of 10^{-2}mm and therefore considered negligble.

The examination of the stress output files reveals modest stress levels, in the order of 10^1 Nmm^{-2} well below the yield stress of 204 Nmm^{-2} for Austenitic Stainless Steel. The highest stress levels were found at the supports, with a typical value of 55 Nmm^{-2} ie 27% of yield. The graphs, figures 3.11 - 3.13, show the stress distribution along the upper and lower beam and also the central web. All the curves tend to maximum towards the ends of the structure and a minimum centrally. The maximum Von Mises stress in these areas is 15.8 Nmm^{-2} ie 7.7% of yield.

3.6.1.2 Lateral Load Case

$\pm$1.1g lateral + 1.0g vertically down

Results were only obtained for the positive lateral load case. The negative load case would produce the mirror image of results discussed here, therefore was not necessary for the assessment of displacement and stress variations. The lateral load case is antisymmetrical and so a full model of the equipment case was used in the analysis. When submitted initially, the displacement output as shown in figure 3.5 was produced. The quilting effect that can be seen was assumed to be the result of unrealistic loading in this load case. The pannier loads were evenly distributed along both the upper and lower beams, which under lateral loading resulted in these lateral loads impinging along the vertical shear panel wall, the central web. In an actual case the equipment these loads are representing are attached via frames and side walls to the shear panel rather than as overhanging weights. These frames and the supporting structures would provide additional vertical and lateral stiffness. The revised lateral load case therefore was modelled with the lateral loads displaced to the upper beam, where they could be distributed through the upper shear panel, the displacement output as seen in figure 3.6, shows the results of the second set of loading conditions.

Several graphs have been plotted to illustrate areas of interest. Graphs are included from both the left and right hand sides of the structure to show the effects of antisymmetric loading. Displacements throughout the whole structure can be seen to be negligble, in the order of 10^{-1}mm. Vertical and lateral displacements have been considered, the longitudinal component being negligable, in the order of 10^{-2}mm. The displacement graphs can be seen in figures 3.14- 3.18. The displacements along the upper right and left beams show both vertical and lateral components to be similar curves, with the right hand curves being slightly more exaggerated, a maximum of 2% larger. Vertical deflections are negative throughout and are of a maximum value at the ends and a minimum centrally, -0.35mm for the right hand side. Lateral deflections are positive showing a tendency for both sides of the case to bow in the positive x direction. Lateral deflections are at a minimum at the ends and rise to a 0.14mm maximum at the centre of the right hand beam. Similarly the vertical component of deflection along the left and right hand lower beams show a similar distribution, a maximum value at both ends with a central plateau minimum of -1.2mm. The lateral components differ from the left to right hand side. The left hand side being at a minimum in the centre, bowing in the negative x direction by 0.18mm, the right hand deflection shows a bow in the positive x direction, maximum of 0.23mm. Along the right hand side central web, the vertical component is almost constant at -0.33mm, the lateral component shows a large rise towards the centre, with a maximum of 1.2mm positive bow.

The deflections discussed above are of a negligble size, however they do indicate the weaknesses in the structure, ie lack of stiffness in the vertical shear panel under lateral loading. The stress output file again shows modest stress levels of the order of 10^1 Nmm^{-2}, these being well below yield for the material. The table, figure 3.19 details stresses at the supports and reveals that these are highly stressed in comparison with the rest of the structure.

Von Mises Stresses at a Support Location

Loadcase	Support Node (488)	Support Node (491)
Vertical (ii)	54.16	57.98
Lateral	104.00	52.40
Longitudinal	56.10	47.52

All stresses are in Nmm^{-2}

Figure 3.19

The graphs, figures 3.20- 3.24 show the Von Mises stress distribution along the regions of 'high' stress in the structure. Again graphs along both left and right hand sides are included to illustrate the effects of antisymmetry.

The upper beams show high stress at the ends and a minimum in the centre. The left hand side is slightly higher stressed than the right hand side, by 6%. Similarly the lower beam exhibits the same stress features along its length, again the left hand side being slightly more exaggerated, by 6%.

Along the right hand central web, high stresses appear at the ends 14 Nmm^{-2}, dropping steeply to a minimum ~ 3 Nmm^{-2} in the centre.

3.6.1.3 Longitudinal Load Case

± 3.0 g Longitudinal + 1.0 g Vertically down

As in the lateral load case only the positive case is considered, the negative load case giving the 'mirror image' of the results described here. The nature of the load case involves both sides of the model being equally loaded and hence only the right hand side of the case is considered.

Displacements through the structure can be seen to be negligble, in the order of 10^{-1} mm. Several graphs along the regions of high displacement can be seen in figs 3.25 - 3.27 and show longitudinal, lateral and vertical components of deflection. The upper beam shows a positive longitudinal displacement, the displacement being constant along the beam at 0.6mm. The vertical displacements show a negative displacement and varies unsymmetrically along the length with maximum displacement being -0.34mm. Lateral displacements are negligble here. The lower beam exhibits a similar constant value of 0.7- 0.9 mm of longitudinal displacement. The vertical deflection here is at a maximum at the ends and a minimum of -1.28mm centrally, with lateral displacements again negligble. The central web has a high positive lateral displacement varying from a minimum at the ends to a maximum of 1.1mm centrally, this high lateral displacement again is due to the lack of stiffness in the vertical shear panel. The longitudinal component shows a similar distribution to the upper beam with deflections between 0.4 - 0.6 mm. The vertical component again is negative and varies unsymmetrically along the length of having a minimum value of -0.344 mm. The stress output file again shows no stress that exceeds yield for the material. The support locations are the most highly stressed with stresses of the order of 10^2 Nmm^{-2}. The Von Mises stress distributions along the upper and lower beams and central webs again exhibit stresses in the order of 10^1 Nmm^{-2}

and can be seen in figures 3.28 -3.30.

3.6.2 Fatigue Load Case

The fatigue analysis involved using three sample nodes from the highly stressed areas of the structure ie the supports and the upper and lower beams. The applied stress range at these locations was determined and compared with standard fatigue data, Reference 3. The results are tabulated in figure 3.31 and details of the calculations can be found in Appendix B2.

Fatigue Analysis Data

Location (Node)	Stress Range Nmm^{-2}	Weld Class	Reserve Factor
Support (488)	83.8	B	1.2
Upper Beam (236)	0.4	F	100
Lower Beam (394)	1.9	F	21

Figure 3.31

The results show that the fatigue reserve factors are high for the majority of the structure and that a grade F weld is acceptable. However the support locations experience a high stress range and would require a very high quality grade B weld to withstand the stated fatigue conditions. This would be impractical and hence it is likely that cracks would initiate and grow at the support locations.

3.6.3 Case Mass

The finite element analysis determined the mass of the unloaded structure to be 360kg.

3.7 Discussion

The analyses revealed that the structure was relatively unstressed when subjected to the service proof and fatigue loads and was 360 kg when unloaded. The results of the investigation, show that there are areas for concern in the case design:-

i. High stresses are experienced at the supports compared with the rest of the structure. The fatigue analysis revealed that high quality grade B welds would be required at the support locations in order to withstand the fatigue loadings. Lower quality welds would cause the case to fail by cracking the supports.

ii. There is a tendency for some lateral deflection when the case is subjected to antisymmetric loading caused by the lack of lateral stiffness in the vertical shear panel separating the supporting upper and lower beams.

Hence, design improvements for the case would be to introduce some vertical stiffeners into the vertical shear panel to prevent the tendency for lateral deflection and to reinforce the support area.

3.8 Conclusions

The analysis of the isotropic case has revealed that the case is over designed, although there are several areas that are exhibit high stresses and displacements and require design improvements. It can be concluded that a redesign in composite materials to produce a more efficient and lighter case is a feasible proposition.

Figure 3.1 Quarter Case Idealisation

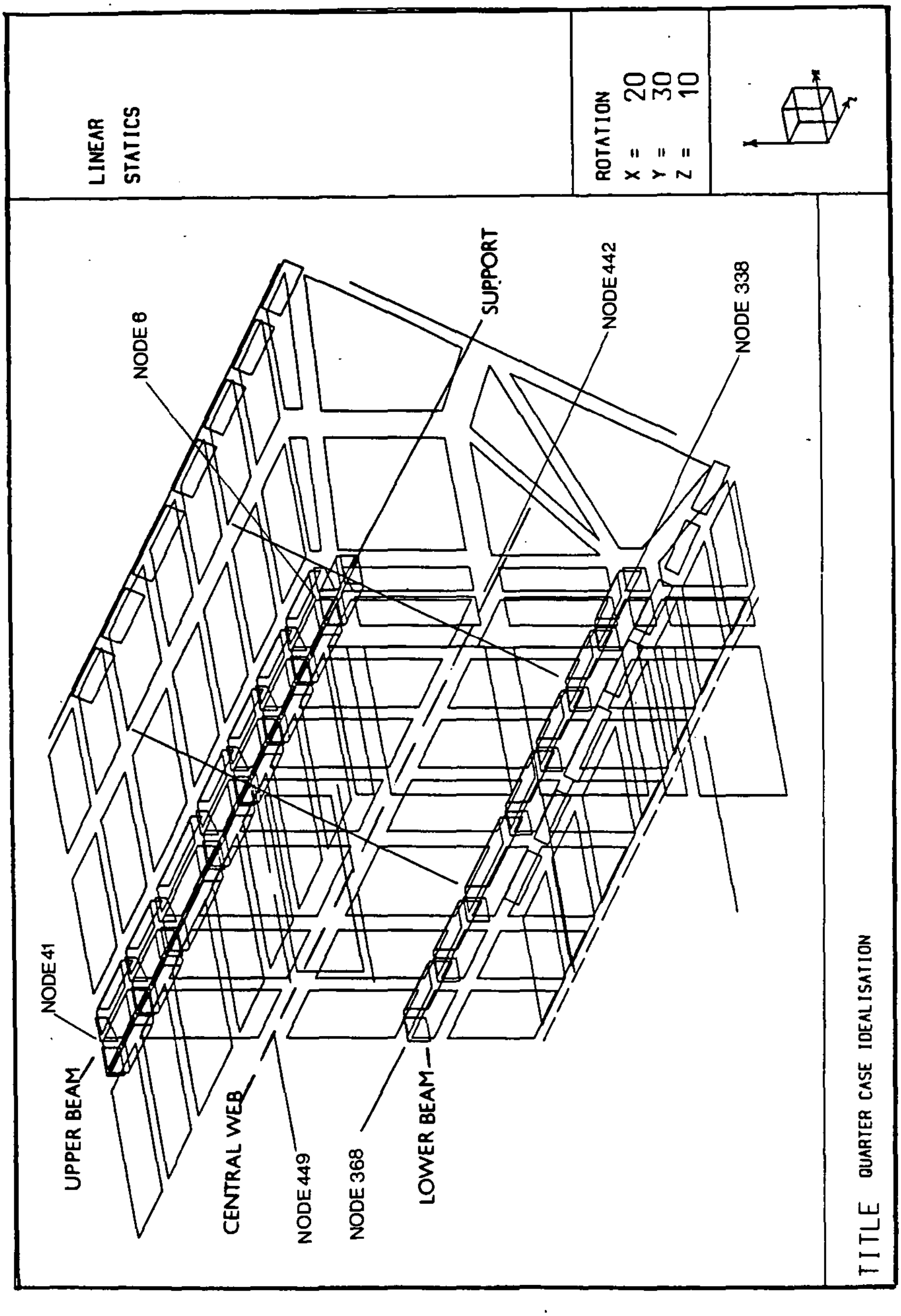

Figure 3.2 Full Model Idealisation

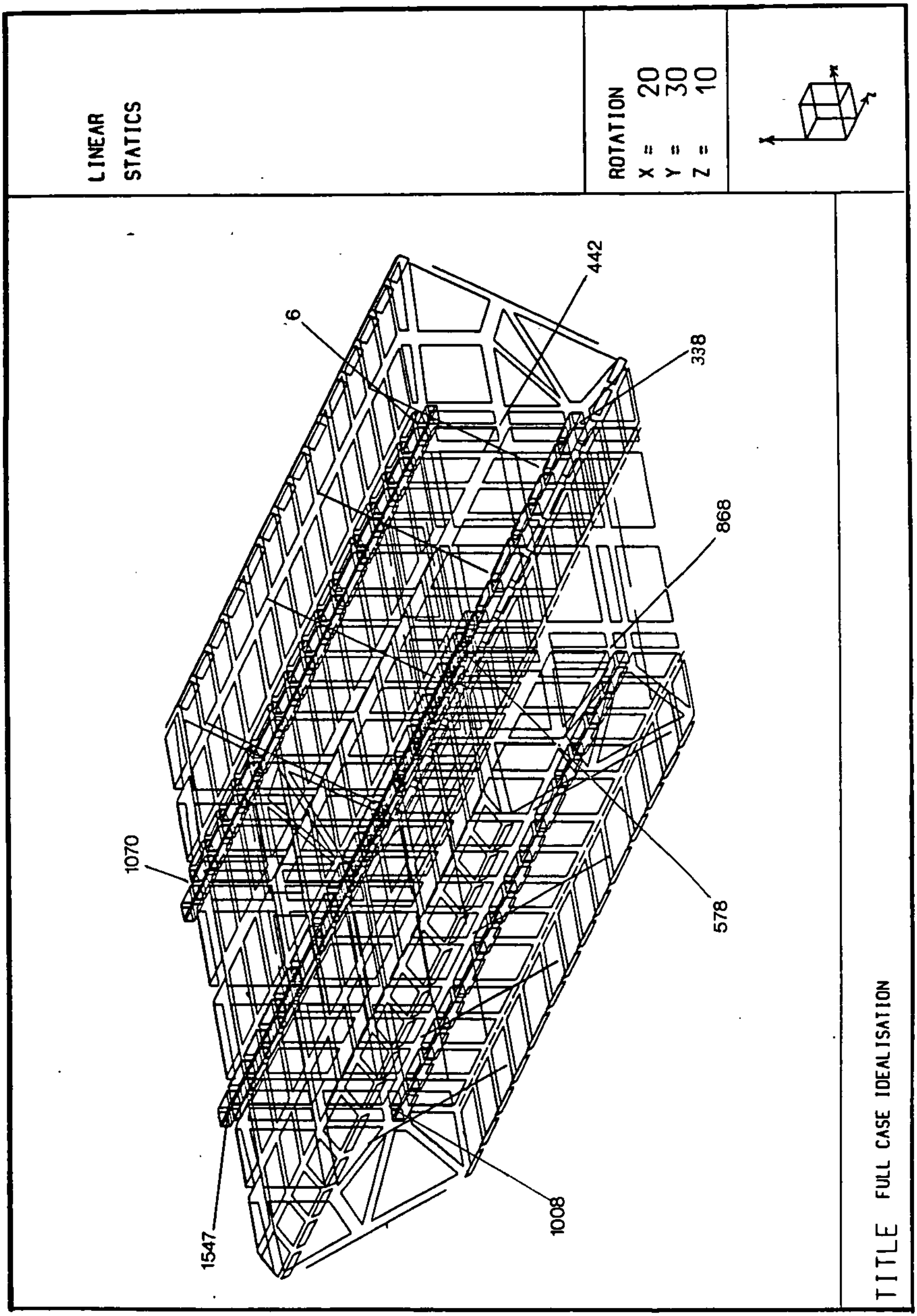

Figure 3.3 Stress Contour Plot for the Full Case (Longitudinal Load Case)

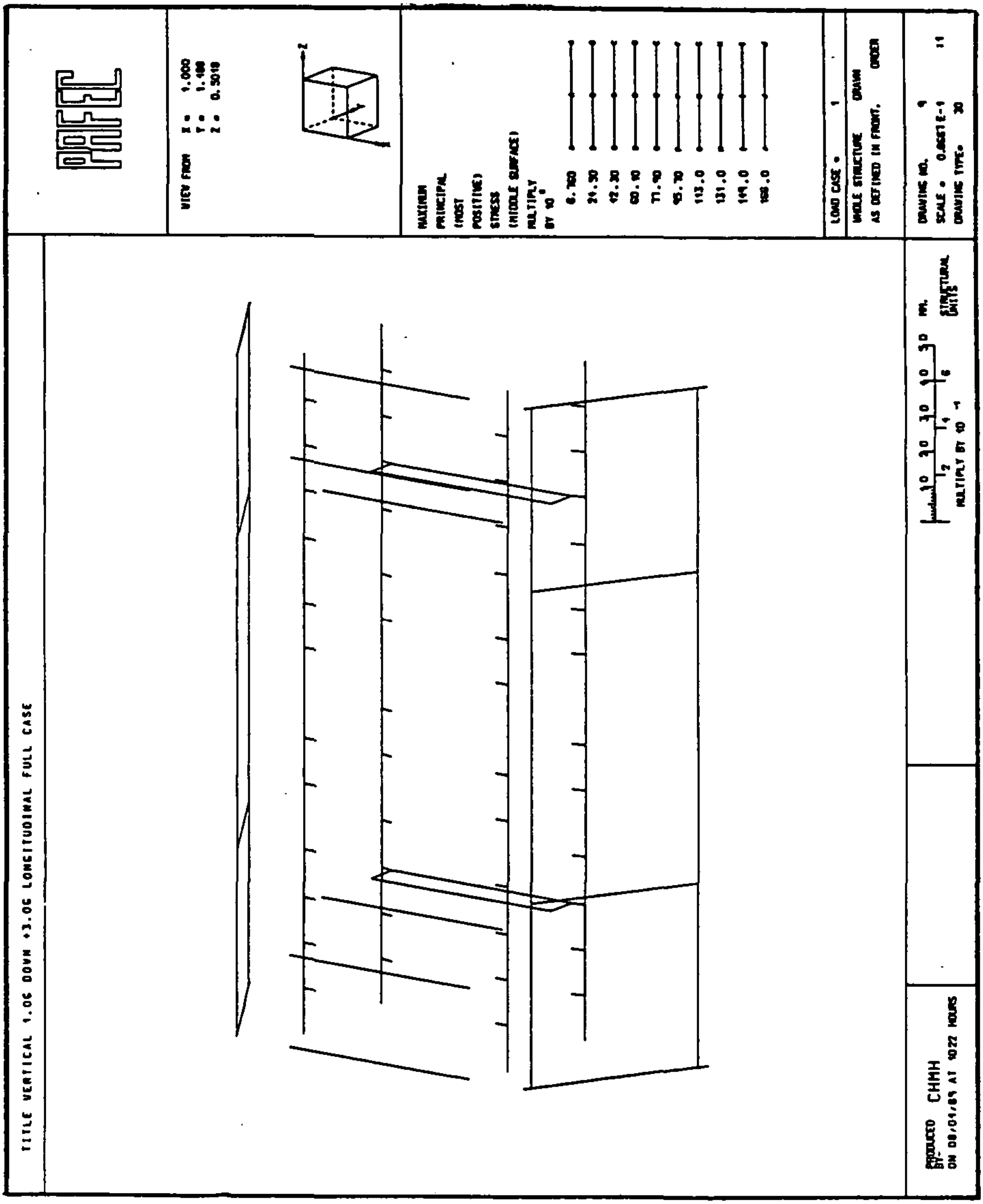

Figure 3.4 Displacement Plot for the Vertical 1.5g down Load Case

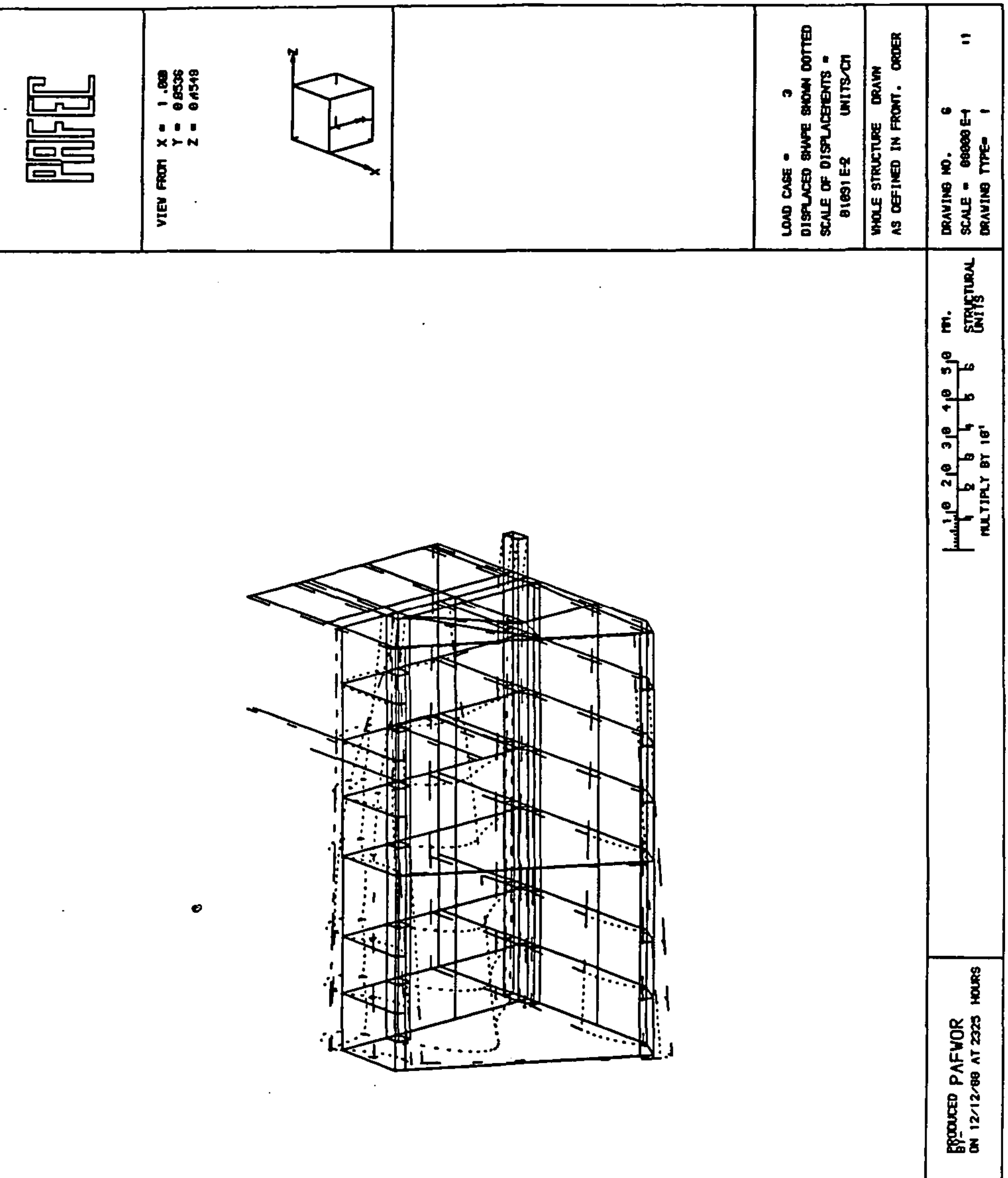

Figure 3.5 Displacement Plot for the Lateral Load Case (Idealisation 1)

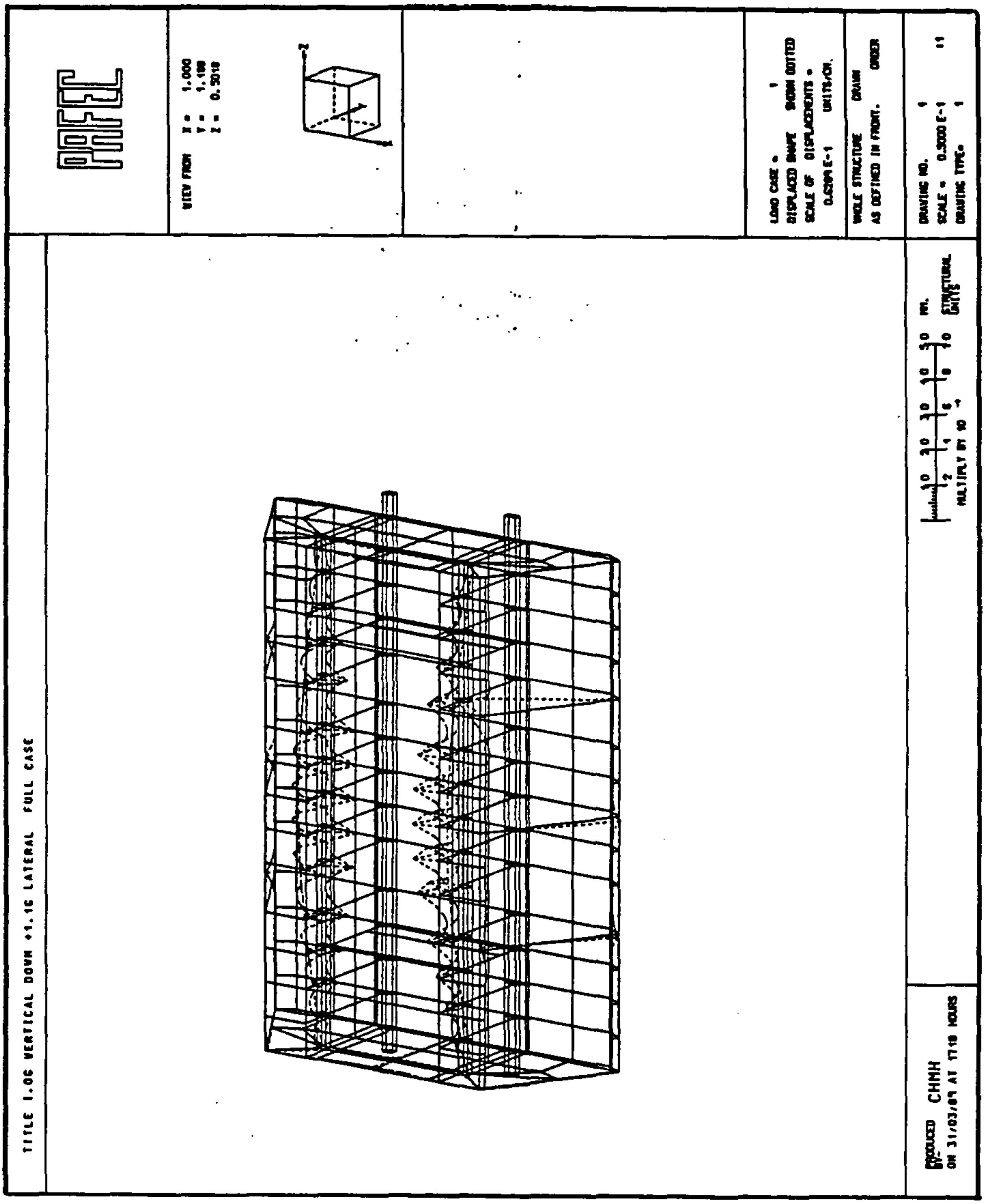

Figure 3.6 Displacement Plot Lateral Load Case (Idealisation 2)

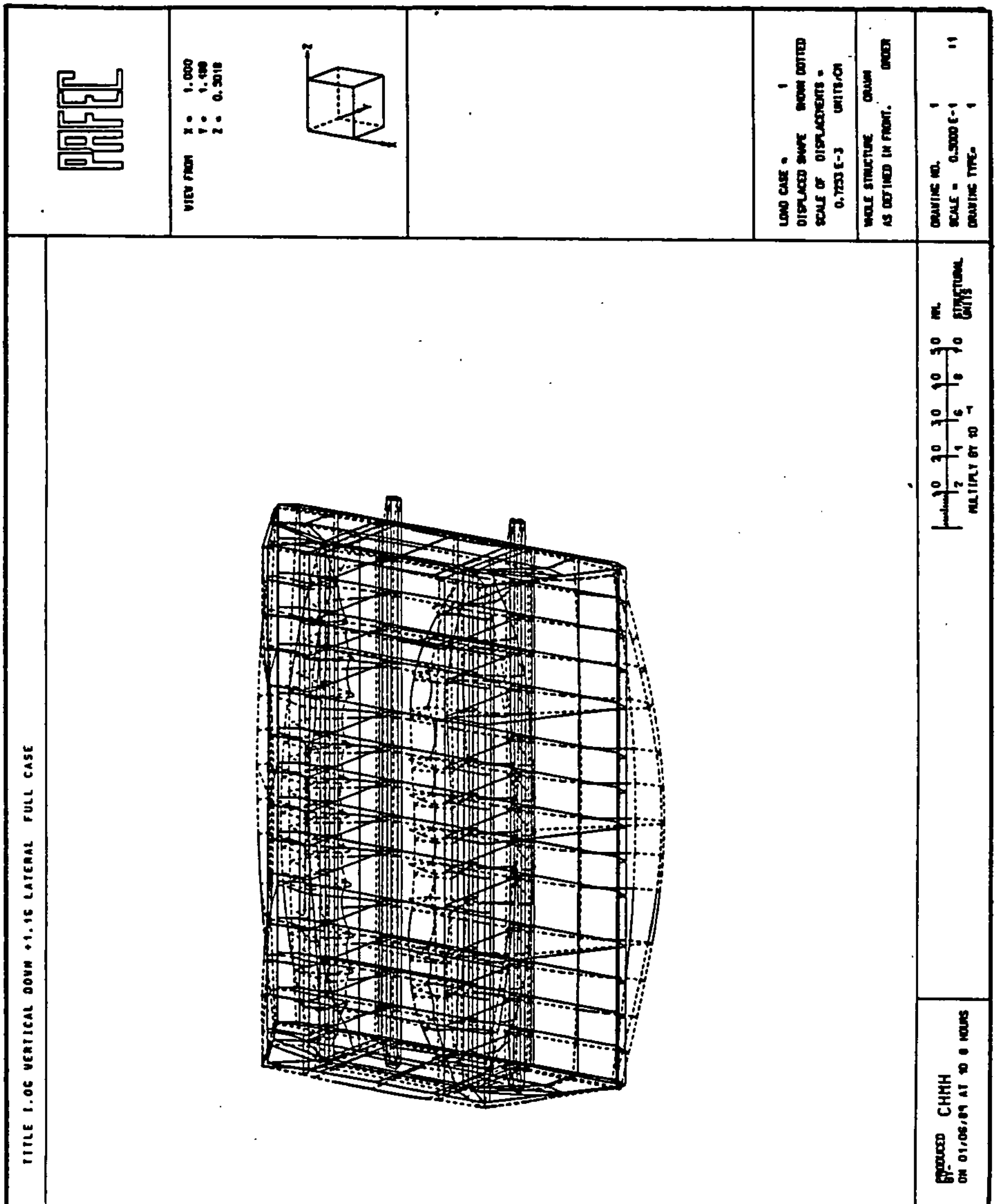

Figure 3.7 Displacement Plot for the Longitudinal Load Case

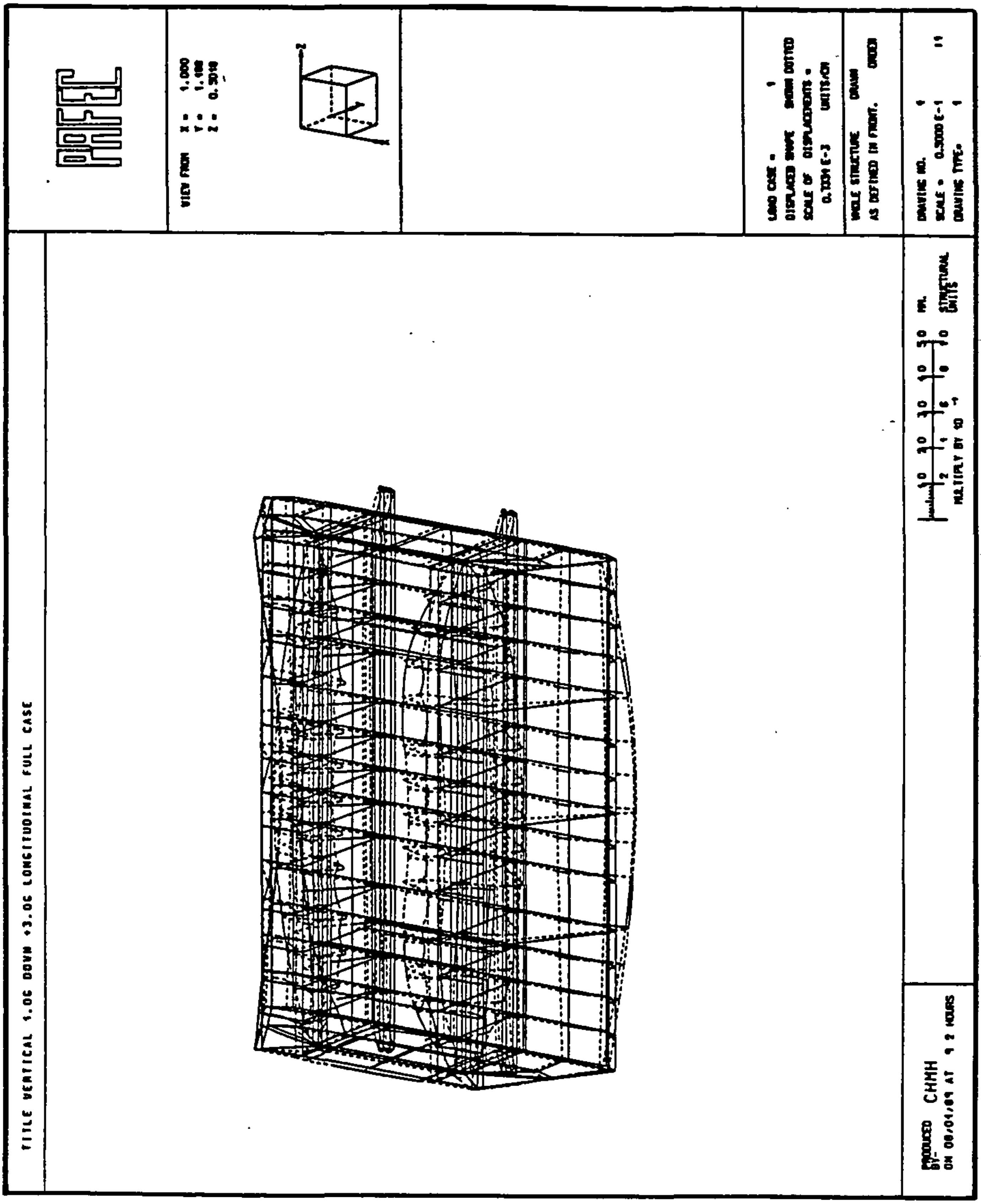

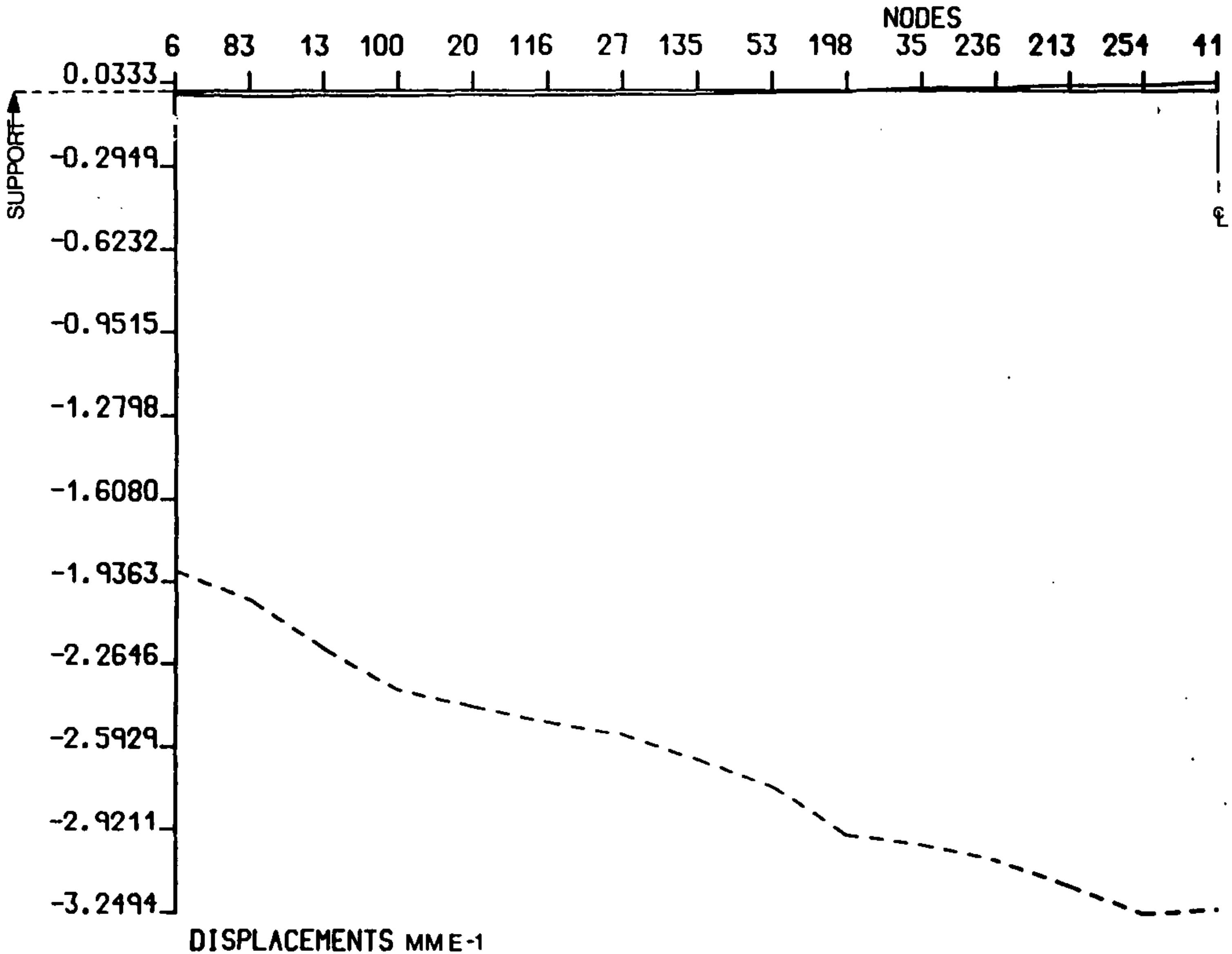

KEY
—— UX DISP.
- - - UY DISP.

LOADCASE
VERTICAL 1.5G
(DOWN)

TITLE UX AND UY DISPLACEMENTS ALONG THE UPPER BEAM

Figure 3.8

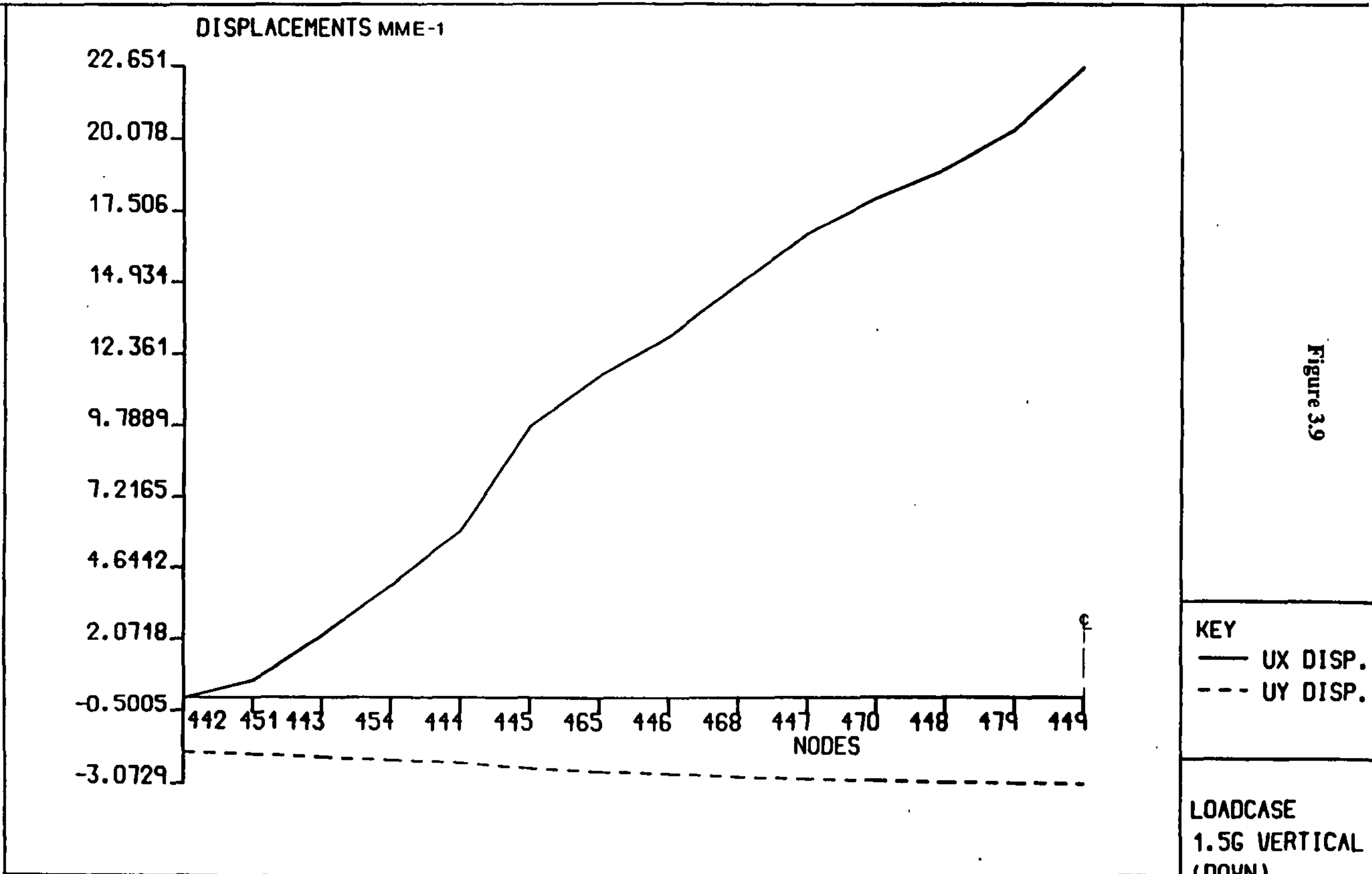

TITLE UX AND UY DISPLACEMENTS ALONG THE CENTRAL WEB

Figure 3.9

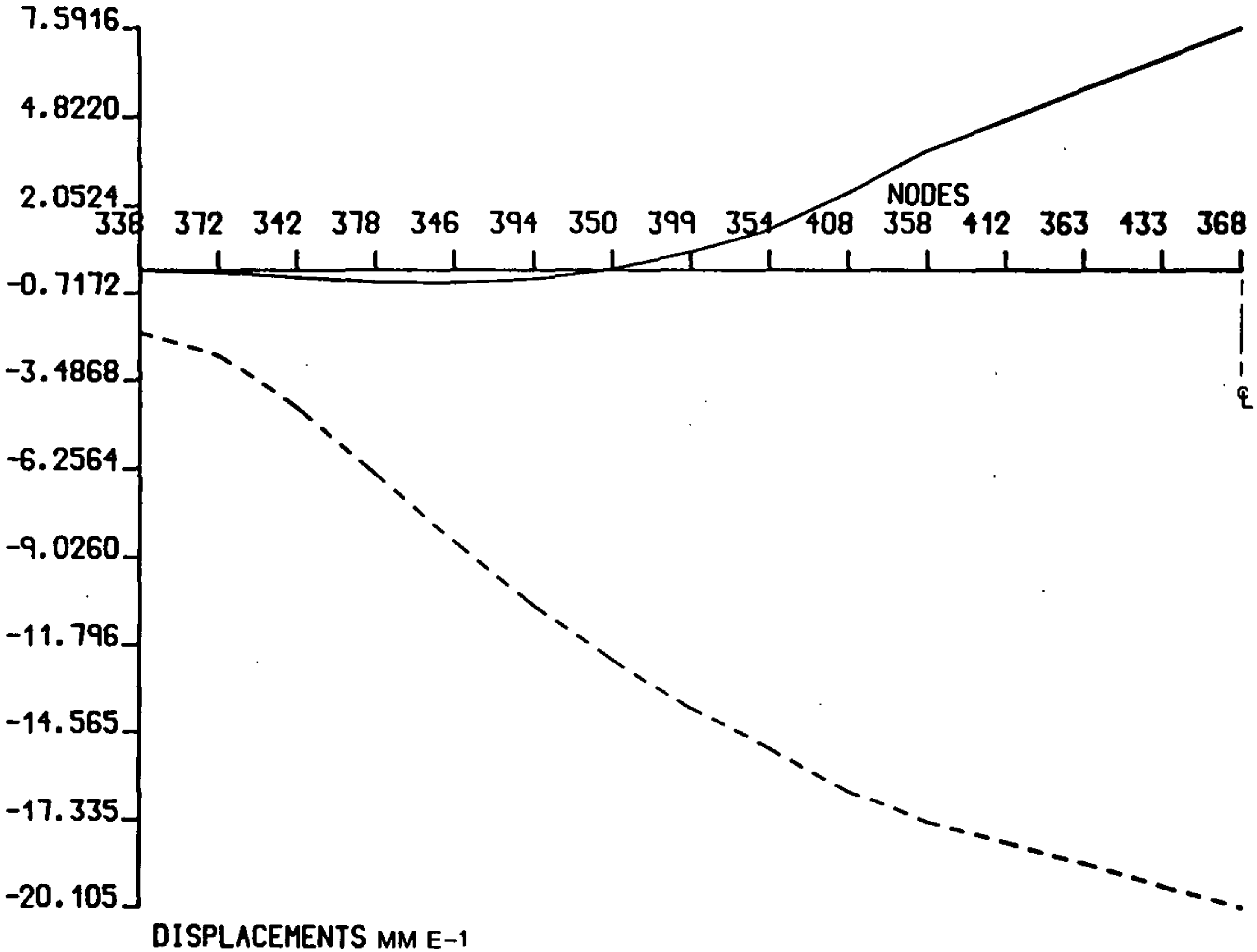

KEY
—— UX DISP.
- - - UY DISP.

LOADCASE
VERTICAL 1.5G
(DOWN)

TITLE UX AND UY DISPLACEMENTS ALONG THE LOWER BEAM

Figure 3.10

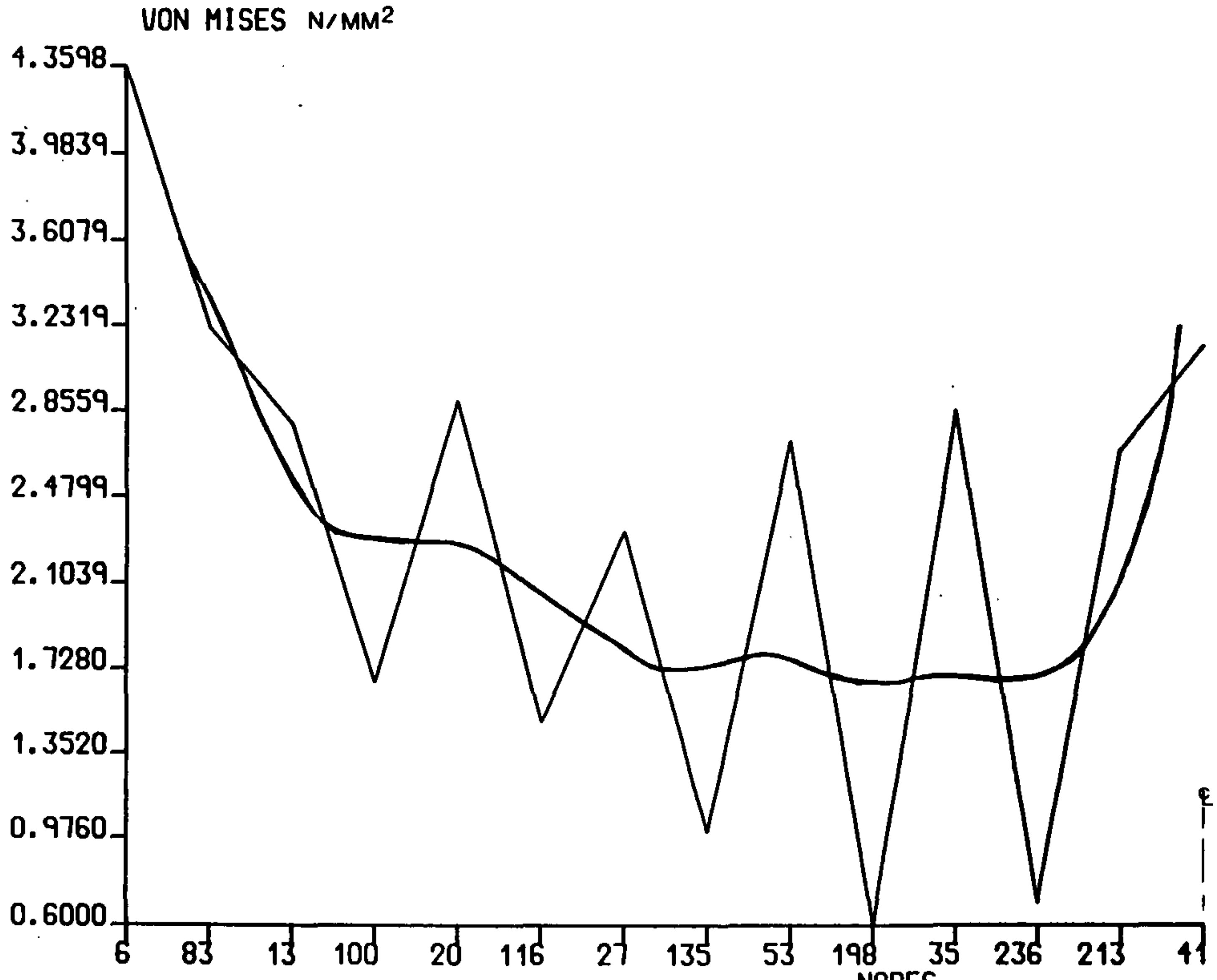

LOADCASE
1.5G VERTICAL
(DOWN)

TITLE VON MISES STRESS ALONG THE UPPER BEAM

Figure 3.11

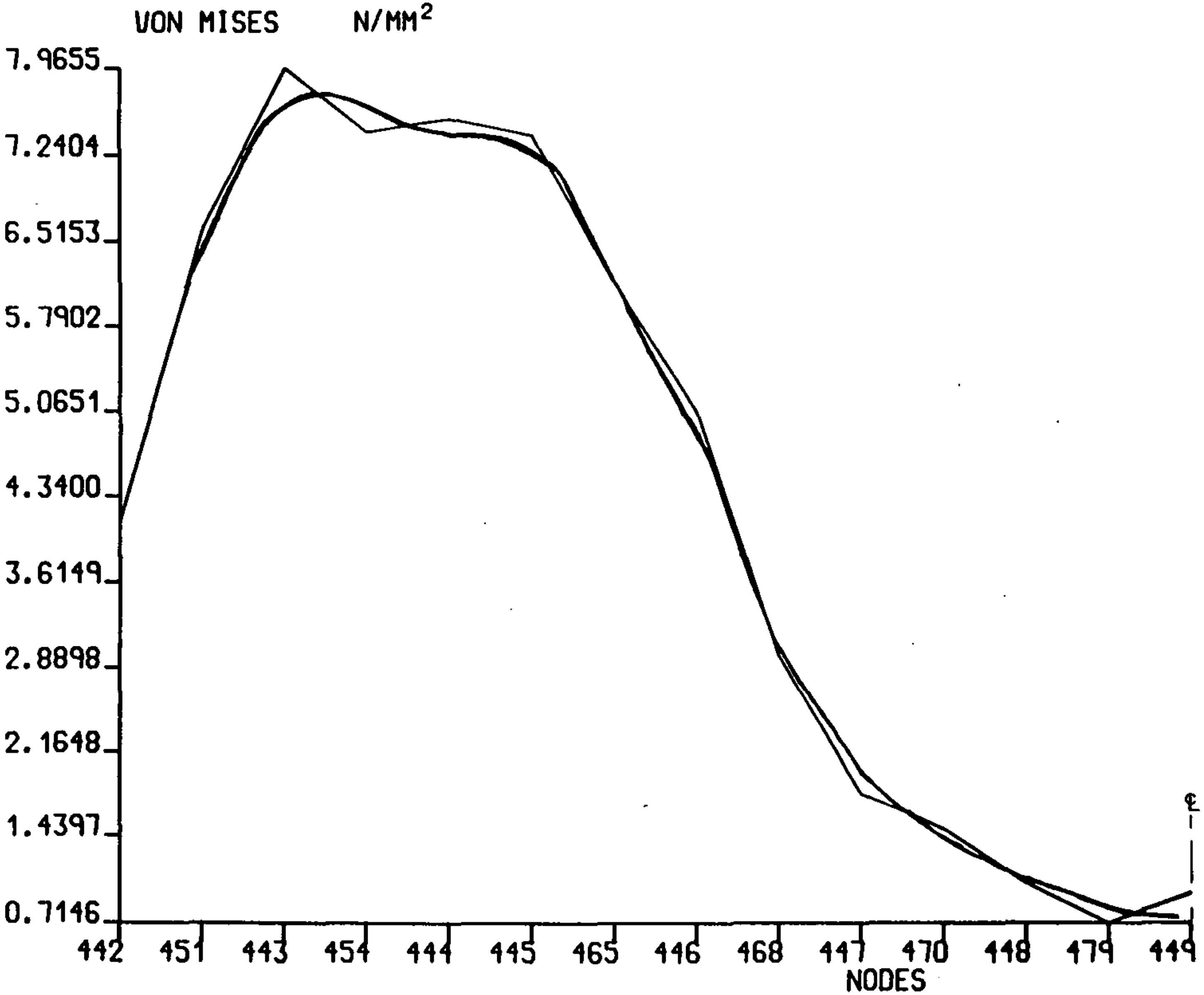

LOADCASE
VERTICAL 1.5G
(DOWN)

TITLE VON MISES STRESS ALONG THE CENTRAL WEB

Figure 3.12

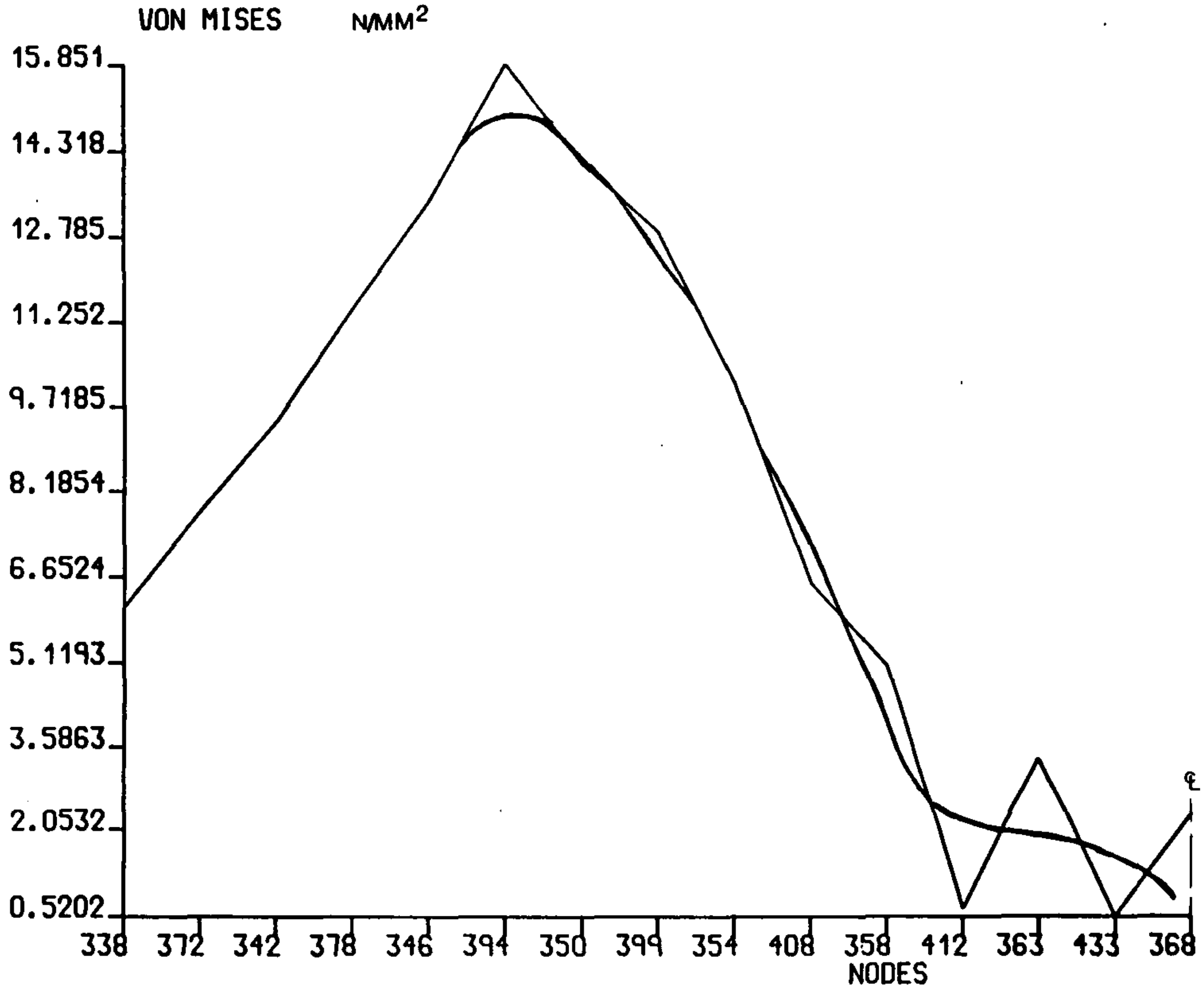

LOADCASE
VERTICAL 1.5G
(DOWN)

TITLE VON MISES STRESS ALONG THE LOWER BEAM

Figure 3.13

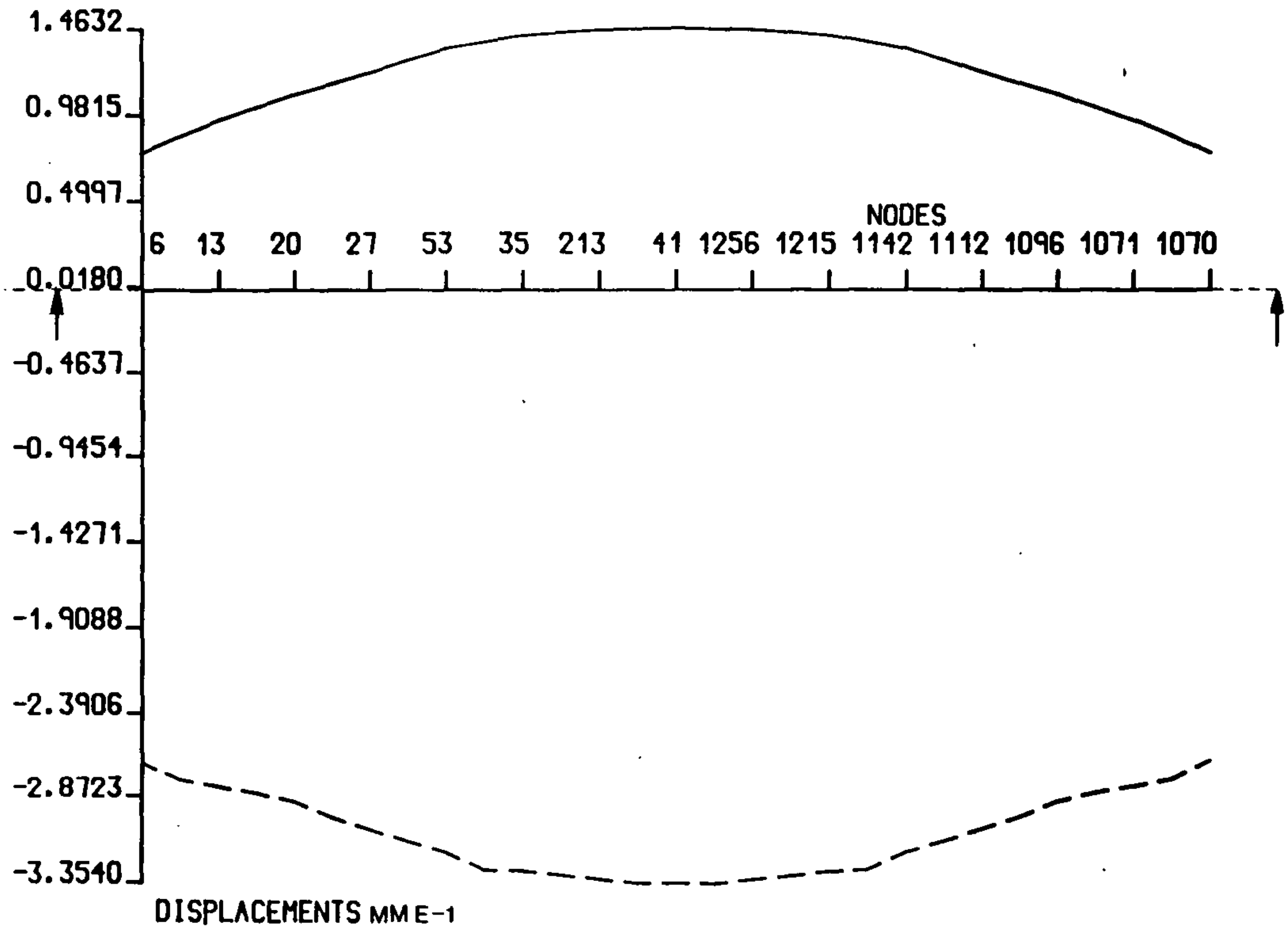

KEY
— UX DISP.
- - UY DISP.

LOADCASE
1.0G VERTICAL (DOWN)
1.1G LATERA

TITLE UX AND UY DISPLACEMENTS ALONG THE RH UPPER BEAM

Figure 3.14

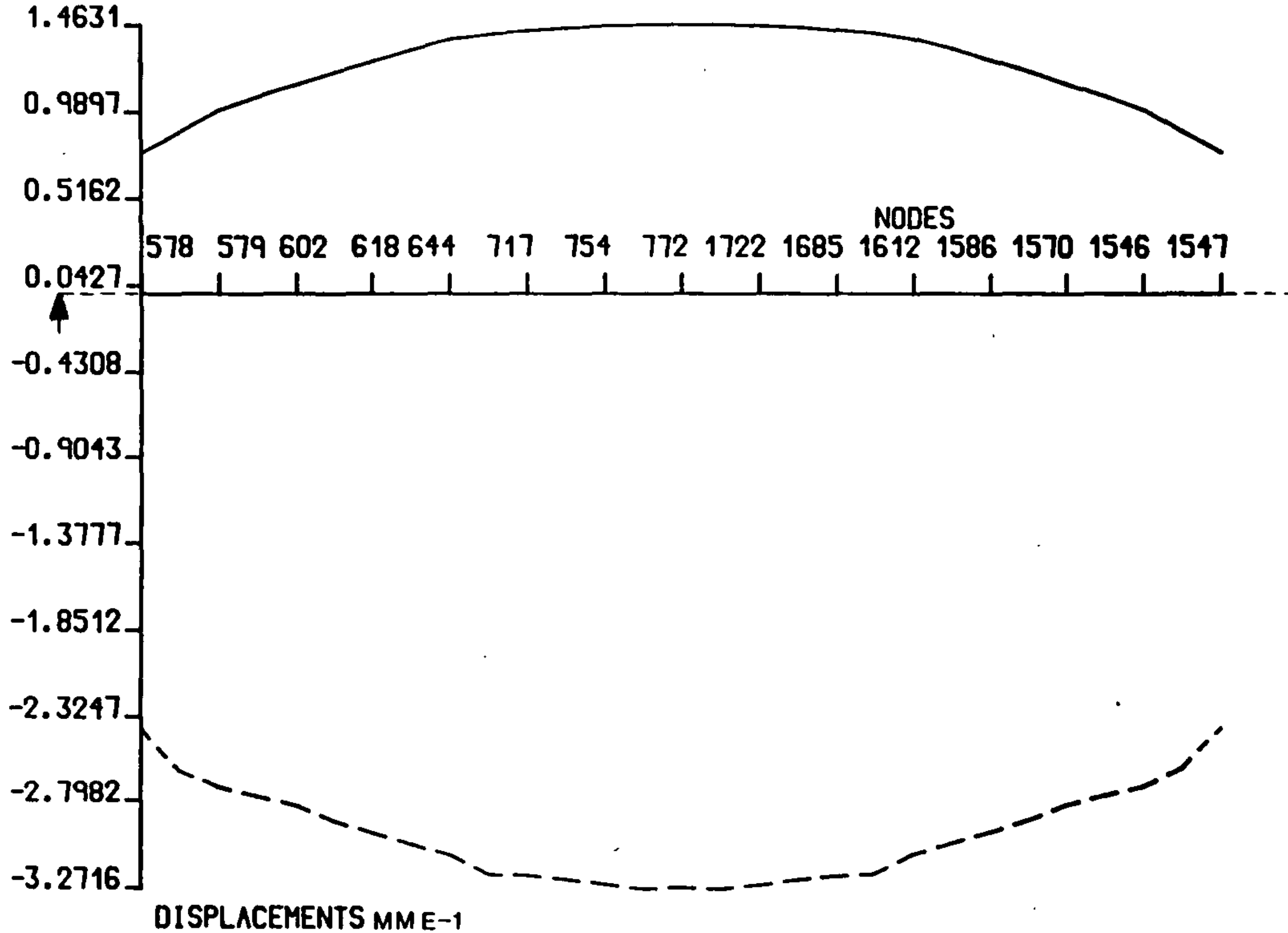

KEY
— UX DISP.
-- UY DISP.

LOADCASE
1.0G VERTICAL
(DOWN)
1.1G LATERAL

TITLE UX AND UY DISPLACEMENTS ALONG THE LH UPPER BEAM

Figure 3.15

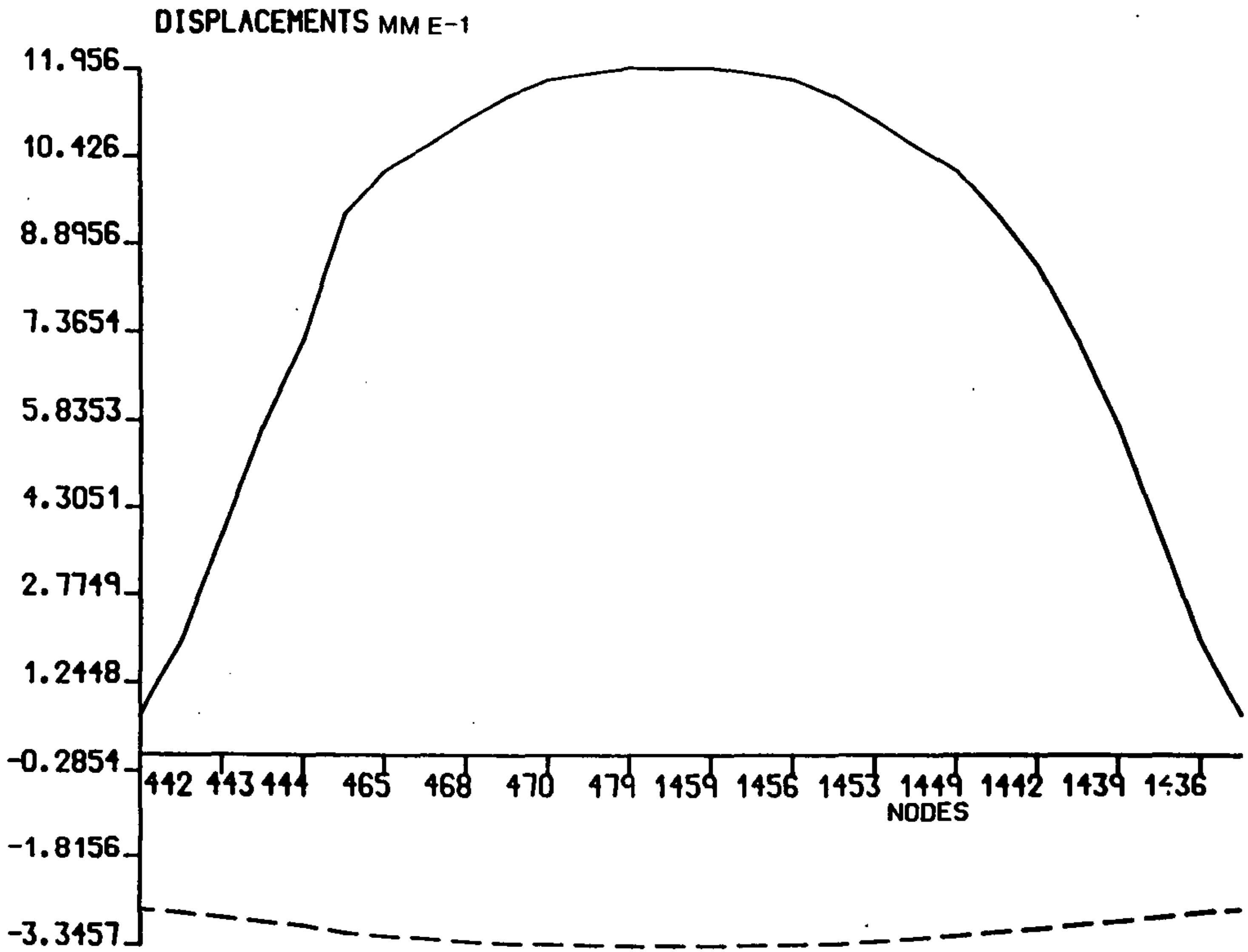

KEY
— UX DISP.
-- UY DISP.

LOADCASE
1.0G VERTICAL
(DOWN)
1.1G LATERAL

TITLE UX AND UY DISPLACEMENTS ALONG THE CENTRAL WEB

Figure 3.16

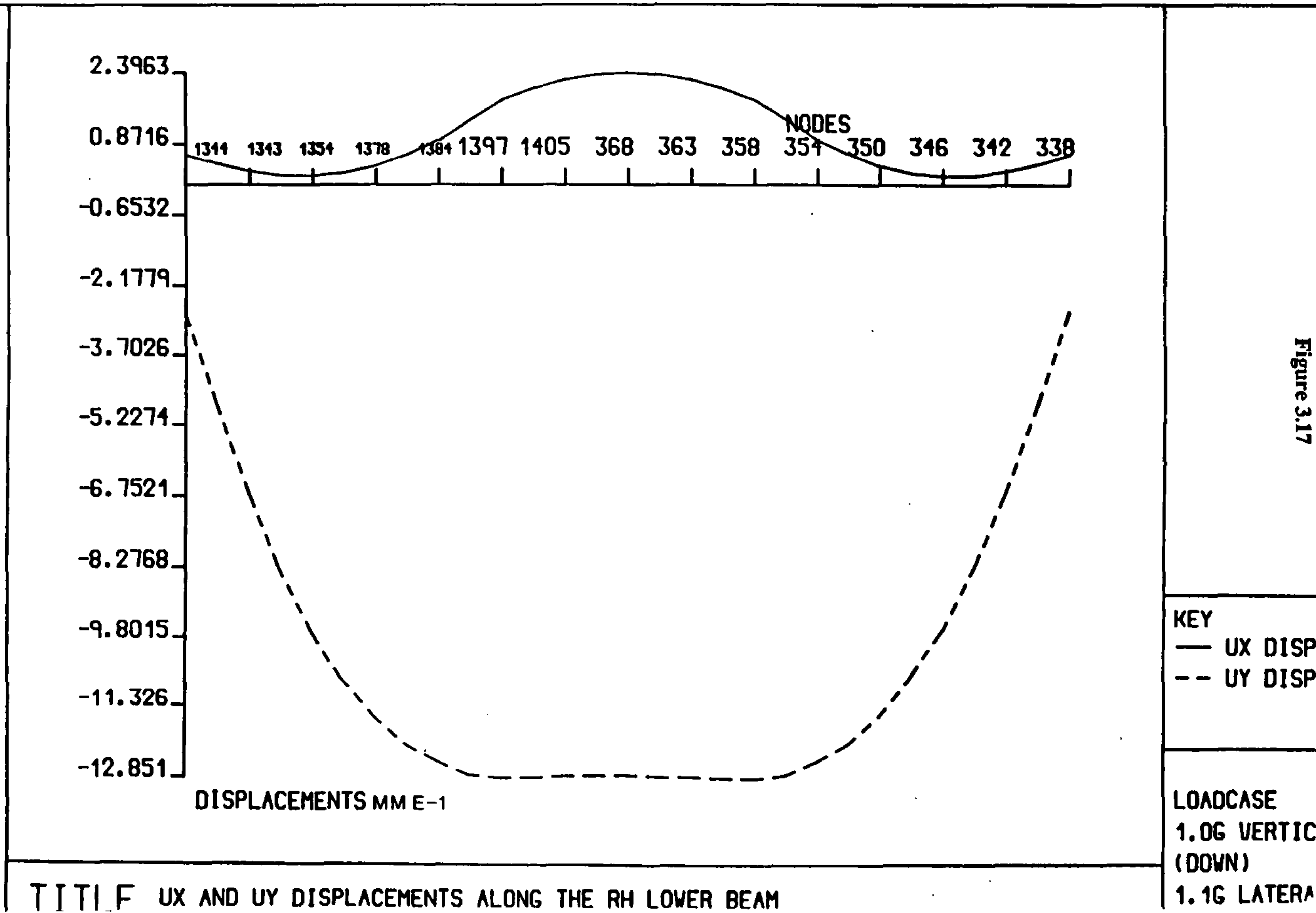
2.3963
0.8716
-0.6532
-2.1779
-3.7026
-5.2274
-6.7521
-8.2768
-9.8015
-11.326
-12.851
NODES
1344 1343 1354 1378 1384 1397 1405 368 363 358 354 350 346 342 338
DISPLACEMENTS MM E-1
KEY
— UX DISP.
-- UY DISP.
LOADCASE
1.0G VERTICA
(DOWN)
1.1G LATERA
TITLE UX AND UY DISPLACEMENTS ALONG THE RH LOWER BEAM

Figure 3.17

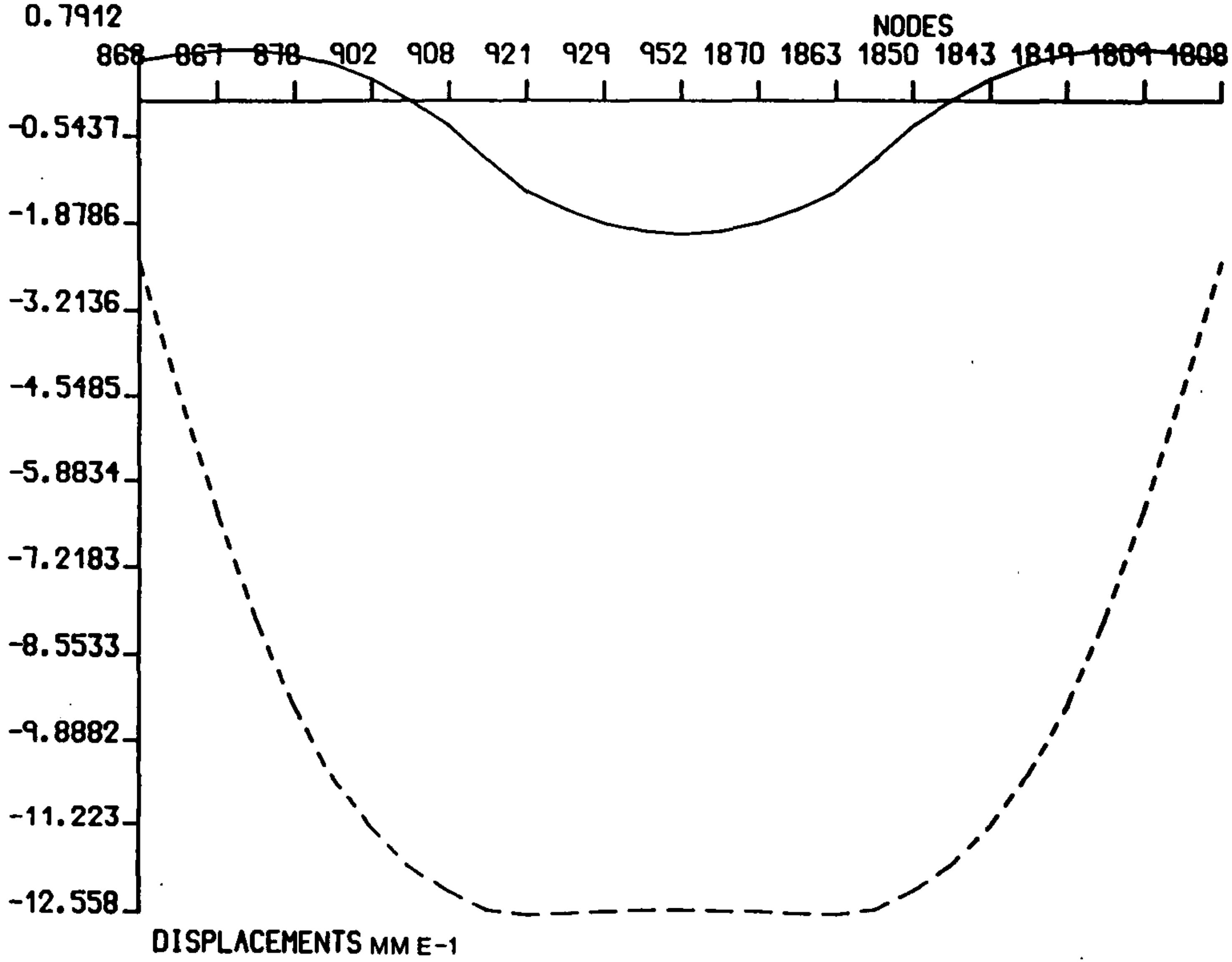

KEY
— UX DISP.
-- UY DISP.

LOADCASE
1.0G VERTICAL
(DOWN)
1.1G LATER[illegible]

TITLE UX AND UY DISPLACEMENTS ALONG THE LH LOWER BEAM

Figure 3.18

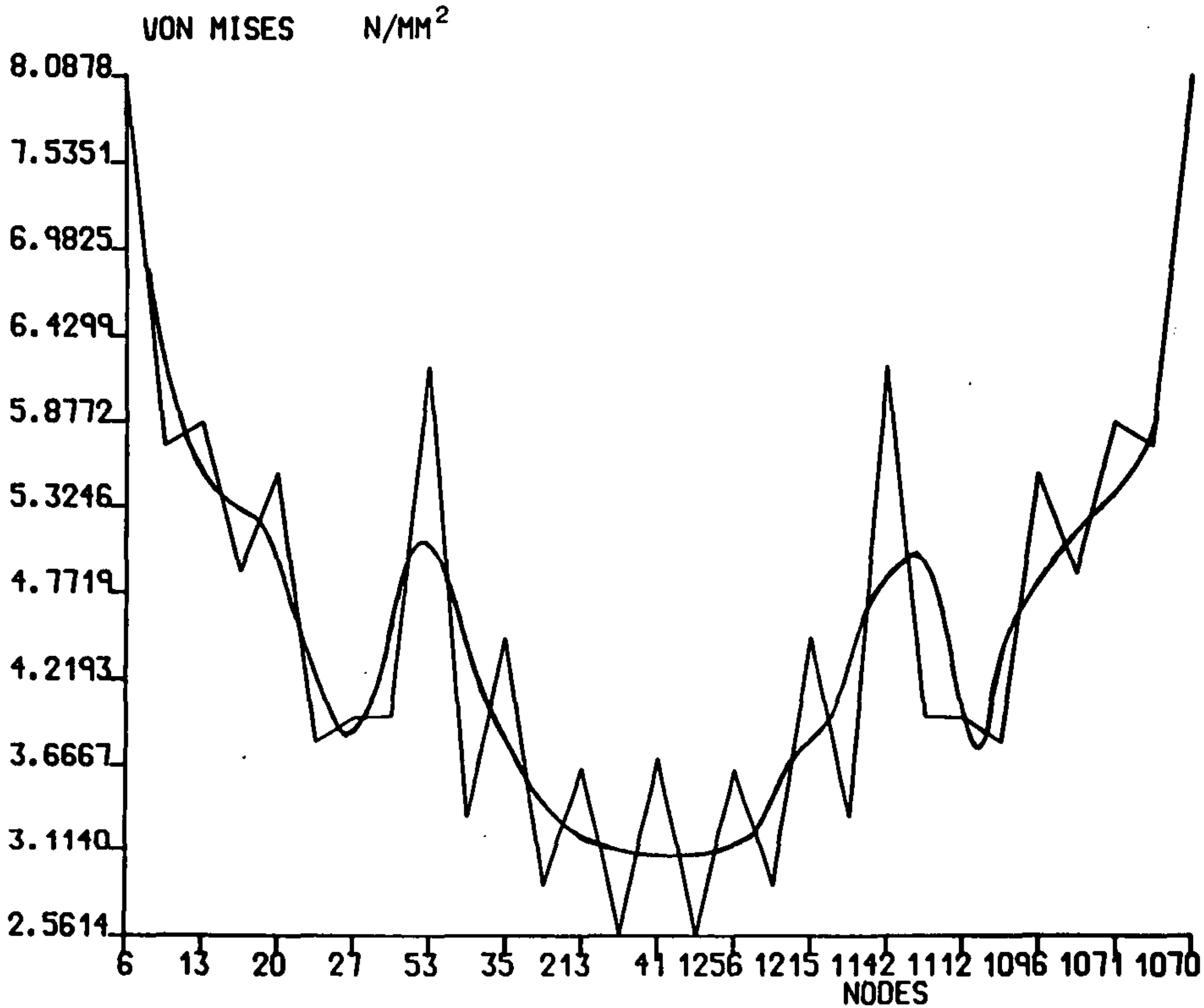

LOADCASE
1.0G VERTICAL
(DOWN)
1.1G LATER'

TITLE VON MISES STRESS ALONG THE RH UPPER BEAM

Figure 3.20

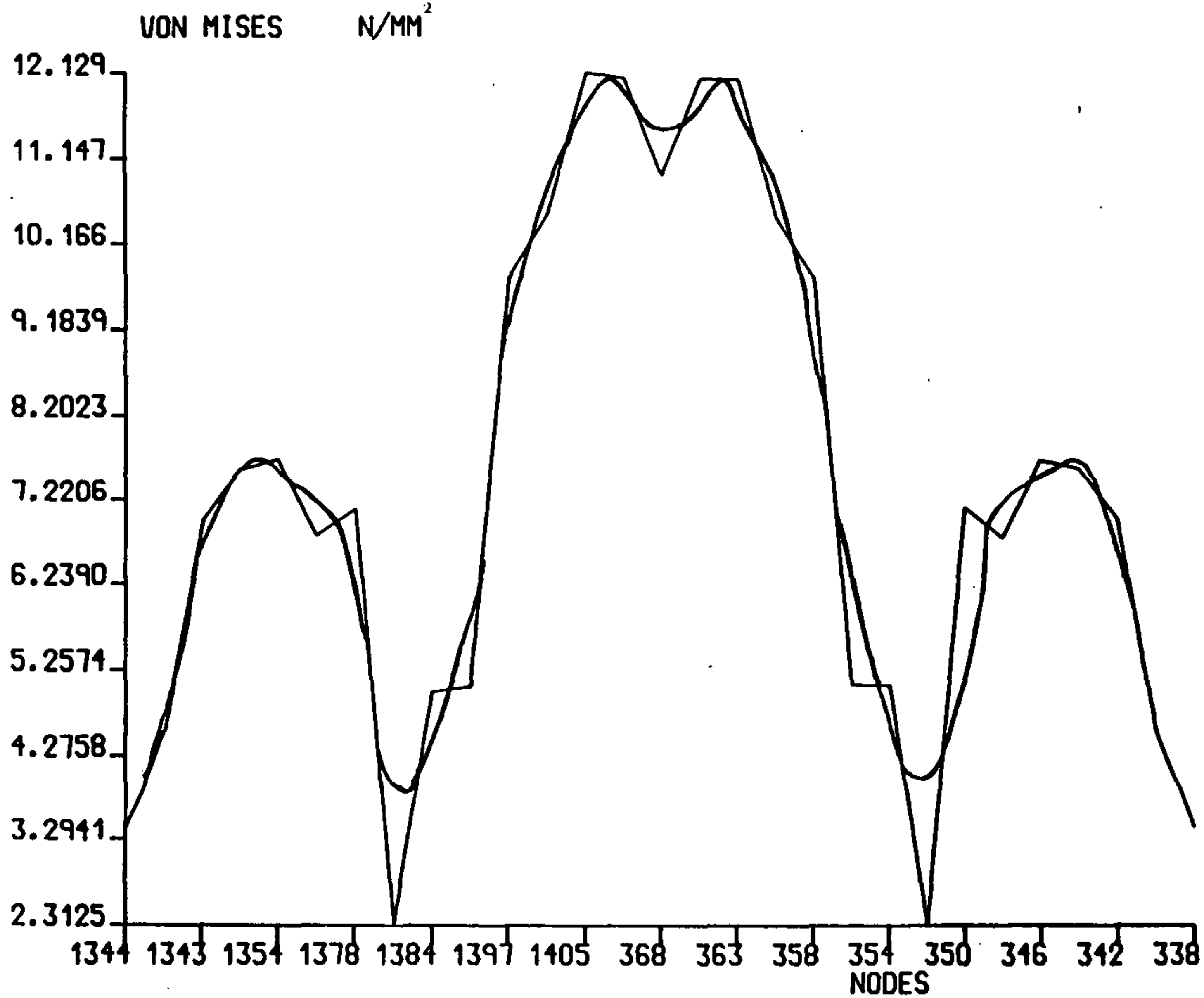

TITLE VON MISES STRESS ALONG THE RH LOWER BEAM

LOADCASE
1.0G VERTICAL
(DOWN)
1.1G LATER...

Figure 3.21

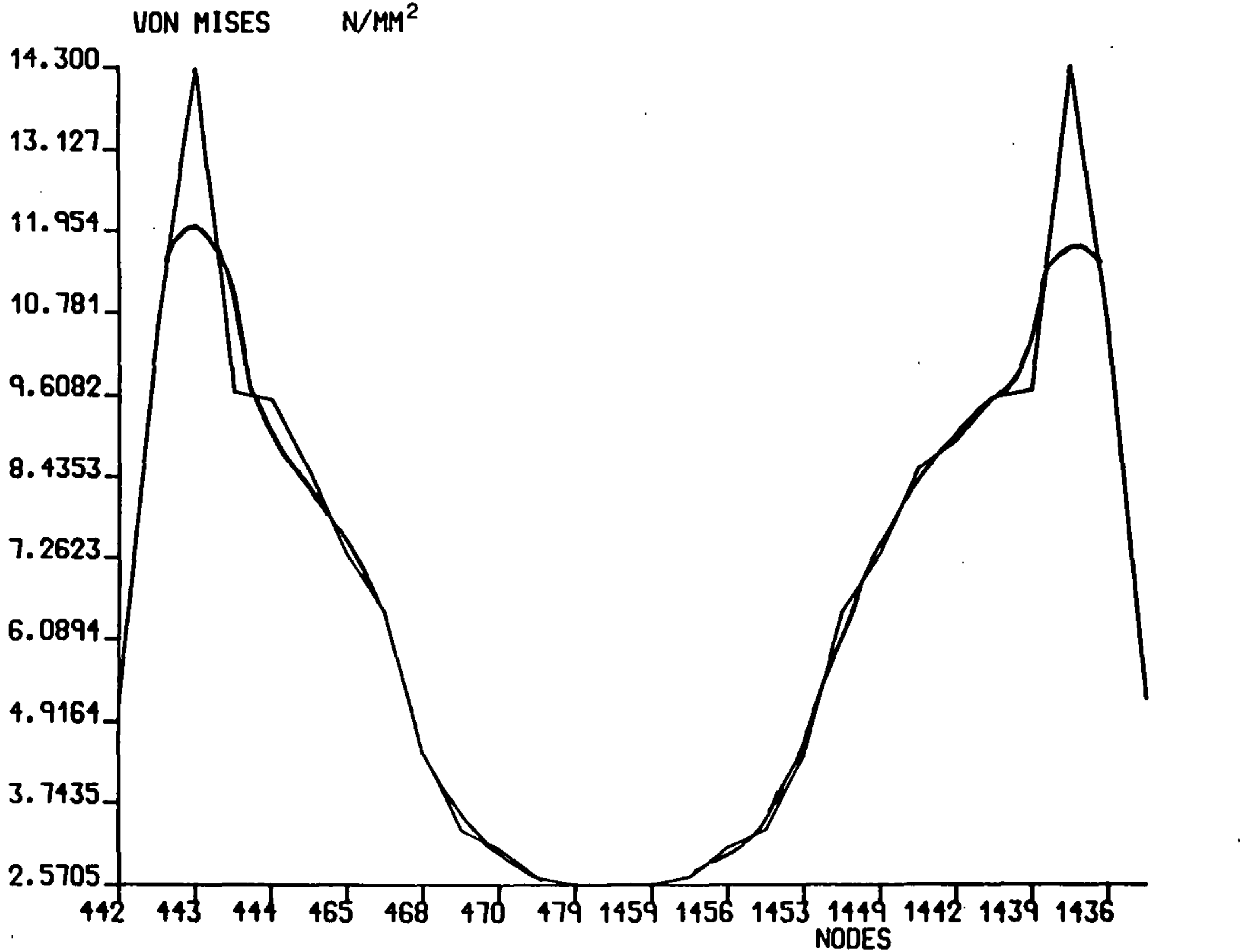

TITLE VON MISES STRESS ALONG THE CENTRAL WEB

LOADCASE
1.0G VERTICAL
(DOWN)
1.1G LATERA'

Figure 3.22

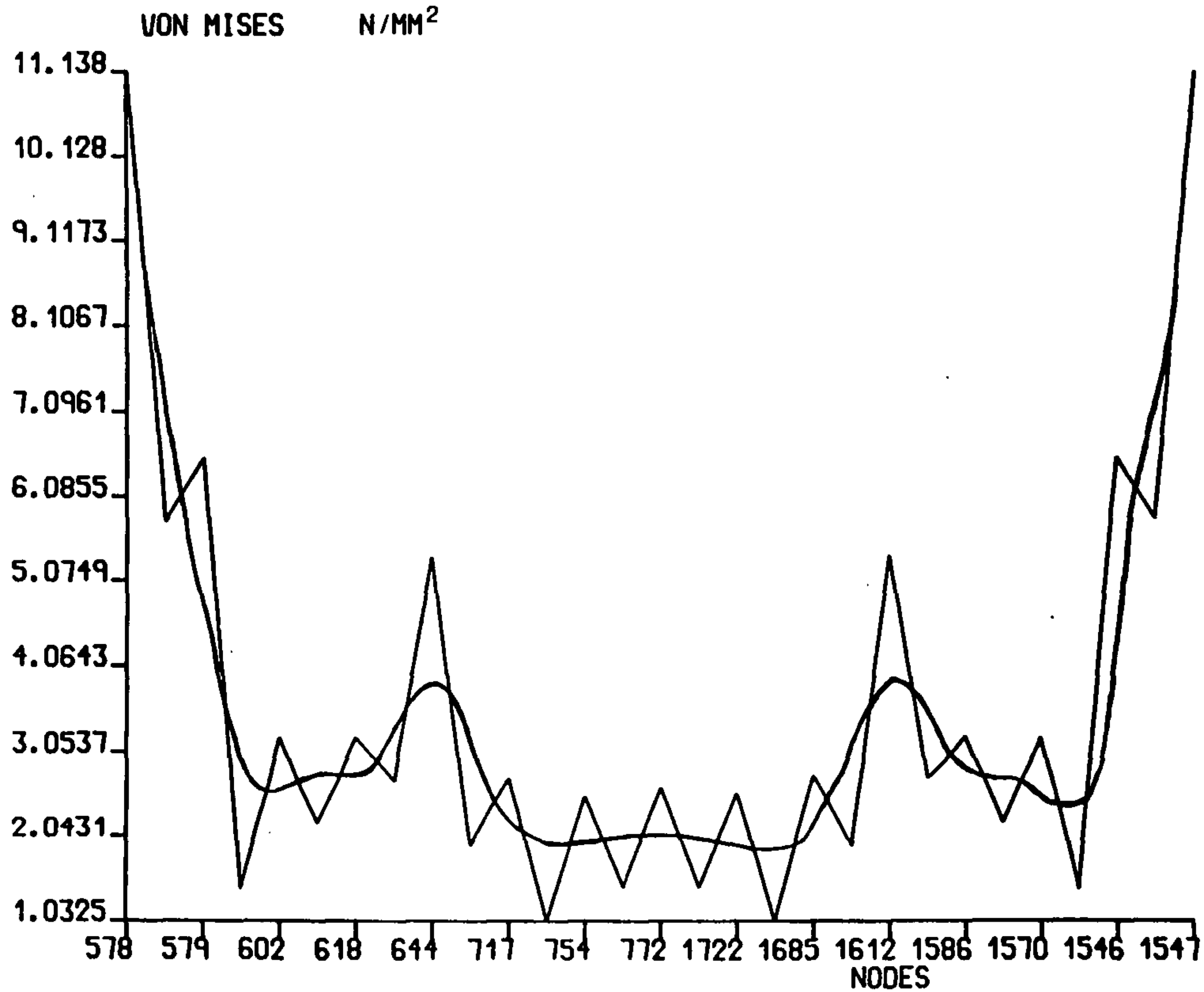

LOADCASE
1.0G VERTICAL
(DOWN)
1.1G LATER''

TITLE VON MISES STRESS ALONG THE LH UPPER BEAM

Figure 3.23

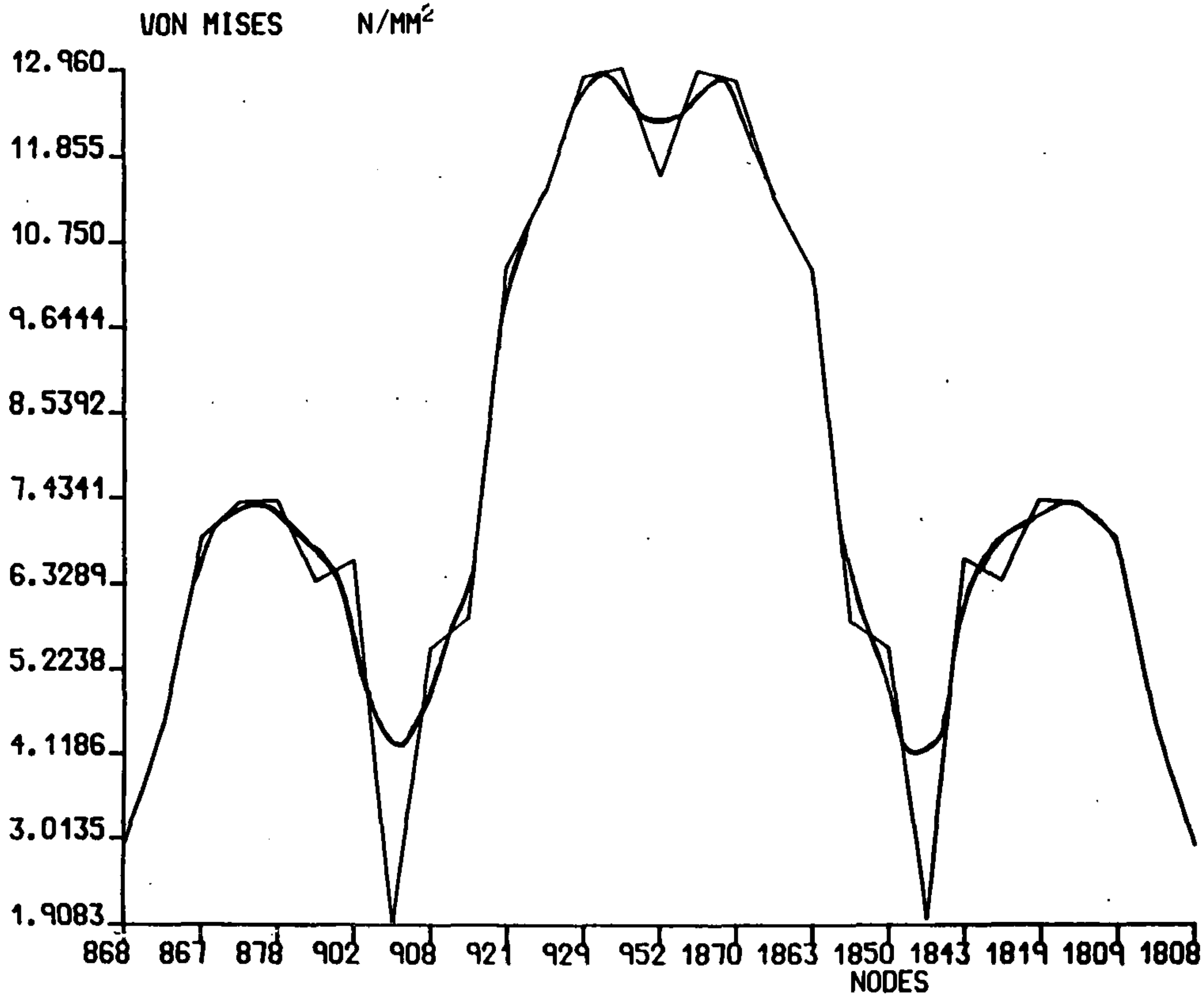

LOADCASE
1.0G VERTICAL
(DOWN)
1.1G LATERA'

TITLE VON MISES STRESS ALONG THE LH LOWER BEAM

Figure 3.24

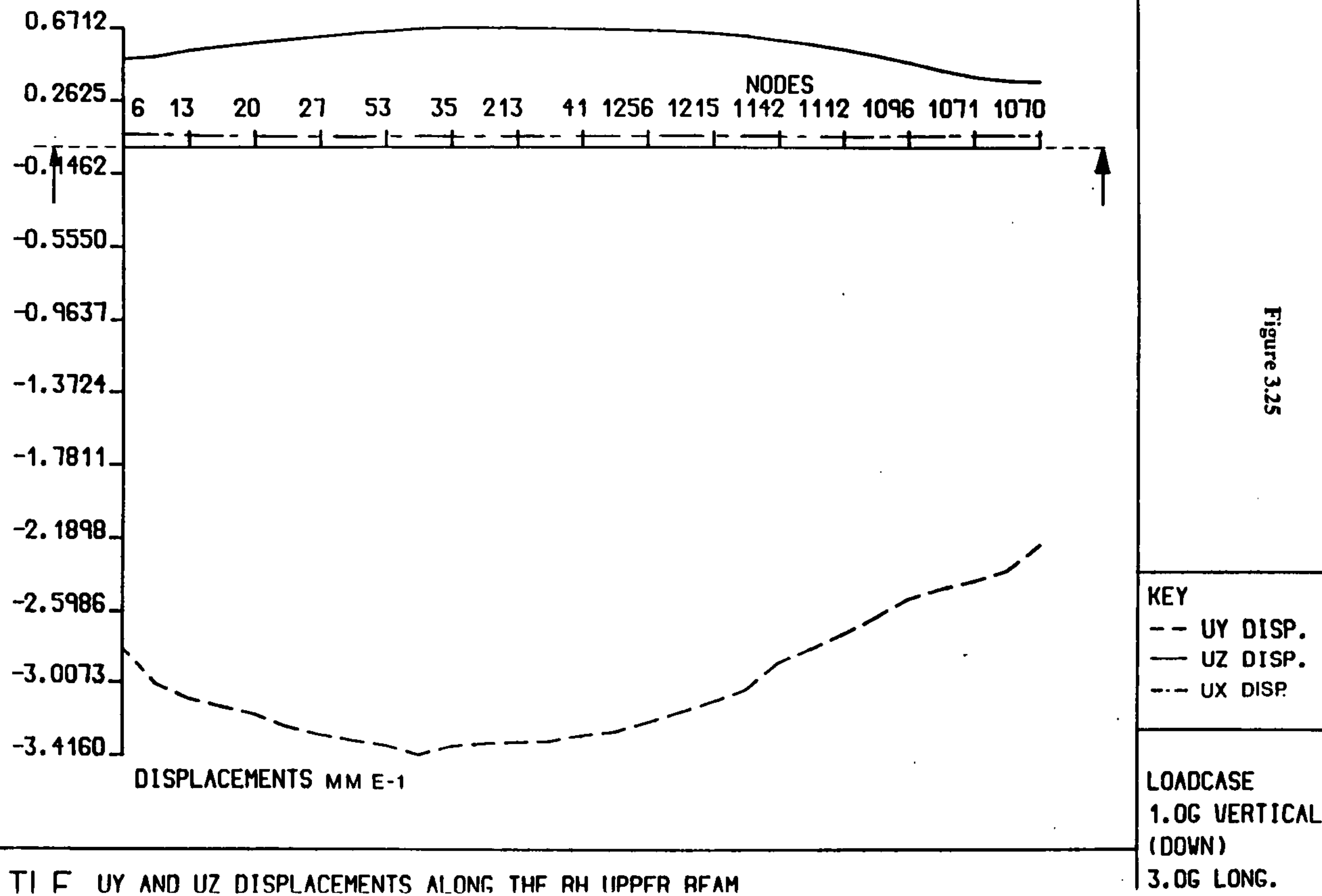

TITLE UY AND UZ DISPLACEMENTS ALONG THE RH UPPER BEAM

Figure 3.25

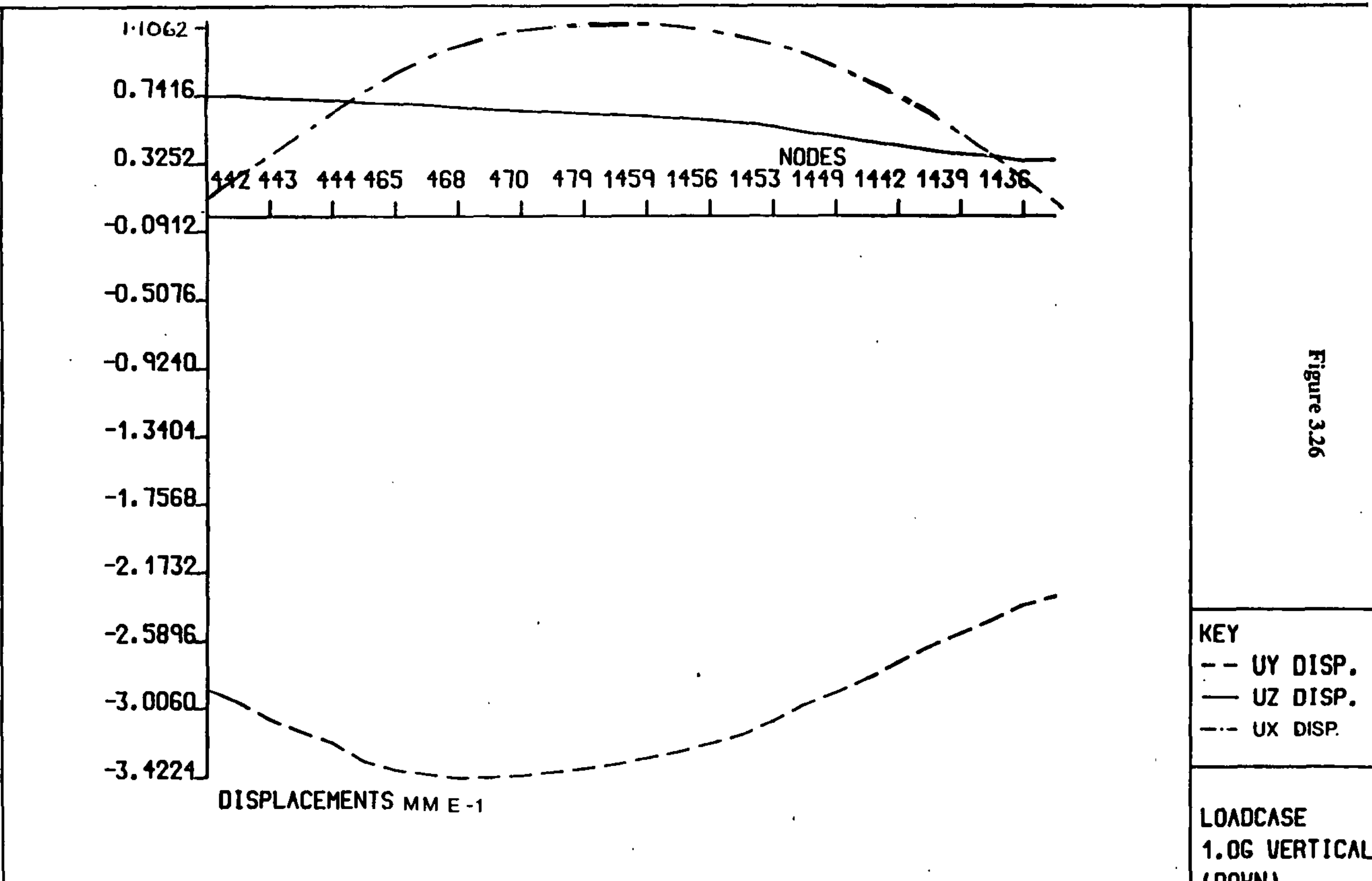

TITLE UY AND UZ DISPLACEMENTS ALONG THE RH CENTRAL WEB

Figure 3.26

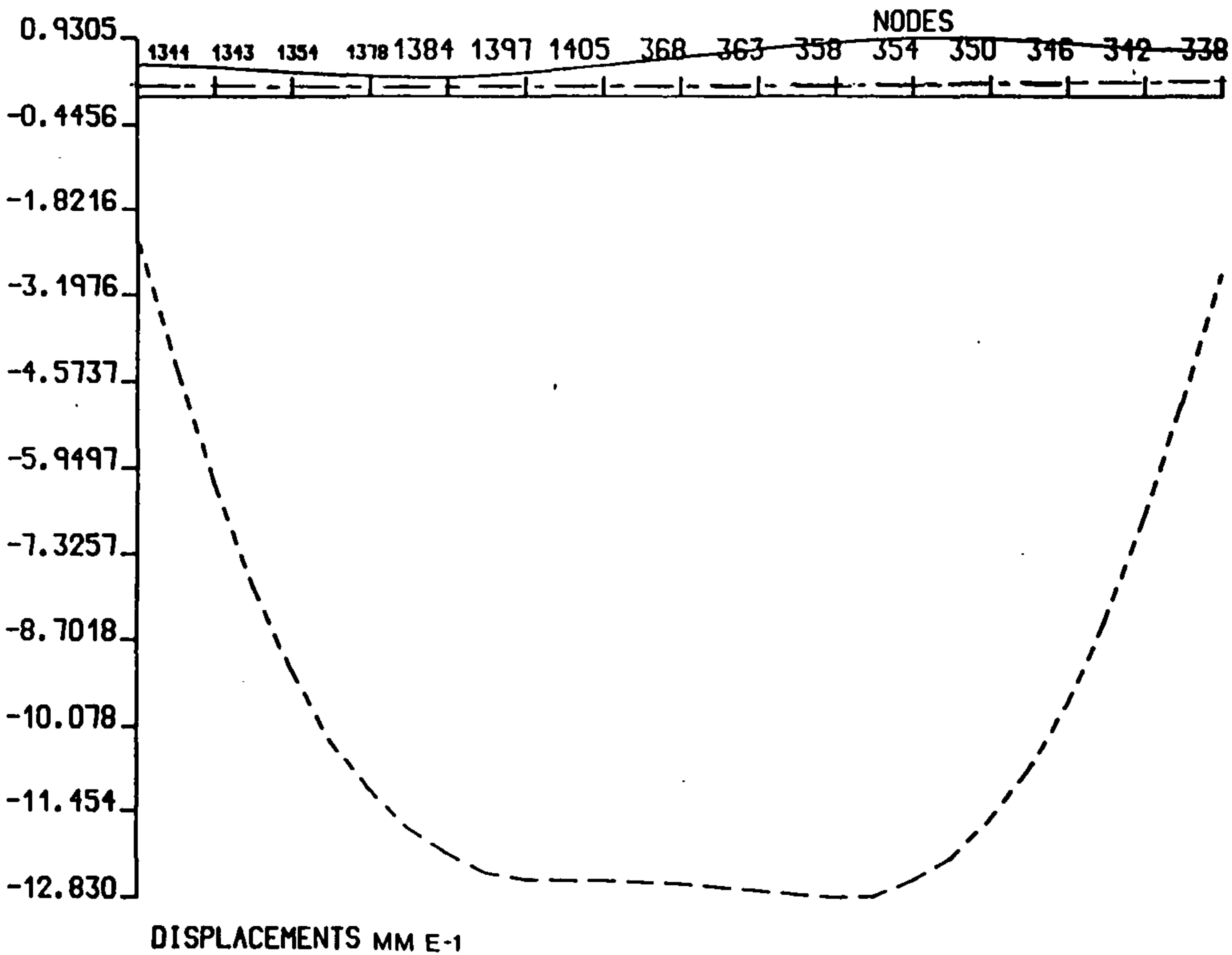

KEY
- - UY DISP.
— UZ DISP.
-·- UX DISP.

LOADCASE
1.0G VERTICAL
(DOWN)
3.0G LONG.

TITLE UY AND UZ DISPLACEMENTS ALONG THE RH LOWER BEAM

Figure 3.27

Figure 4.15 Generally Orthotropic Lamina in Tension, Test 3, Element 44215

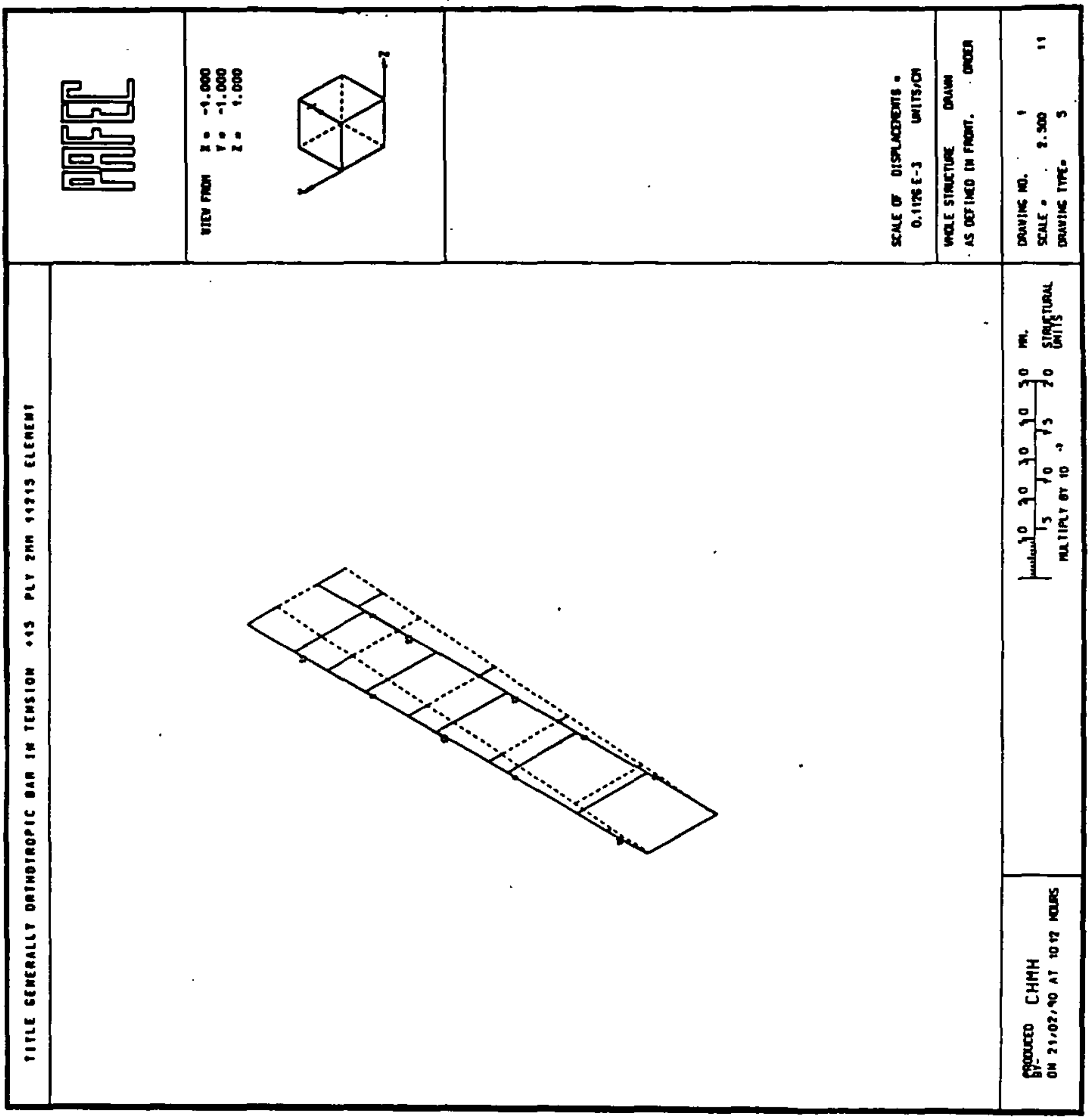

Figure 4.16 Generally Orthotropic Lamina in Tension, Test 3, Element 43215

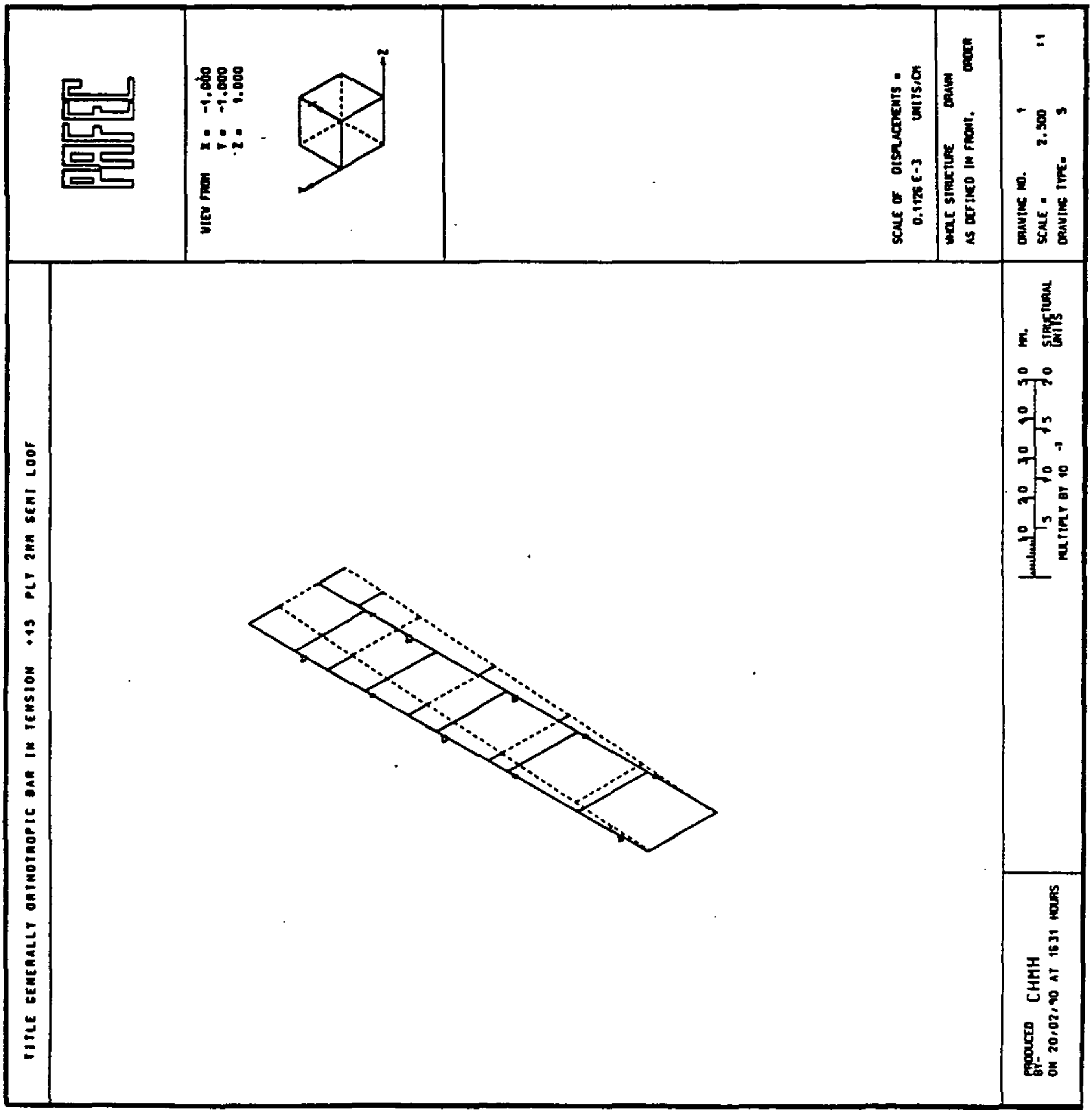

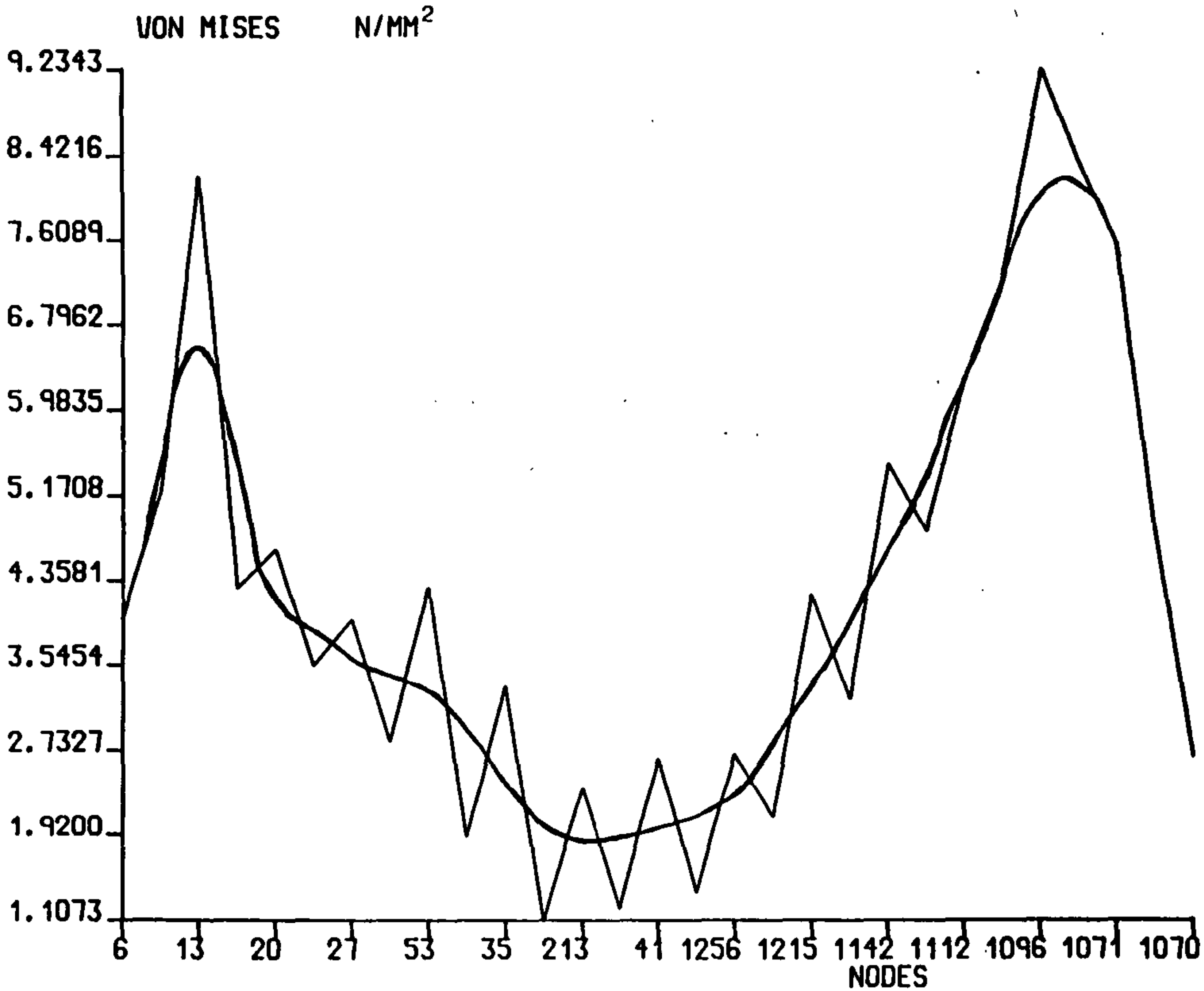

TITLE VON MISES STRESS ALONG THE RH UPPER BEAM

LOADCASE
1.0G VERTICAL
(DOWN)
3.0G LONG

Figure 3.28

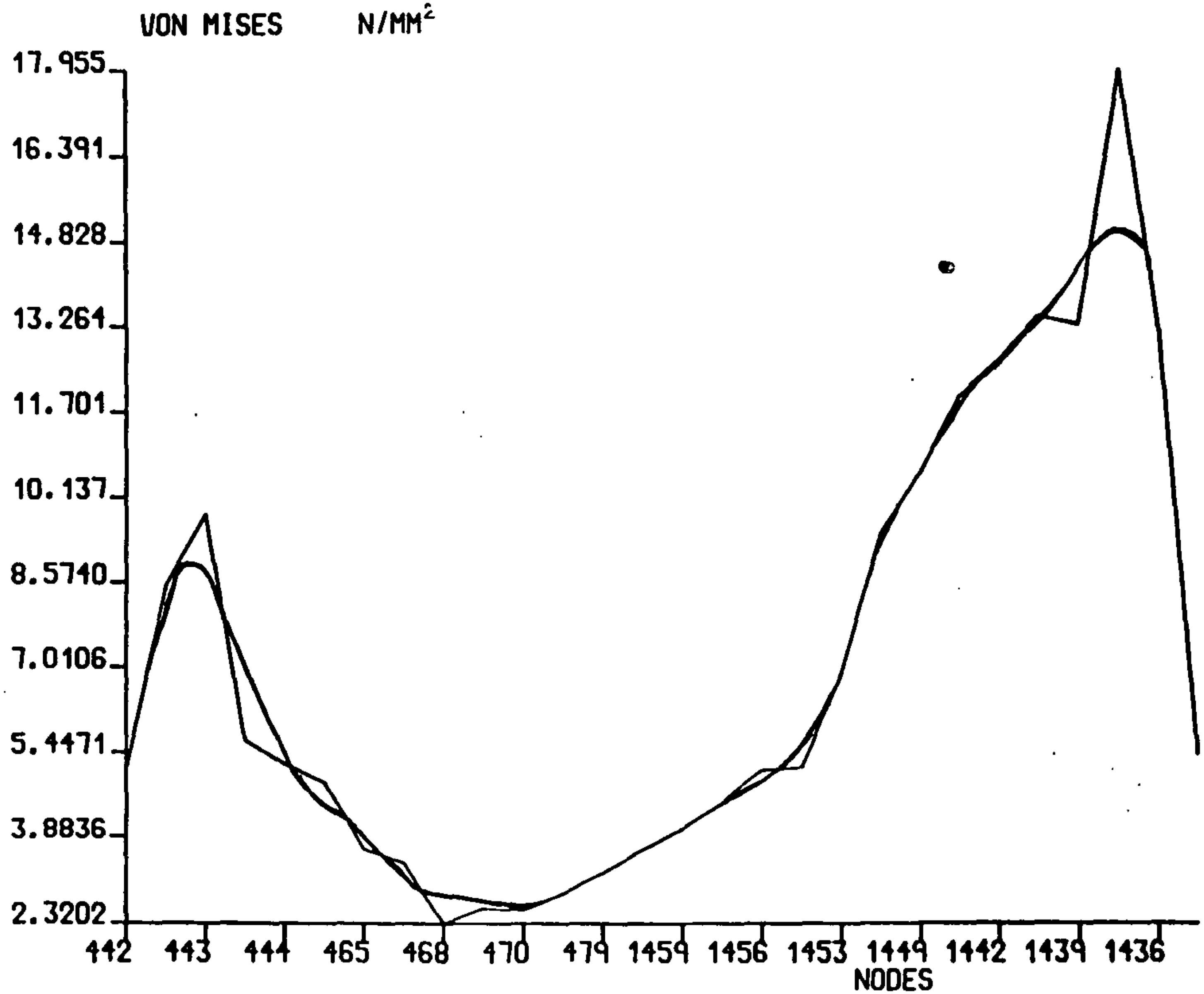

TITLE VON MISES STRESS ALONG THE RH CENTRAL WEB

LOADCASE
1.0G VERTIC
(DOWN)
3.0G LONC

Figure 3.29

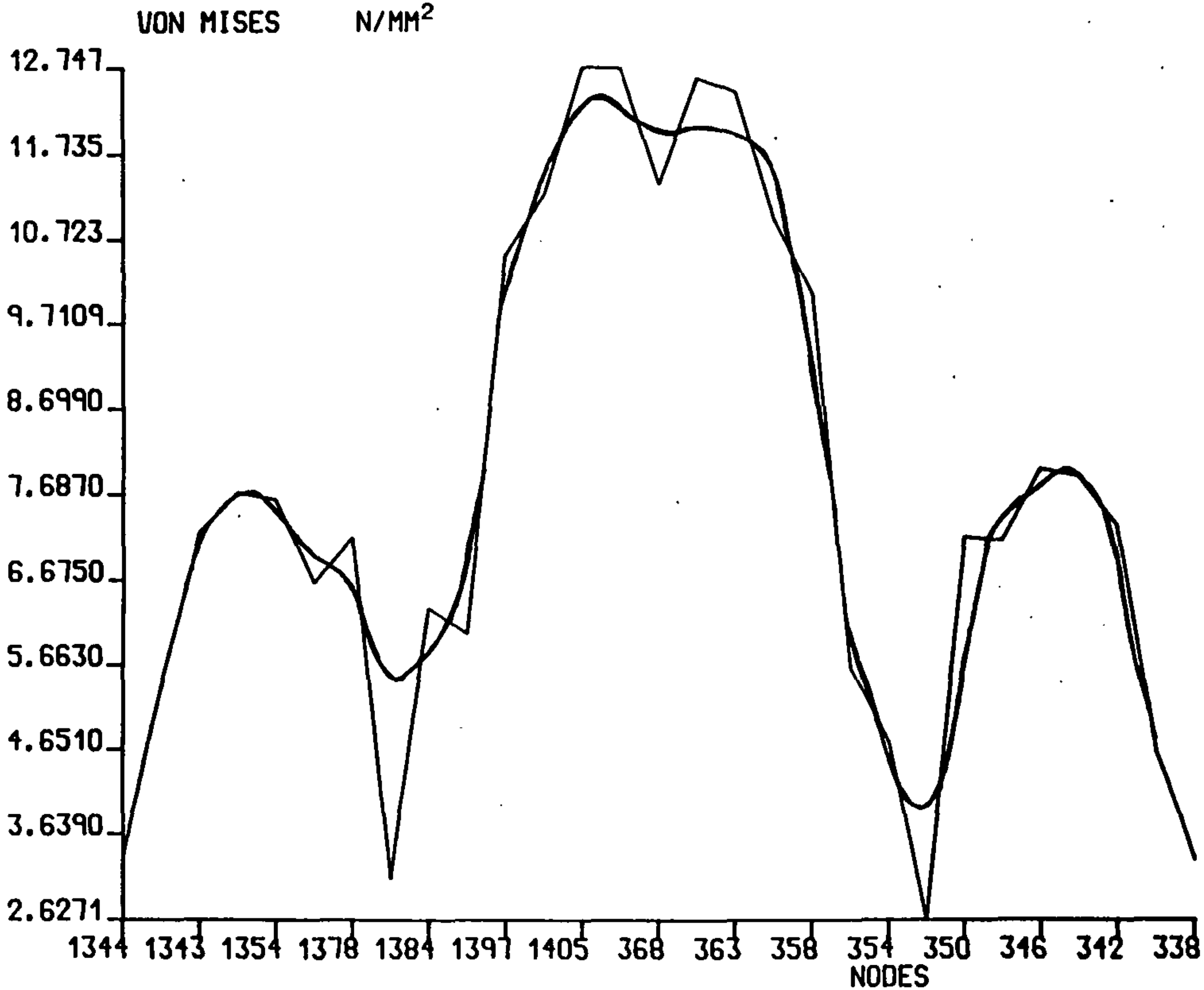

TITLE VON MISES STRESS ALONG THE RH LOWER BEAM

LOADCASE
I.0G VERTICAL
(DOWN)
3.0G LONG.

Figure 3.30

CHAPTER 4

Orthotropic Element Testing

4.1 Introduction

Single element testing has been the subject of several papers in the past, References 4 and 5, however little work has been performed in evaluation of orthotropic elements. Hence, in order to justify the use of Pafec Finite Element software in the analysis of a composite equipment case, the performance in terms of accuracy of displacements and stress analysis of three orthotropic elements was investigated, via a series of element tests.

The results of the tests were assessed using a proven laminate design analysis package, CoALA and 'first principle' calculations, where applicable. Finally the most appropriate element for the problem in hand was selected.

4.2 Orthotropic Element Selection

The composite equipment case will be in essence a thin plate structure , hence the elements tested were all thin plate elements capable of modelling orthotropic properties. Three element families were selected, with their second order quadrilateral element being used. The elements tested are described below, see Reference 1 for more detail.

i. The 36215 iso-parametric membrane element used only for in plane stress situations.

ii. The 44215 facet shell element used where both in-plane and out-of-plane effects are important.

iii. The 43215 semi-Loof curved shell element, again used where both in-plane and out-of-plane effects are important. The semi-Loof is a more sophisticated element than the 44215 and can be used in curved and folded shell problems, however it can be degenerated to a flat plate as in the following tests.

4.3 The Element Test Model

The evaluation of the Pafec orthotropic elements was carried out with a series of tests involving idealised loading and support conditions appropriate in the stress analysis of composite materials. As the composite case will be subjected to both bending and tension, each element was tested to see if it accurately modelled a variety of composite material properties in tension and, where applicable, in bending.

The model used for the element tests was a cantilever bar 50mm long and 10mm wide, idealised into five elements each with an aspect ratio of unity, see figure 4.1.

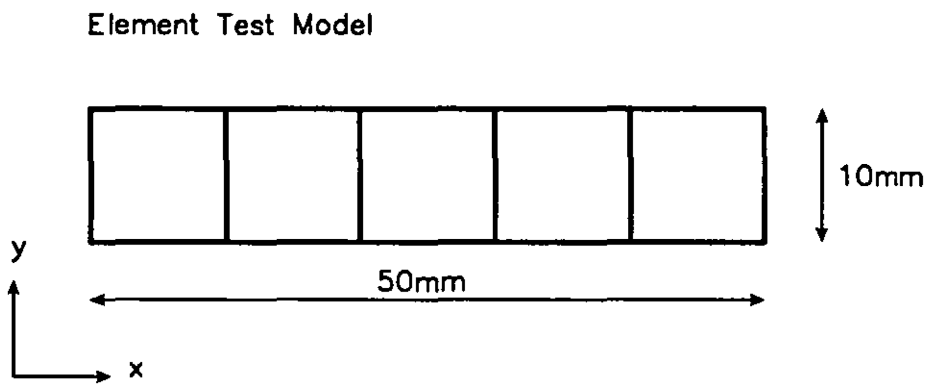

Figure 4.1

The bar was modelled in a unidirectional Carbon/Epoxy composite, using typical material constants for a fibre volume fraction of 60% as tabulated in figure 4.2.

Material constants for a Carbon /Epoxy composite ($V_f = 60\%$)

Material Constants	Value
Young's Modulus:–	
Longitudinal E_1	140.0 GN/m^2
Transverse E_2	10.0 GN/m^2
Shear Modulus	5.0 GN/m^2
Poisson's Ratio ν_{12}	0.3

Figure 4.2

Three common lay-ups were used in the tests as described below and illustrated in figure 4.3.

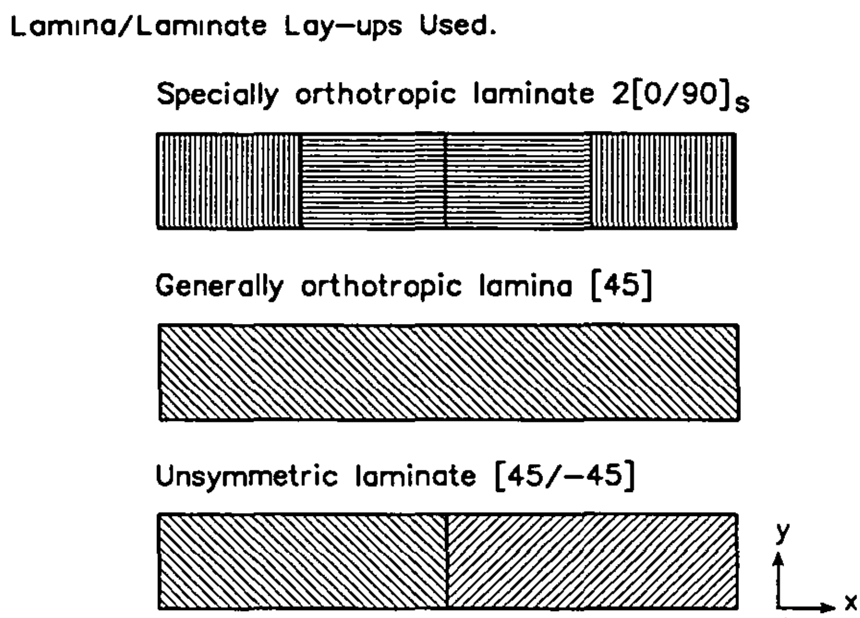

Figure 4.3

i. Symmetric laminate using specially orthotropic plies ie those with a fibre orientation of 0° and 90°. The laminate lay-up is $2[0/90]_s$.

ii. Generally orthotropic lamina, fibre orientation of 45°.

iii. Unsymmetric laminate, lay-up [45/-45].

The theoretical properties of these materials are described in section 4.5.

4.4 Element Tests

Each element type was tested with the three different lay-ups in tension, tests 1, 3 and 5. Bending tests were performed on the 44215 and 43215 elements with the symmetric laminate and lamina, properties, tests 2 and 4 respectively. The unsymmetric laminate was not tested in bending, as there was no satisfactory basis for comparison with a proven system. The test models were loaded and restrained as shown in figure 4.4. The loads applied conformed with the formulation for elements with mid side nodes.

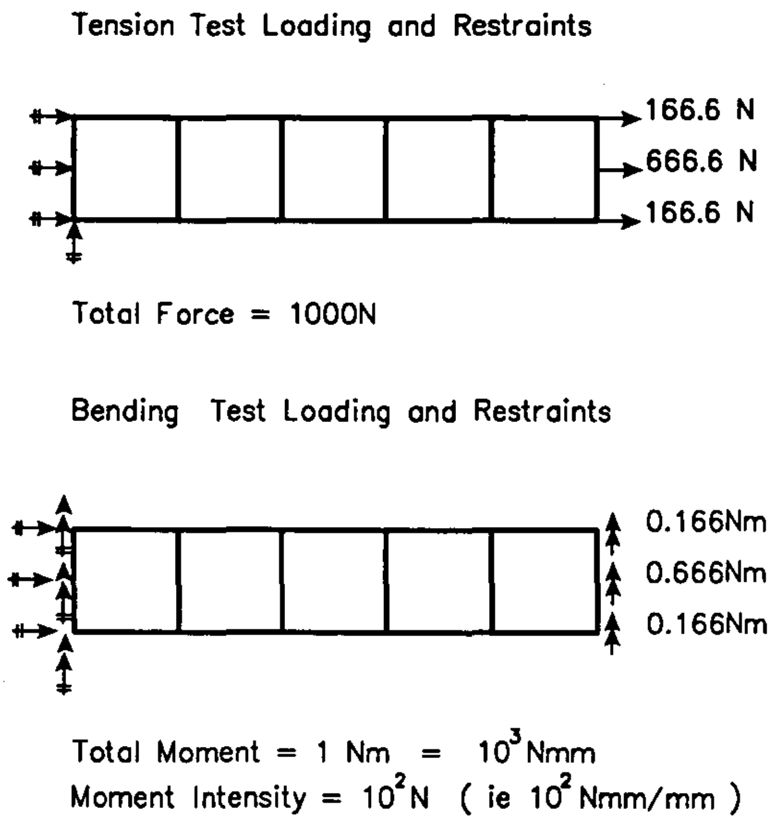

Figure 4.4

A summary of the tests performed can be seen in figure 4.5.

Tests Performed

No.	Elements	Lay-up	Test	Ply mm
1	36215 44215 43215	$2[0/90]_s$	Tension	1
2	44215 43215	$2[0/90]_s$	Bending	1
3	36215 44215 43215	[+45]	Tension	2
4	44215 43215	[+45]	Bending	2
5	36215 44215 43215	[+45/−45]	Tension	1

Figure 4.5

The laminate design analysis package , CoALA was used as a check on the resultant stresses and displacements obtained from the element tests, together with hand calculations in the simpler cases for further verification, detailed in Appendix C2 - C5. CoALA software is a commercially available package from Cranfield Institute of Technology and provides a detailed analysis of a lamina or laminate under a specific loadcase. It computes laminate stiffness, elastic and physical engineering constants, strain, strength and stress analyses on a ply to ply basis, see Reference 6 . Sample output from Pafec and CoALA for test 3 can be found in Appendix C1.

4.5 Theoretical Effects

Theoretical laminate analysis, detailed in Reference 7 predicts various effects from these test situations as described below:-

4.5.1 Test 1

Symmetric laminate in tension, theory predicts that there is 'in-plane orthotropy' ie no shear coupling effects, ie straight extension.

4.5.2 Test 2

Symmetric laminate in bending, similarly theory predicts 'bending orthotropy', ie no bend-twist coupling effect.

4.5.3 Test 3

Generally orthotropic lamina in tension, here the shear coupling terms are present in the stiffness matrix. Hence shear is predicted along with extensional effects.

4.5.4 Test 4

Generally orthotropic lamina in bending, the presence of fibres at orientations of other than 0 and 90 involve the bend-twist coupling terms in the bending matrix.

4.5.5 Test 5

Unsymmetric laminate in tension, theory predicts that membrane-bending coupling effects are introduced in the stiffness matrix. These terms mean that in-plane loads cause both in-plane and out-of-plane deformations and vice versa.

4.6 Results

The stress results from the element tests are tabulated in the tables 4.6 - 4.8. Table 4.6 details the results of the tension tests 1, 3 and 5. Table 4.7 details the results from test 2 and table 4.8 the results from test 4. Displacement results are tabulated in tables 4.9 - 4.10, table 4.9 detailing the results from the tension tests and table 4.10 the results from the bending tests. Pafec displacement plots can be seen, figures 4.11 - 4.23.

4.6.1 Tension Tests

4.6.1.1 Stress Results

The results from the tension tests 1, 3 and 5 can be seen in tables 4.6. The resulting output from the tests gave a variety of stress data, with both packages tested generating a ply by ply stress solution. The Pafec 36215 element details both in plane principal stresses and stresses along the material axes. The 44215 element provides stresses on the 'positive', 'neutral' and 'negative' surfaces in the material directions ie along and transverse to the fibre direction. The 43215 semi-Loof element provides 'upper' and 'lower' surface stresses again in the material directions. CoALA provides mid ply stresses only. The stresses tabulated from both packages are those at the mid ply in the principal material direction .

On examination of table 4.6 it can be seen that the three element types tested produced similar stress results in tests 1 and 3. There were slight discrepancies in the value of shear, however as the order of magnitude for this result is 10^{-7} Nmm^{-2}, they can be ignored. Comparison with the CoALA results show an accurate correlation in magnitude and direction for direct stress. The Pafec results for shear are of the same order of magnitude as the CoALA results, which being minimal can be approximated to zero, the theoretical value for shear in such a test. A hand calculation can be found in Appendix C2 which correlates exactly with both Pafec and CoALA providing further verification.

Comparison of the Pafec results for test 5, figure 4.6 the unsymmetric laminate in tension show that they correlate accurately in shear, however significant differences occur in the values of direct stress between the plane stress element, 36215 and the bending elements, 44215 and 43215. On comparison with the CoALA results for this test, it can be seen that direct stress values obtained by the bending elements are very accurate, typically with a 0.02% variation from the CoALA result. The plane stress element proved less accurate, in direct stress there was a maximum deviation of

26.3% from the CoALA results. The value of shear obtained from all elements compared exactly with the CoALA result, however directions were reversed in Pafec.

4.6.1.2 Displacement Results

The displacement plots, figures 4.11 - 4.19 display the various coupling effects predicted in section 4.5, for the tension tests. Each element exhibits straight extension when tested in tension with symmetric laminate properties, test 1, figures 4.11- 4.13 verifying that no shear coupling took place. This was due to there being only specially orthotropic plies present in the laminate. The test 3 displacement plots figures 4.14 - 4.16 shows the effect of shear coupling terms in the stiffness matrix by the presence of both shear and extensional displacements. The displacement plots for test 5 for elements 44215 and 43215, figures 4.18 and 4.19 show the effect of both extension and curvature for the unsymmetric laminate case, predicted by the presence of membrane-twist terms in the stiffness matrix. The plot for the 36215 element, figure 4.17 in this case does not give a fair representation of the effects, due to it not being able to achieve the out-of-plane effects.

Comparison of actual displacement results between elements can be seen in table 4.9, with displacements at the three nodes along the loaded end of the cantilever being tabulated. Theoretical calculations for test 1, using both CoALA derived constants and composite analogies can be found in Appendix C3 to verify the Pafec data. It can be seen that the results obtained for the three elements correlate exactly in tests 1 and 3 and with the theoretical values. Test 5, the unsymmetric laminate showed that there was accurate correlation between the two bending elements for in plane displacements, with out of plane displacements showing some deviation. The displacements here for the in plane element along the bar were found to be 87% of the equivalent value recorded for the out of plane elements with transverse displacements being 19% greater than those derived by the bending elements. Obviously, the in plane element produced no out of plane displacements.

4.6.2 Bending Tests

4.6.2.1 Stress Results

The results from the bending tests 2 and 4 can be seen in tables 4.7 and 4.8 respectively. As in the tension tests the stresses tabulated from both packages are at the mid ply in the principal material direction (ie along and transverse to the fibre direction).

Comparisons were made between the neutral surface stresses obtained at the centroid of the mid bar element for the Pafec test model, element 3, these being the equivalent stresses to those obtained at the centroid of the CoALA single element. On comparison of the results for the symmetric laminate in bending, test 2, between the Pafec 44215 element and CoALA it can be seen that the Pafec results are greater for direct stress. Direct stress in the fibre direction in the outer plies were 78% greater and for the inner plies was 2.5 times greater. Direct stress perpendicular to the material direction was 1.5 times greater in the outer plies and 82% greater in the inner plies. Shear values obtained for the 44215 element were of an order of magnitude smaller than those derived by CoALA. On considering stress directions, the directions obtained by the 44215 element for shear correspond with CoALA, however direct stress directions are opposite throughout the depth of the laminate.

The Pafec 43215 element performs more consistently in test 2 to the 44215 element. Comparing mid ply stresses, interpolated across the depth of the ply with the CoALA mid ply stresses it can be seen that the values obtained for direct stress are greater than the CoALA results. Direct stress values in the outer plies along the material direction were found to be 33% greater, with inner ply stresses being 28% greater. Direct stresses transverse to the material direction were consistently greater, by 33% in both inner and outer plies. The results for shear were similar to the 44215 element, with the shear values obtained being of an order of magnitude smaller than the CoALA derived results. Stress directions obtained by the 43215 element were the same as those from the 44215 element, ie they corresponded with CoALA in shear and were opposite in direct stress.

The results for the generally orthotropic lamina bending test, test 4 are shown in figure 4.8. Here, the CoALA results are taken to a variation to test 4. This variation involved using two 45 plies to idealise a single lamina of 45. This was necessary due to CoALA only calculating centroidal stresses, which meant on analysis of a single lamina, CoALA correctly predicts zero stress and hence provides no basis for comparison with the Pafec results.

The uni-directional lamina test predicted stresses at the centroid of each lamina which by extrapolation through the depth of the lamina gives the results detailed in table 4.8. The results from the 44215 element shows that the positive and negative surface stresses are greater than CoALA, 2.6 times in the fibre direction, 1.9 times transverse to the fibre and 1.9 times greater in shear. The neutral surface stresses tend to zero in Pafec and are exactly zero in CoALA, which corresponds to bending theory. The results from the 43215 element in this case show that the stress results are of the same order of magnitude as CoALA, being in general about 66% of the equivalent CoALA result. Extrapolating over the depth of the ply shows that mid ply stresses are zero, which again corresponds with CoALA and bending theory. Both elements predict the same stress directions as CoALA. The results of a first principles calculation can be seen in Appendix C4, which verifies that the direct and shear results generated by CoALA are correct.

4.6.2.2 Displacement Results

The displacement plots for these tests can be seen in figures 4.20 - 4.23 feature the various coupling effects predicted in section 4.5. The plots for the symmetric laminate in bending show that both elements types exhibit pure bending with no bend-twist effects, figures 4.20 and 4.21. The generally orthotropic lamina in bending does feature these effects, as exhibited by both element types in figures 4.22 - 4.23.

On comparison of the actual values obtained for displacements, tables 4.9 and 4.10, it can be seen that the 44215 element produces greater displacements. It should be noted that in order to obtain realistic values for displacements the applied test moment was reduced from 10^7 Nmm to 10^4 Nmm. Theoretical values derived for the symmetric laminate in bending, see Appendix C5, show that the 44215 elements are more accurate than the 43215 results, being 13.2% too large and the 43215 results being 29.7% too small. The generally orthotropic lamina in bending showed again that the 44215 element produced larger displacements than the 43215 element, in both cases displacements were not constant across the width of the bar, due to the presence of the bend twist coupling effect.

4.7 Discussion

The justification of using CoALA to verify the Pafec results obtained in the element tests was assured by a series of 'first principles' calculations, which can be found in Appendices C2 - C5. To summarise the results from the tests, it can be said that the use of the Pafec orthotropic mid side noded quadrilateral elements, 36215, 44215, 43215 for the analysis of plane stress situations using single laminae or symmetric laminates is justified in terms of both displacement and stress analysis.

Bending applications, involving the 44215 and 43215 elements showed that for the symmetric laminate application direct stress results were higher than the CoALA generated results. The semi-Loof element produced stresses which were 33.3% greater through the depth of the laminate. The 44215 element again produced higher stresses which although were not a consistant amount greater through the depth of the laminate can be assumed to be twice the equivalent CoALA result. Lamina stresses obtained again were greater for the 44215 element by a factor of 2 and less for the semi-Loof, 66% of the CoALA values. Displacements values obtained in both the symmetric laminate and lamina test showed that the 44215 element produced a more accurate value than the semi-Loof element.

The results for the symmetric laminate tension test establish that the direct stresses are significantly different between the plane stress element and CoALA, although the shear stresses correlated. The stresses generated by the bending elements corresponded accurately with CoALA.

The actual application of Finite Element Analysis in this research involves a composite case subjected to tension and local bending, using generally and specially orthotropic laminae. The above results demonstrate that the element to use is the 44215 plate bending element, providing accurate results for stress and displacement in tension which covers the majority of the structure and reasonable results for displacement in bending, with stress results here providing a safety factor of more than 2 for lamina applications.

4.8 Conclusions

It can be concluded that the most appropriate element to use for the analysis of the composite structure in terms of accuracy of stress analysis and displacements for the ares under plane stress is the 44215, facet shell element. Where, local bending is important the 44215 will give conservative stress results.

The poor stress results for the laminated elements under bending is a cause for concern for the vendors and users of Pafec and these conclusions have been transmitted to that company.

Fig 4.6 Stress Results for Tension Tests 1, 3 and 5

Mid Ply Stresses				
Test No.	Ply	σ_1	σ_2	τ_{12}
Pafec Element 36215				
1	0	46.700	0.867	0.397E−7
	90	−0.867	3.299	0.169E−6
	90	−0.867	3.299	0.169E−6
	0	46.700	0.867	0.397E−7
3	45	25.000	25.000	−25.000
5	45	45.83	4.166	25.000
	−45	45.83	4.166	−25.000
Pafec Element 44215				
1	0	46.700	0.867	0.140E−6
	90	−0.867	3.300	1.200E−6
	90	−0.867	3.300	1.200E−6
	0	46.700	0.867	0.140E−6
3	45	25.000	25.000	−25.000
5	45	36.850	13.030	25.000
	−45	36.850	13.030	25.000
Pafec Element 43215				
1	0	46.700	0.867	0.350E−7
	90	−0.867	3.300	0.350E−7
	90	−0.867	3.300	0.350E−7
	0	46.700	0.867	0.350E−7
3	45	25.000	25.000	−25.000
5	45	36.850	13.030	25.000
	−45	36.850	13.030	−25.000
CoALA Results				
1	0	46.701	0.868	0.157E−7
	90	−0.868	3.298	0.166E−6
	90	−0.868	3.298	0.166E−6
	0	46.701	0.868	−0.157E−7
3	45	25.000	25.000	−25.000
5	45	36.952	13.048	25.000
	−45	36.952	13.048	−25.000

All Stresses in Nmm^{-2}

Fig 4.7 Stress Results for the Symmetric Laminate In Bending, Test 2

Mid Ply Stresses				
Element	Ply	σ_1	σ_2	τ_{12}
Pafec Element 44215				
1	0	-0.531E2	-0.183E1	-0.103E2
	90	0.364E1	-0.133E1	0.345E1
	90	-0.364E1	0.133E1	-0.345E1
	0	0.531E2	0.183E1	0.103E2
2	0	-0.554E2	-0.515	-0.148E1
	90	0.758E1	-0.116E1	0.495
	90	-0.758E1	0.116E1	-0.495
	0	0.554E2	0.515	0.148E1
3	0	-0.567E2	-0.105E1	-0.151
	90	0.340	-0.134E1	0.504E-1
	90	-0.340	0.134E1	-0.504E-1
	0	0.567E2	0.105E1	0.151
4	0	-0.566E2	-0.905	-0.105E-1
	90	0.103E1	-0.132E1	0.350E-2
	90	-0.103E1	0.132E1	-0.350E-2
	0	0.566E2	0.905	0.105E-1
5	0	-0.565E2	-0.984	0.826E-3
	90	0.649	-0.132E1	-0.276E-3
	90	-0.649	0.132E1	0.276E-3
	0	0.565E2	0.984	-0.826E-3
Pafec Element 43215				
1	0	-0.423E2	-0.665	-0.670E-2
	90	0.825	-0.985	0.224E-2
	90	-0.825	0.985	-0.224E-2
	0	0.423E2	0.665	0.670E-2
2	0	-0.425E2	-0.572	-0.593E-1
	90	0.127E1	-0.980	0.197E-1
	90	-0.127E1	0.980	-0.197E-1
	0	0.425E2	0.572	0.593E-1
3	0	-0.424E2	-0.564	-0.316
	90	0.131E1	-0.980	0.645E-1
	90	-0.131E1	0.980	-0.645E-1
	0	0.424E2	0.564	0.316
4	0	-0.424E2	-0.561	-0.923
	90	0.131E1	-0.980	0.307
	90	-0.131E1	0.980	0.307
	0	0.424E2	0.564	0.923
5	0	-0.424E2	-0.564	-0.440E1
	90	0.132E1	-0.980	0.146E1
	90	-0.132E1	0.980	-0.146E1
	0	0.424E2	0.564	0.440E1
CoALA Results				
	0	0.318E2	0.426	-0.144E1
	90	-0.987	0.734	0.416E1
	90	0.987	-0.734	-0.416E1
	0	-0.318E2	-0.426	0.144E1

All stresses in Nmm^{-2}

Fig 4.10 Displacements Results for the Bending Tests 2 and 4

Test 2 – Symmetric Laminate in Bending									
Element Type	Node (i)			Node (ii)			Node (iii)		
	ux	uy	uz	ux	uy	uz	ux	uy	uz
44215	0	0	−1.17	0	0	−1.35	0	0	−1.26
43215	0	0	−2.02	0	0	−2.02	0	0	−2.02
CoALA	0	0	−1.89	0	0	−1.89	0	0	−1.89
Test 4 – Generally Orthotropic Lamina in Bending									
Element Type	Node (i)			Node (ii)			Node (iii)		
	ux	uy	uz	ux	uy	uz	ux	uy	uz
44215	0	0	−0.94	0	0	−0.89	0	0	−0.84
43215	0	0	−1.39	0	0	−1.31	0	0	−1.22

Results shown for an applied moment of 10^4 Nmm
All displacements in mm
ux displacements are along the bar
uy displacements are perpendicular to the length of the bar
uz out of plane displacements

Figure 4.11 Symmetric Laminate in Tension, Test 1, 36215 Element

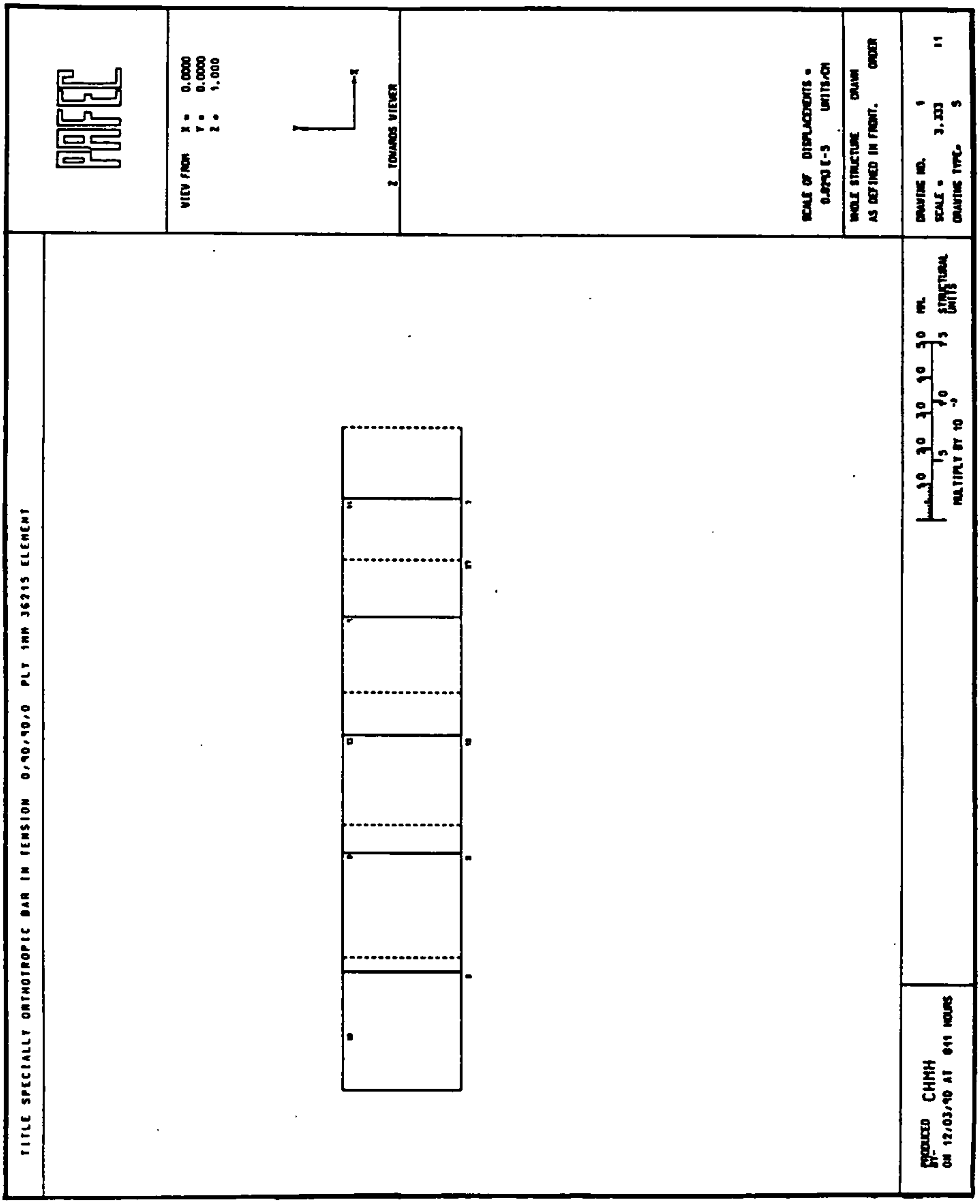

Figure 4.12   Symmetric Laminate in Tension, Test 1, 44215 Element

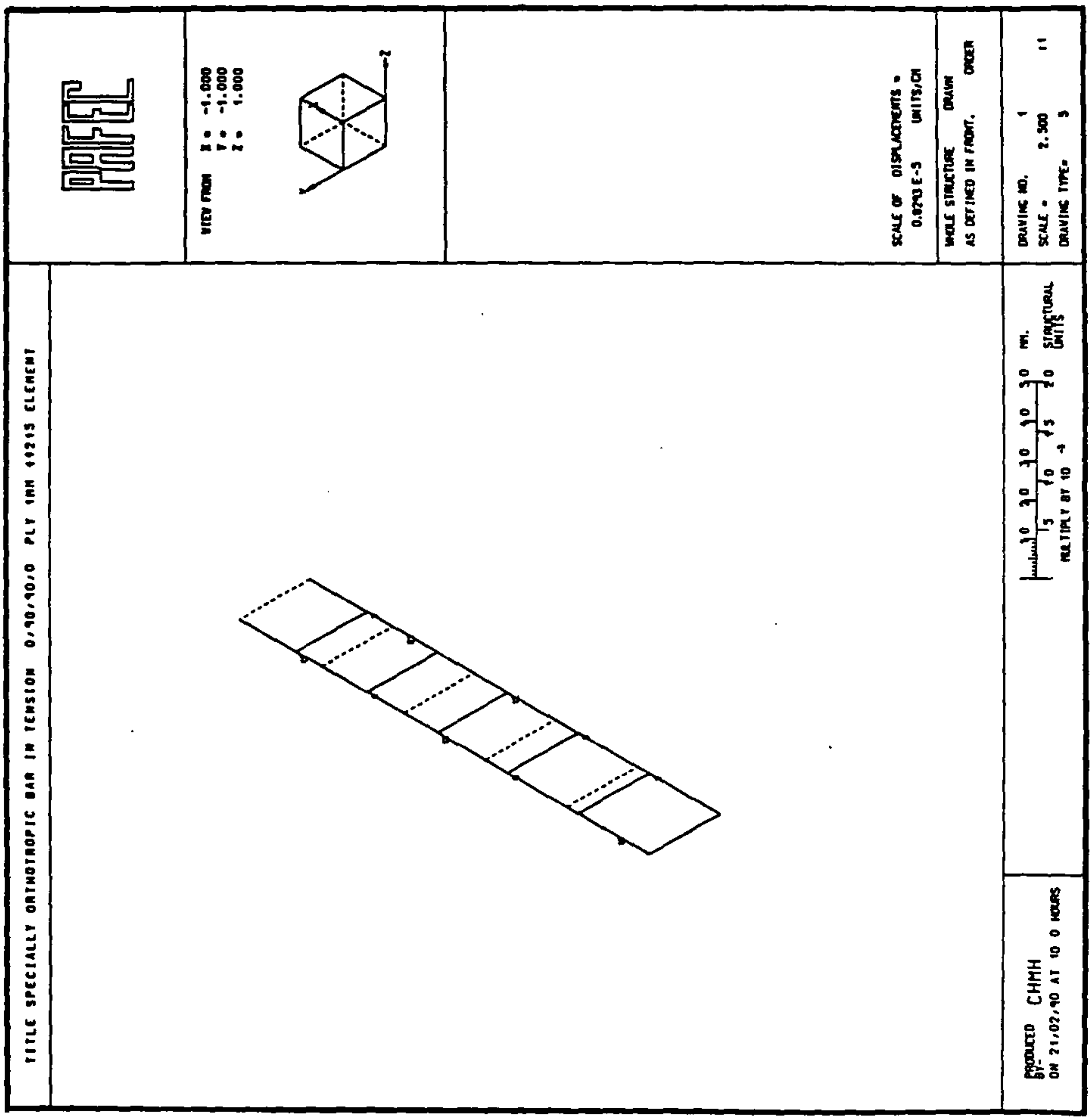

Figure 4.13 Symmetric Laminate in Tension, Test 1, Element 43215

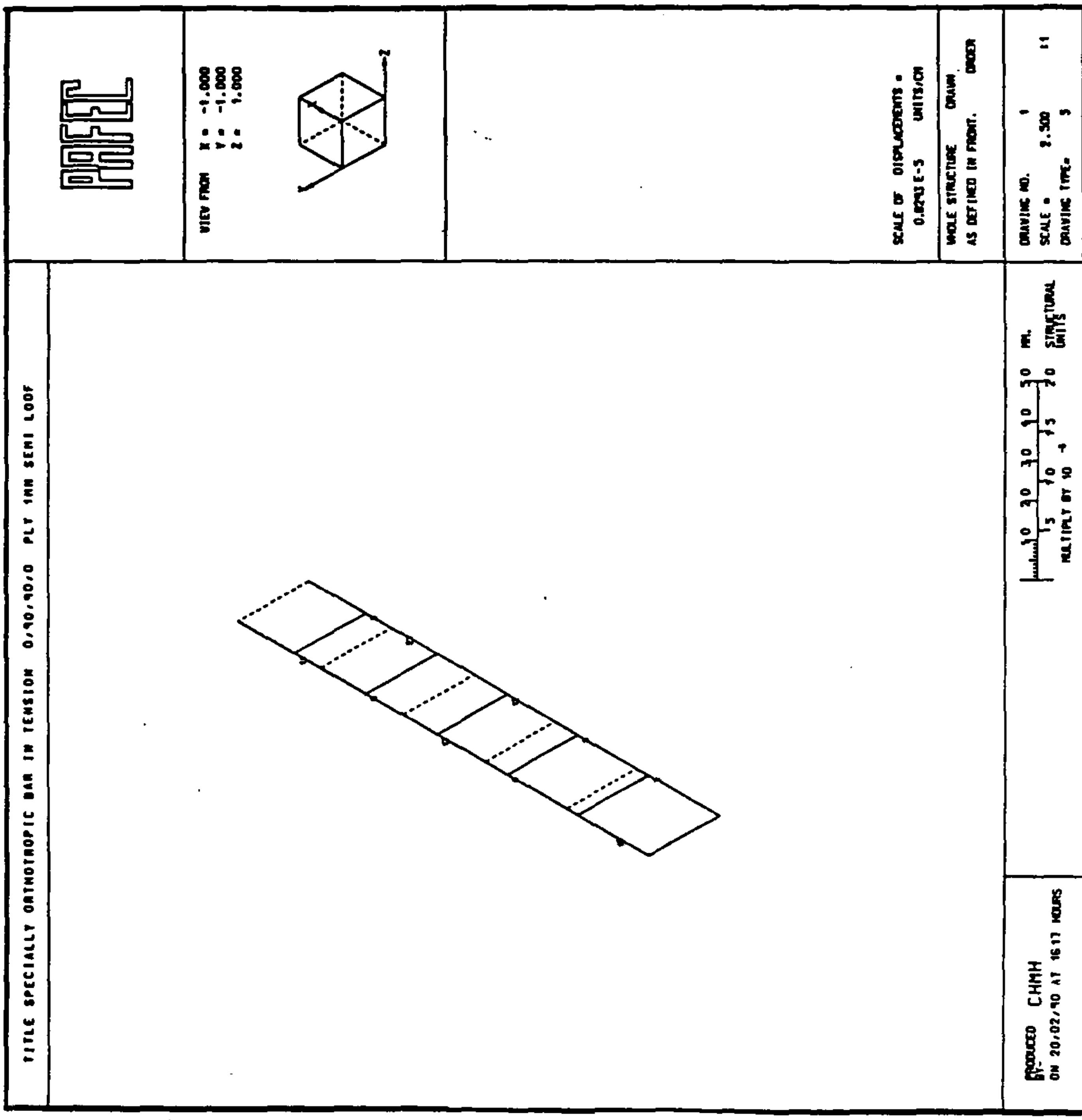

Figure 4.14   Generally Orthotropic Lamina in Tension, Test 3, Element 36215

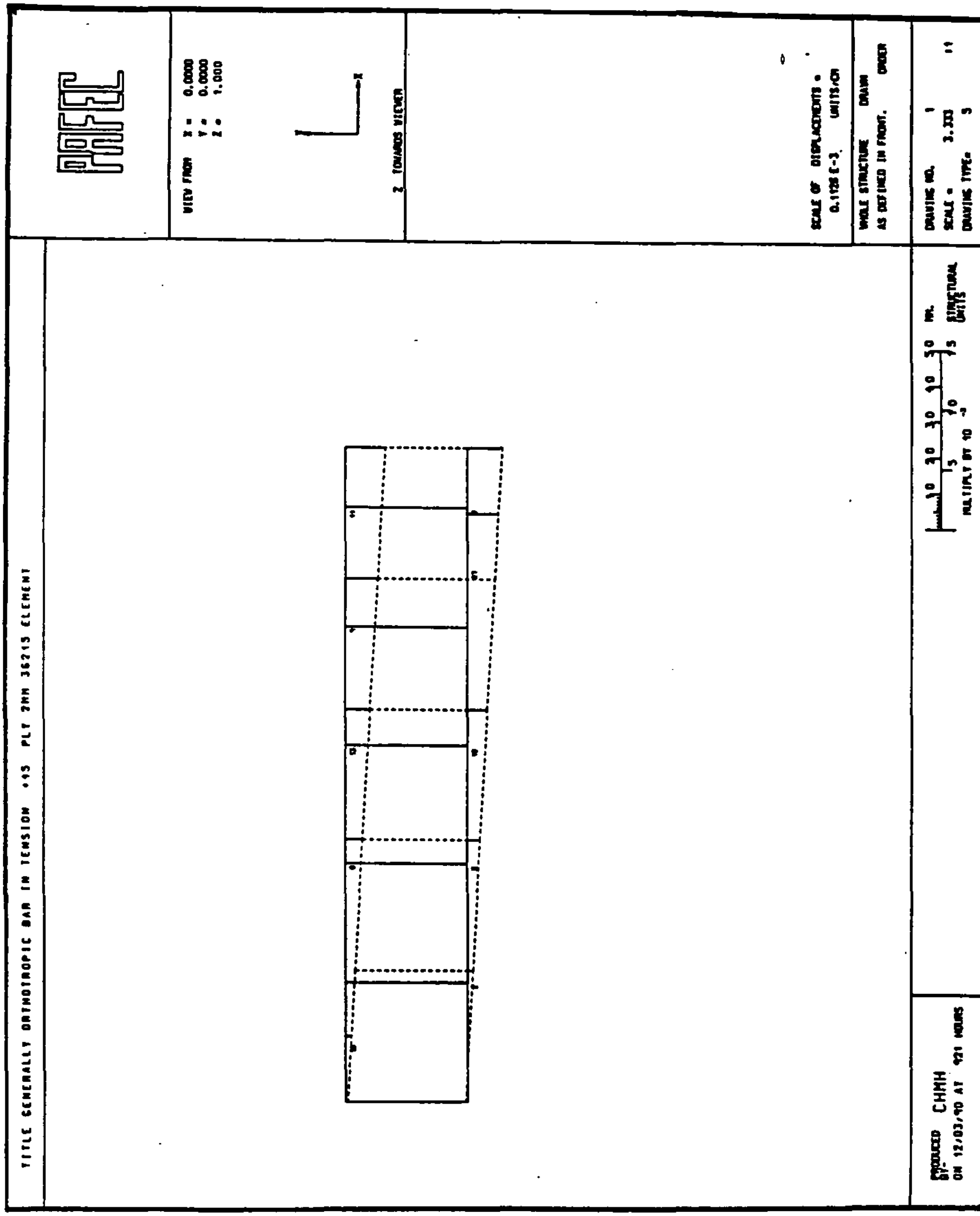

Figure 4.15 Generally Orthotropic Lamina in Tension, Test 3, Element 44215

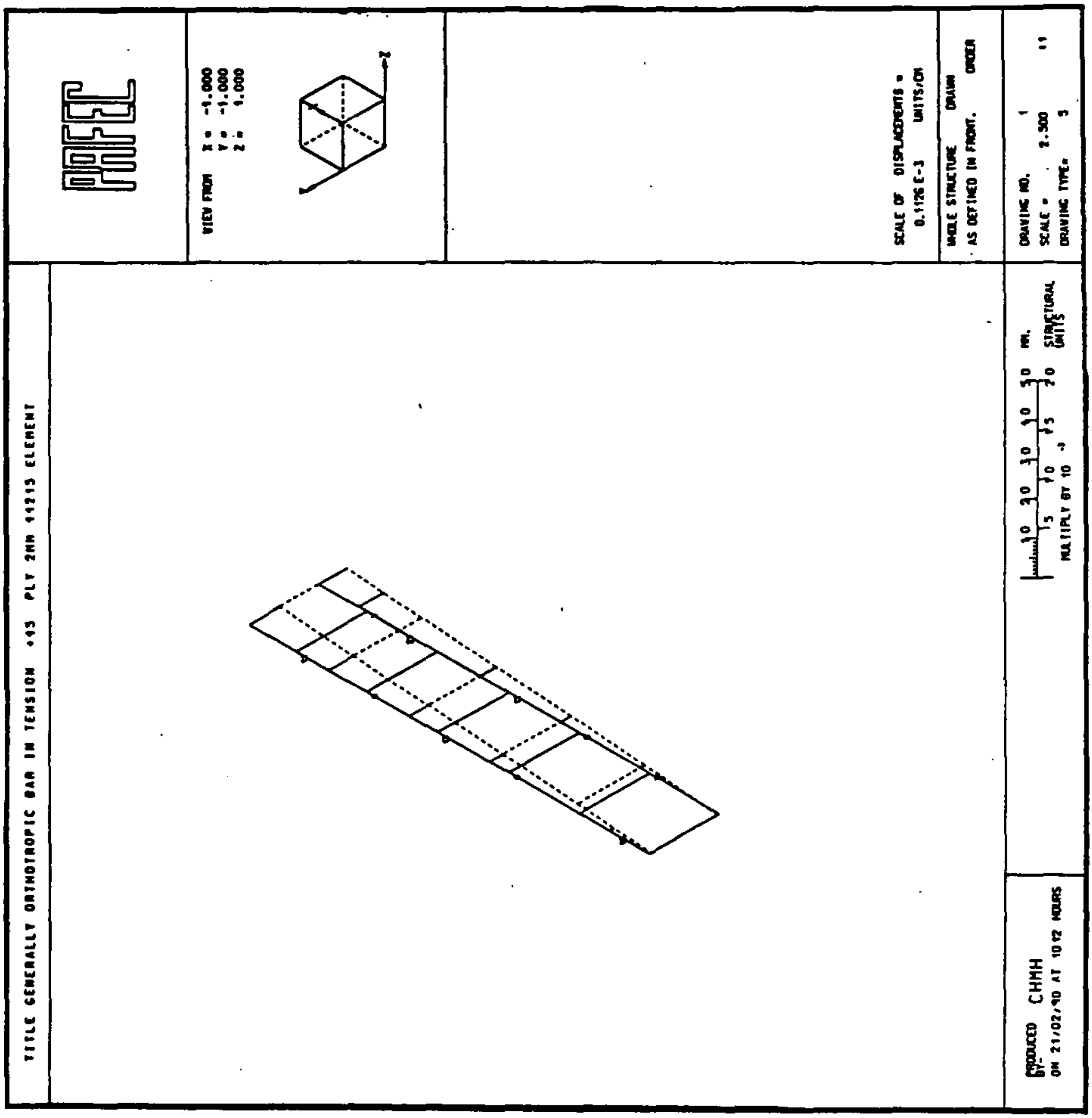

Figure 4.16 Generally Orthotropic Lamina in Tension, Test 3, Element 43215

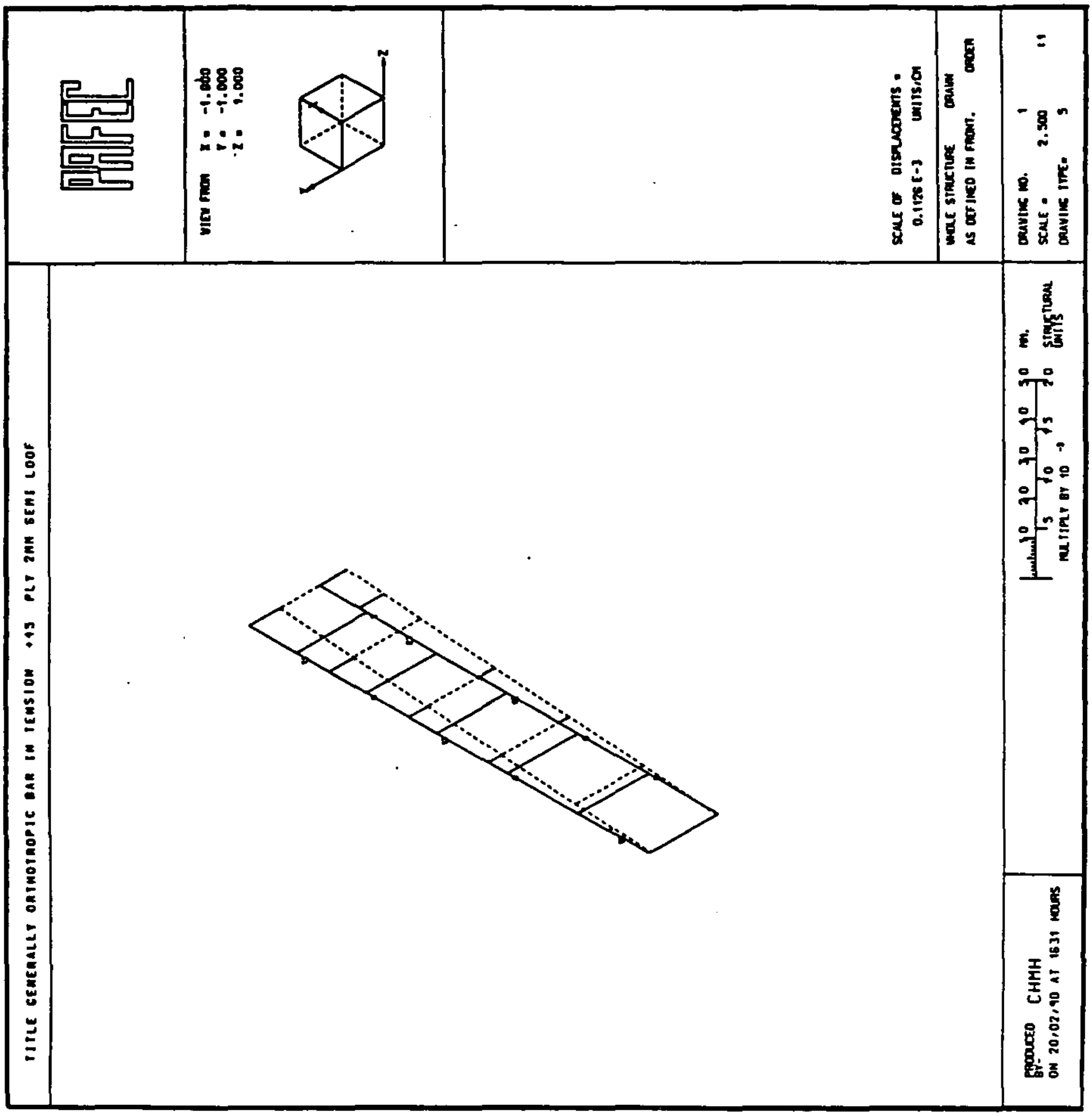

Figure 4.17 Unsymmetric Laminate in Tension, Test 5, Element 36215

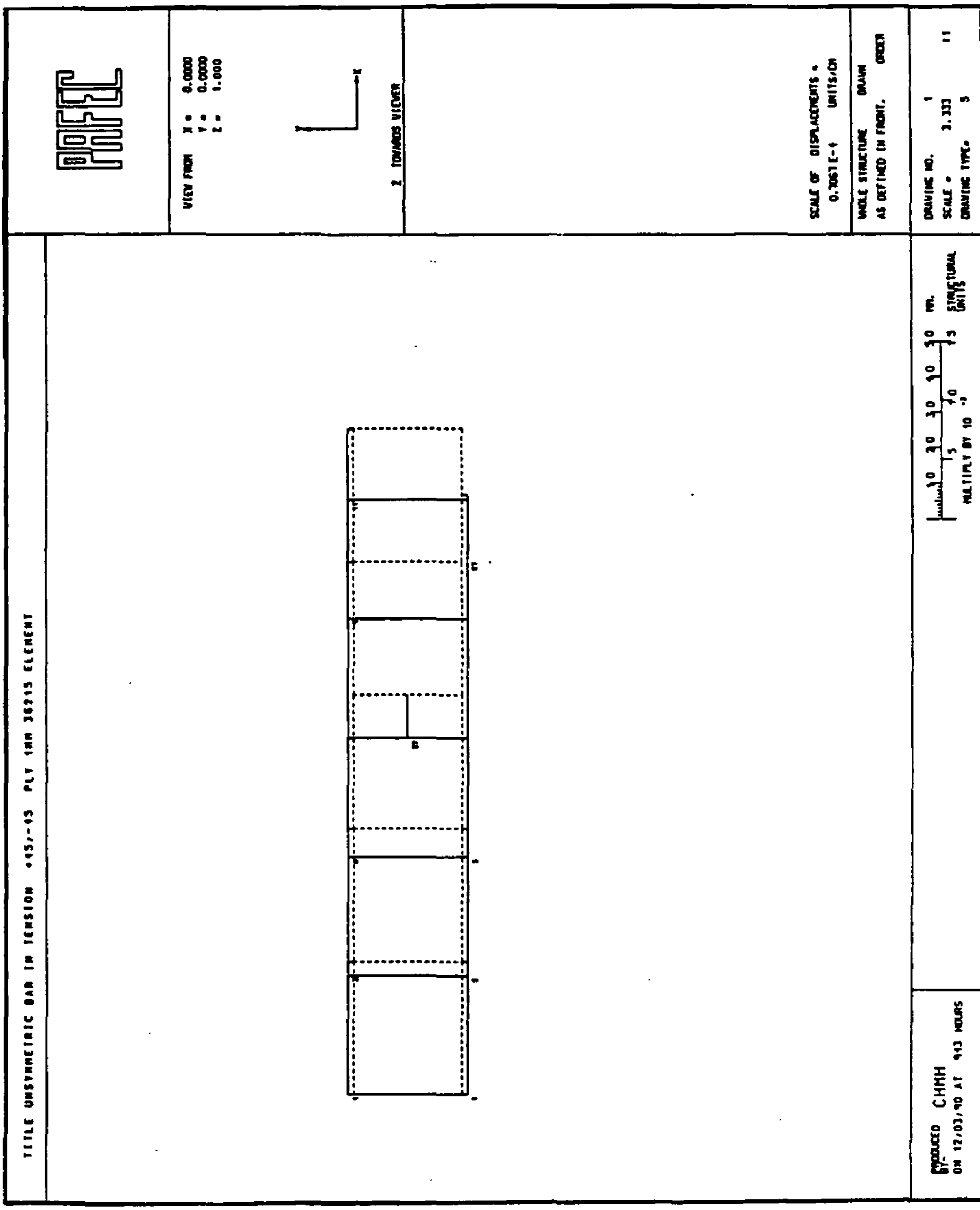

Figure 4.18 Unsymmetric Laminate in Tension, Test 5, Element 44215

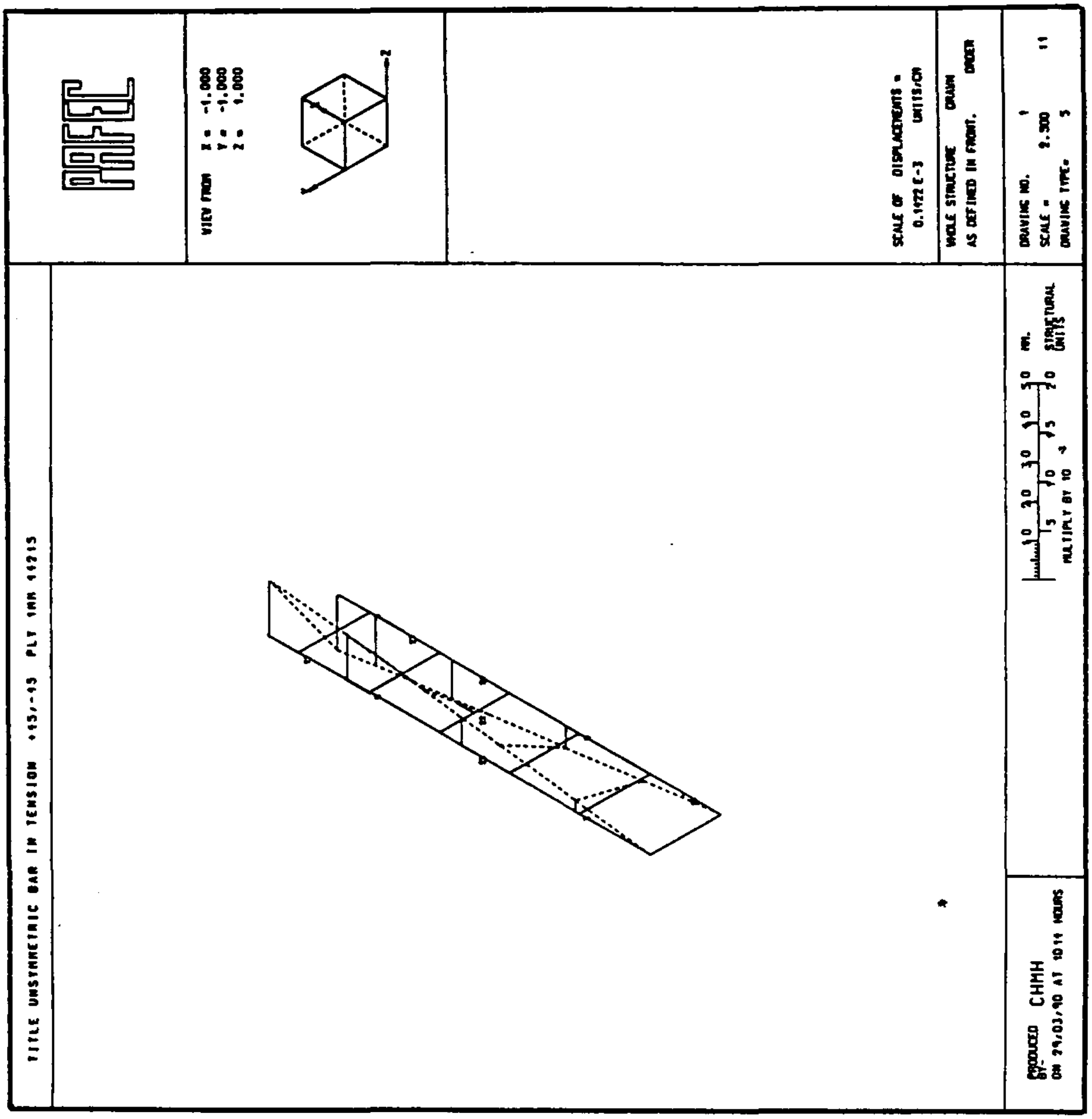

Figure 4.19 Unsymmetric Laminate in Tension, Test 5, Element 43215

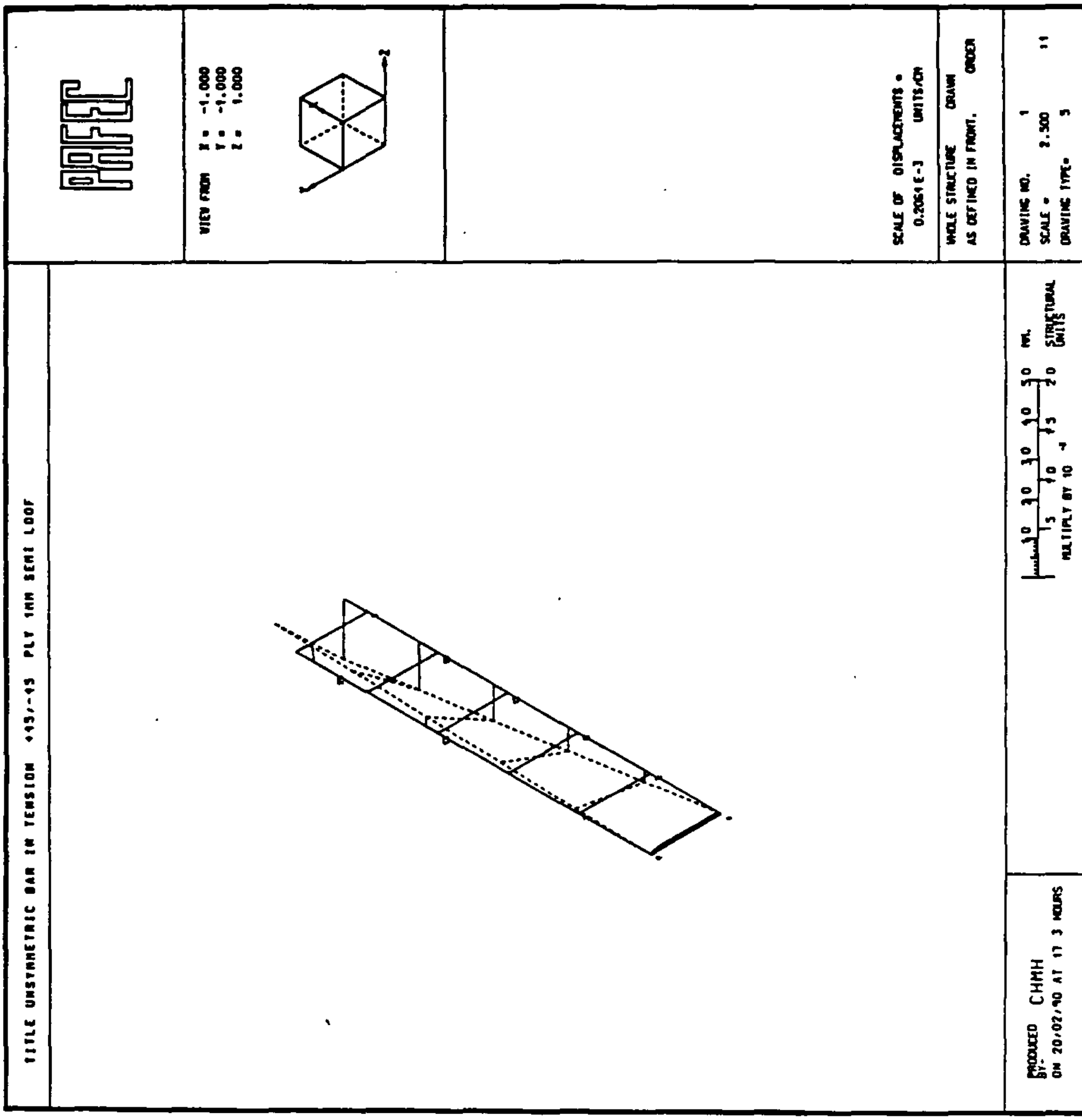

Figure 4.20 Symmetric Laminate in Bending, Test 2, Element 44215

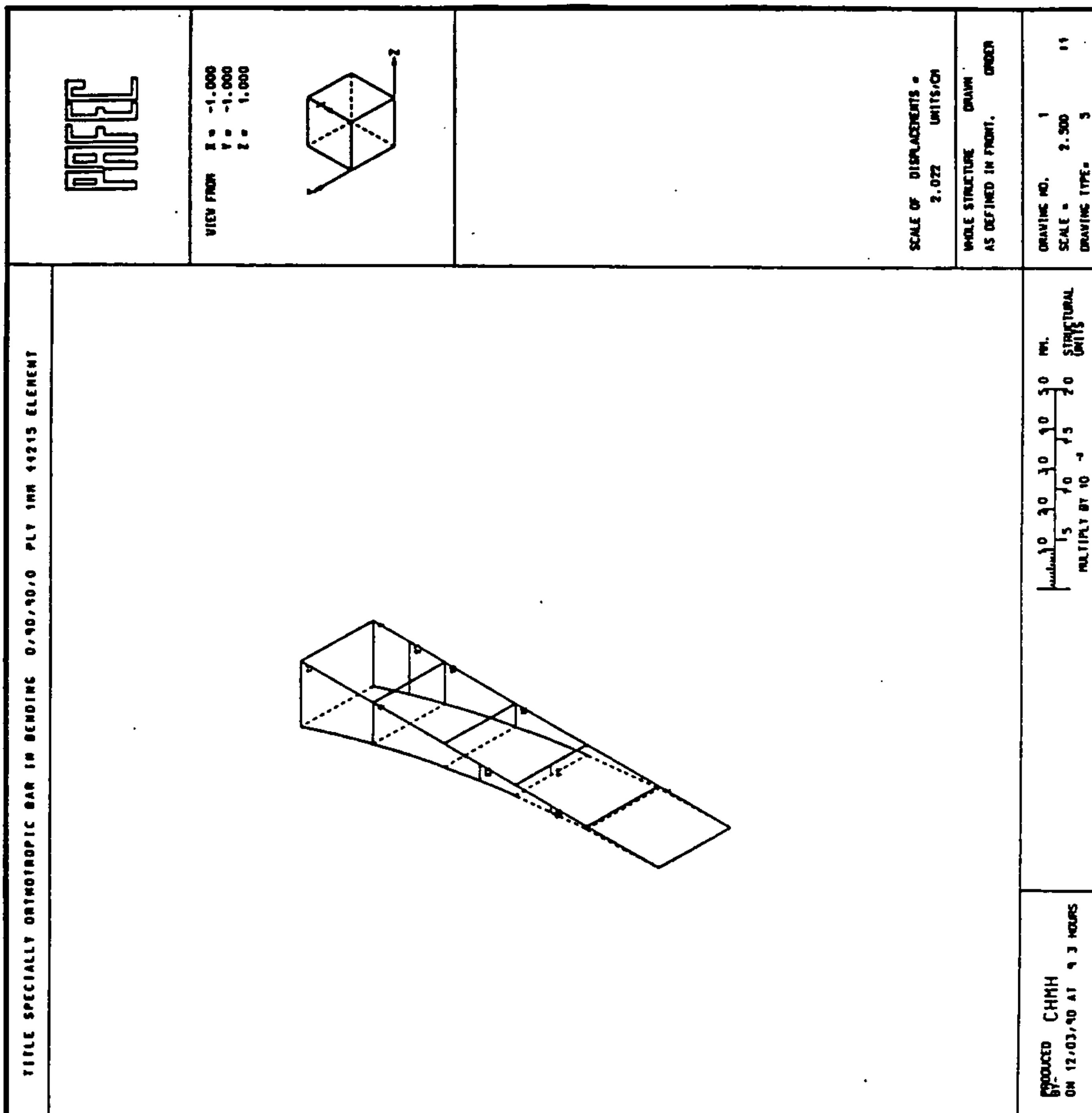

Figure 4.21 Symmetric Laminate in Bending, Test 2, Element 43215

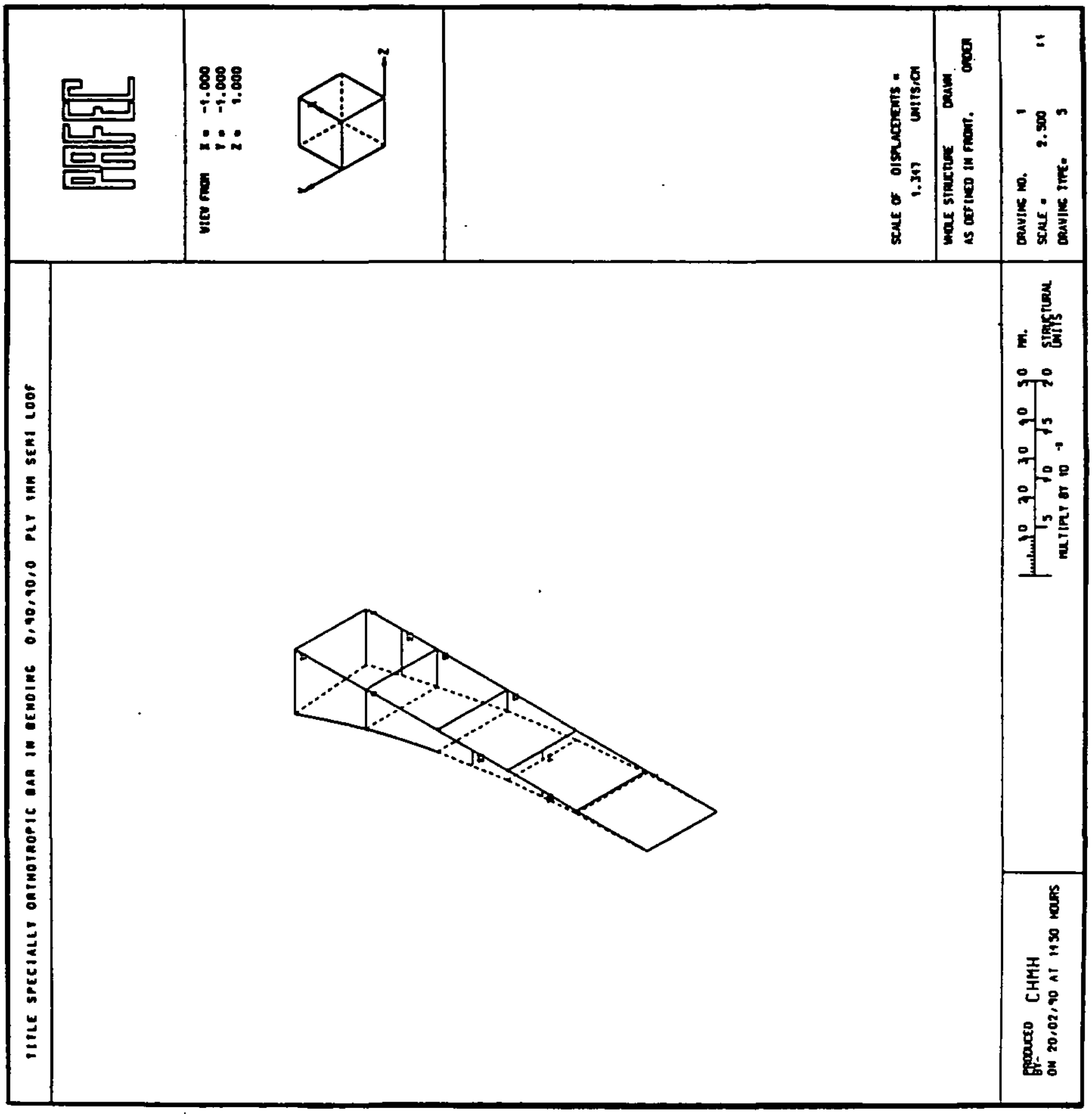

Figure 4.22 Generally Orthotropic Lamina in Bending, Test 4, Element 44215

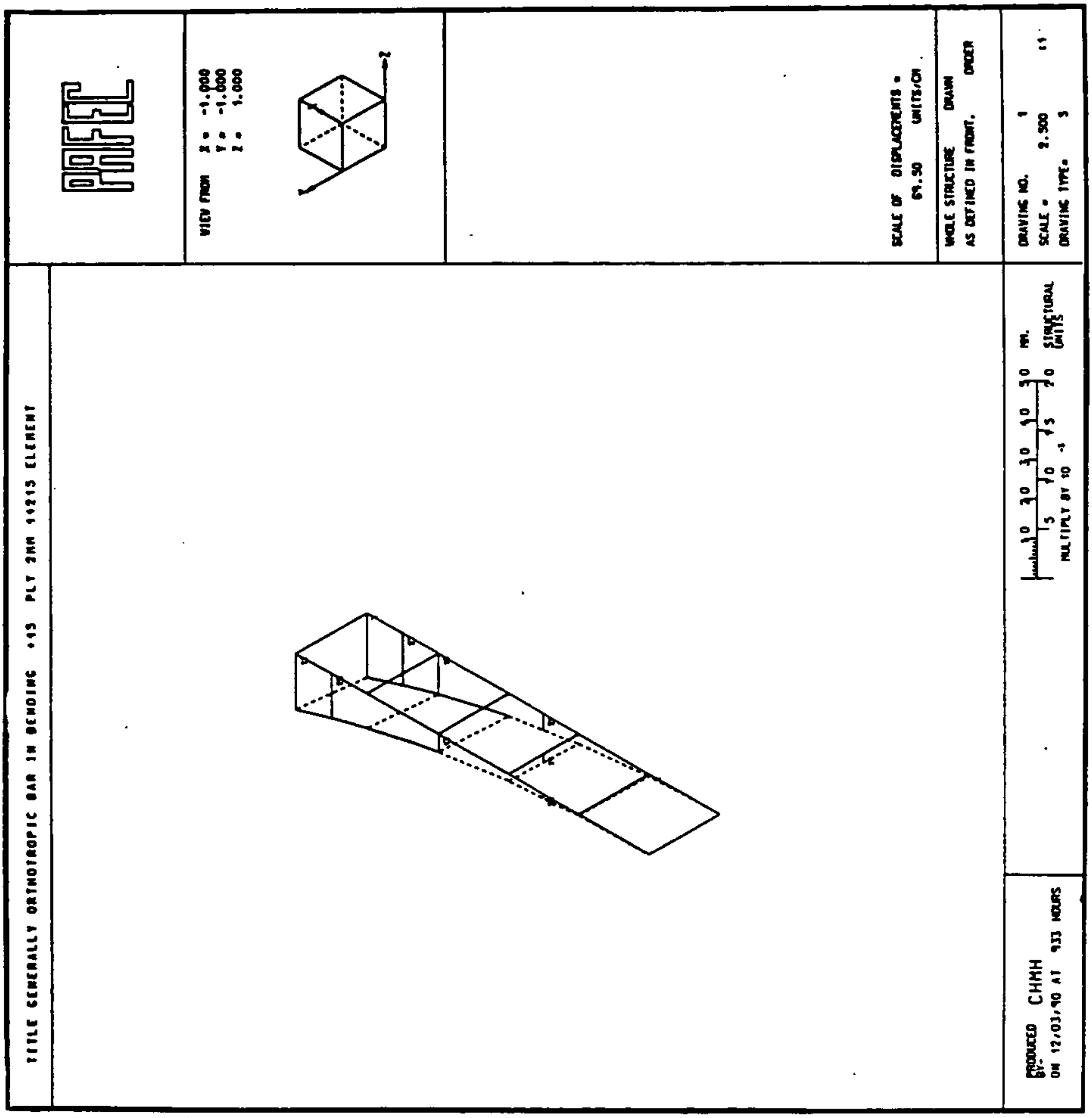

Figure 4.23 Generally Orthotropic Lamina in Bending, Test 4, Element 43215

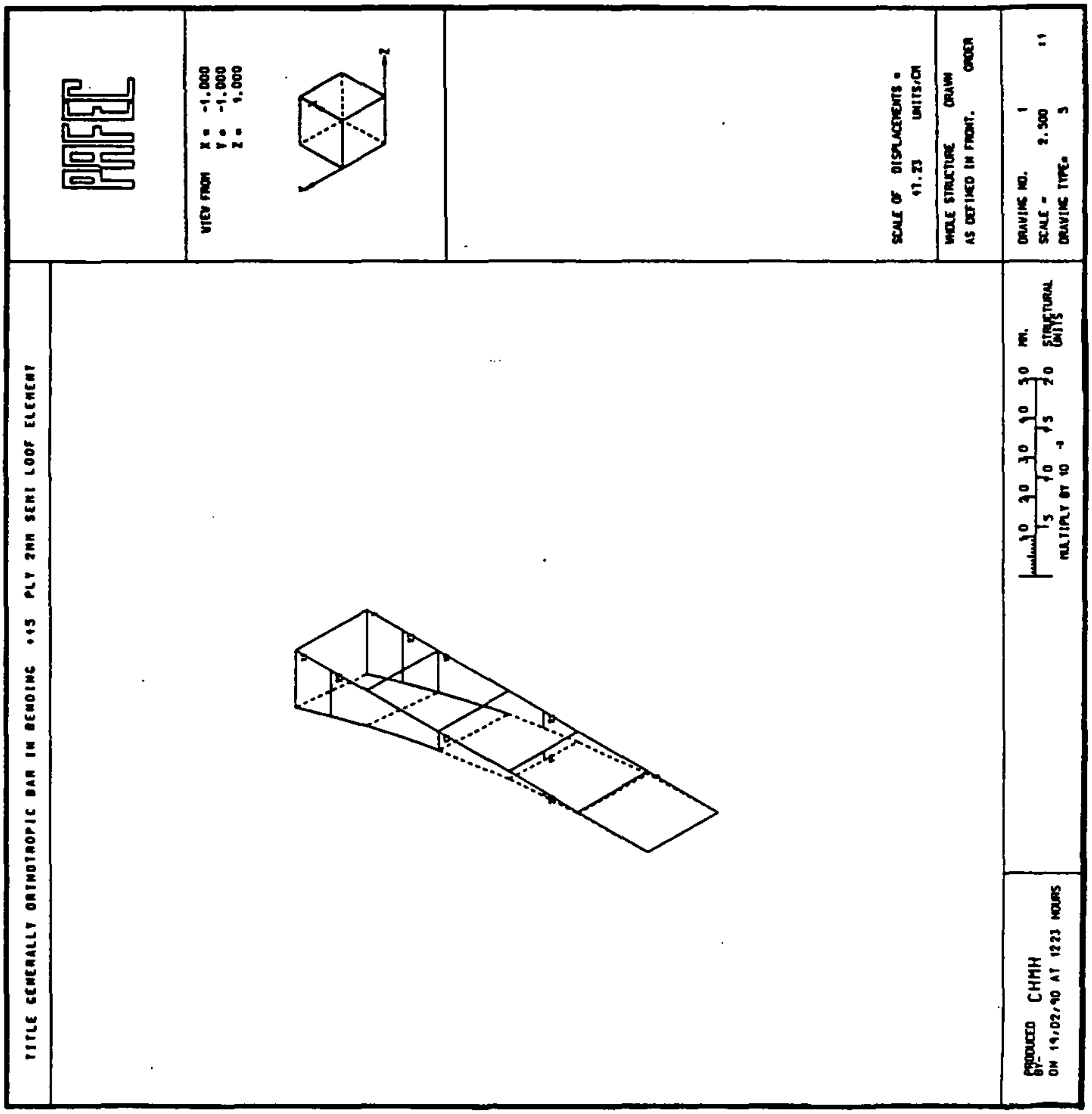

CHAPTER 5

Composite Case Development

5.1 Introduction

This chapter investigates the design and development of a composite undercarriage equipment case using Finite Element Analysis. It discusses case rationalisation, initial design calculations, the finite element analysis process and finally details the results and recommendations.

The investigation so far into equipment case design has revealed that they tend to be overdesigned and have several inherent problems; weak support design leading to high local stresses and a tendency to exhibit excessive flexiblity due to the 'open frame' design. These points have been taken into consideration in the following case development.

The confidence of using the Pafec orthotropic finite elements in such an analysis has also been assured through extensive element testing, see chapter 4.

5.2 Case Rationalisation

The investigation of previous cases has shown that they are of a skeletal nature. The main structure consists of two parallel, longitudinal side beams of deep section with appropriately positioned load bearing cross members, the outer skin and panniers provide no significant contribution to the strength of the case.

The design of the two longitudinal beams was considered initially as these form the basis of the case and are used to provide the support mechanisms for all the equipment carried and also the case itself. In previous designs, these structures have been found to be lacking in lateral stiffness and have been highly stressed in the area of the case supports.

On establishing an efficient beam design, under vertical and longitudinal loading conditions, the structure was extended with the addition of cross members, to form the basic skeletal case. This was subjected to lateral load conditions.

5.3 Preliminary Design Calculations

Design calculations were carried out to establish some size guidelines for the longitudinal beams structure. The structure was modelled as a uniform beam, simply supported at both ends. The beam was considered to carry two loads:-

i. A uniformly distributed load of 2.1 kN/m, representing the equipment carried by the case and its self weight.

ii. Two point loads of 3 kN to represent half the choke load, the heaviest single item of equipment.

Figure 5.1 illustrates the model.

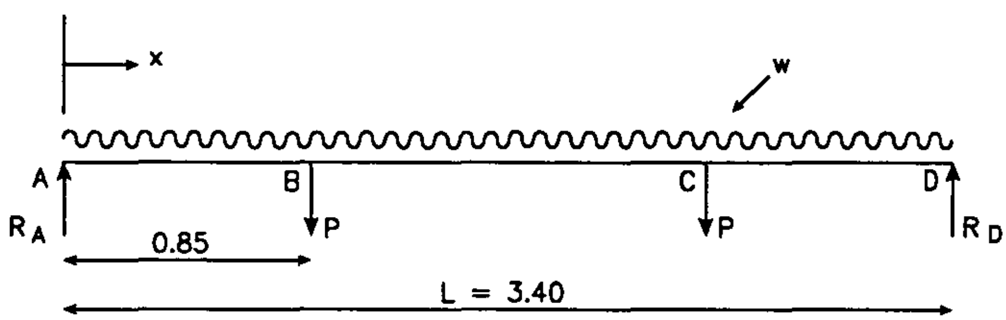

Figure 5.1

Considering vertical equilibrium

$$R_A + R_D = wL + 2P = 7.14 + 6.0 = 13.14 \text{ kN}$$

Where w=2.1 kN/m, L=3.4 m and P=3 kN.

The loading is symmetrical, hence,

$R_A = R_D = 13.14/2 = 6.57$ kN

Maximum bending moment occurs centrally.

Considering section BC

$$\text{Bending Moment } M = R_A x - wx^2 - P(x - 0.85)$$

Centrally x = 1.7m, hence

$$M = 5.14 \text{ kNm}$$

The depth of the case is 0.8m, hence the approximate compressive and tensile loads in the top and bottom flanges respectively can be calculated from,

End Load = Bending Moment / Depth

ie. End Load = 5.14/ 0.8 = 6.5 kN

The end load was adjusted to 7.0 kN to provide a small reserve factor against changes in the loading pattern which must occur due to alterations of the equipment layout at a later date. Considering a ballpark figure for allowable direct stress of 100 MN/m^2 for a Glass Fibre/ Epoxy Resin composite structure.

Hence from,

Beam flange cross section = End Load / Direct Stress

Flange cross section = $7 \times 10^3 / 100 \times 10^6 = 70 \times 10^{-6}$ m^2

ie. **Flange cross section = 70 mm^2**

The above calculations show that the cross sectional area of a beam flanges to carry the specified loads is very small, so it can be deduced that the above model is not strength critical and the material cross section required are dictated by stiffness considerations. The initial size guidelines were taken from similar features in the standard metal isotropic case modified to take account of the composite material specification.

5.4 Longitudinal Beam Idealisation

These are symmetrical about the vertical axis, hence half the structure was modelled. The dimensions for the structure, 3.4 x 0.8 m were taken from the hybrid case analysed in chapter 3. The model consists of a thin vertical web with vertical stiffeners, positioned at either end and at a point centrally where the choke load is located. Upper and lower horizontal flanges complete the structure providing further stiffness. The upper flange is extended to provide the case support, with a triangular gusset panel to aid load transfer.

The structure was modelled using two composite materials. The web, vertical stiffeners, outer portions of the upper and lower horizontal flanges and gusset panel at the support were modelled in a woven glass lamina of varying thickness dependent on the location. The initial material sizings being, 4mm thick for the web and outer portions of the flanges and 8 mm thick material for the vertical stiffeners The inner portion of the upper and lower flanges were modelled in a unidirectional lamina consisting of glass rovings in an epoxy resin to provide longitudinal stiffness. This portion of the flange was initially designed 50mm wide using 8mm thick unidirectional material. The torsional stiffness of the flanges was increased by the use of woven cloth to form the outer edges of the upper and lower flanges, the total flange width being 150 mm. These dimensions give an initial flange cross section of 1000 mm^2, well above the preliminary design calculations of 70 mm^2. A volume fraction analysis of both materials can be found in section 5.4.2 of this chapter.

5.4.1 Finite Element Modelling

5.4.1.1 Model 1

The initial coarse mesh model, can be seen in figures 5.2 and 5.3 shows the small degree of mesh refinement at the support locations . The mid side noded orthotropic facet shell elements, 44215 and 44115 (a triangular element) were used. These elements were the most reliable of the orthotropic elements tested in tension and bending situations. It was shown that stress and displacement results achieved by the 44215 element in the tension tests correlated accurately with the proven analysis package, CoALA and theoretical calculations. In bending the element did not function as well, with the stress results achieved being a factor of 2 too great and the displacements being 7 % too great. The use of the triangular 44115 elements was restricted, as these elements by the nature are not as accurate in terms of stress and displacement analysis as their quadrilateral counterparts.

The initial model had 166 nodes, 599 elements and 3174 degrees of freedom.

5.4.1.2 Model 2

The results of the above analysis could not be viewed with confidence in the support region. The model was refined around the support location using the same element types. The original gusset panel was replaced by two similar panels offset by 25mm from the central axis. A small rib of woven cloth was added across the edge of the upper flange to reduce transverse flexibility. Extra longitudinal gusset panels were included into the web to aid load transfer. The stiffness of the supports was increased by reinforcing the triangular gusset plates to double thickness, 8 mm and the top surface elements surrounding the exact support location to five times the original thickness, 40 mm. This later development simulating a washer to distribute the load. The final design scheme is shown in figure 5.4 and the refined support can be seen in figure 5.5.

The final model had 688 nodes, 186 elements and 3510 degrees of freedom.

5.4.2 Material Selection

The two materials selected for the composite case were:-

i. A unidirectional lamina, consisting of 8 mm diameter Glass Rovings in an epoxy resin.

ii. A woven glass cloth lamina, again in an epoxy resin.

Laminas were selected as it was considered too complex and expensive to specify multi-layer composites at this stage, especially as the structure being considered was subjected to direct stresses with no torsional effects, an ideal situation for the use of unidirectional materials.

A volume fraction analysis was carried out on each of these materials to determine their Young's' and Shear Moduli.

5.4.2.1 The Uni-directional lamina

Properties:-

E for fibre $E_F = 38$ GPa

E for matrix $E_M = 3$ GPa

Considering a fibre volume fraction of 0.6, hence

$V_F = 0.6$

$V_M = 0.4$

Rule of Mixtures Theory , Reference 10 details:-

Modulus in fibre direction $E_1 = E_F V_F + E_M V_M$ . . . (1)

Modulus in transverse direction $1/E_2 = V_F/E_F + V_M/E_M$ . . . (2)

An accepted approximation for the in plane Shear Modulus gives,

$G_{12} = 0.4 \times E_1$ . . . (3)

Hence on substitution,

$E_1 = 24.0$ GPa

$E_2 = 6.7$ GPa

$G_{12} = 9.6$ GPa

The Pafec orthotropic material module within the data file requires these properties to be transformed into the appropriate compliances, as detailed in the following matrix.

$$\begin{bmatrix} \epsilon_1 \\ \epsilon_2 \\ \psi_{12} \end{bmatrix} = \begin{bmatrix} S_{11} & S_{12} & 0 \\ S_{21} & S_{22} & 0 \\ 0 & 0 & S_{66} \end{bmatrix} \begin{bmatrix} \sigma_1 \\ \sigma_2 \\ \tau_{12} \end{bmatrix}$$

From composite theory, Reference 11.

$$S_{11} = 1/E_1 \qquad \ldots (4)$$

$$S_{22} = 1/E_2 \qquad \ldots (5)$$

$$S_{12} = -\vartheta_{12}/E_2 \qquad \ldots (6)$$

$$S_{66} = 1/G_{12} \qquad \ldots (7)$$

Hence on substitution in (4), (5), (6) and (7) the compliances for the unidirectional laminate are,

$$S_{11} = 4.167 \times 10^{-11} \ \ Pa^{-1}$$

$$S_{22} = 1.496 \times 10^{-10} \ \ Pa^{-1}$$

$$S_{12} = -1.083 \times 10^{-11} \ \ Pa^{-1}$$

$$S_{66} = 1.042 \times 10^{-10} \ \ Pa^{-1}$$

5.4.2.2 The Woven Glass Cloth lamina

A similar analysis for the woven material gives,

Properties:-

E for fibre $E_F = 38$ GPa

E for matrix $E_M = 3$ GPa

Considering a fibre volume fraction of 0.6, hence

$$V_F = 0.6$$

$$V_M = 0.4$$

An accepted approximation for the in plane Shear Modulus gives,

$G_{12} = 0.4 \times E_1$

On substitution into equations (1) and (3) from the previous analysis gives,

$E_1 = 9.6$ GPa

$E_2 = 9.6$ GPa

$G_{12} = 3.8$ GPa

Note E_2 is assumed to be the same as E_1 due to the nature of the woven material.

The compliances are, on substitution into (4), (5), (6) and (7):-

$S_{11} = 0.104 \times 10^{-9}$ Pa^{-1}

$S_{22} = 0.104 \times 10^{-9}$ Pa^{-1}

$S_{12} = -2.708 \times 10^{-11}$ Pa^{-1}

$S_{66} = 2.630 \times 10^{-10}$ Pa^{-1}

5.4.3 Load Cases

The standard load cases can be found in Appendix A1, the cases considered in this analysis as follows:-

5.4.3.1 Proof Load Cases

The equipment mountings must be able to withstand the mass of the equipment when subjected to the following accelerations, all loads being reacted at the supports.

Two proof load cases were applied to the structure:-

i. Vertical 1.5g down

ii. Longitudinal ±3.0g + 1.0g vertical down

It should be noted that the vertical 1.0g up case, load case (i) in Appendix A1 has not been applied here, the vertical 1.5g down being a 'worst case'. Only the positive longitudinal case was analysed, it was assumed that on obtaining satisfactory results in this case, the negative case would produce satisfactory results. A lateral load case was not applied here, a true indication of lateral stiffness can only be established on testing a model of the whole case structure.

5.4.3.2 Fatigue Load Case

All equipment mountings must be designed to have a fatigue life of not less than 10^7 cycles for the loads produced by the following accelerations acting on the mass of the equipment, ie choke and pannier loads.

i. Vertical 1.0g down $\pm$ 0.3g

ii. Longitudinal $\pm$0.2g

Lateral effects were not considered here ($\pm$0.3g) standard case, Appendix A1. The fatigue life determined from the summation of the effects of vertical and longitudinal loads is anticipated to be much greater than the stated requirements.

5.4.5 Load Case Idealisation

The structure is assumed to carry half the mass of the equipment in the case and half the mass of the case itself. The following loads were applied:-

i. A uniformly distributed load of 2.1 kN/m, along the length of the longitudinal beam to represent equipment loading and self weight.

ii. Choke load, total mass 1.2 tonnes applied as a point load at two locations on each side structure.

The structure was loaded under vertical and longitudinal load cases with loads applied along the central axis of the upper flange, in the required ratio 1:4:1 across each of the second order elements used.

The structure was restrained in the vertical, lateral and longitudinal directions along the axis of symmetry and at the support node in the vertical and lateral directions. The longitudinal direction was not restrained at the support to allow a slotted hole to be modelled. In the analysis of the first model, the support node was taken to be the central node at the edge of the upper flange extension, however in the refined model the restraint was applied 7 mm from the edge at the next suitable node in order to model the mounting position more realistically.

5.5 Skeletal Model Idealisation

5.5.1 Finite Element Modelling

The side structure was extended to form a skeletal case. This was achieved by the addition of four lateral cross members, placed at either end of the case and internally at the choke mounting locations. The cross members were modelled as vertical webs the full height of the case, with upper and lower horizontal flanges to providing further stiffness. The cross members were modelled in the same materials as the longitudinal beams with the web, stiffeners and initially the outer portions of the upper and lower flanges being modelled in the woven cloth composite, the inner portion of the flanges being modelled in the unidirectional laminate to provide lateral stiffness.

5.5.1.1 Model 1

Even though the case displays two axes of symmetry, it was necessary to model half the case as the model is to be subjected to an antisymmetric load case. The side structure used previously was extended by the addition of two cross members, with a certain amount of remodelling being done around the cross member locations. The half model of the case was achieved by mirroring about the longitudinal axis. The model was idealised again using the facet shell elements, 44215 and 44115, with again the use of triangular elements being kept to a minimum. The model can be seen in figure 5.6.

5.5.1.2 Model 2

The analysis of model 1 revealed that there was high lateral deflections. To overcome this the stiffness of the upper and lower flanges on the beams and cross members was increased, by using unidirectional rovings across the full width of the flanges instead of having a central core of rovings and outer portion of woven cloth. Woven cloth would be wrapped around the flanges to provide an outer skin and increased torsional stiffness, this was not modelled. The depth of the flanges was also increased to 32mm, again to increase stiffness. To effect the above changes, no remodelling was required, material properties of the appropriate groups of elements were changed in the Pafec data file.

5.5.2 Material Selection

See section 5.4.2

5.5.3 Load Cases

The skeletal case was tested under lateral load conditions and as in previous specifications, the equipment mountings must be able to withstand the mass of the equipment when subjected to the following loading, all loads being reacted at the supports. The actual loading tested was:-

$\pm$ 1.1g + 1.0g vertical down

It should be noted that only the positive lateral case was analysed, it was assumed that on obtaining satisfactory results in this case, the negative case would produce satisfactory results. As the skeletal model was analysed under the lateral load case only, no fatigue analysis was performed.

5.5.3 Load Case Idealisation

The skeletal case was tested under lateral loading conditions, subjected to the same loads as the longitudinal beams, ie the uniformly distributed load to represent equipment and self weight and the point loads to represent the choke. In the previous model all loads were applied along the upper surface of the side structure as their load paths passed straight through the structure, when loaded vertically and laterally. To simulate realistic loading in the lateral load case, loads were applied along the upper and lower flanges to achieve the effect of equipment being distributed throughout the case.

Restraints were applied at the axis of symmetry to prevent longitudinal displacements An additional restraint was also applied in this plane to prevent rotation around the vertical axis. At the supports vertical and lateral displacements were restrained, longitudinal displacements were allowed, to simulate the effect of a slotted hole mounting.

5.6 Results

The displacement plots obtained from the proof load analyses for side structure and skeletal model can be seen in figures 5.7 - 5.10. There are no stress contour plots included, these plots can only be obtained for composite material analyses by using PIGS version 4.3 and later releases to post-process. Unfortunately this revision of software was not available at the time of the research.

On identification of the areas of high displacement, several graphs have been plotted via PIGS post-processor to clarify the results for each load case. The stress output files were examined and areas of high stress have been plotted out manually. Figures 5.11 - 5.13 details the direct stress at the element centroid in the material direction along the positive surface for elements along the upper flange and the support locations in both for the two side structure models analysed. Figures 5.14- 5.15 provides the same information for the skeletal model.

5.6.1 Longitudinal Beams

5.6.1.1 Vertical Load Case

The analysis of the first model, revealed the structure to be relatively unstressed, with stresses of the order 10^6 Nm^{-2} throughout the structure. These stresses being well within the maximum working stress level of 10^8 Nm^{-2}, which is approximately half the Ultimate Tensile Strength of the glass rovings used, these giving a safety factor of 2. The support area however was highly stressed with stresses of the order of 10^8 Nm^{-2} being found, with actual values higher than the working level, see figure 5.11. Elements in the gusset panels were also more highly stressed with stresses of the order of 10^7 Nm^{-2}. Local elements to the support area in the main web, however experienced low stresses of the order of 10^6 Nm^{-2}.

The displacement curves for the first model, figures 5.16 - 5.18 show that there is a maximum vertical displacement of 4.72 mm centrally along the upper surface under the vertical 1.5g down load case. with approximately 3.00 mm deflection across the first element of the support area. Transversely across the top flange at the support position there was a symmetrical deflection of 3.12 mm as shown in figure 5.17. Lateral displacements were minimal throughout, of the order of 10^{-3} mm, as can be seen in figure 5.18.

The structure was then modified several times to improve the design in the support location, as described in section 5.4.1.2. The mesh was refined in the support area, to enable more accurate results to be obtained. Modelling refinements included the addition of a small transverse rib of woven cloth across the termination of the upper flange to prevent transverse flexibility. The gusset plate elements and the upper flange support elements were increased in thickness, the gusset elements by a factor of two and the support elements by a factor of 5. This model was then analysed under vertical and longitudinal load cases.

The refined model subjected to the vertical load case, again showed that the majority of the case was relatively unstressed, with stresses of the order of 10^6 Nm^{-2}. The support location experienced higher stresses of the order of 10^7 Nm^{-2}, however these are well within the maximum working stress level of 10^8 Nm^{-2}, see figure 5.12. Displacements for the vertical load case showed a reduction in vertical displacements, with a maximum of 2.70mm occurring centrally and a proportionate deflection over the support region. Across the support displacements were minimal of the order of 10^{-2} mm. Graphs of these displacements can be seen in figures 5.19 - 5.20. On checking lateral and longitudinal displacements throughout the structure, both were found to be negligible. Displacement plots are also included for both models analysed here and can be seen in figures 5.7 - 5.8.

5.6.1.2 Longitudinal Load Case

When subjected to the longitudinal load case, again the majority of the case was relatively unstressed, with stresses of the order of 10^6 Nm^{-2} throughout the structure. The support location experienced higher stresses of the order of 10^7 Nm^{-2}, however these are still well within the maximum working stress level of 10^8 Nm^{-2}, see figure 5.13 . Displacements in the vertical direction along the upper flange increased for this load case and were at a maximum of 3.07 mm centrally with a proportionate deflection over the support region. Across the support displacements were minimal of the order of 10^{-5} mm. Graphs of these displacements can be seen in figures 5.21 - 5.22. Lateral displacements throughout the structure were minimal throughout the structure, of the order of 10^{-3}mm. Longitudinal displacements at the mounting point were minimal, maximum of 1.24mm and in the real case would be absorbed by a slotted hole or similar mechanism at one end mounting. A displacement plot can be seen in figure 5.9.

5.6.1.3 Fatigue Load Case

The support area of the structure which experienced the highest stresses was considered in the fatigue analysis. A typical stress range experienced by a node at the support was calculated to be 1.46×10^7 Nm^{-2}. From standard data sheets the fatigue strength of a Glass/Epoxy composite ($V_F = 60\%$) at 10^7 cycles is approximately 20% of its Ulimate Tensile Strength. The U.T.S of the material used in this analysis is 3.24×10^8 Nm^{-2} , hence the maximum stress range allowable is 6.4×10^7 Nm^{-2}. Hence the stress range experienced is well within the allowable range, with a reserve factor of 4.4 and the fatigue life of the case is assured for 10^7 cycles.

5.6.1.4 Mass of the structure

The mass of the longitudinal beams were 29.2kg for the first model and 31.2kg for the refined model. These masses being quoted for a full single complete beam.

5.6.2 Skeletal Case

5.6.2.1 Lateral Load Case

The analysis of the first model revealed the majority of the structure to be relatively unstressed, with stresses of the order of 10^6 Nm^{-2} or lower throughout. However there were several areas of high stress identified as shown in figure 5.14, where stresses of the order of 10^7 Nm^{-2} were found. These occurred at the intersection points between the side structures and lateral cross members. These high stresses are to be expected as there is no fillet modelled at the corners to smooth the stress distribution.

High lateral displacements were experienced see figure 5.23 with a maximum of 22.89 mm at the centre of the right hand side upper flange, at the supports the lateral displacement is negligible. Figure 5.23 also shows that the model does not bend in a smooth manner, there is a sharp gradient to the graph before the location of the internal cross member. The gradient at this position is substantially reduced as would be expected, with the cross member providing lateral bending stiffness. Towards the centre of the case the gradient of the curve increases and is a maximum at the centre. An example of lateral displacements through the depth of the case can also be seen in figure 5.24, and shows that the deflection is relatively uniform through the depth of the case, the lower flange being displaced an extra 5.4% at this position. Vertical displacements are low, negligible in the support locations with a typical maximum displacement of 1.04 mm occurring at the centrally, figure 5.25.

These results showed a lack of lateral stiffness and a lack of strength at the points where the cross members merge, which led to the development of the second model.

The second model with redesigned upper and lower flanges showed on analysis that the regions of high stress were substantially lower, of the order of 10^6 Nm^{-2}. Stresses throughout the structure were again of the order of 10^6 Nm^{-2} or lower, see figure 5.1.

Lateral displacements, figures 5.26 - 5.29, were greatly reduced to what was thought as an acceptable 3.05 mm occurring centrally along the right hand upper flange. Displacements along the left hand flanges again were acceptable and 2.3% greater than the right hand side. A deflection of 3.12 mm occurred centrally along the left hand side upper flange. The case deformed laterally in the same manner as before, as can be seen from the similar shaped curves in figures 5.26 - 5.29 to figure 5.23. The graphs show that there is small deflections at the ends of the case rising to a maximum centrally. Lateral displacements through the depth of the case were found to increase proportionately, figures 5.30 - 5.31. The graphs of displacement in the longitudinal direction along the two cross members, figures 5.32 - 5.33 detail very small displacements, and deform in an 's' shape. The displacements are minimal of the order 10^{-3} mm and hence there is no cause for concern due to non-linear effects. Vertical displacements along the flanges were at a maximum centrally , 0.47mm is the maximum displacement along the right hand side upper flange is a typical value. The lower flanges exhibited smaller vertical deflections, 4.8% smaller. The vertical displacements along the left hand flanges were substantially greater , with a maximum vertical displacement occurring centrally along the upper flange of 0.65 mm, 18% greater. Again the lower flange exhibited smaller vertical displacements than the upper flange , 1.2% smaller centrally. Unlike the lateral displacement curves, figures 5.34 -5.37, the vertical displacements graphs do not have similar curves showing that both sides of the case do not deform symmetrically in the vertical sense. However, as these displacements are negligible any unsymmetrical deformation is very slight and can be ignored.

5.6.2.2 Mass of the structure

The mass of the resulting unloaded skeletal case was found to be 222kg, for a full model.

5.7 Discussion

The resulting design for a skeletal case on analysis reveals that it compares very well with the similar analysis of the isotropic case, chapter 3. The model is relatively unstressed throughout, with higher stresses occurring around the support locations and the junctions of the lateral cross members and the main body of the case. However, these can be alleviated by the addition of a fillet at the intersection points. Lateral stiffness again proved to be a cause for concern in the initial model of the case, however with the change of flange design to one of completely unidirectional rovings, a satisfactory level of stiffness was achieved. The displacements obtained were of a similar order to those experienced by the isotropic case and well within the working limits of normal traction engineering. A fatigue analysis using stress results from the 'highest' stressed area of the refined model established that the structure would not suffer from fatigue damage, up to 10^7 cycles.

The mass of the skeletal case compares extremely favourably, the isotropic case having a mass of 360kg and the composite skeletal model a mass of 222kg, with further refinements additional weight savings could be achieved. Of course the mass of the skeletal model will increase with the addition of outer panels, covers and internal frameworks, a reasonable estimate of total weight would be 260 kg, giving a total saving of 100kg ie a weight advantage of 0.72:1.

Changing the flange material to a carbon fibre composite would theoretically enable further weight reduction, its greater value of Young's Modulus would acheive a case of equivalent structural integrity using less material. However, practically this would be of no benefit as a minimum thickness design could not be used due to manufacturing difficulties.

5.8 Conclusions

The skeletal model analysed was relatively unstressed, with acceptable stresses at the support locations. Deflections throughout the structure were minimal and acceptable. On further refinement the final mass of 222kg could be reduced, however it still compares favourably with the mass of the isotropic case analysed.

Figure 5.2 Longitudinal Beam Idealisation - First Model

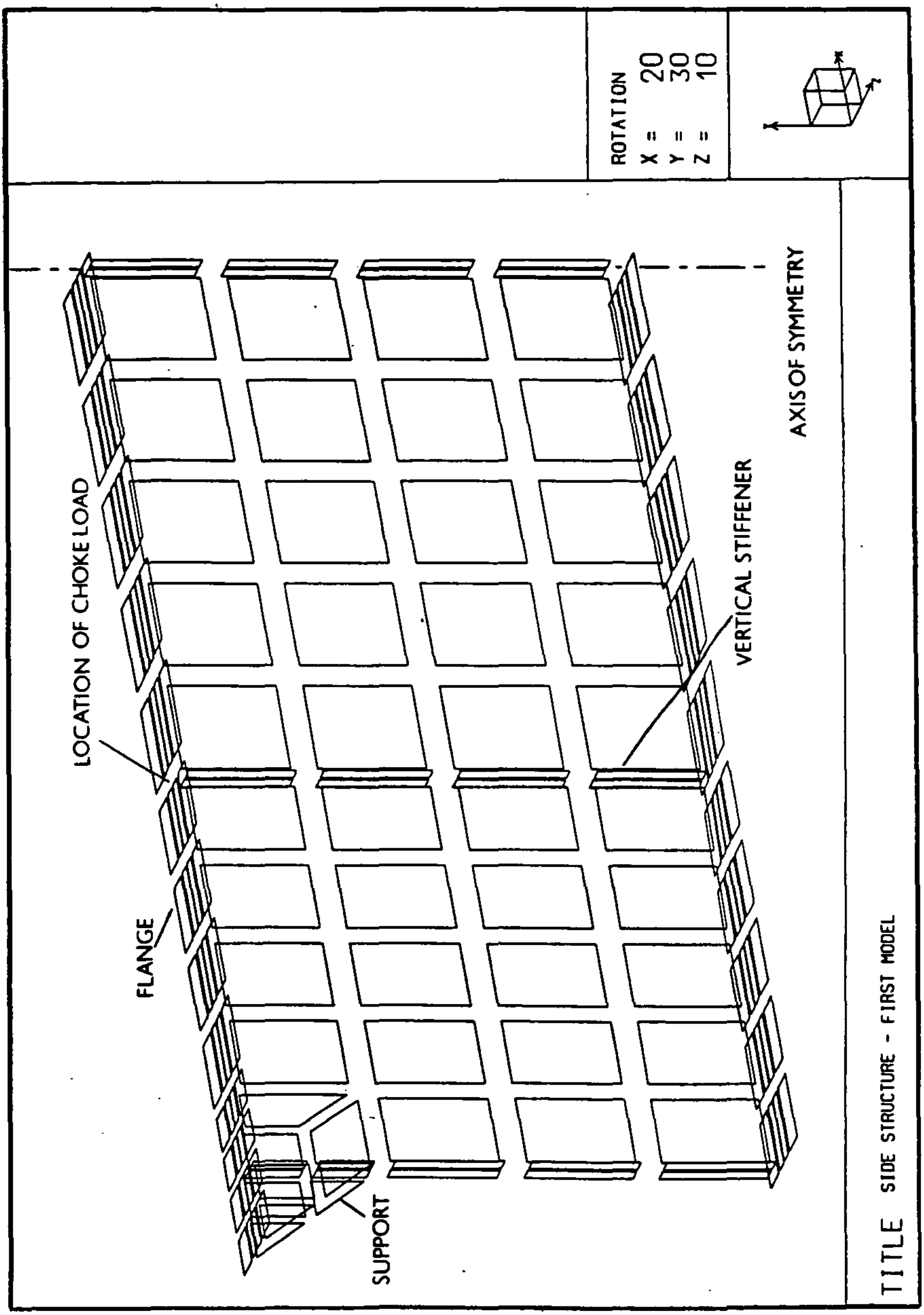

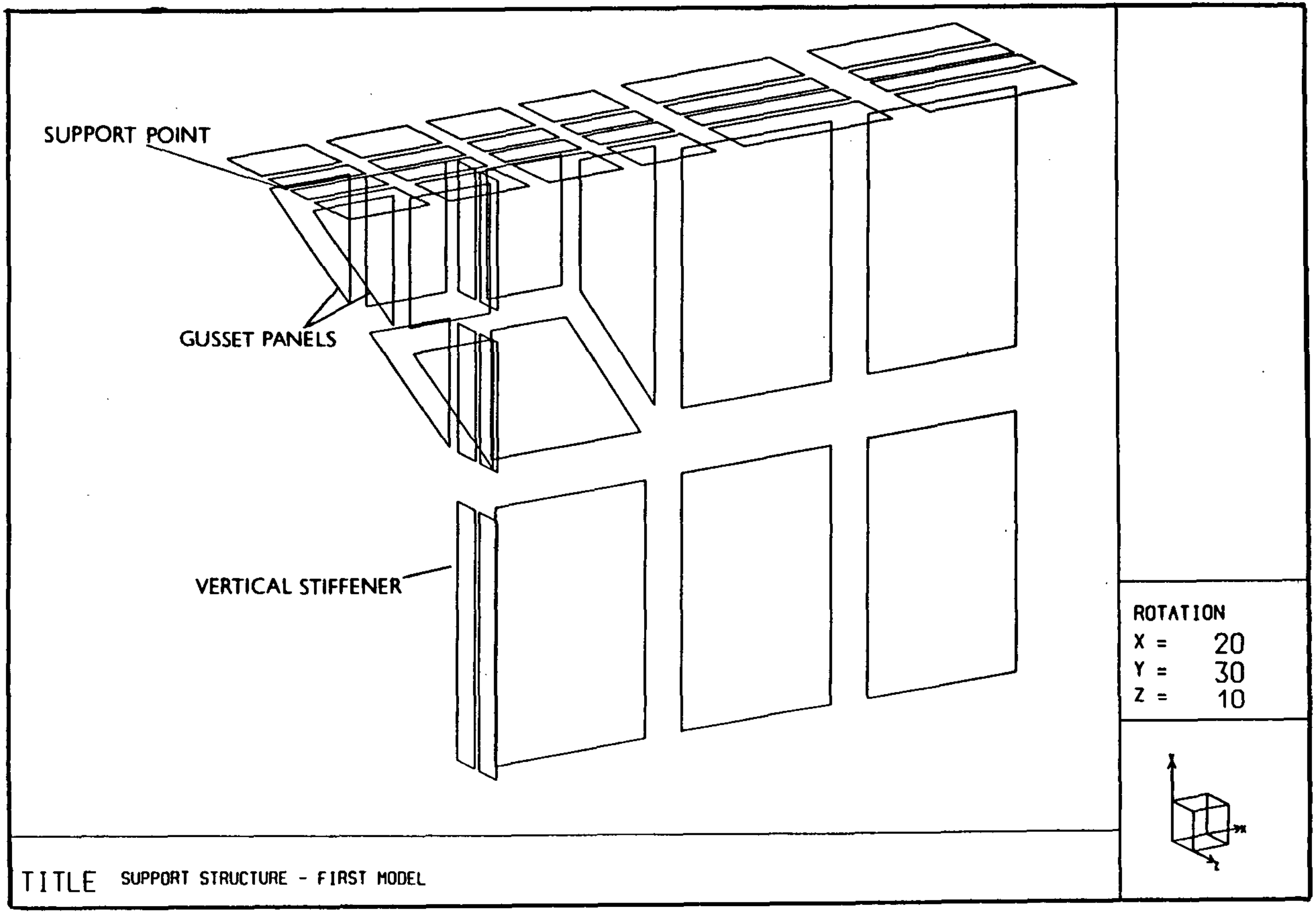

Figure 5.3 Support Structure Idealisation - First Model

Figure 5.4 Longitudinal Beam Idealisation - Refined Model

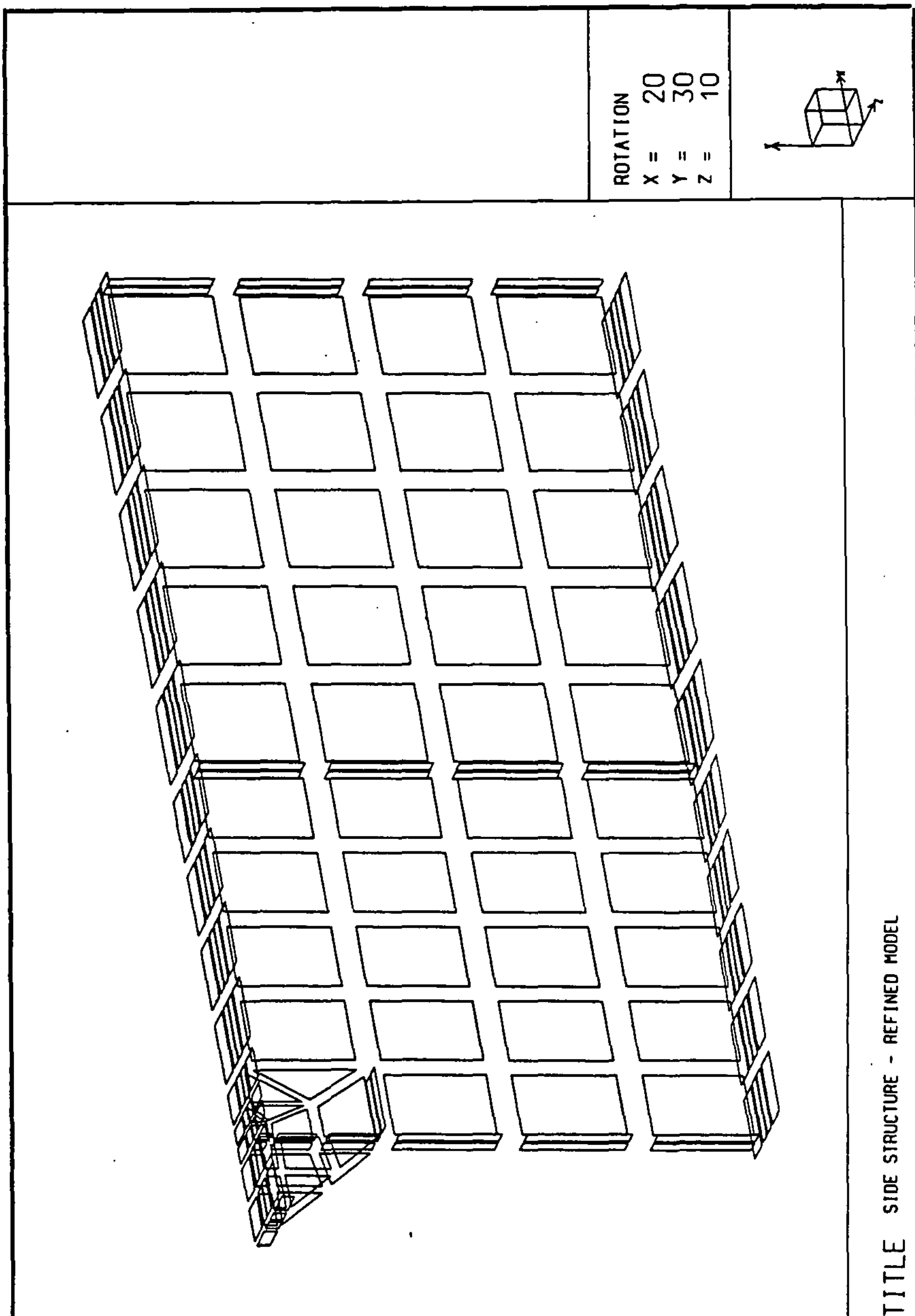

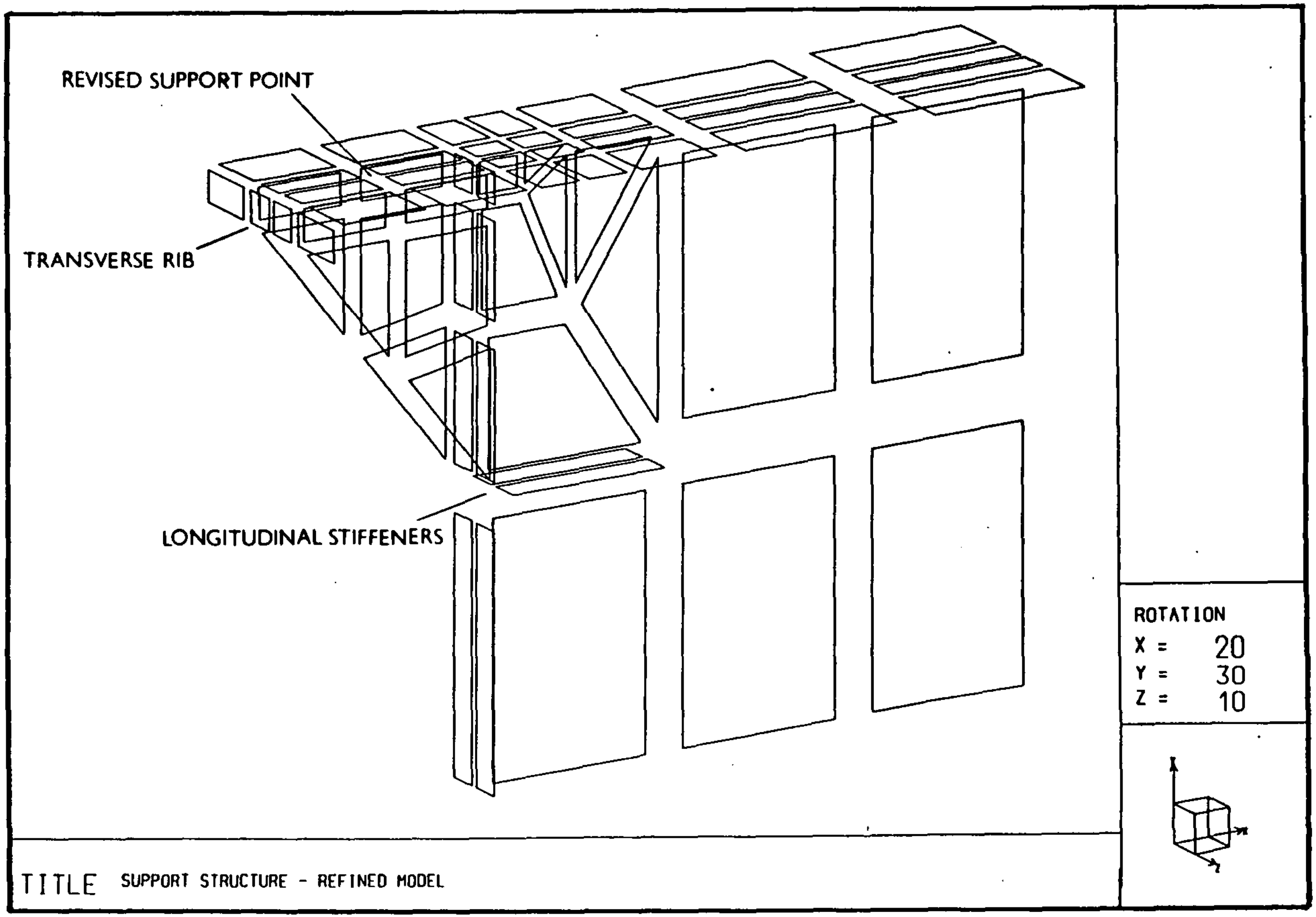

Figure 5.5 Support Structure Idealisation - Refined Model

Figure 5.6 Skeletal Model Idealisation

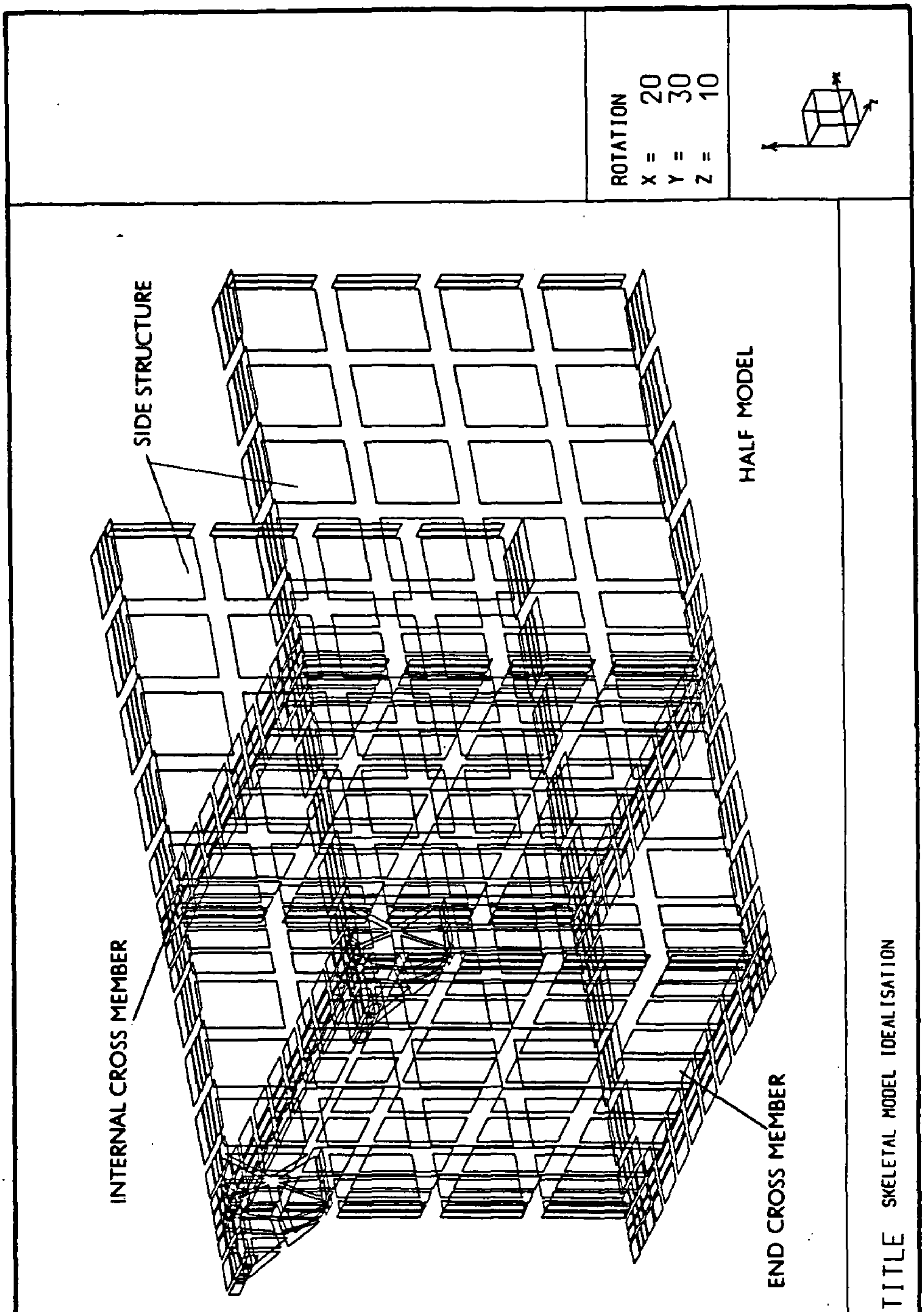

Figure 5.7 Displacement Plot Vertical 1.5g Load Case - First Model

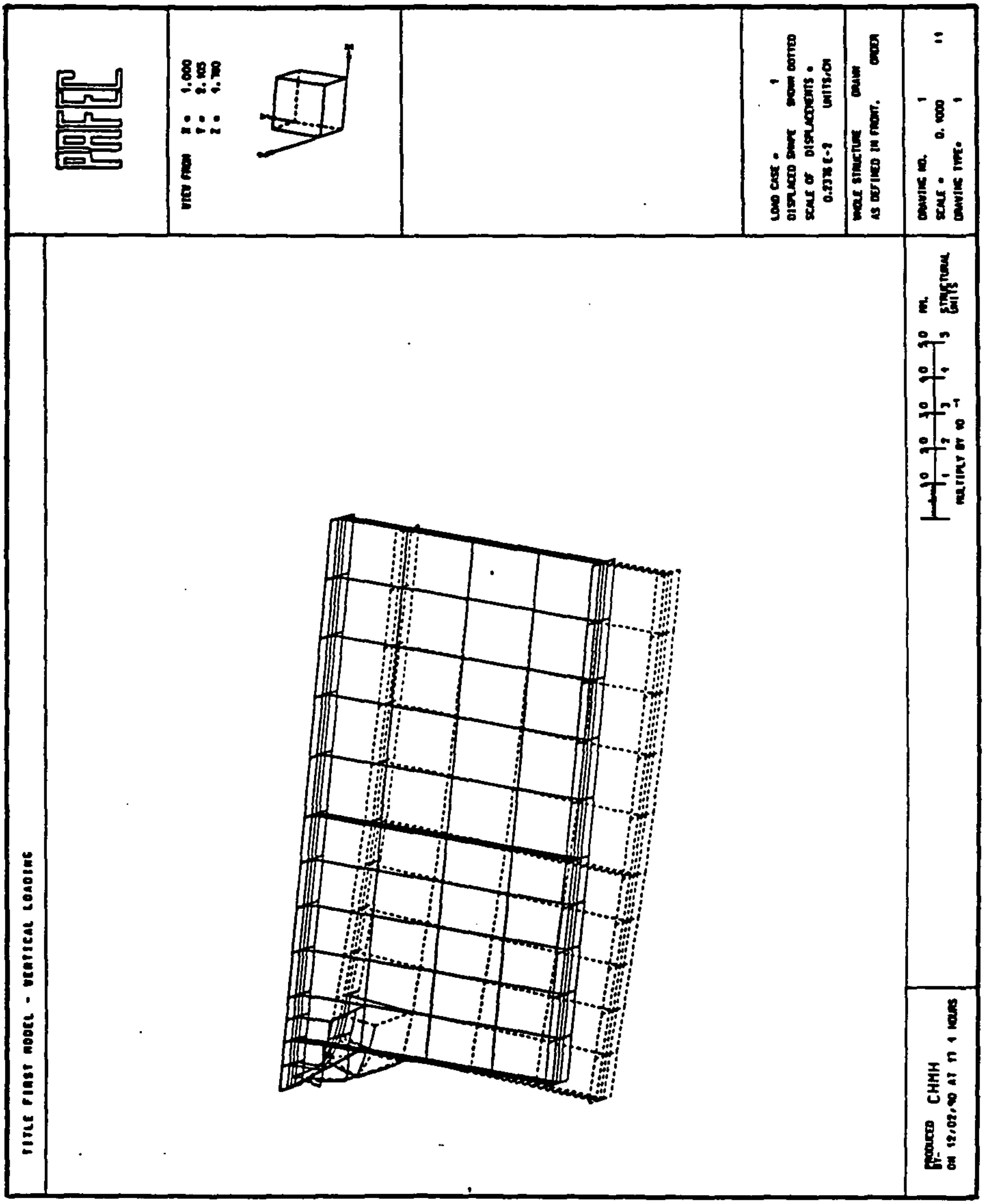

Figure 5.8 Displacement Plot Vertical 1.5g Load Case - Refined Model

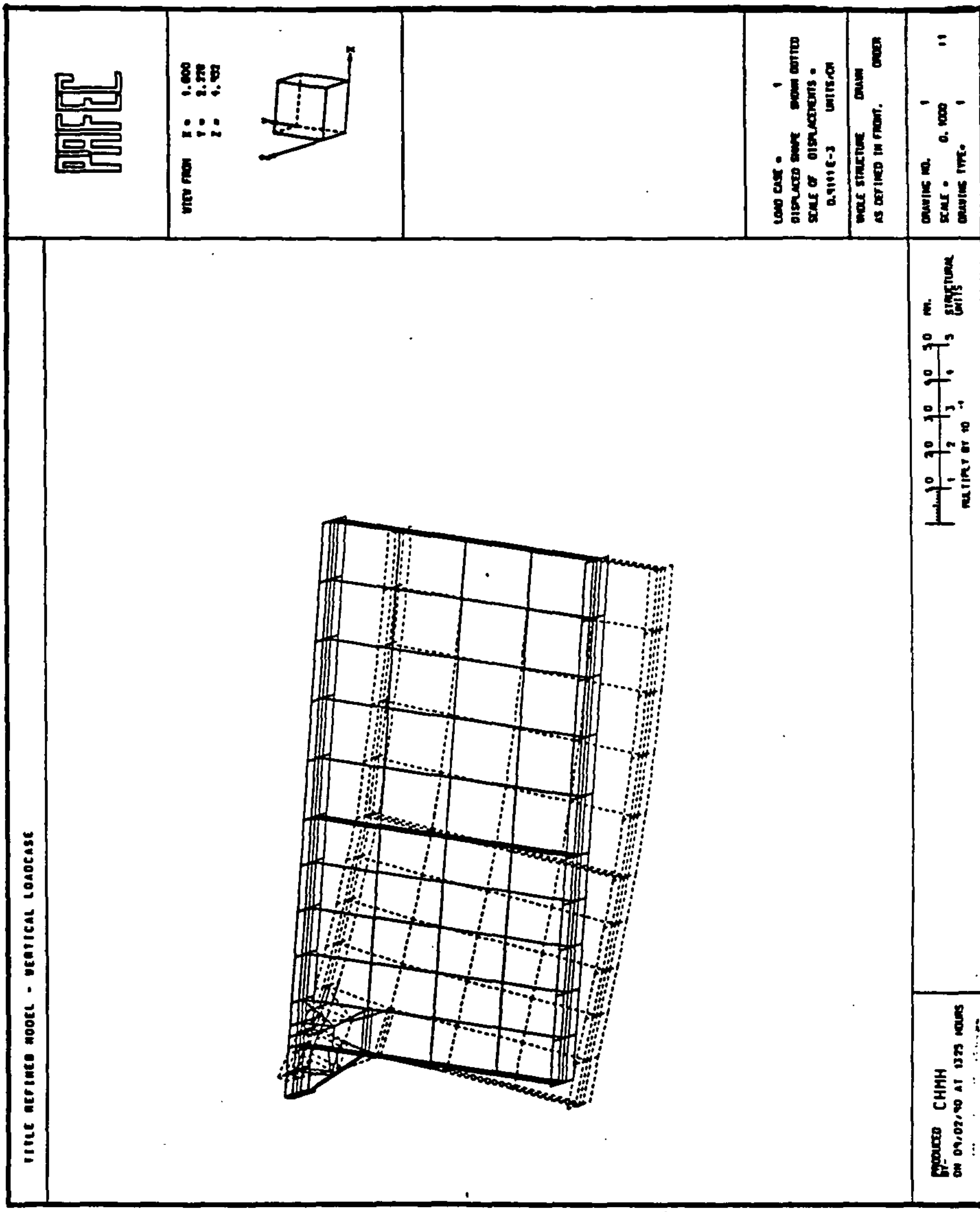

Figure 5.9 Displacement Plot Longitudinal Load Case - Refined Model

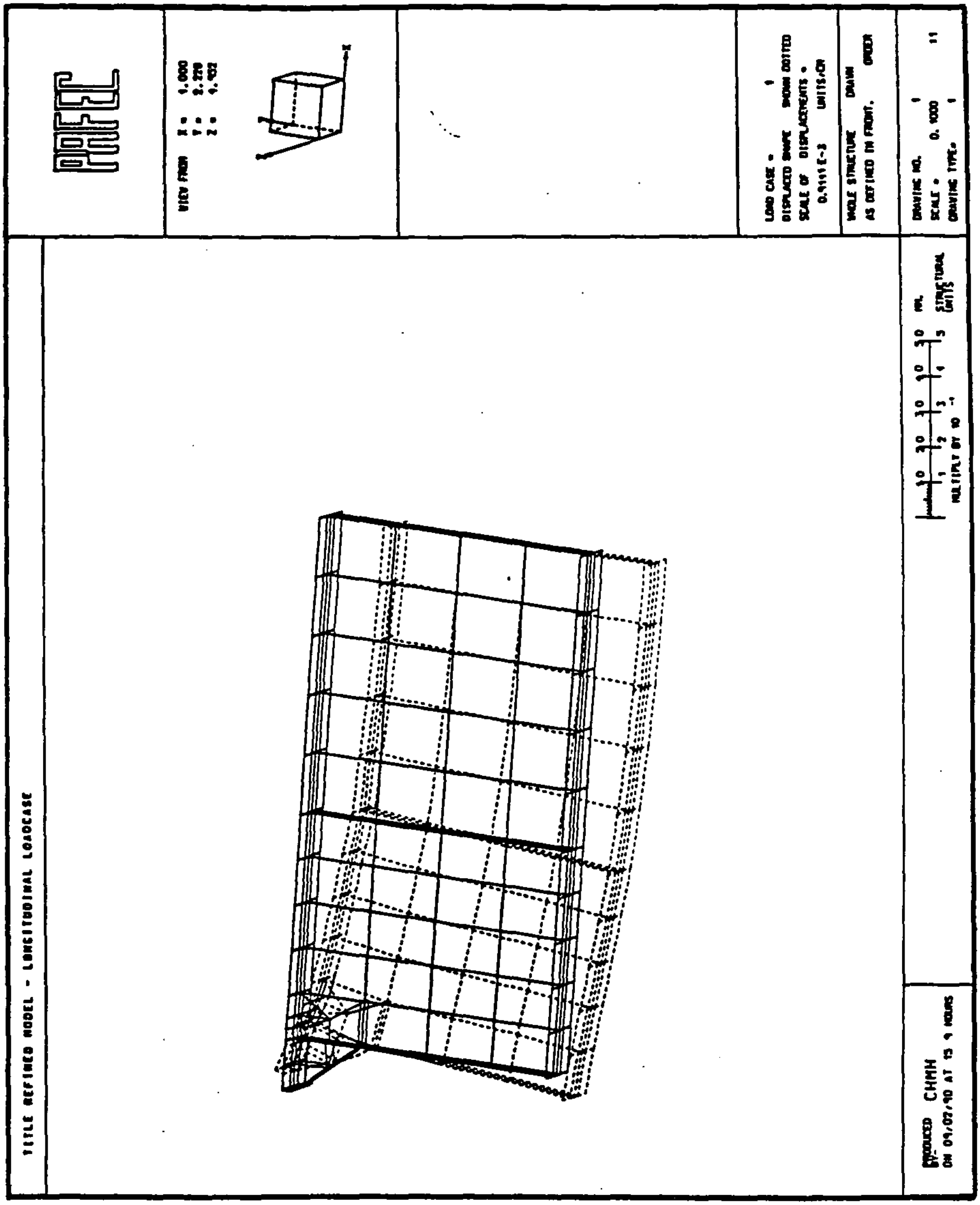

Figure 5.10 Displacement Plot Lateral Load Case - Skeletal Model 2

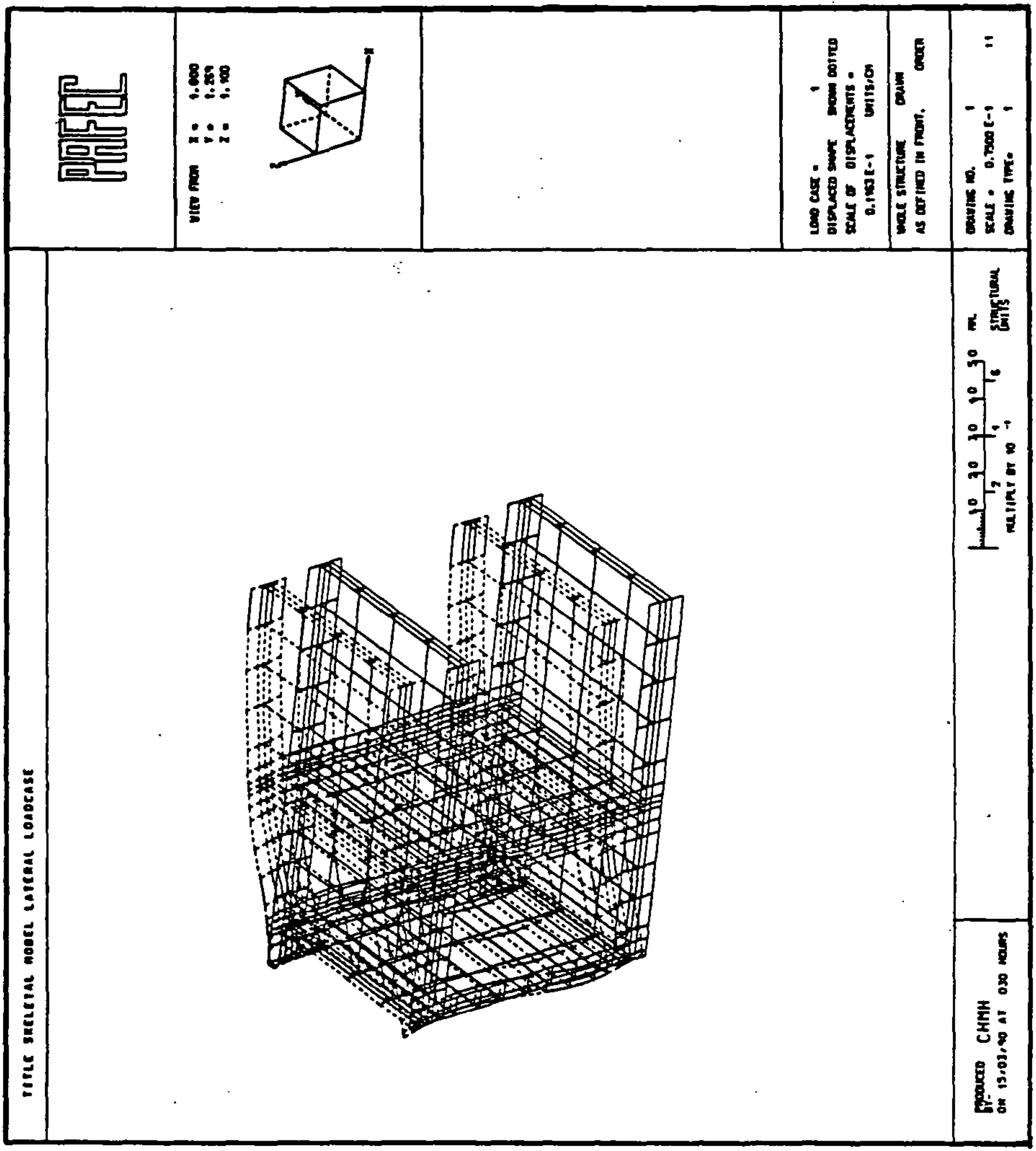

Figure 5.11 Direct Stress Distribution at the Support and along the Upper Flange.
A Longitudinal Beam, Vertical Load Case – First Model

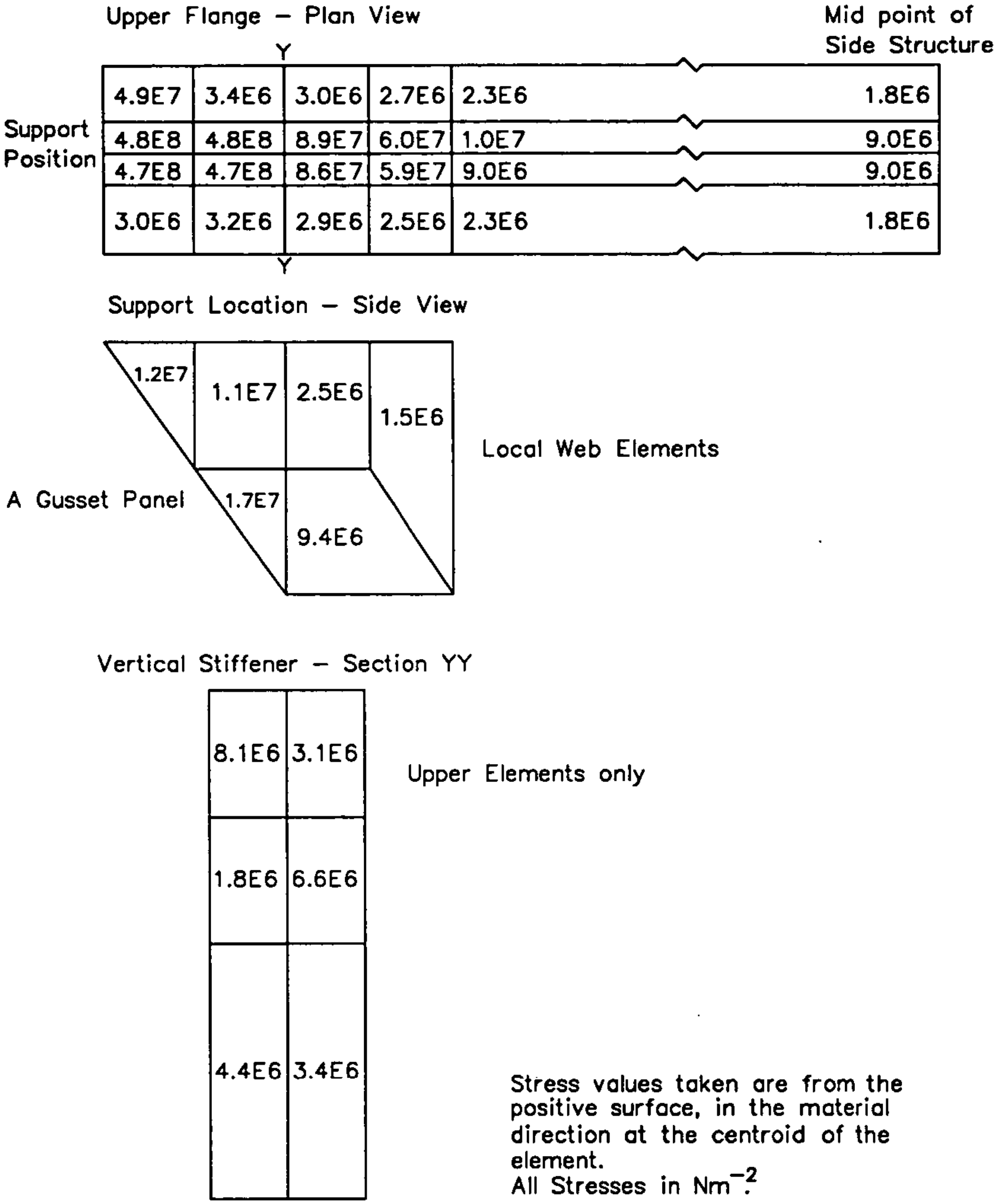

Stress values taken are from the positive surface, in the material direction at the centroid of the element.
All Stresses in Nm^{-2}.

Figure 5.12 Direct Stress Distribution at the Support and along the Upper Flange. A Longitudinal Beam, Vertical Load Case – Refined Model

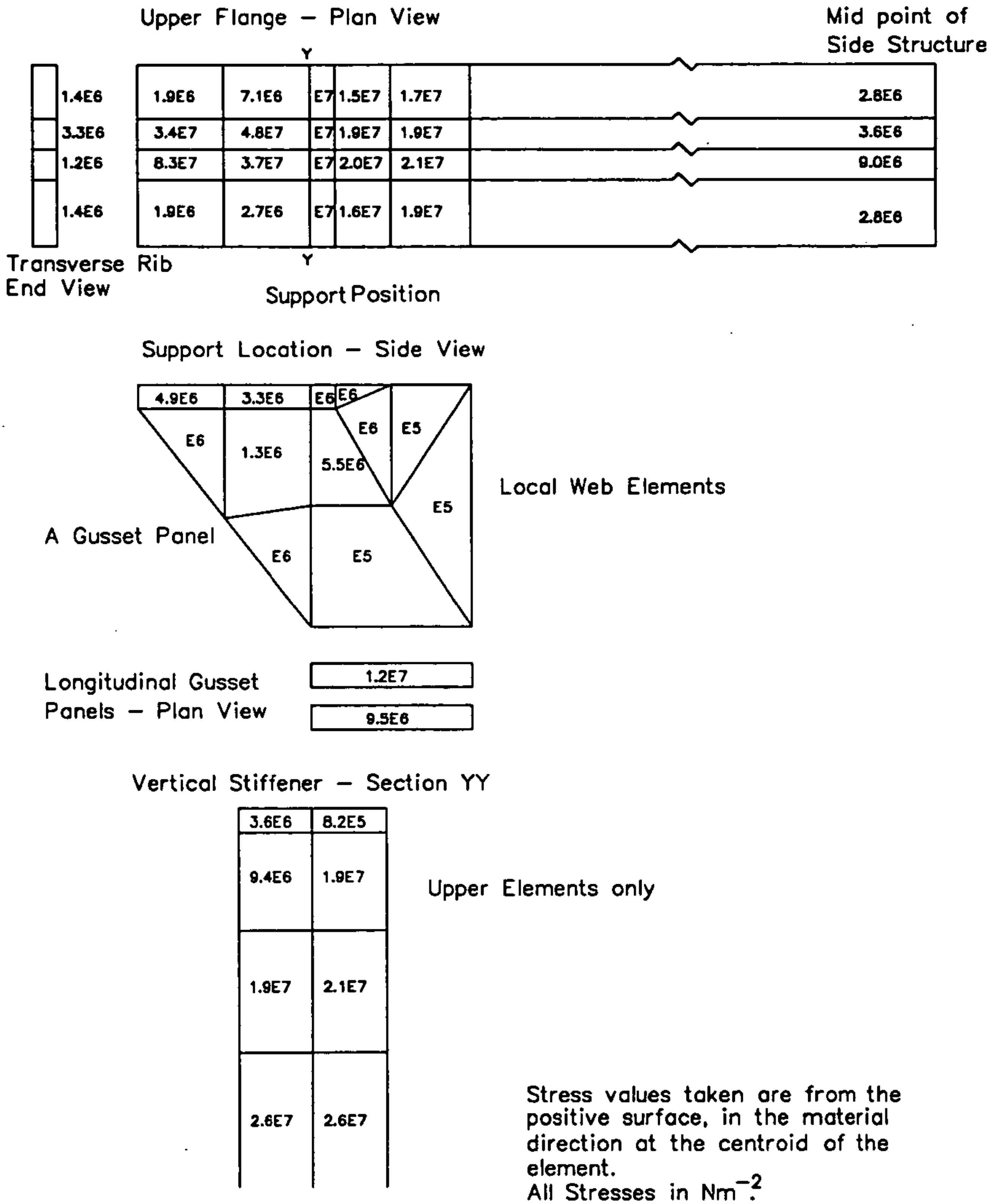

Figure 5.13 Direct Stress Distribution at the Support and along the Upper Flange.
A Longitudinal Beam, Longitudinal Load Case — Refined Model

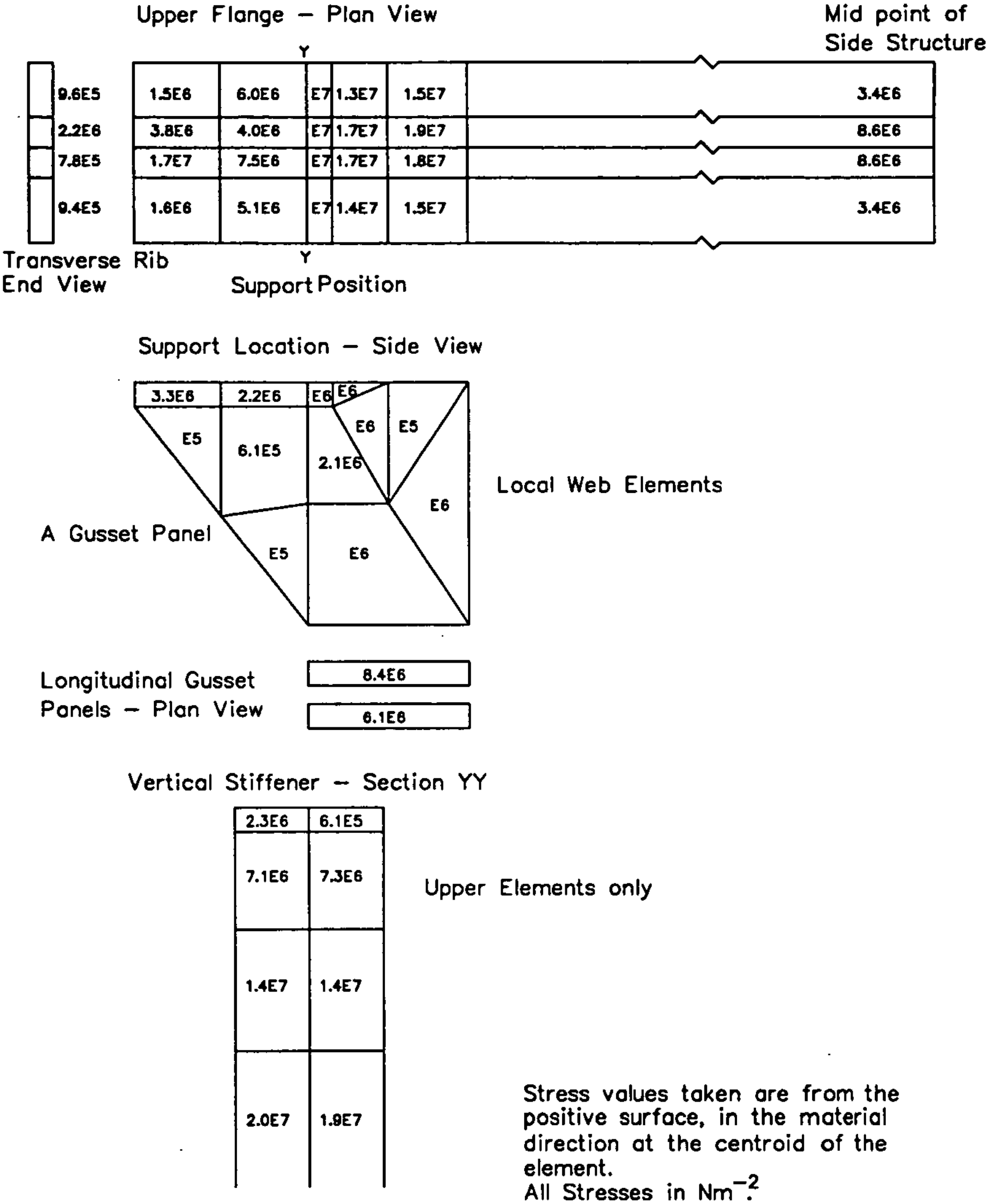

Stress values taken are from the positive surface, in the material direction at the centroid of the element.
All Stresses in Nm^{-2}.

Figure 5.14 Direct Stress Distribution at the Support and along the Upper Flange
Skeletal Model, Lateral Load Case – Model #1

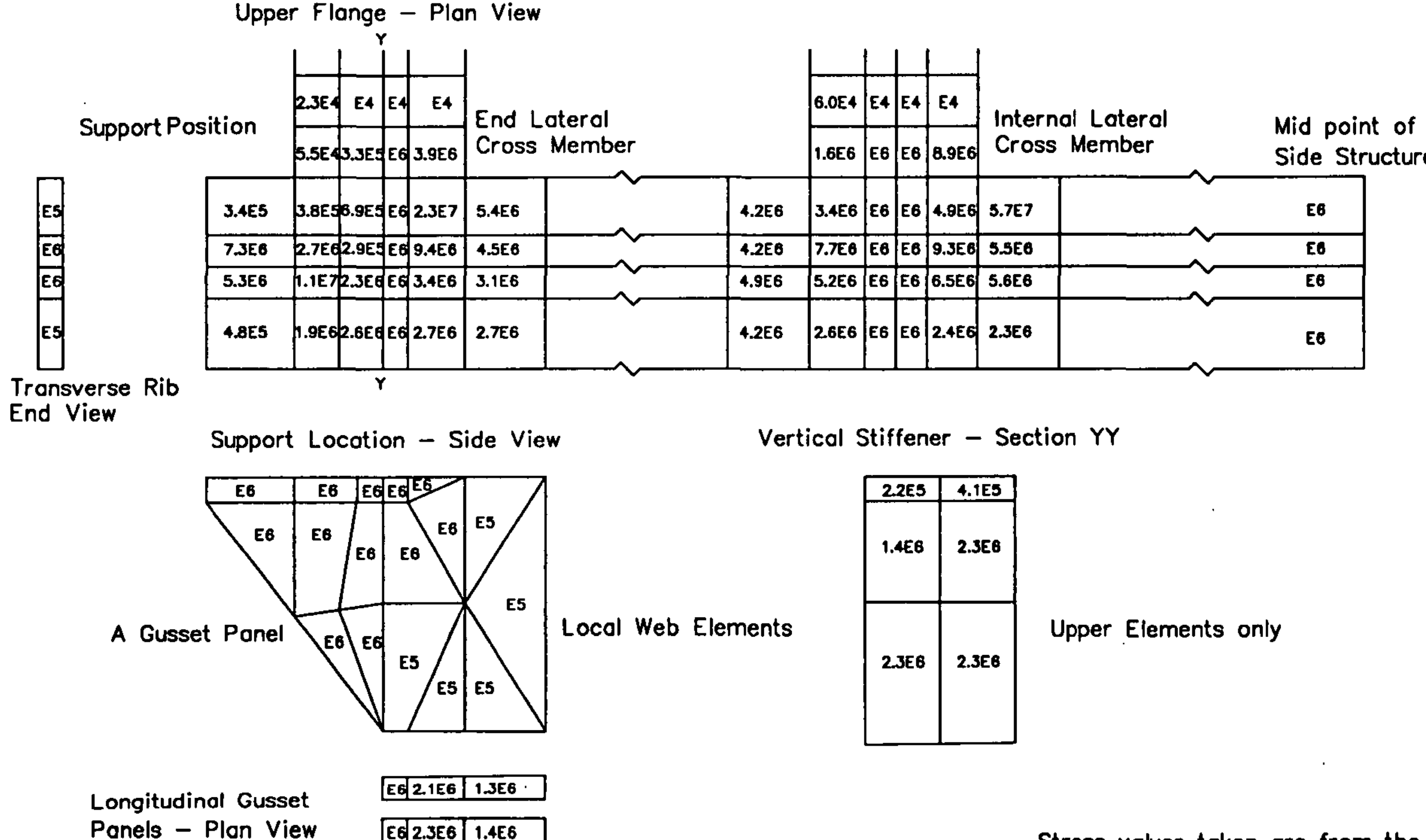

Stress values taken are from the positive surface, in the material direction at the centroid of the element.
All Stresses in Nm^{-2}.

Figure 5.15 Direct Stress Distribution at the Support and along the Upper Flange
Skeletal Model, Lateral Load Case – Model #2

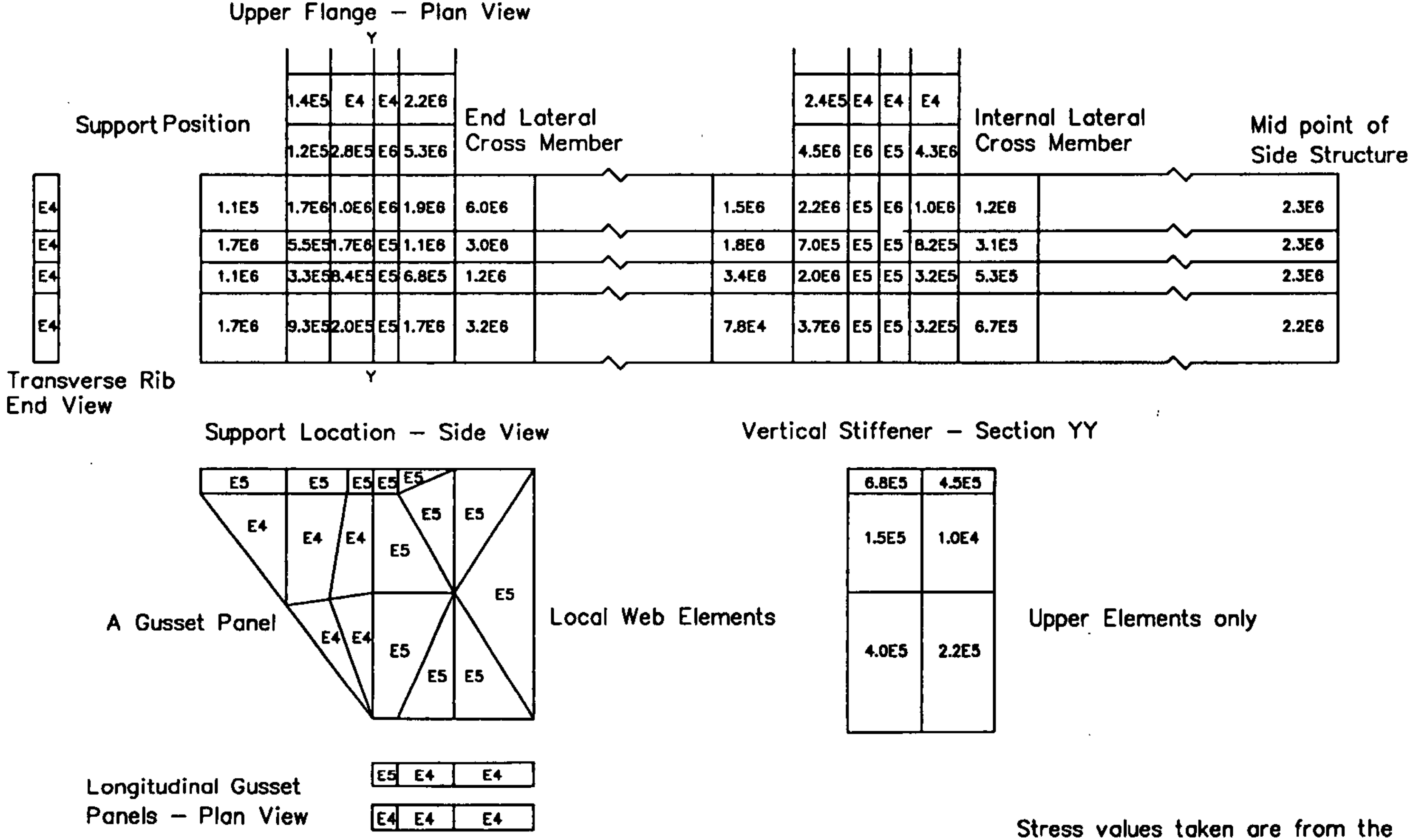

Stress values taken are from the positive surface, in the material direction at the centroid of the element.
All Stresses in Nm^{-2}.

5-32

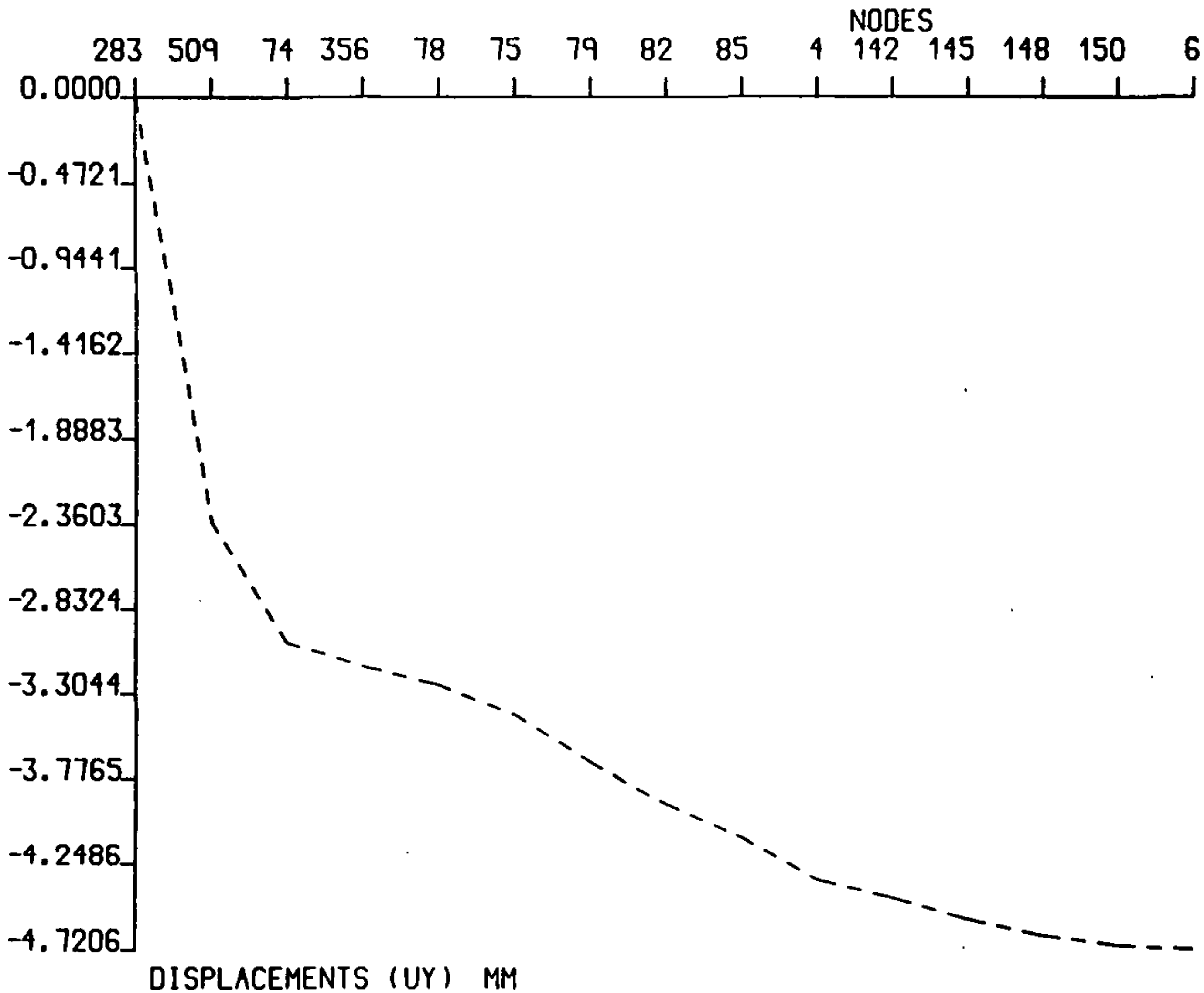

KEY
— UX DISP.
- - UY DISP.

LOADCASE
1.5G VERTICAL
(DOWN)

TITLE VERTICAL (UY) DISPLACEMENTS ALONG THE UPPER FLANGE - FIRST MODEL

Figure 5.16

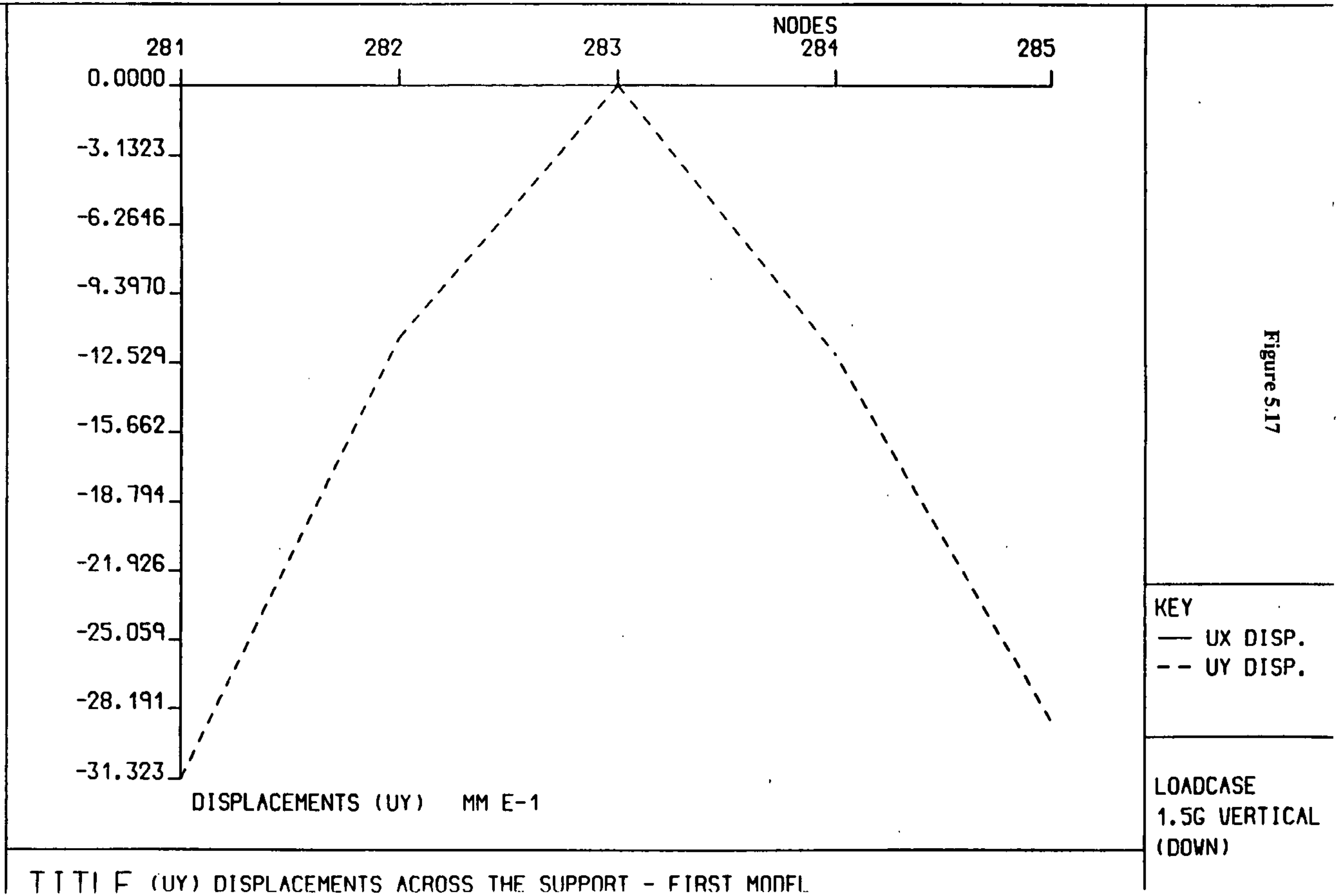
NODES
281
282
283
284
285
0.0000
-3.1323
-6.2646
-9.3970
-12.529
-15.662
-18.794
-21.926
-25.059
-28.191
-31.323
DISPLACEMENTS (UY) MM E-1
KEY
UX DISP.
UY DISP.
LOADCASE
1.5G VERTICAL
(DOWN)
TITLE (UY) DISPLACEMENTS ACROSS THE SUPPORT - FIRST MODEL

Figure 5.17

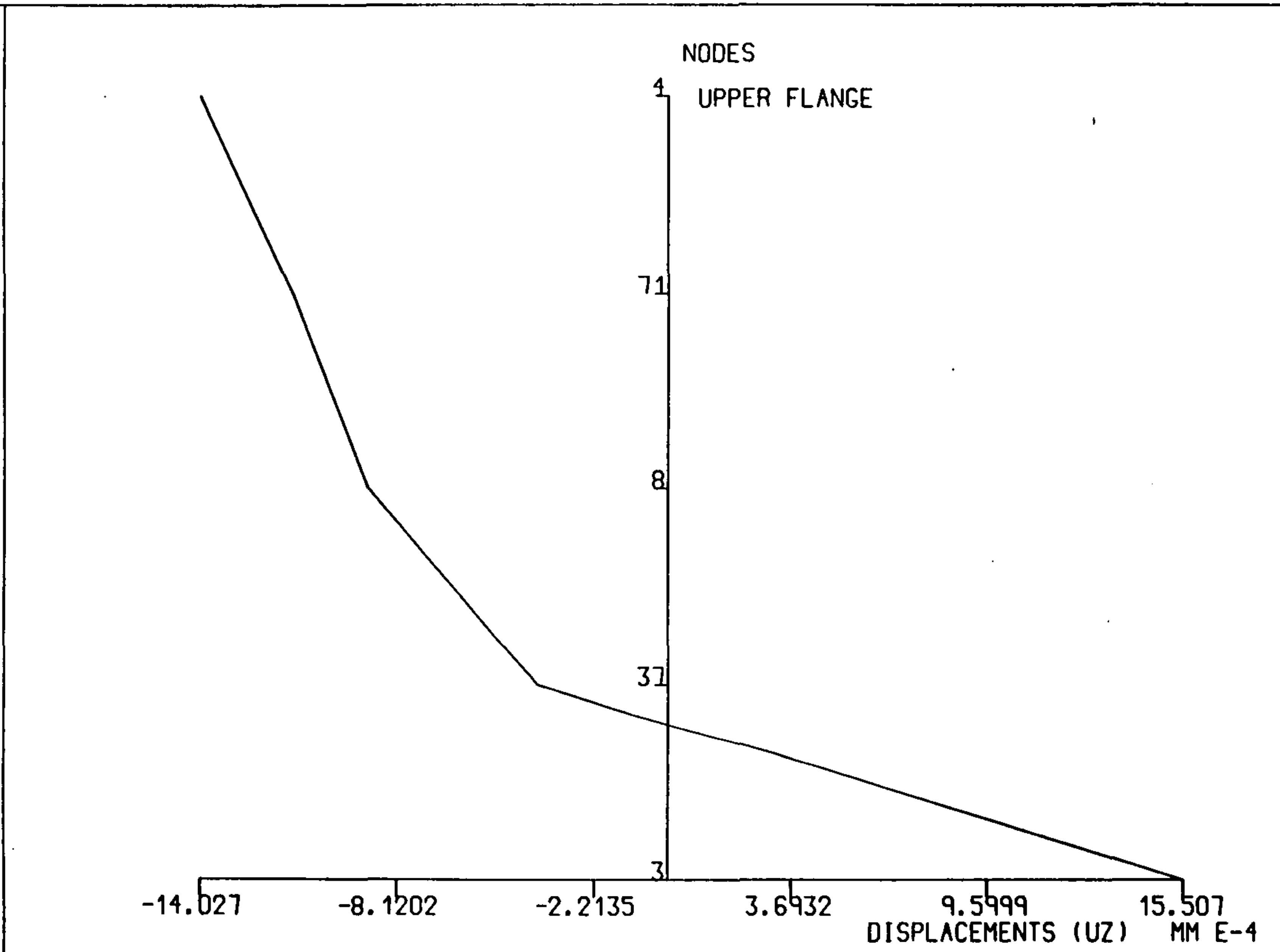

KEY
— UZ DISP.

LOADCASE
1.5G VERTICAL
(DOWN)

TITLE LATERAL (UZ) DISPLACEMENTS THROUGH THE CHOKE LOAD PATH - FIRST MODEL

Figure 5.18

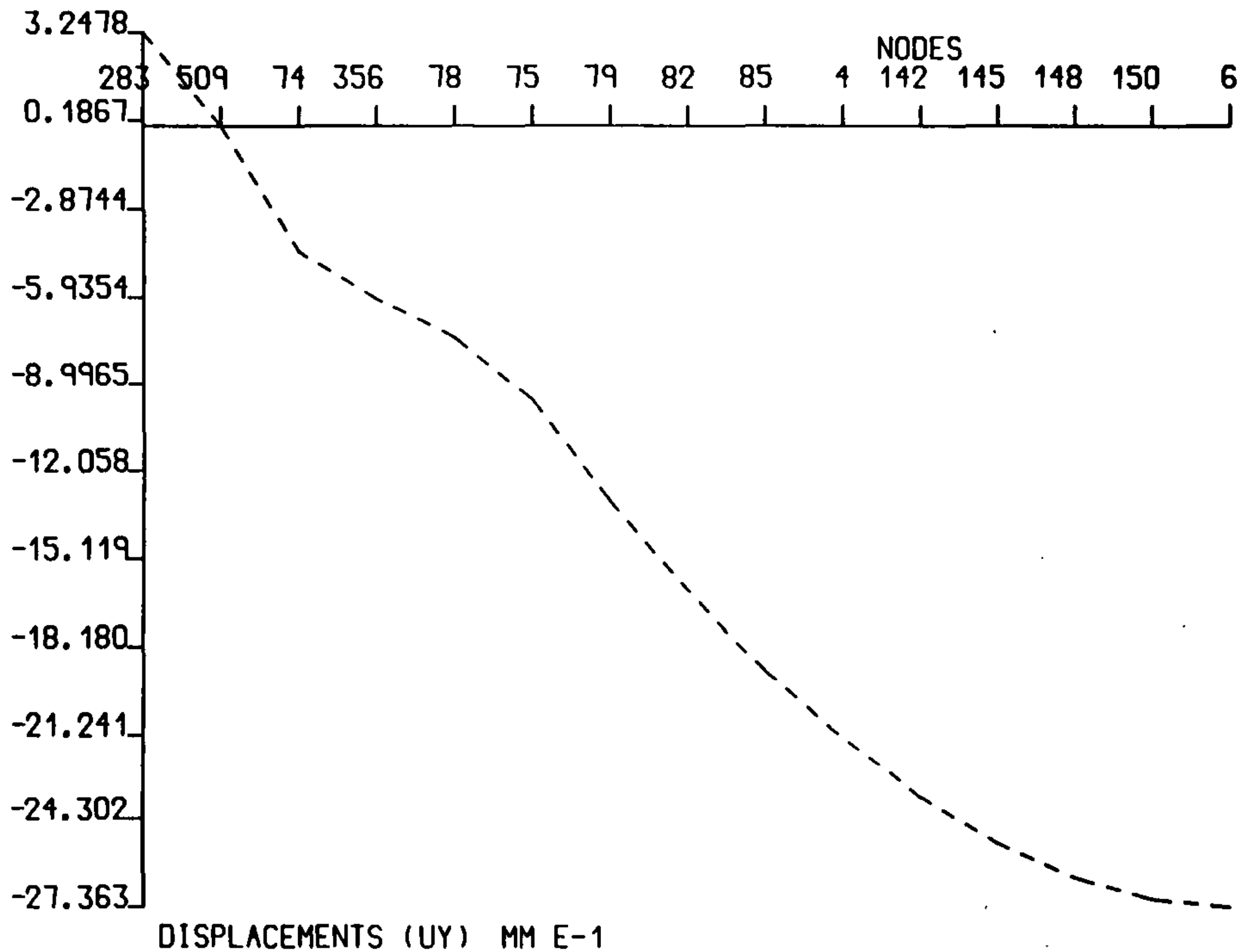

KEY
— UX DISP.
-- UY DISP.

LOADCASE
1.5G VERTICAL
(DOWN)

TITLE VERTICAL (UY) DISPLACEMENTS ALONG THE UPPER FLANGE - REFINED MODEL

Figure 5.19

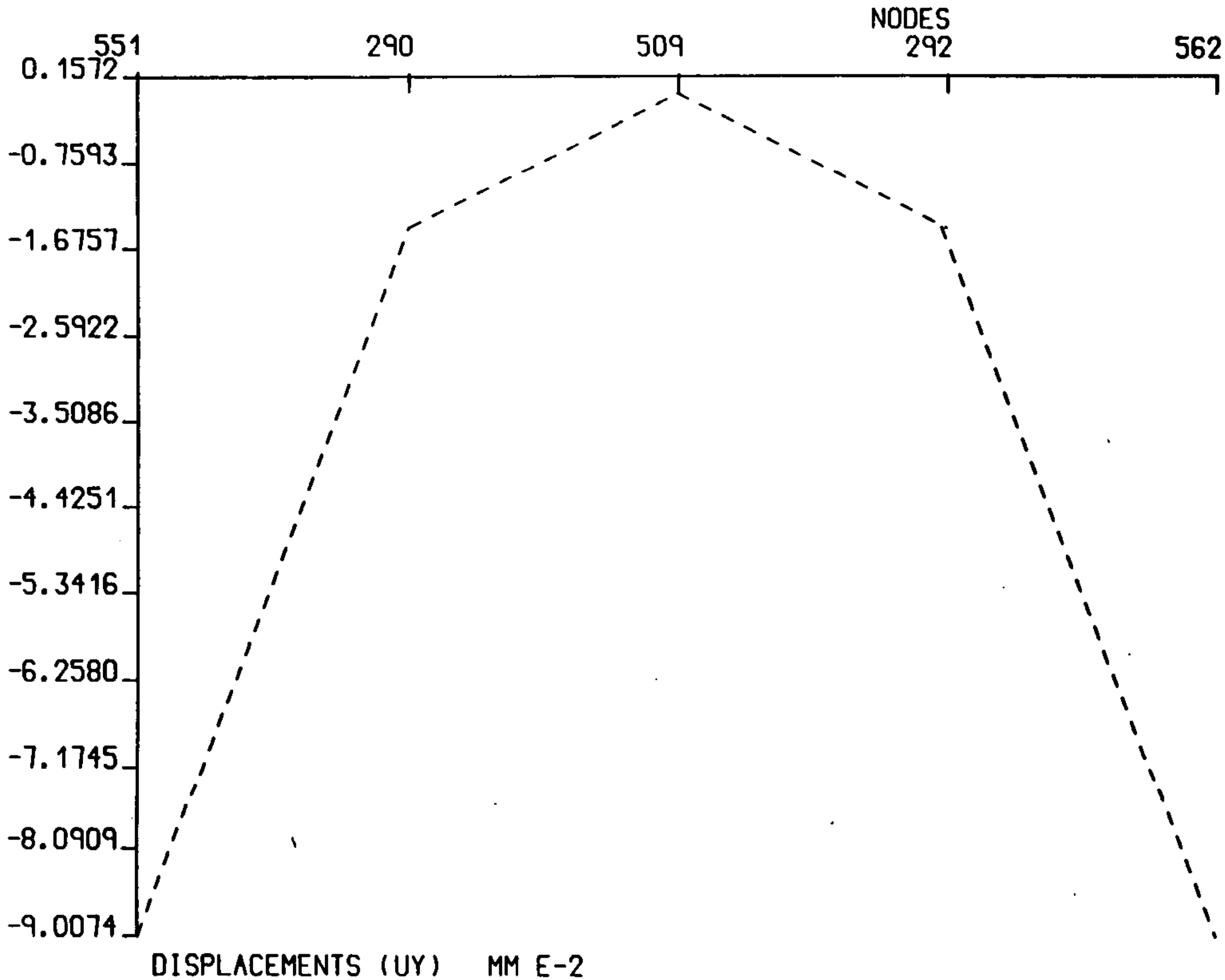

KEY
— UX DISP.
-- UY DISP.

LOADCASE
1.5G VERTICAL
(DOWN)

TITLE (UY) DISPLACEMENTS ACROSS THE SUPPORT - REFINED MODEL

Figure 5.20

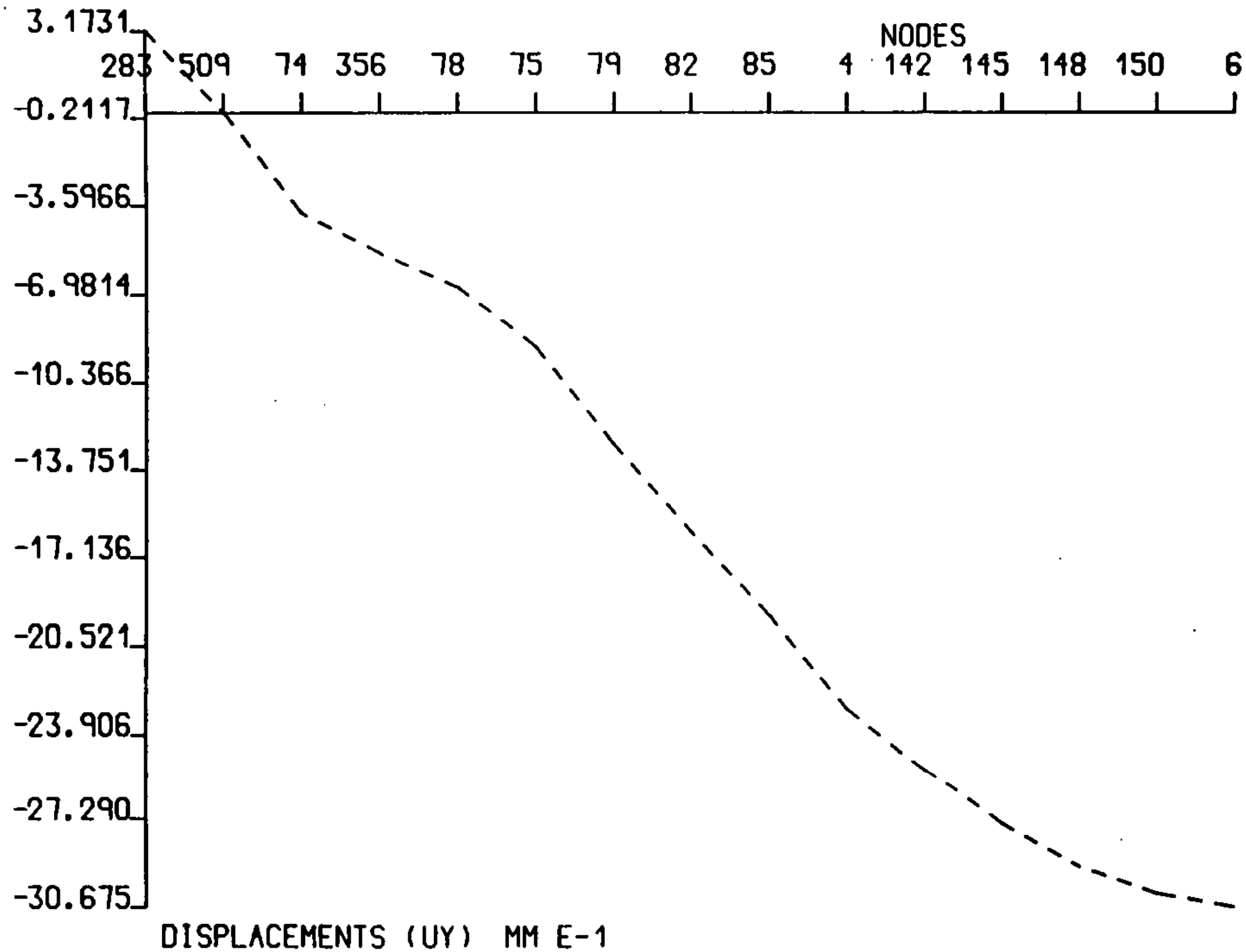

KEY
— UX DISP.
- - UY DISP.

LOADCASE
1.0G VERTICAL
(DOWN)
3.0G LONG.

TITLE VERTICAL (UY) DISPLACEMENTS ALONG THE UPPER FLANGE - REFINED MODEL

Figure 5.21

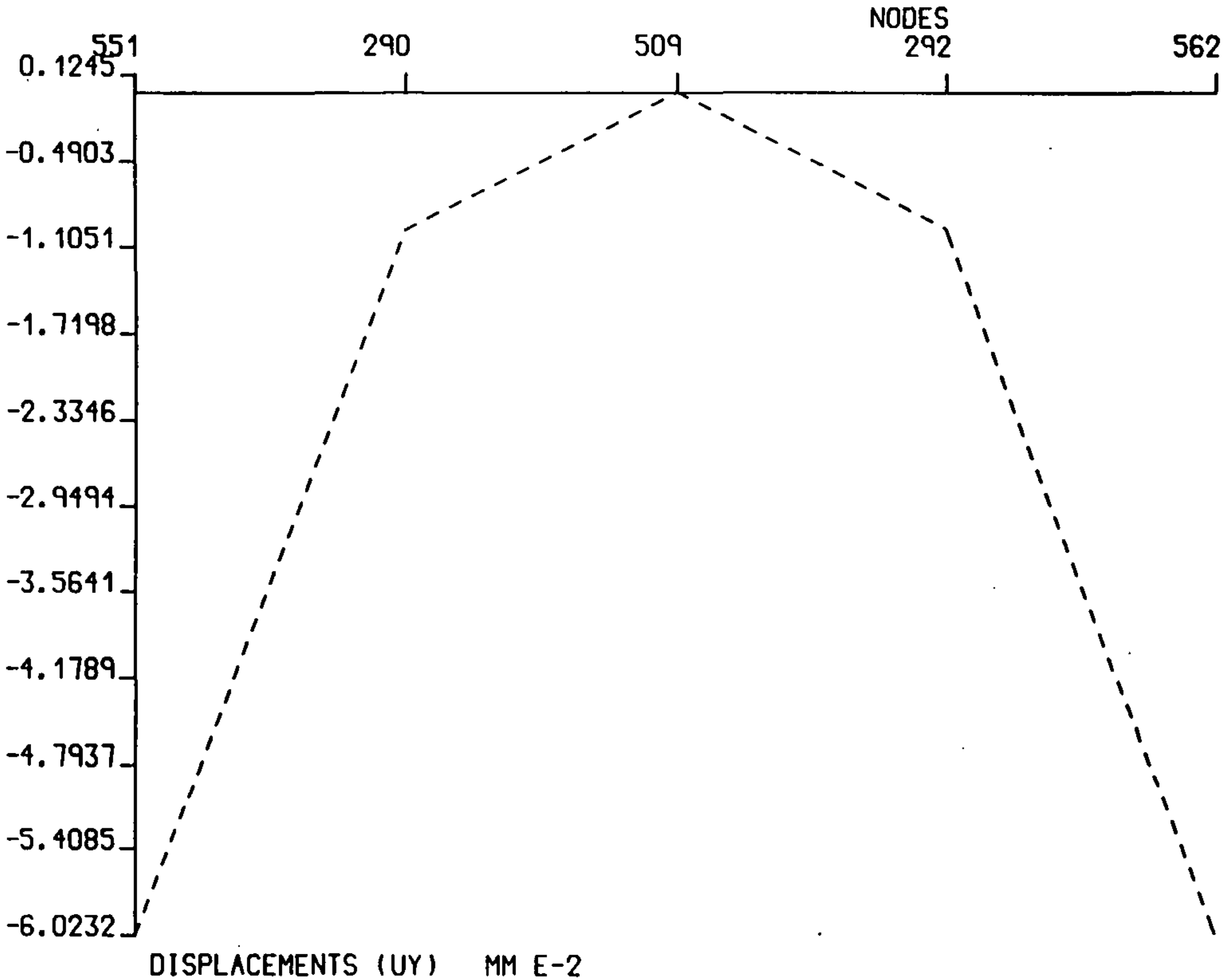

TITLE VERTICAL (UY) DISPLACEMENTS ACROSS THE SUPPORT - REFINED MODEL

KEY
— UX DISP.
-- UY DISP.

LOADCASE
1.0G VERTICAL
(DOWN)
3.0G LONG

Figure 5.22

5-40

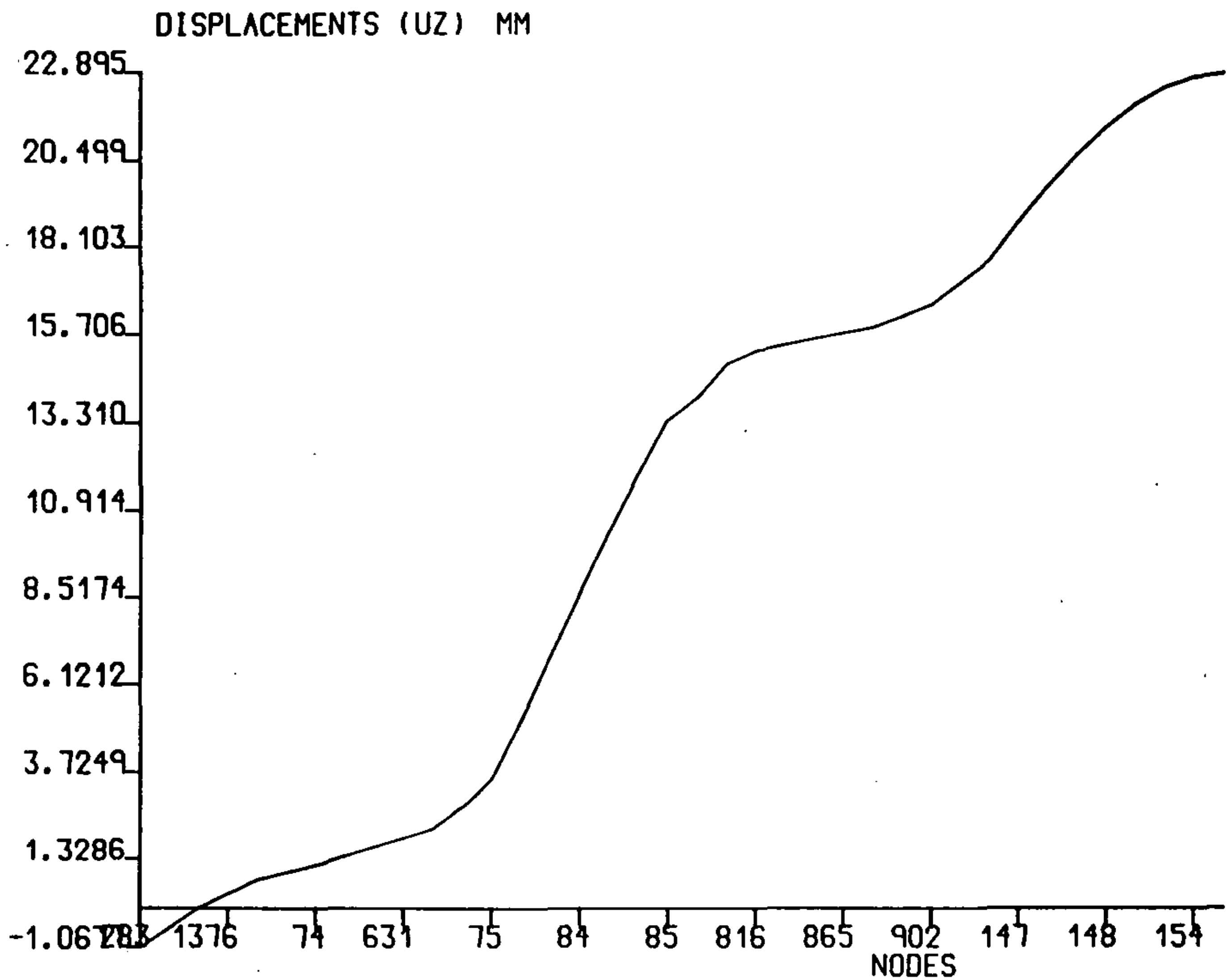

KEY
— UZ DISP.
- - UY DISP.

LOADCASE
1.0G VERTICAL
(DOWN)

TITLE LATERAL (UZ) DISPLACEMENTS ALONG THE RHS UPPER FLANGE - SKELETAL MODEL

Figure 5.23

Figure 5.24

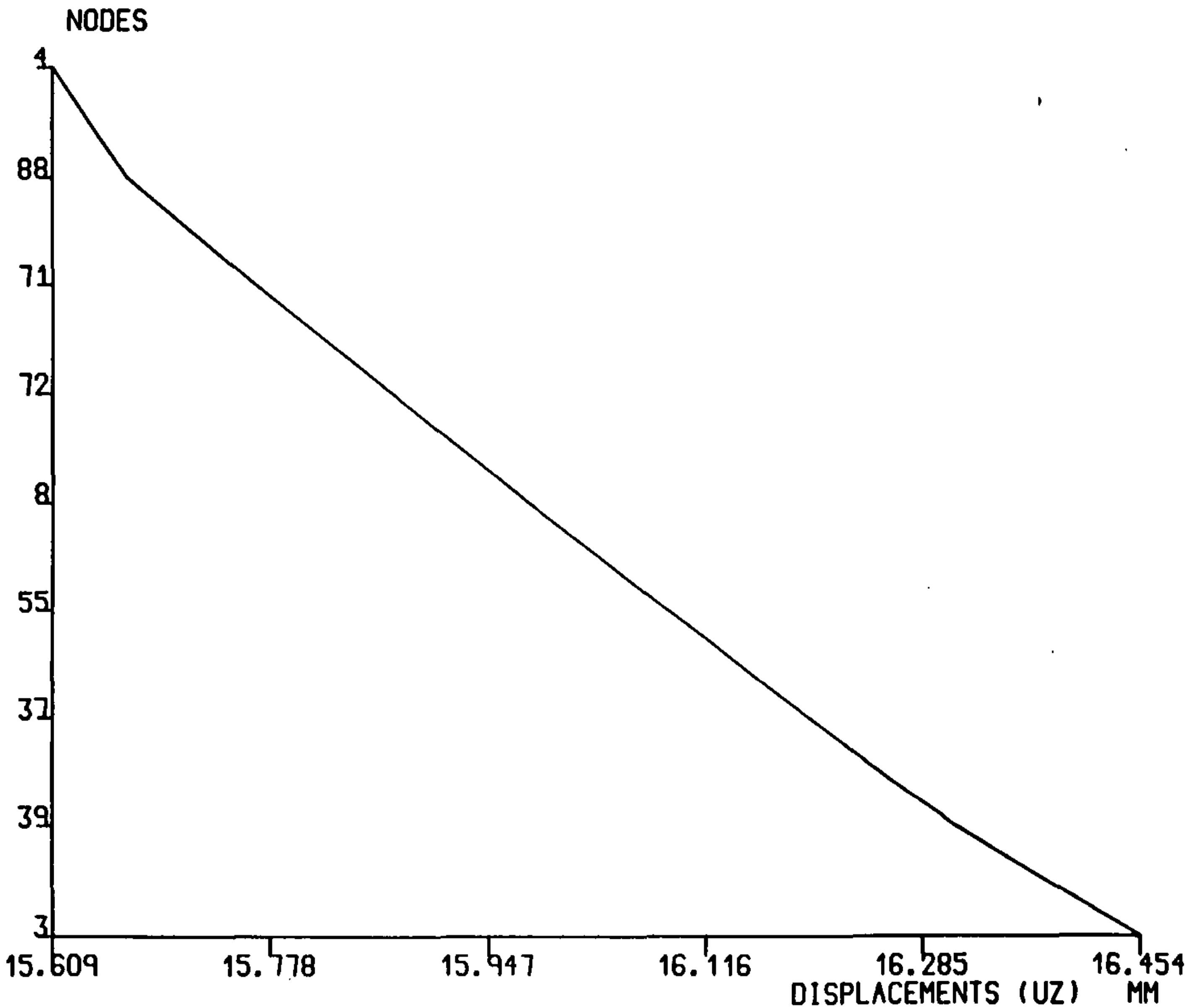

KEY
— UZ DISP.

LOADCASE
1.0G VERTICAL
(DOWN)
1.1G LAT

TITLE LATERAL (UZ) DISPLACEMENTS ALONG THE RHS CHOKE LOCATION SKELETAL MODEL

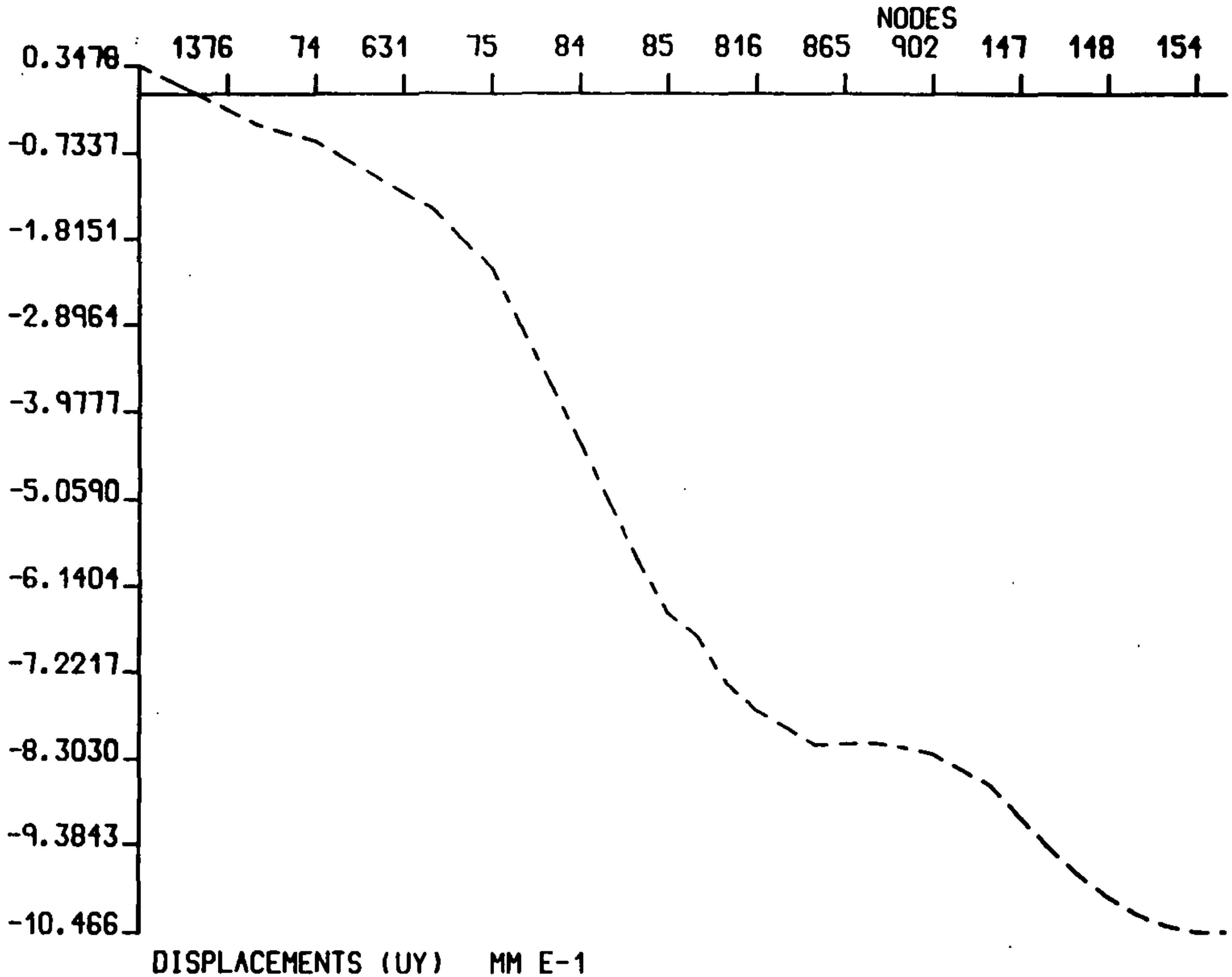

KEY
— UX DISP.
-- UY DISP.

LOADCASE
1.0G VERTICAL
(DOWN)

TITLE VERTICAL (UY) DISPLACEMENTS ALONG THE RHS UPPER FLANGE - SKELETAL MODEL

Figure 5.25

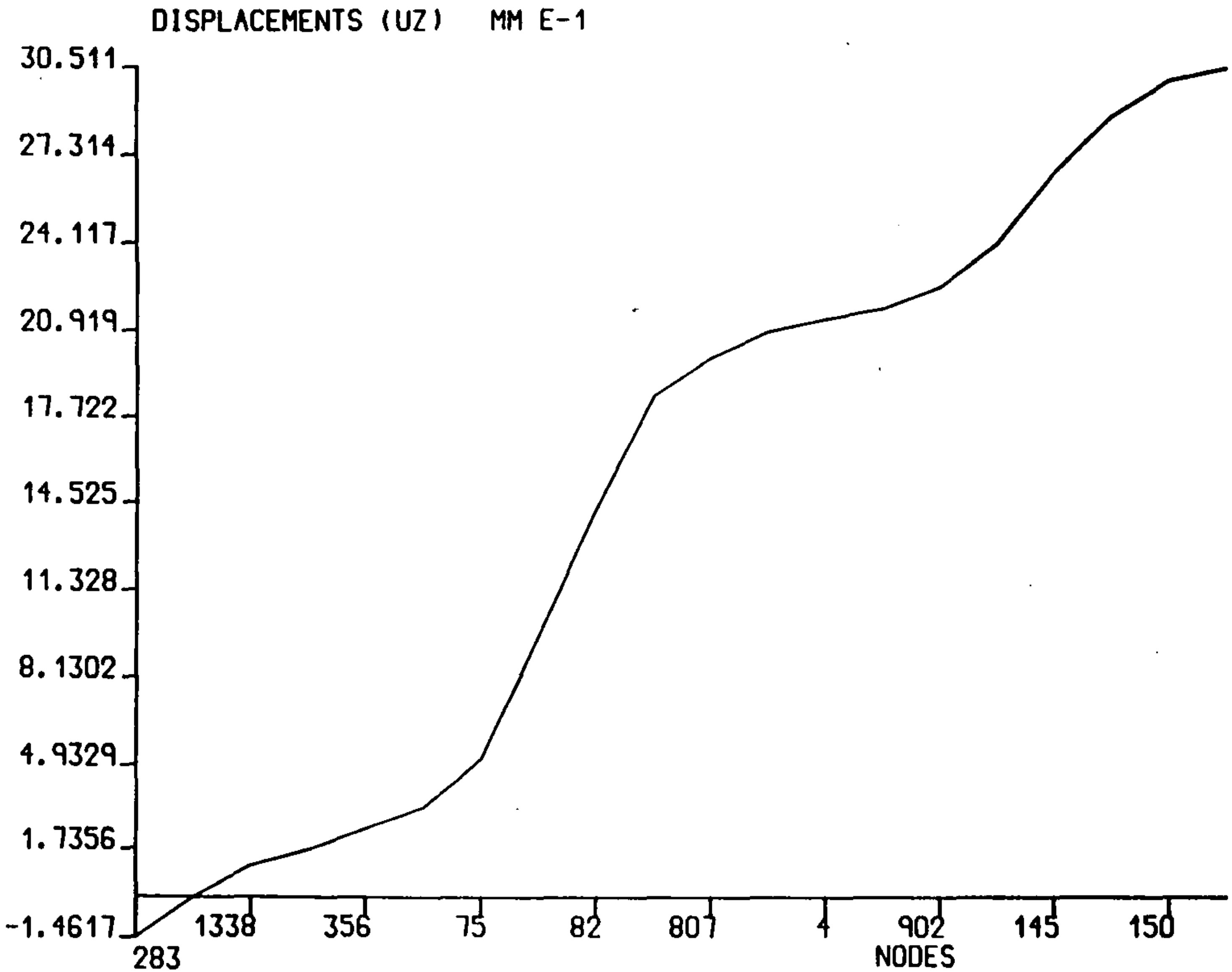

KEY
— UZ DISP.
-- UY DISP.

LOADCASE
1.0G VERTICAL
(DOWN)
1.1G LAT

TITLE LATERAL (UZ) DISPLACEMENTS ALONG THE RHS UPPER FLANGE - SKELETAL MODEL #2

Figure 5.26

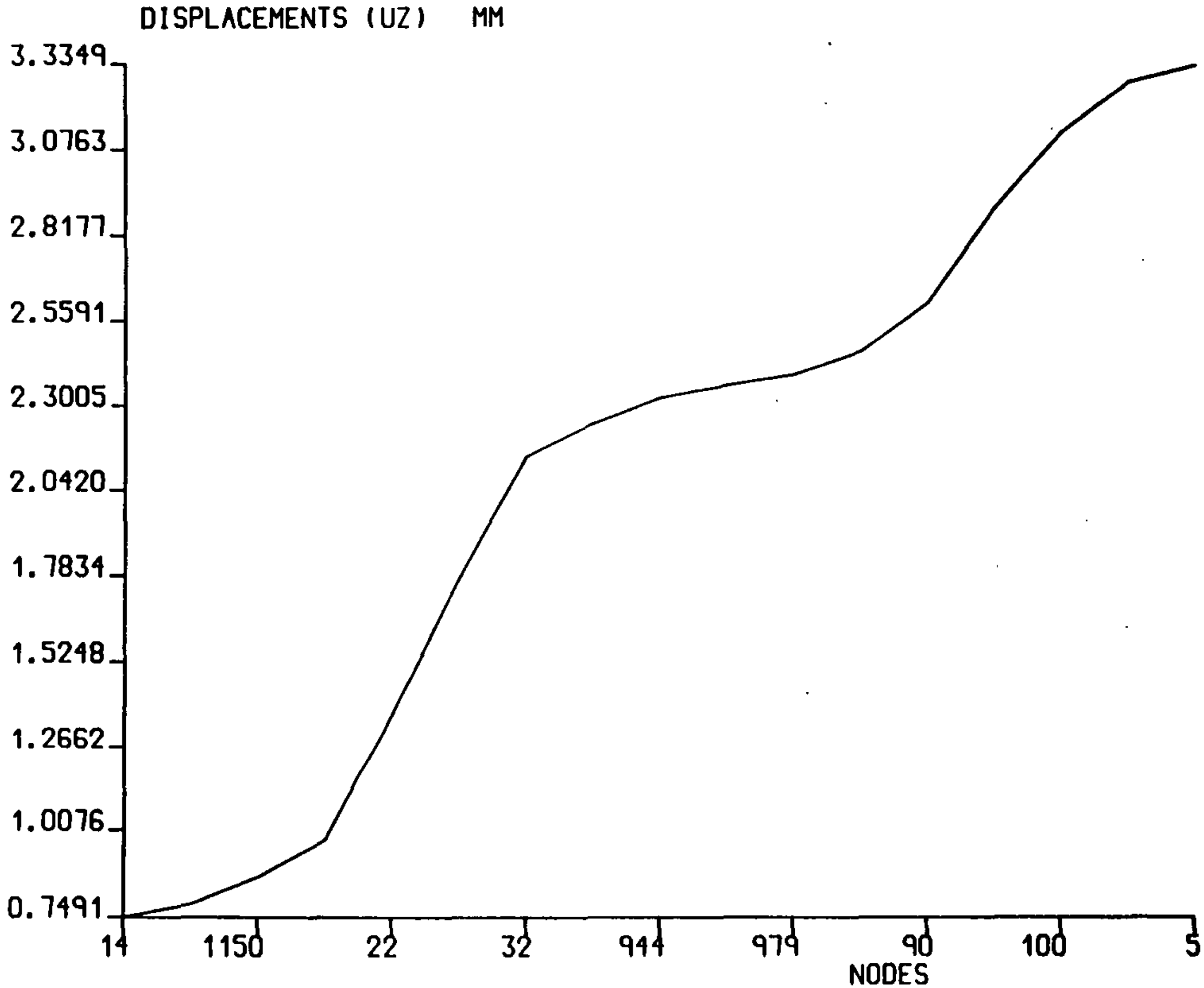

KEY
—— UZ DISP.
- - UY DISP.

LOADCASE
1.0G VERTICAL
(DOWN)

TITLE LATERAL (UZ) DISPLACEMENTS ALONG THE RHS LOWER FLANGE - SKELETAL MODEL #2

Figure 5.27

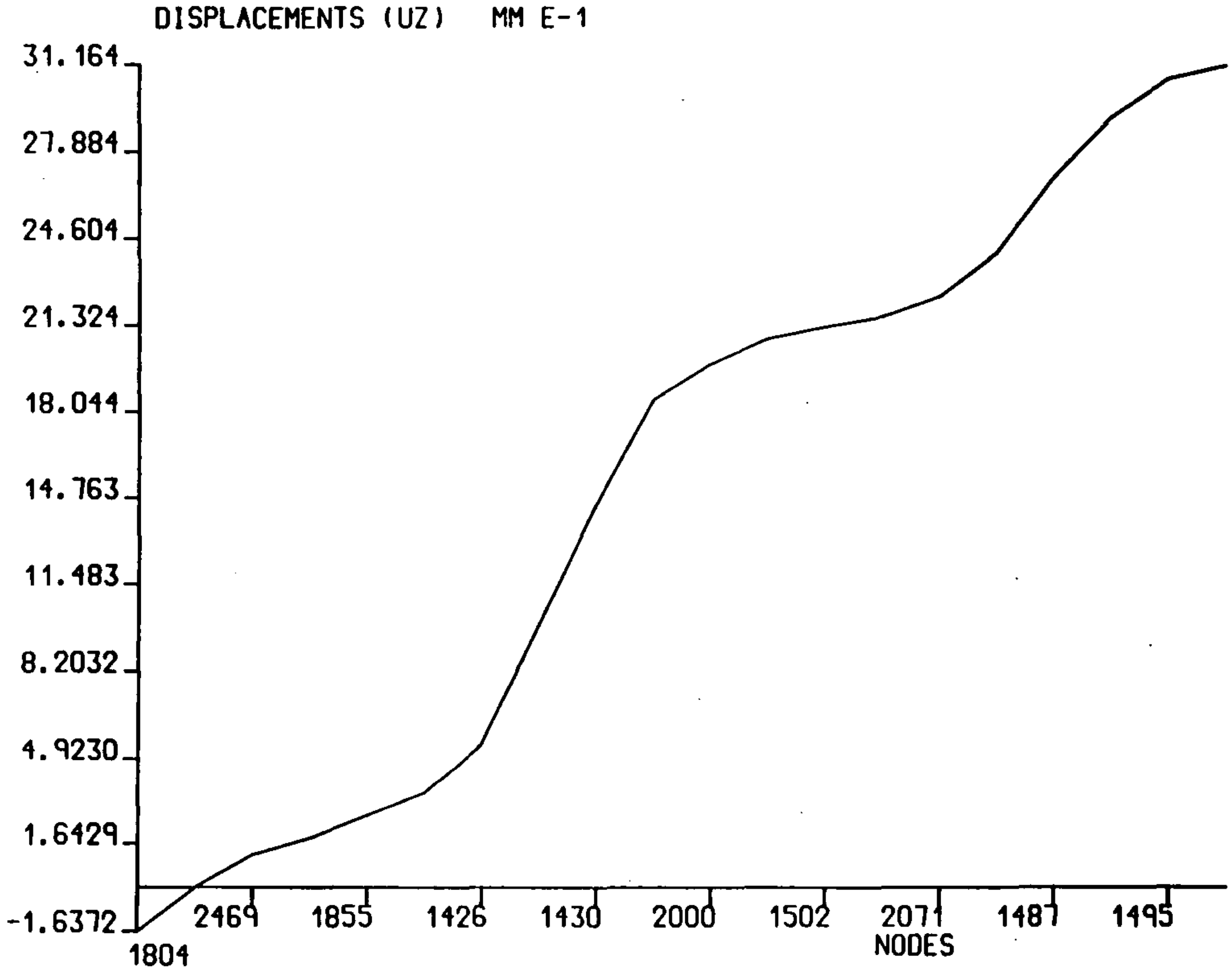

KEY
— UZ DISP.

LOADCASE
1.0G VERTICAL
(DOWN)
1.1G LAT.

TITLE LATERAL (UZ) DISPLACEMENTS ALONG THE LHS UPPER FLANGE - SKELETAL MODEL #2

Figure 5.28

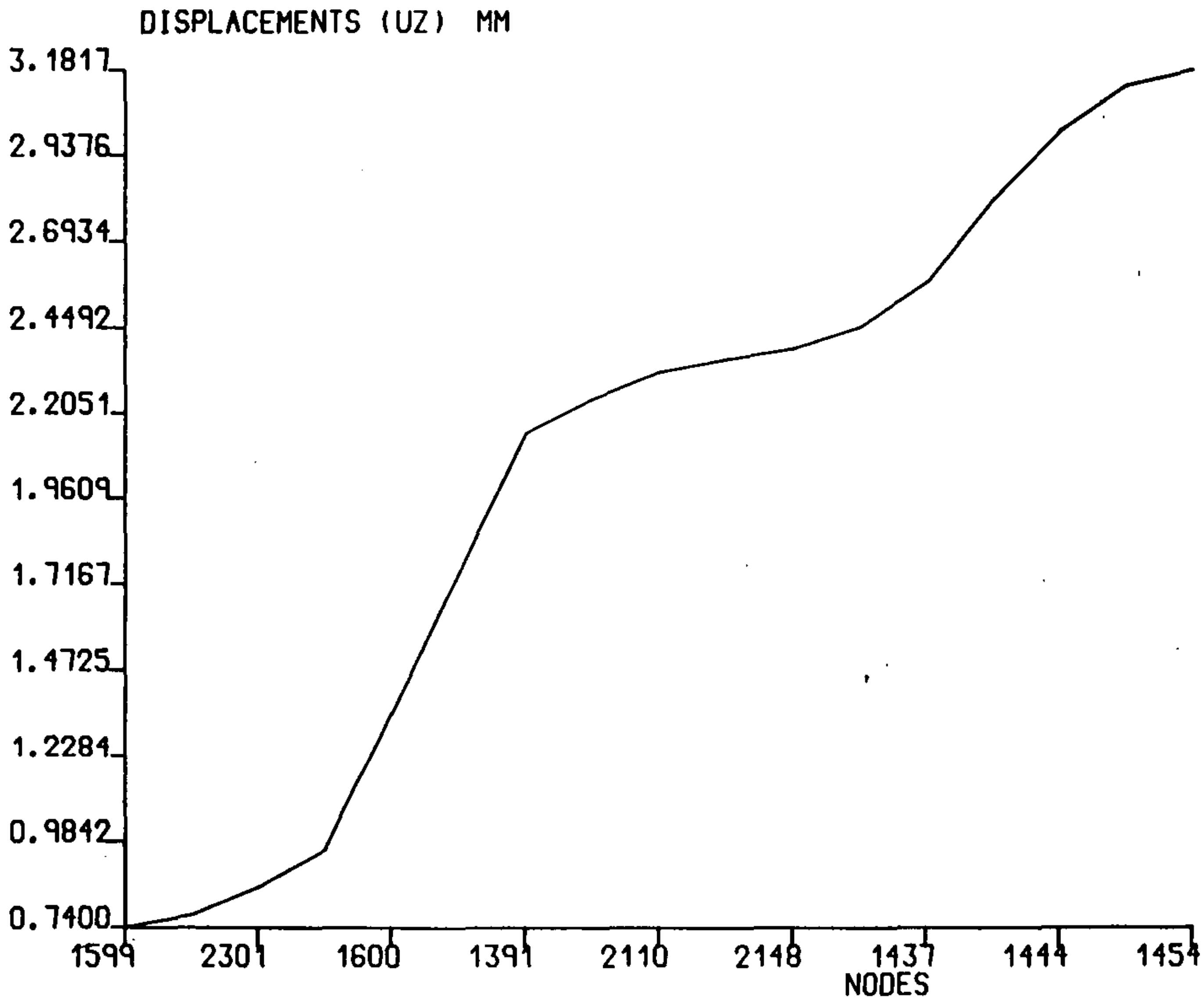

KEY
— UZ DISP.

LOADCASE
1.0G VERTICAL
(DOWN)

TITLE LATERAL (UZ) DISPLACEMENTS ALONG THE LHS LOWER FLANGE - SKELETAL MODEL #2

Figure 5.29

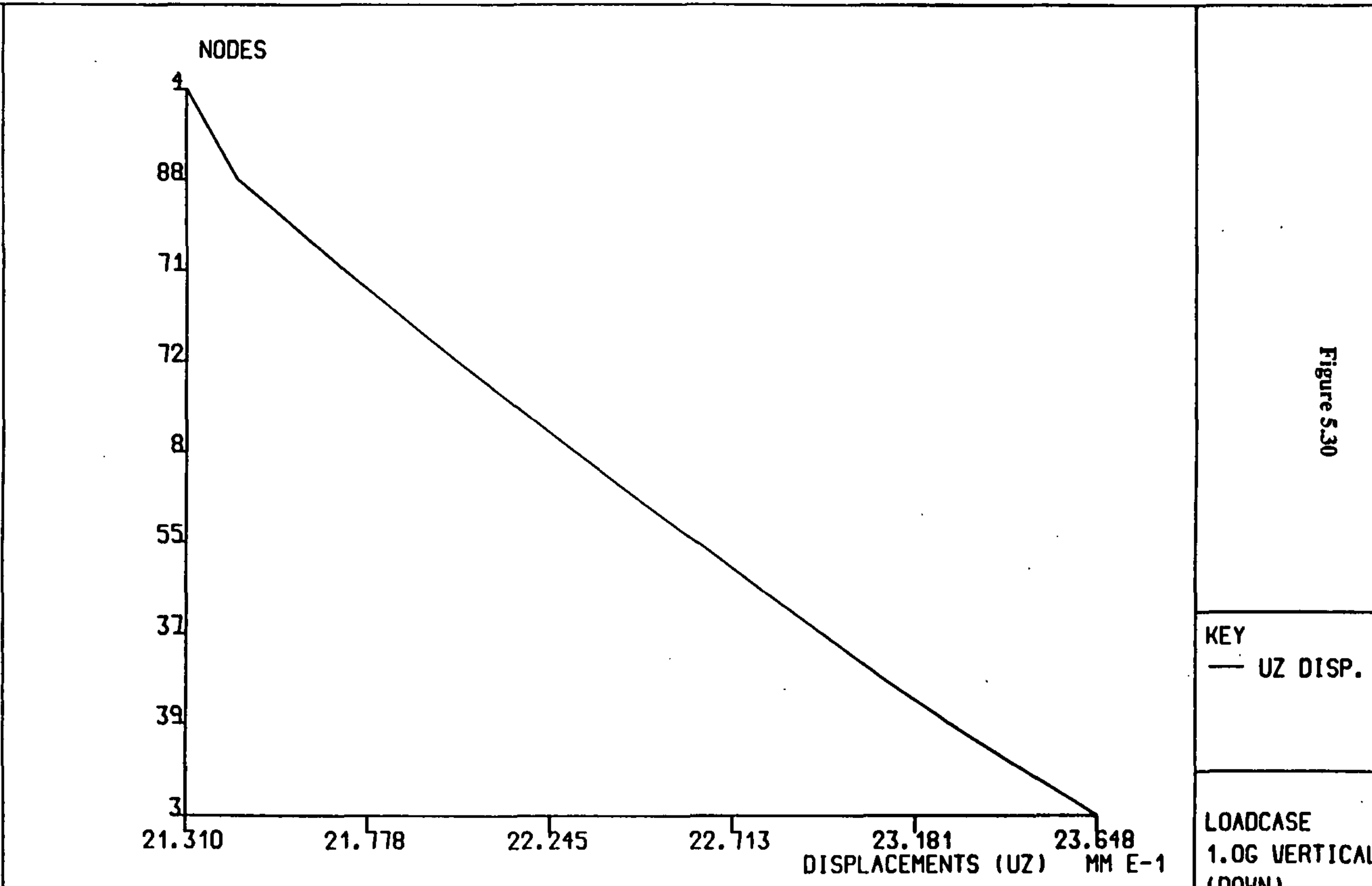

TITLE LATERAL (UZ) DISPLACEMENTS ALONG THE RHS CHOKE LOCATION SKELETAL MODEL #2

Figure 5.30

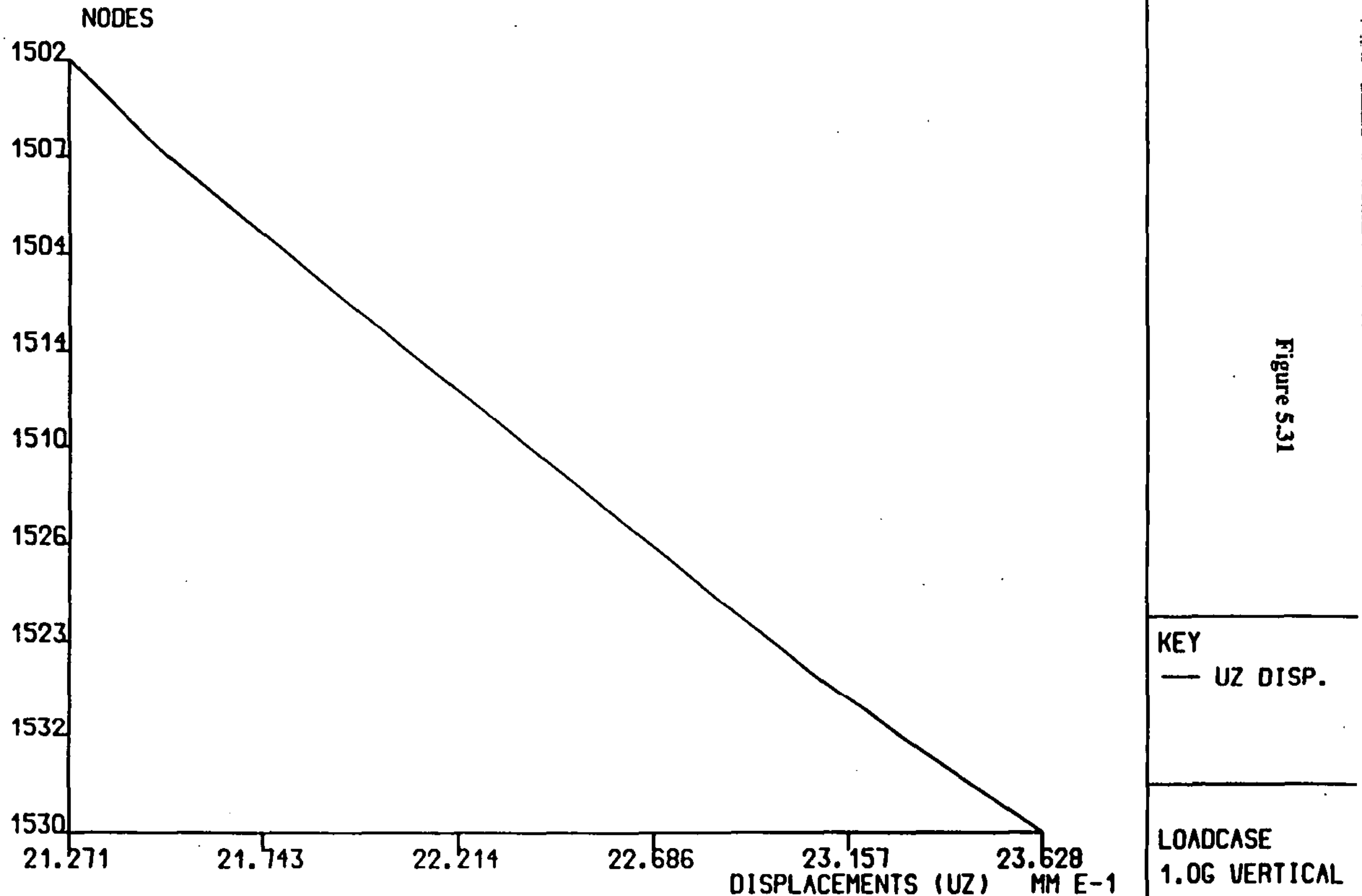

TITLE LATERAL (UZ) DISPLACEMENTS ALONG THE LHS CHOKE LOCATION SKELETAL MODEL #2

Figure 5.31

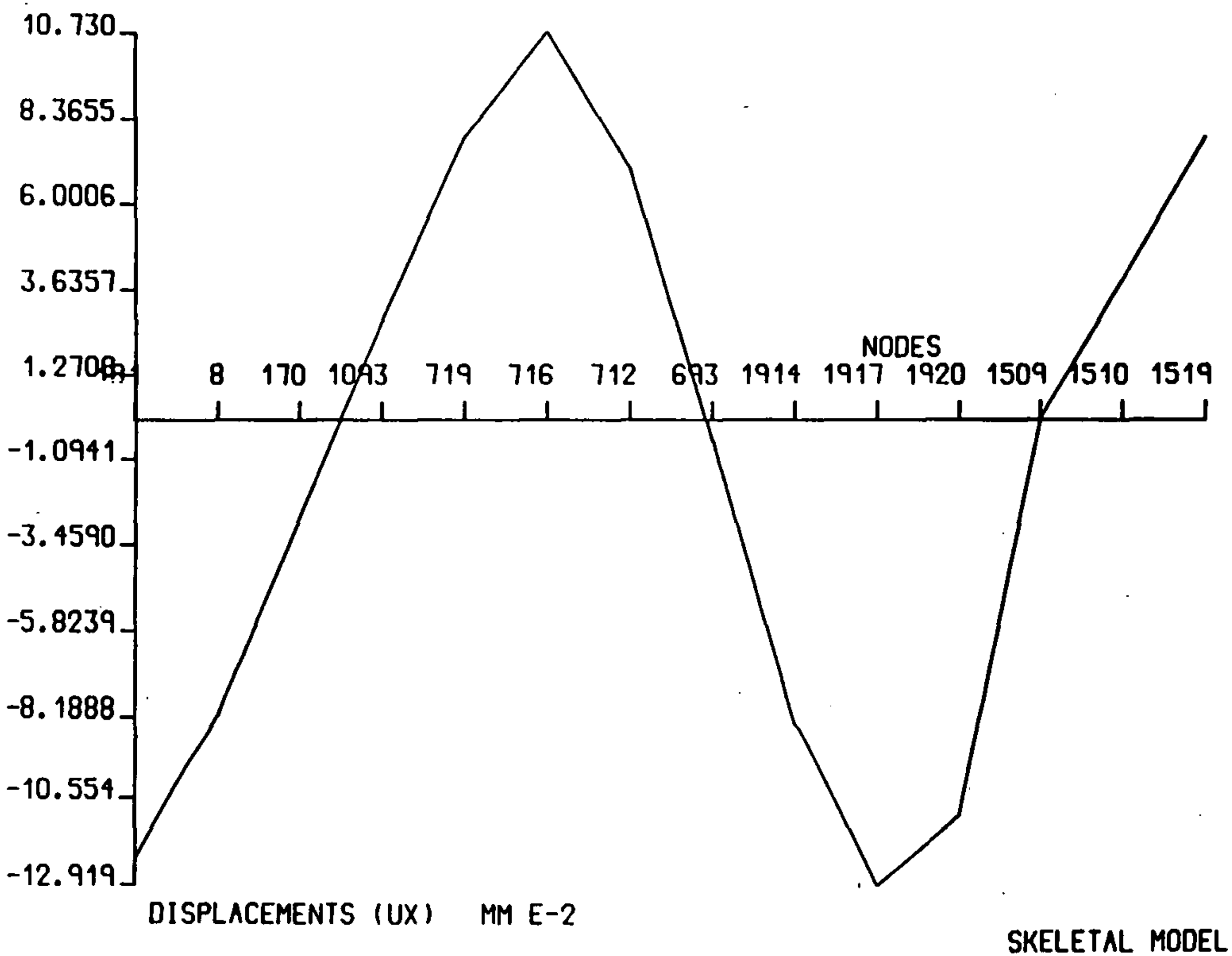

KEY
— UX DISP.
-- UY DISP.

LOADCASE
1.0G VERTICAL
(DOWN)
1.1G LAT.

TITLE LONGITUDINAL DISPLACEMENTS ALONG THE SECOND LATERAL CROSS MEMBER

Figure 5.32

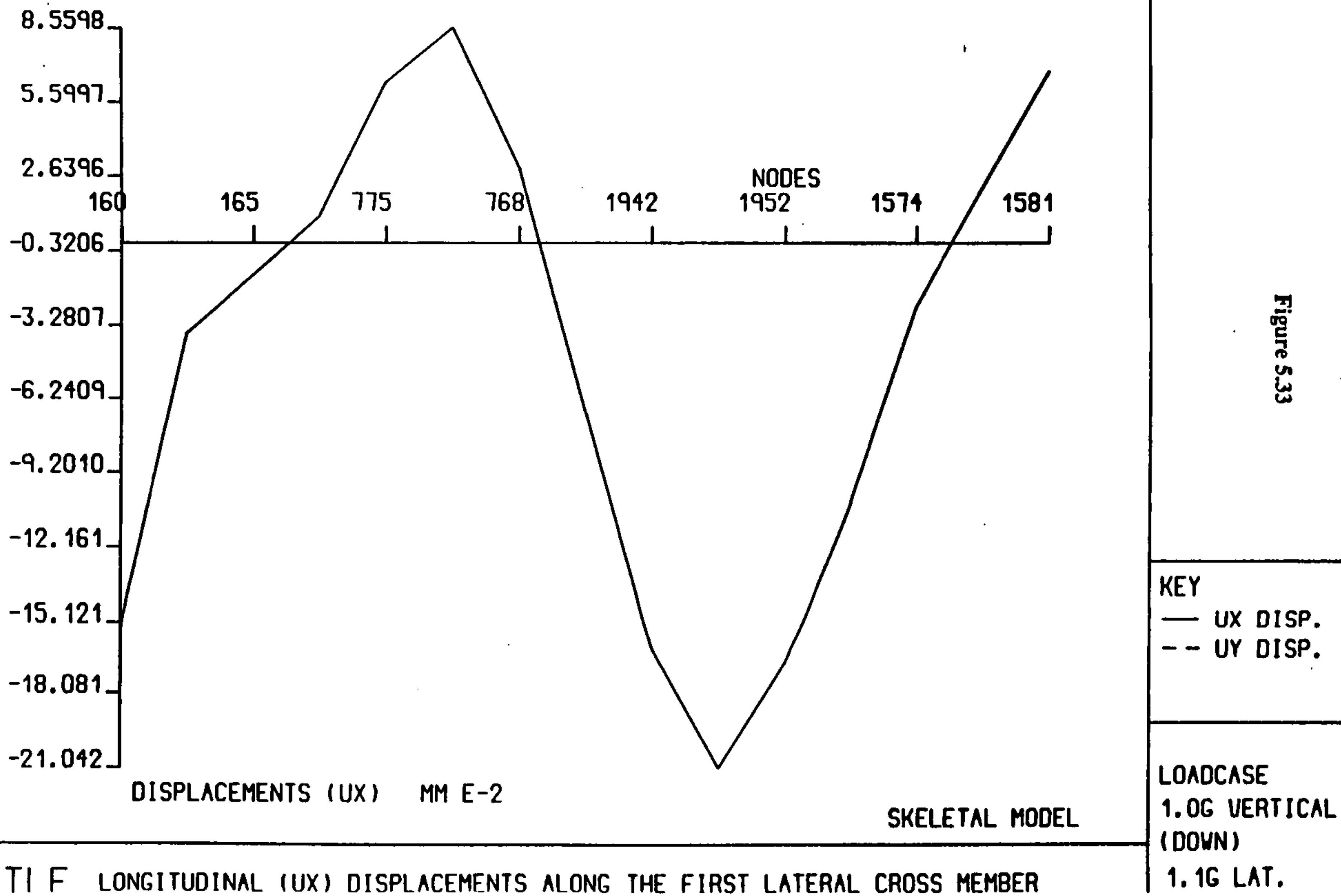

TITLE LONGITUDINAL (UX) DISPLACEMENTS ALONG THE FIRST LATERAL CROSS MEMBER

Figure 5.33

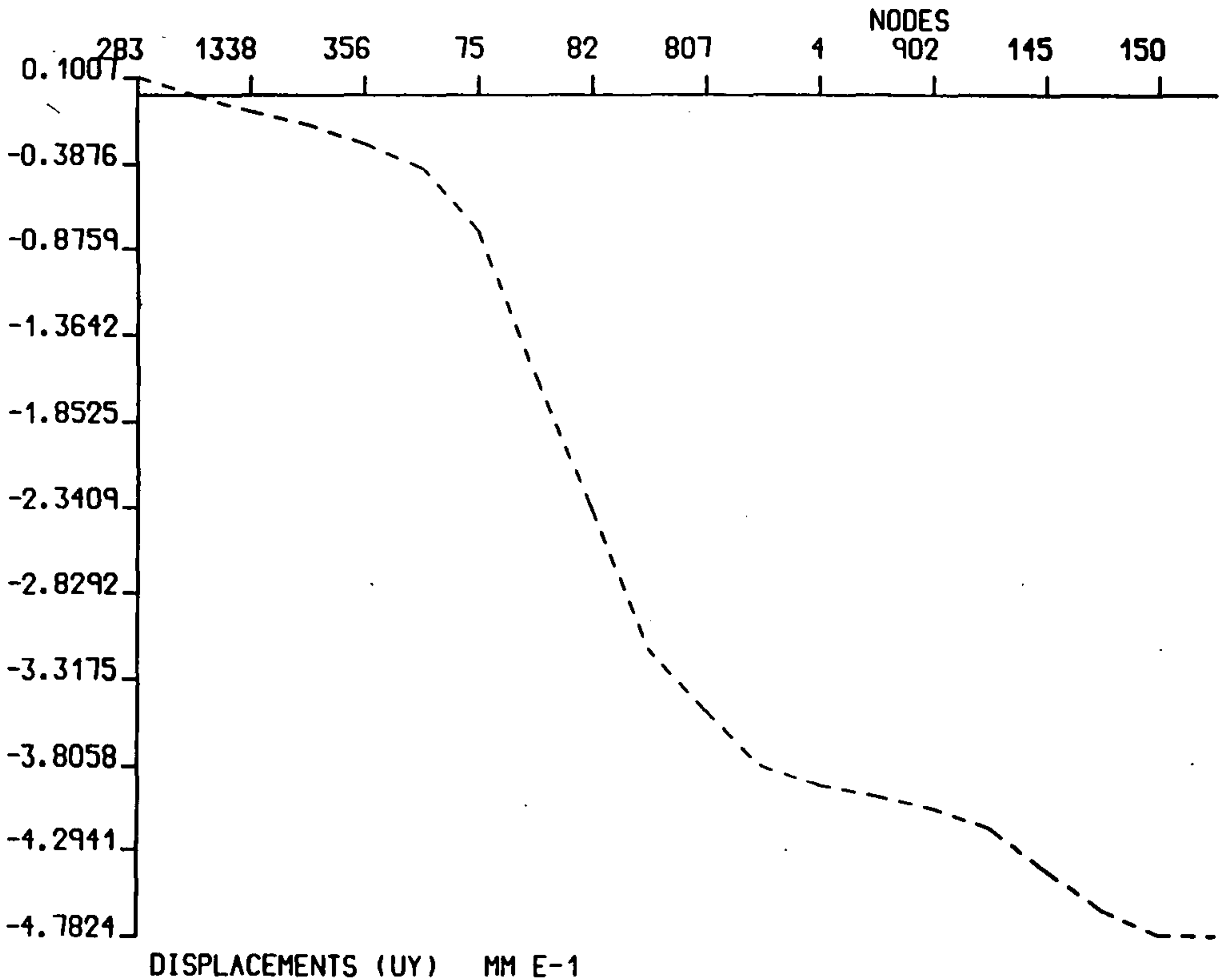

KEY
— UX DISP.
- - UY DISP.

LOADCASE
1.0G VERTICAL
(DOWN)

TITLE VERTICAL (UY) DISPLACEMENTS ALONG THE RHS UPPER FLANGE - SKELETAL MODEL #2

Figure 5.34

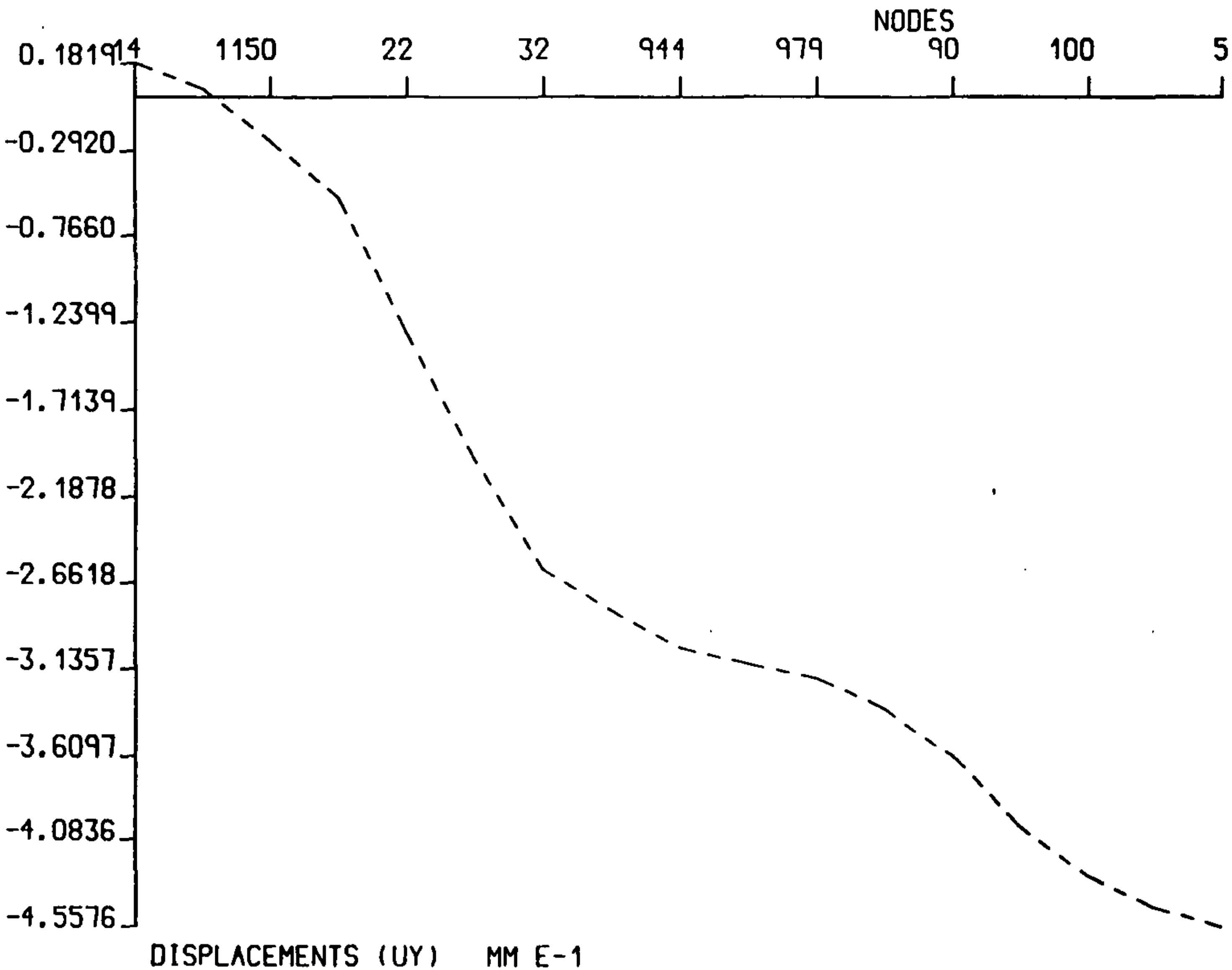

KEY
— UX DISP.
-- UY DISP.

LOADCASE
1.0G VERTICAL
(DOWN)

TITLE VERTICAL (UY) DISPLACEMENTS ALONG THE RHS LOWER FLANGE - SKELETAL MODEL #2

Figure 5.35

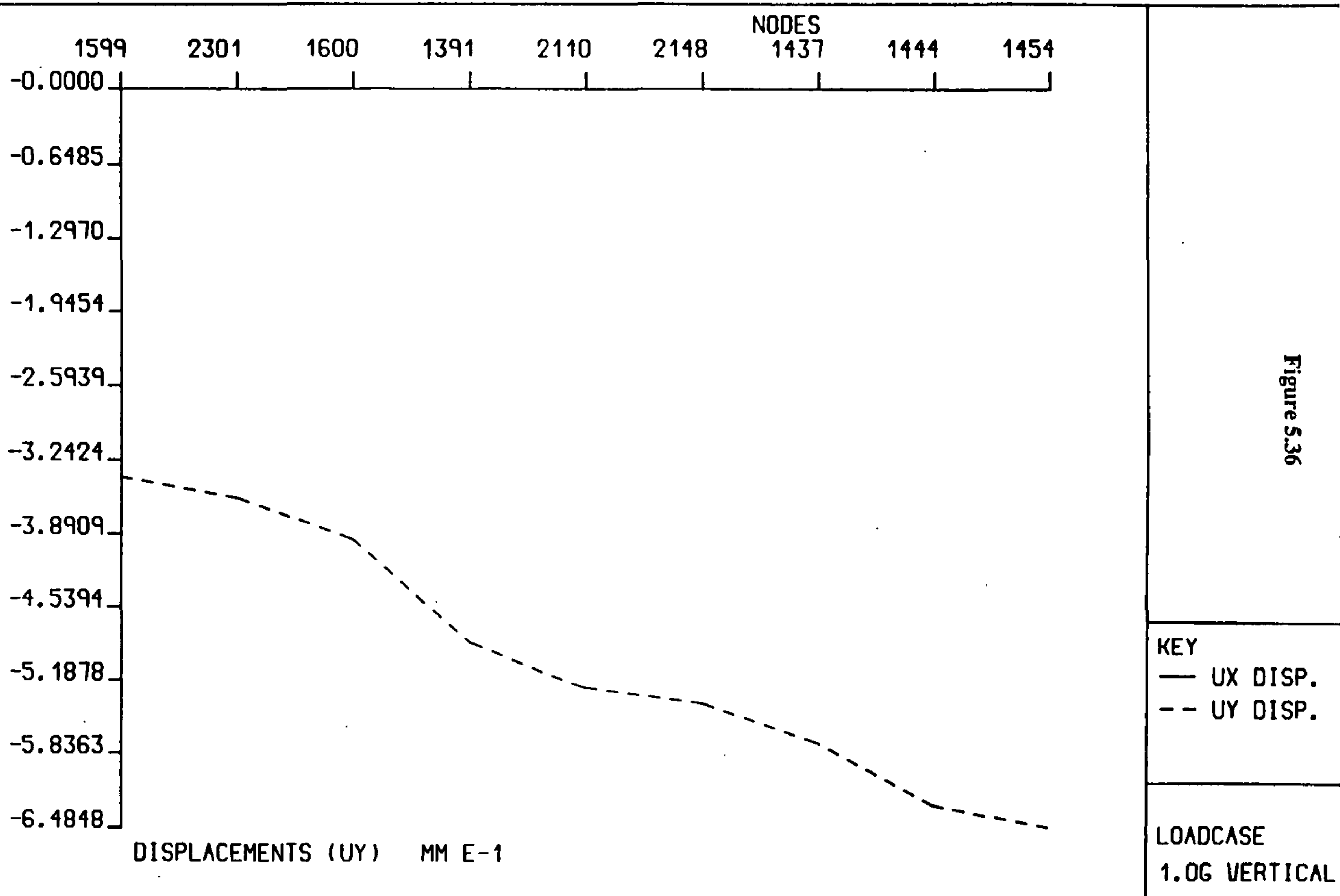

TITLE VERTICAL (UY) DISPLACEMENTS ALONG THE LHS LOWER FLANGE - SKELETAL MODEL #2

Figure 5.36

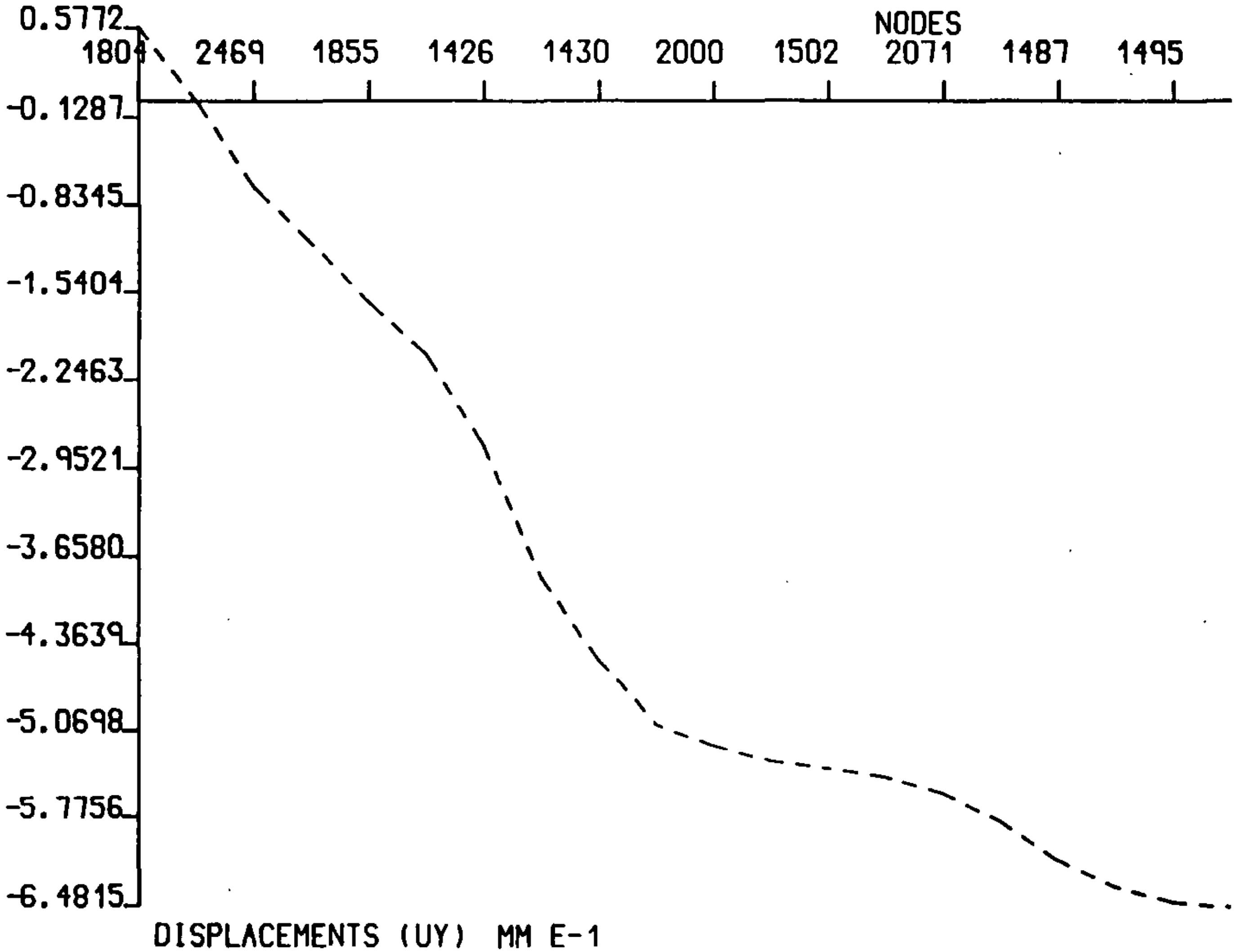

KEY
— UZ DISP.
-- UY DISP.

LOADCASE
1.0G VERTICAL
(DOWN)

TITLE VERTICAL (UY) DISPLACEMENTS ALONG THE LHS UPPER FLANGE - SKELETAL MODEL #2

Figure 5.37

CHAPTER 6

Composite Case Design Proposals

6.1 Introduction

The case design investigated in chapter 5 was for the purpose of analysis reduced to a skeletal structure consisting of longitudinal and lateral beams of idealised cross section. This idealisation would require some change to make it a practical manufacturing proposition. The following chapter details some possible construction features which would maintain similar stress levels to those derived in the analysis and suit the properties and manufacturing processes of glass fibre composite materials. Not all features are shown, but the principles illustrated could be extended to all parts of the design.

6.2 Design Features

The principal design features discussed below are illustrated in figures 6.2 - 6.4, with figure 6.1 detailing their exact locations in the model.

6.2.1 Main Flanges

The flange design adopted in the skeletal model is shown in figure 6.2, and consists of a rectangular section of unidirectional material. An outer layer of woven cloth would be wrapped around the section to provide protection and consolidate the junction between the flange and vertical web as described in section 6.1.2.

Figure 6.1 Side View of the Skeletal Model

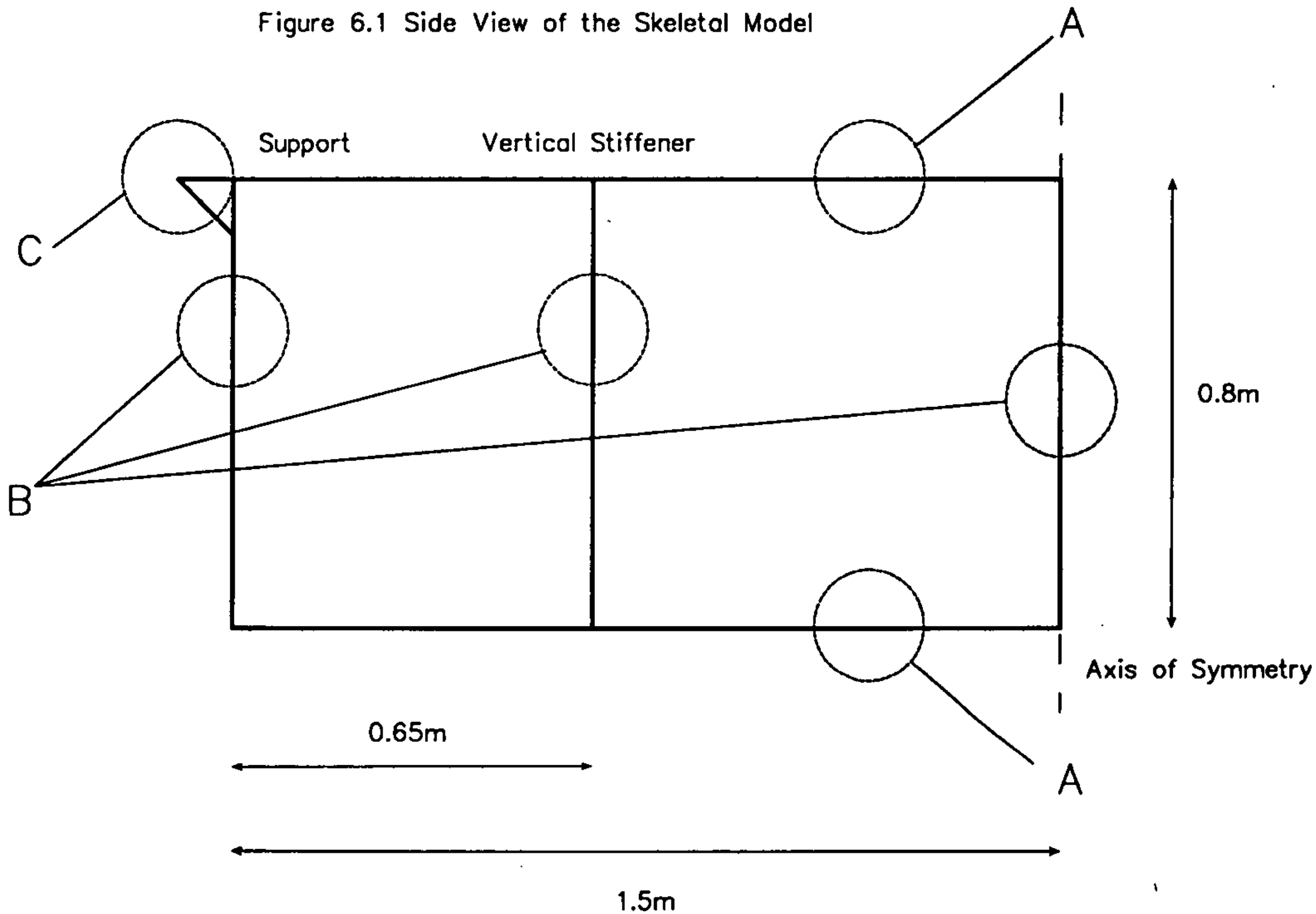

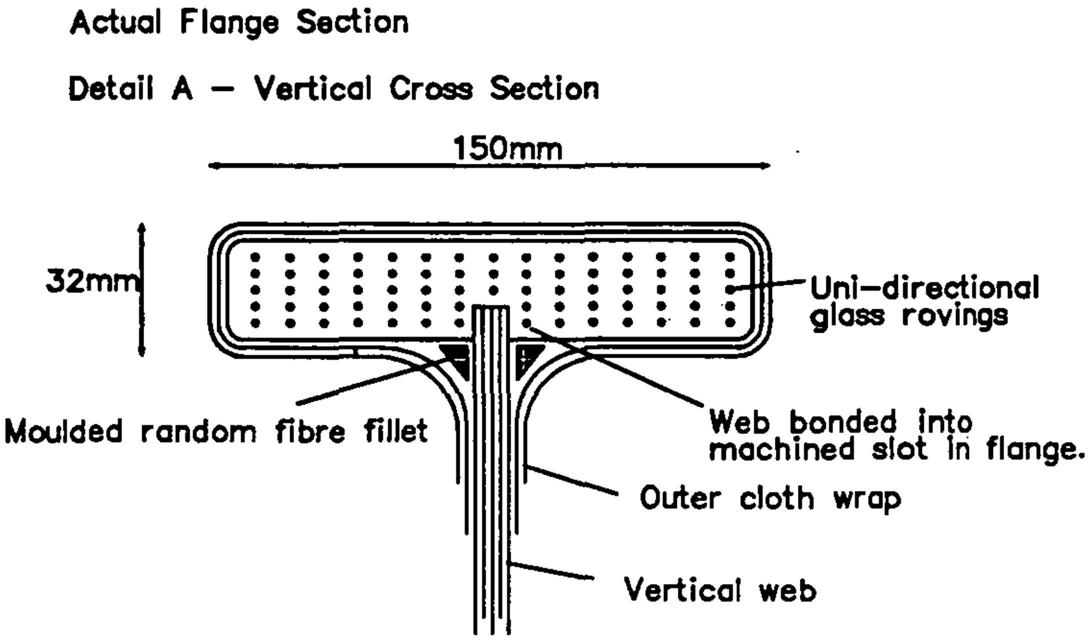

Figure 6.2

6.2.2 The Webs

The webs are modelled as flat sheets of woven material of constant thickness. In practice these would be moulded separately from the flanges, with integral thickened sections for the vertical stiffeners as shown in figure 6.3. Assembly would be by bonding the web panels into moulded slots in the flanges, figure 6.2. In addition an external layer of woven material applied by wet lay up methods would be added after assembly around the flanges extending onto the webs, figure 6.2. This layer would provide protection for the load carrying members and joints from external damage.

6.2.3 Lateral Cross Members

The lateral cross members are proposed to be of identical construction to the side members. The method of attachment to the side structure is again via a moulded slot in the appropriate vertical stiffener, figure 6.3. At the merger point for the longitudinal and lateral flanges, some interleaving would be required to avoid a plane of pure matrix material, with continuity being maintained longitudinally.

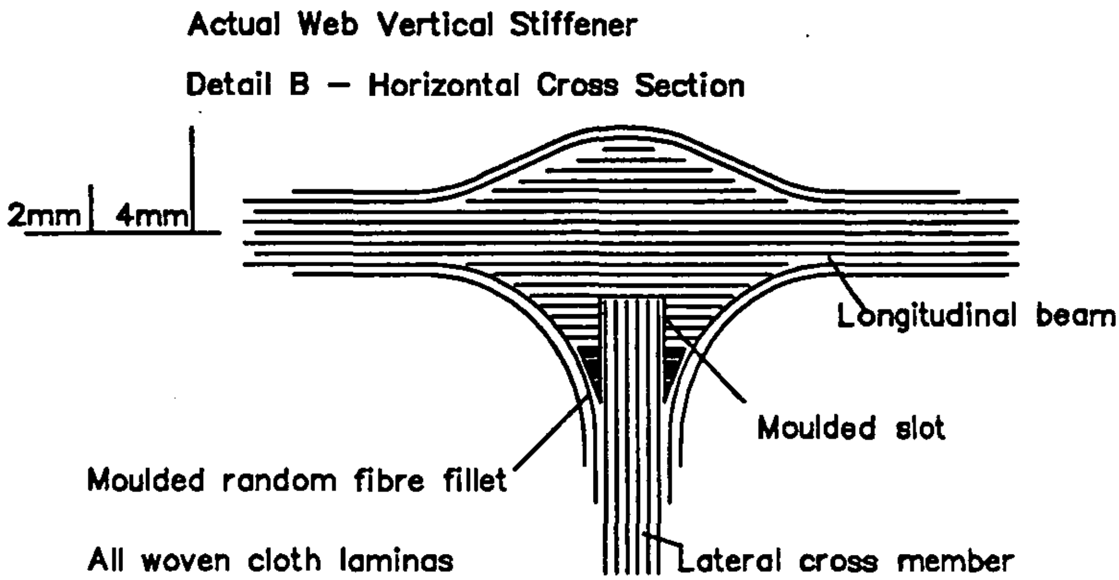

Figure 6.3

6.2.4 Main Mounting Points

The main method of mounting must be in the form of metal bushed holes. Composite material is unsuitable for the high bolt clamping loads, due to the potential failure of the matrix material in compression resulting in local delamination. The bushes may be bonded in or arranged to provide a controlled 'nip' as shown in figure 6.4.

Mounting Point Details

Detail C – Vertical Cross Section through Upper Flange

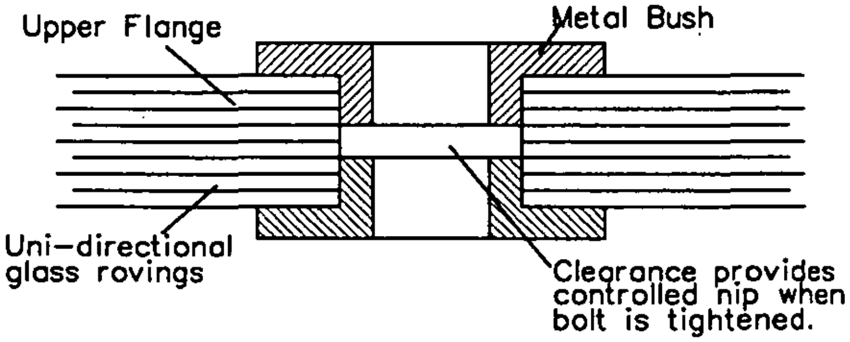

Figure 6.4

In order to achieve the modelled conditions the main mountings must have minimal longitudinal restraint. This could be achieved by a slotted hole in the metal locomotive chassis or preferably by a short swinging link or rubber bushed mounting.

6.2.5 Attachment Points

It is proposed to use threaded metal inserts bonded in at the various equipment and cable clamping positions. Similarly integral brackets could be formed as part of the structure, to reduce complexity and assist rapid assembly.

6.2.6 Protection from Service Damage

The size guidelines proposed for the flanges, although adequate for the load cases, may not be sufficient to withstand the general handling abuse likely to be experienced in railway service. Additional protective laminas could be added in areas subjected to damage without excessively increasing the weight.

6.3 Further Refinements of Design

Alternative materials such as Carbon fibre or Kevlar could be introduced into the structure to improve local areas. Carbon fibre has a high Youngs's Modulus, approximately 3 times that of glass and would be useful in reducing deflections. Carbon is also 50% stronger and 33% lighter than glass. Kevlar has high strength but a relatively low Young's modulus making it very flexible and ideal for areas subjected to high impact damage.

These specialised fibres are much more costly than glass and thus likely only to be used in local areas, rather than in the main members of the equipment case.

CHAPTER 7

Conclusions

The research concludes that:-

7.1 The Finite Element Analysis of Composite Structures has proven to be an effective method of analysing practical applications of these structures.

7.2 Extensive element testing has shown that the Pafec 75 Suite of Finite Element software is a reasonably effective package to use for this purpose.

7.3 The proposed composite undercarriage equipment case has been shown to have acceptable stress levels, minimal deflections and satisfactory fatigue life under the standard railway service load conditions.

7.4 The main advantages associated with composite construction compared with a conventional steel structure are; reduced weight, reduced complexity and high resistance to corrosion. On application to an equipment case these should result in reduced manufacturing and operating costs in the long term, however initial investment would be required to develop the manufacturing processes and tooling.

7.5 The analyses have shown that a weight advantage ratio for a composite structure of 0.72:1 is easily achieved with low risk stress levels and a relatively simple design, with the additional advantage of integral equipment mounting positions to reduce complexity.

7.6 In addition to the engineering advantages, there is the marketing advantage of incorporating advanced technology in engineering products, which may justify the additional development costs.

REFERENCES

1. Pafec Data Prep Manual

2. Warnock F. and Benham P.P.,"Mechanics of Solids and Strength of Materials," Pitman Publications; 1969, pp 364-369.

3. Gurney T. R., "Fatigue Design Rules for Welded Steel Joints," The Welded Institue Research Bulletin; Vol 17, May 1976.

4. Sharman P.W.,"Stress Quality Testing of Iso-parametric Membrane Elements in Uniform Thickness and Stiffened Benchmarks," NAFEMS Conference; May 1987.

5. Somashekar B.R. and Prathap G.,"A field consistency error model for the single element test for the eight noded brick element," Quality Assurance in FEM Technology, Edited by J.Robinson; 1987, pp 171 - 180.

6. Dahto D., "CoALA Primer," Cranfield Institute of Technology Publication; 1987.

7. Hoskins B.C. and Baker A.A., "Composite Materials for Aircraft Structures," AIAA Education Series; 1985, pp 108 - 111.

8. Hoskins B.C. and Baker A.A., "Composite Materials for Aircraft Structures," AIAA Education Series; 1985, pp 95 - 98.

9. Todd J.D., "Structural Theory and Analysis," The Macmillan Press Ltd.;1979, pp 138 - 152.

10. Vinson J.R. and Sierakoski R.L., "The Behaviour of Structures Composed of Composite Materials," Martinus Nijhoff Publishers; 1986, pp 29 - 49.

11. Hoskins B.C. and Baker A.A., "Composite Materials for Aircraft Structures," AIAA Education Series; 1985, pp 64 -67.

APPENDIX A1

Typical Loading Conditions for Undercarriage Equipment Cases

i. Proof Load Cases

The equipment mountings must be able to withstand the mass of the equipment and the case self-weight when subjected to the following accelerations, all loads being reacted at the supports.

i.	Vertical	1.0g (up).
ii.	Vertical	1.5g (down).
iii.	Lateral	± 1.1g + 1.0g vertical (down).
iv.	Longitudinal	± 3.0g + 1.0g vertical (down).

ii. Fatigue Load Cases

All equipment mountings shall be designed to have a fatigue life of not less than 10^7 cycles for the loads produced by the following accelerations acting on the mass of the equipment.

i.	Vertical	1.0g (down) + 0.3g.
ii.	Lateral	± 0.3g.
iii.	Longitudinal	± 0.2g.

APPENDIX B1

Engineering Drawing of a Typical Undercarriage Equipment Case,

(Courtesy of Brush Electrical Machines Ltd.)

Enclosed at the back of the thesis.

APPENDIX B2

Fatigue Analysis of Welded Joints

The fatigue analysis requires the applied stress range to be determined at the welded joints in the structure. Three sample locations were taken at the most highly stressed areas ie the upper and lower beams and the support locations.

Stress ranges were calculated by subtracting stresses obtained from the following superimposed loadcases:-

Stress 1 = Vertical 1.3g down + 0.3g lateral + 0.2g longitudinal ... (1)

Stress 2 = Vertical 0.7g down - 0.3g lateral - 0.2g longitudinal ... (2)

A typical calculation for node 488, located at a support is as follows:-

Maximum principal stresses, taken along the middle surface at node 488 are:-

Vertical 1.3g down	106 Nmm^{-2}
Vertical 0.7g down	57 Nmm^{-2}
Lateral +0.3g	19 Nmm^{-2}
Longitudinal +0.2g	1.8 Nmm^{-2}

Hence substituting in (1) and (2) gives,

Stress 1 = 124 Nmm^{-2} ? 127

Stress 2 = 40 Nmm^{-2} ? 36

Stress range = 84 Nmm^{-2} 91

The resulting stress range is thus **84 Nmm^{-2}**. 96

On refering to Gurney, Reference 3 reveals that a class B ? is required for this stress range over 10^7 cycles. A maximum allowable stress range here would be 100 Nmm^{-2} , hence a class B weld would have a reserve factor of **1.2**

APPENDIX C1

Sample Output from CoALA and Pafec for Test 3

```
  CCCCCCCC                   AAAAAA     LL              AAAAAA
  CCCCCCCC                   AAAAAA     LL              AAAAAA
CC                         AA      AA   LL            AA      AA
CC              000000     AA      AA   LL            AA      AA
CC              000000     AA      AA   LL            AA      AA
CC            00      00   AAAAAAAAAA   LL            AAAAAAAAAA
CC            00      00   AAAAAAAAAA   LL            AAAAAAAAAA
CC            00      00   AA      AA   LL            AA      AA
  CCCCCCCC      000000     AA      AA   LLLLLLLLLL    AA      AA
  CCCCCCCC      000000     AA      AA   LLLLLLLLLL    AA      AA
```

COLLEGE of AERONAUTICS LAMINATE ANALYSIS

Cranfield Institute of Technology

M A T E R I A L   P R O P E R T I E S

MATERIAL 1 HS-Carbon/Epoxy UD

(E 1	E 2)	.1400E+06	.1000E+05
(G 12	NU 12)	.5000E+04	.3000E+00
(X.t	X.c)	.1500E+04	.1200E+04
(Y.t	Y.c)	.5000E+02	.2500E+03
(S	)	.7000E+02	
(ex.t	ex.c)	.1050E-01	.6500E-02
(ey.t	ey.c)	.5000E-02	.2500E-01
(e.s	)	.1400E-01	
(ALPHA 1	ALPHA 2)	-.3000E-06	.2800E-04
(BETA 1	BETA 2)	.1000E-01	.3000E+00

L O A D   C A S E   1

L A M I N A T E   C O N F I G U R A T I O N

PLY NUMBER	PLY THICKNESS	MATERIAL NUMBER	PLY ANGLE	TEMP. DIFF.	MOIST. %
1	.2000E+01	1	45.00	.00	.00

L O A D   C A S E   1

NON-MECHANICAL (THERMAL AND MOISTURE) LOADS

UNRESTRAINED RESIDUAL STRESSES AND STRAINS

P L Y   S T R E S S E S (at centroid)

NO.	f 1	f 2	f 12	Failure index TSAI-WU	M.O.F
1	.00000E+00	.00000E+00	.00000E+00	.00000E+00	0

P L Y   S T R A I N S (at centroid)

NO.	e 1	e 2	e 12	Failure index TSAI-WU	M.O.F
1	.00000E+00	.00000E+00	.00000E+00	.00000E+00	0

L O A D   C A S E   1

E Q U I V A L E N T   P R O P E R T I E S

	Membrane Mode	Bending Mode Top Surface	Bending Mode Bottom Surface
ALPHA x	.00000E+00	.00000E+00	.00000E+00
ALPHA y	.00000E+00	.00000E+00	.00000E+00
ALPHA xy	.00000E+00	.00000E+00	.00000E+00
BETA x	.00000E+00	.00000E+00	.00000E+00
BETA y	.00000E+00	.00000E+00	.00000E+00
BETA xy	.00000E+00	.00000E+00	.00000E+00

E Q U I V A L E N T   T H E R M A L   L O A D S

NxT = .00000E+00   NyT = .00000E+00   NxyT = .00000E+00

MxT = .00000E+00   MyT = .00000E+00   MxyT = .00000E+00

E Q U I V A L E N T   M O I S T U R E   L O A D S

NxC = .00000E+00   NyC = .00000E+00   NxyC = .00000E+00

MxC = .00000E+00   MyC = .00000E+00   MxyC = .00000E+00

L O A D   C A S E 1

APPLIED MECHANICAL LOADS

Nx = .10000E+03   Ny = .00000E+00   Nxy = .00000E+00

Mx = .00000E+00   My = .00000E+00   Mxy = .00000E+00

RESULTANT (MECHANICAL + RESIDUAL) STRESSES AND STRAINS

P L Y   S T R E S S E S (at centroid)

NO.	f 1	f 2	f 12	Failure Index TSAI-WU	M.O.F
1	.25000E+02	.25000E+02	-.25000E+02	.56957E+00	2

P L Y   S T R A I N S (at centroid)

NO.	e 1	e 2	e 12	Failure Index TSAI-WU	M.O.F
1	.12500E-03	.24464E-02	-.50000E-02	.56957E+00	2

LAMINATE CONSTITUTIVE EQUATION FOR THE ANALYSED CONFIGURATION

"A.B.D" STIFFNESS MATRIX

.8850E+05	.6850E+05	.6542E+05	:	.0000E+00	.0000E+00	.0000E+00
.6850E+05	.8850E+05	.6542E+05	:	.0000E+00	.0000E+00	.0000E+00
.6542E+05	.6542E+05	.7247E+05	:	.0000E+00	.0000E+00	.0000E+00
.0000E+00	.0000E+00	.0000E+00	:	.2950E+05	.2283E+05	.2181E+05
.0000E+00	.0000E+00	.0000E+00	:	.2283E+05	.2950E+05	.2181E+05
.0000E+00	.0000E+00	.0000E+00	:	.2181E+05	.2181E+05	.2416E+05

"a.b.d" COMPLIANCE MATRIX

.3786E-04	-.1214E-04	-.2321E-04	:	.0000E+00	.0000E+00	.0000E+00
-.1214E-04	.3786E-04	-.2321E-04	:	.0000E+00	.0000E+00	.0000E+00
-.2321E-04	-.2321E-04	.5571E-04	:	.0000E+00	.0000E+00	.0000E+00
.0000E+00	.0000E+00	.0000E+00	:	.1136E-03	-.3643E-04	-.6964E-04
.0000E+00	.0000E+00	.0000E+00	:	-.3643E-04	.1136E-03	-.6964E-04
.0000E+00	.0000E+00	.0000E+00	:	-.6964E-04	-.6964E-04	.1671E-03

LAMINATE EQUIVALENT ENGINEERING ELASTIC CONSTANTS

	Membrane Mode	Bending Mode
Ex	.13208E+05	.13208E+05
Ey	.13208E+05	.13208E+05
Gxy	.89744E+04	.89744E+04
NUxy	.32075E+00	.32075E+00
NUyx	.32075E+00	.32075E+00
mx	.61321E+00	.61321E+00
my	.61321E+00	.61321E+00

```
TITLE GENERALLY ORTHOTROPIC BAR IN TENSION (+45) PLY THICKNESS=2MM
CONTROL
1
STRESS
CLEAR.FILES
PHASE=7
PICS.STRESS.FILE
CONTROL.END
C
C
C     *** THE NODES MODULE IS PRINTED
C     *** USING GLOBAL CARTESIAN AXES
C
NODES
Z=            0.00000
   NODE         X                 Y
     1       0.00000           0.00000
     2       0.10000E-01       0.00000
     3       0.10000E-01       0.10000E-01          50 mm x 10 mm
     4       0.00000           0.10000E-01
     5       0.20000E-01       0.00000
     7       0.50000E-01       0.00000
     8       0.20000E-01       0.10000E-01
     9       0.40000E-01       0.10000E-01
    10       0.40000E-01       0.00000
    11       0.50000E-01       0.10000E-01
    12       0.30000E-01       0.00000
    13       0.30000E-01       0.10000E-01
    14       0.50000E-02       0.00000
    15       0.10000E-01       0.50000E-02
    16       0.50000E-02       0.10000E-01
    17       0.00000           0.50000E-02
    18       0.15000E-01       0.00000
    19       0.20000E-01       0.50000E-02
    20       0.15000E-01       0.10000E-01
    21       0.25000E-01       0.00000
    22       0.30000E-01       0.50000E-02
    23       0.25000E-01       0.10000E-01
    24       0.35000E-01       0.00000
    25       0.40000E-01       0.50000E-02
    26       0.35000E-01       0.10000E-01
    27       0.45000E-01       0.00000
    28       0.50000E-01       0.50000E-02
    29       0.45000E-01       0.10000E-01
C
ELEMENTS
GROU=1
ELEM= 36215
PROP=1
   NUMB  TOPO
     1     1     2     4     3    14    17    15    16
     2     2     5     3     8    18    15    19    20
     3     5    12     8    13    21    19    22    23
     4    12    10    13     9    24    22    25    26
     5    10     7     9    11    27    25    28    29
C

1

LAMINATES
NUMB ORTH.MATERIAL.NUMBER   LOWER   UPPER RAD1  RAD2 AXIS.SET   ANG1  ANG2  ANG3
  1        1               -0.001   0.001        0 0 0 45 0 0
C
ORTHOTROPIC.MATERIAL
NUMBER   SXX   SYY   SZZ   SXY   SYZ   SZX   SHXY   SHYZ   SHZX
1
  1    7.69E-12 1.43E-10  0  -2.15E-12  0  0  1.66E-10   0  0
C
LOADS
CASE      NODE      DIRE      HARN      VALU
 1    7         1          0       166.666  }
 1   28         1          0       666.666  } tension = 1000N
 1   11         1          0       166.666  }
C
RESTRAINTS
NODE.NUMBER     PLANE     DIRECTION
  1               1          1
  17          0          2
C
OUT.DRAW
DRAW   PLOT
  1      5
  2     30
END.OF.DATA
0END OF DATA          0 ERRORS
```

```
                                              PPPPP  AAAAA FFFFF EEEEE CCCCC
SYSTEM LEVEL   6.2                            P   P  A   A FF    E     C   CC
JULY 1986                                     P   P  A   A FF    E     C
                                              PPPPP  AAAAA FFF   EEE   C
                                              PP     AA  A F     EE    C
PHASE NO.  7                                  PP     AA  A F     EE    C
STARTS HERE                                   PP     AA  A F     EE    C
                                              PP     AA  A F     EEEEE CCCCC
LEVEL TAKEN - 07/28/86  AT  1:55 PM
```

TITLE GENERALLY ORTHOTROPIC BAR IN TENSION +45 PLY THICKNESS=2MM

```
***************************************
*                                     *
* STATICS  SOLUTION BY BLOCK FRONT    *
*        IN DOUBLE PRECISION          *
*                                     *
*  STRUCTURE CONTAINS     52 FREEDOMS *
*                          5 ELEMENTS *
*    AND THE FRONT SIZE IS    16      *
*                                     *
***************************************
```

0 *** A BLOCKED FRONT SOLUTION HAS BEEN REQUESTED ***
0 THE BLOCK SIZE IS 272
1
0D I S P L A C E M E N T S   F O R   L O A D   C A S E   1

0SAMPLE OF LARGEST DISPLACEMENTS

0

NODE	UX	NODE	UY	NODE	RESULTANT
11	0.1952426E-03	11	-0.1703635E-03	11	0.2591204E-03
28	0.1952424E-03	28	-0.1691380E-03	28	0.2583161E-03
7	0.1952418E-03	7	-0.1679124E-03	7	0.2575149E-03
29	0.1757184E-03	29	-0.1534495E-03	29	0.2332889E-03
27	0.1757177E-03	27	-0.1509983E-03	27	0.2316834E-03
9	0.1561940E-03	9	-0.1365356E-03	9	0.2074573E-03

NOTE - (2) THE HISTOGRAM INDICATES THE MAGNITUDE OF THE RESULTANT TRANSLATION AT EACH NODE. EACH STAR * REPRESENTS 0.2591E-04 UNITS
(3) A STAR * IN A DISPLACEMENT COLUMN INDICATES THAT A CONSTRAINT HAS BEEN APPLIED.
(4) ONLY STRUCTURAL NODES ARE GIVEN IN THE TABLE BELOW
1

CASE 1 NODE NUMBER	TRANSLATIONS MULTIPLIED BY 1E 6 UX	UY	RESULTANT TRANSLATION MULTIPLIED BY 1E 6 U	HISTOGRAM	SCALED COORDINATES MULTIPLIED BY 1E 0 X	Y
1	*	1.226	1.226		0.00	0.00
2	39.048	-32.602	50.869	**	0.010	0.00
3	39.048	-35.053	52.474	**	0.010	0.010
4	*	-1.226	1.226		0.00	0.010
5	78.097	-66.429	102.53	****	0.020	0.00
7	195.24	-167.91	257.51	**********	0.050	0.00
8	78.097	-68.880	104.13	****	0.020	0.010
9	156.19	-136.54	207.46	********	0.040	0.010
10	156.19	-134.08	205.85	********	0.040	0.00
11	195.24	-170.36	259.12	**********	0.050	0.010
12	117.15	-100.26	154.19	******	0.030	0.00
13	117.15	-102.71	155.79	******	0.030	0.010
14	19.524	-15.688	25.046	*	0.005	0.00
15	39.048	-33.827	51.663	**	0.010	0.005
16	19.524	-18.139	26.650	*	0.005	0.010
17	*	*	*		0.00	0.005
18	58.573	-49.515	76.698	***	0.015	0.00
19	78.097	-67.655	103.33	****	0.020	0.005
20	58.573	-51.967	78.303	***	0.015	0.010
21	97.621	-83.343	128.36	*****	0.025	0.00
22	117.15	-101.48	154.99	******	0.030	0.005
23	97.621	-85.794	129.96	*****	0.025	0.010
24	136.67	-117.17	180.02	*******	0.035	0.00
25	156.19	-135.31	206.65	********	0.040	0.005
26	136.67	-119.62	181.63	*******	0.035	0.010
27	175.72	-151.00	231.68	*********	0.045	0.00
28	195.24	-169.14	258.32	**********	0.050	0.005
29	175.72	-153.45	233.29	*********	0.045	0.010

```
SYSTEM LEVEL    6.2                       PPPPP  AAAAA FFFFF EEEEE CCCCC
JULY 1986                                 P   P  A   A FF    E     C   CC
                                          P   P  A   A FF    E     C
                                          PPPPP  AAAAA FFF   EEE   C
                                          PP     AA  A F     EE    C
PHASE NO.  9                              PP     AA  A F     EE    C
STARTS HERE                               PP     AA  A F     EE    C
                                          PP     AA  A F     EEEEE CCCCC
LEVEL TAKEN - 07/28/86  AT  1:55 PM
```

TITLE GENERALLY ORTHOTROPIC BAR IN TENSION +45 PLY THICKNESS=2MM

MODULE 196 WORKSPACE MODULE DELETED IN R09808
DEFAULT STRESS.ELEMENTS MODULE CREATED.
1

ELEMENT TYPE 36215 8-NODE ISOPARAMETRIC QUADRILATERAL(PLANE STRESS) ORTHOTROPIC

PRINCIPAL STRESSES - SIGMA-1 IS THE MAXIMUM VALUE OF STRESS IN THE PLANE OF THE ELEMENT
SIGMA-2 IS THE MINIMUM VALUE OF STRESS IN THE PLANE OF THE ELEMENT

ANGLE OF SIGMA-1 - THE FIRST ANGLE , M-SIG1 , IS THE ANGLE BETWEEN THE MATERIAL DIRECTION AND SIGMA-1 . THE SECOND ANGLE , EX-M , IS THE ANGLE BETWEEN THE ELEMENT X-AXIS AND THE MATERIAL DIRECTION . BOTH ANGLES ARE MEASURED IN A POSITIVE SENSE ABOUT THE ELEMENT Z-AXIS

MATERIAL STRESSES - STRESS COMPONENTS REFERRED TO MATERIAL AXES

ELEM NO	LOAD CASE	NODE NO	PRINCIPAL STRESSES SIGMA-1	SIGMA-2	MAX. SHEAR STRESS	ANG. OF. SIG-1 M-SIG1	EX-M	......MATERIAL. STRESSES....... SIGMA-X	SIGMA-Y	SIGMA-XY
1	1	1	5.000E 07	-3.320E 02	2.500E 07	-45.0	45.0	2.500E 07	2.500E 07	-2.500E 07
1	1	14	5.000E 07	-9.200E 01	2.500E 07	-45.0	45.0	2.500E 07	2.500E 07	-2.500E 07
1	1	2	5.000E 07	6.800E 01	2.500E 07	-45.0	45.0	2.500E 07	2.500E 07	-2.500E 07
1	1	17	5.000E 07	-6.000E 01	2.500E 07	-45.0	45.0	2.500E 07	2.500E 07	-2.500E 07
1	1	*	5.000E 07	-1.200E 02	2.500E 07	-45.0	45.0	2.500E 07	2.500E 07	-2.500E 07
1	1	15	5.000E 07	-2.600E 02	2.500E 07	-45.0	45.0	2.500E 07	2.500E 07	-2.500E 07
1	1	4	5.000E 07	-1.000E 02	2.500E 07	-45.0	45.0	2.500E 07	2.500E 07	-2.500E 07
1	1	16	5.000E 07	-4.600E 02	2.500E 07	-45.0	45.0	2.500E 07	2.500E 07	-2.500E 07
1	1	3	5.000E 07	-8.960E 02	2.500E 07	-45.0	45.0	2.500E 07	2.500E 07	-2.500E 07
2	1	2	5.000E 07	-5.640E 02	2.500E 07	-45.0	45.0	2.500E 07	2.500E 07	-2.500E 07
2	1	18	5.000E 07	4.080E 02	2.500E 07	-45.0	45.0	2.500E 07	2.500E 07	-2.500E 07
2	1	5	5.000E 07	6.960E 02	2.500E 07	-45.0	45.0	2.500E 07	2.500E 07	-2.500E 07
2	1	15	5.000E 07	-1.800E 02	2.500E 07	-45.0	45.0	2.500E 07	2.500E 07	-2.500E 07
2	1	*	5.000E 07	-6.000E 01	2.500E 07	-45.0	45.0	2.500E 07	2.500E 07	-2.500E 07
2	1	19	5.000E 07	-6.280E 02	2.500E 07	-45.0	45.0	2.500E 07	2.500E 07	-2.500E 07
2	1	3	5.000E 07	-1.480E 02	2.500E 07	-45.0	45.0	2.500E 07	2.500E 07	-2.500E 07
2	1	20	5.000E 07	-8.760E 02	2.500E 07	-45.0	45.0	2.500E 07	2.500E 07	-2.500E 07
2	1	8	5.000E 07	-2.300E 03	2.500E 07	-45.0	45.0	2.500E 07	2.500E 07	-2.500E 07
3	1	5	5.000E 07	-3.080E 02	2.500E 07	-45.0	45.0	2.500E 07	2.500E 07	-2.500E 07
3	1	21	5.000E 07	8.560E 02	2.500E 07	-45.0	45.0	2.500E 07	2.500E 07	-2.500E 07
3	1	12	5.000E 07	7.840E 02	2.500E 07	-45.0	45.0	2.500E 07	2.500E 07	-2.500E 07
3	1	19	5.000E 07	-2.760E 02	2.500E 07	-45.0	45.0	2.500E 07	2.500E 07	-2.500E 07
3	1	*	5.000E 07	-1.720E 02	2.500E 07	-45.0	45.0	2.500E 07	2.500E 07	-2.500E 07
3	1	22	5.000E 07	-1.308E 03	2.500E 07	-45.0	45.0	2.500E 07	2.500E 07	-2.500E 07
3	1	8	5.000E 07	-4.120E 02	2.500E 07	-45.0	45.0	2.500E 07	2.500E 07	-2.500E 07
3	1	23	5.000E 07	-1.348E 03	2.500E 07	-45.0	45.0	2.500E 07	2.500E 07	-2.500E 07
3	1	13	5.000E 07	-3.560E 03	2.500E 07	-45.0	45.0	2.499E 07	2.500E 07	-2.500E 07
4	1	12	5.000E 07	-1.028E 03	2.500E 07	-45.0	45.0	2.500E 07	2.500E 07	-2.500E 07
4	1	24	5.000E 07	1.280E 03	2.500E 07	-45.0	45.0	2.500E 07	2.500E 07	-2.500E 07
4	1	10	5.000E 07	1.772E 03	2.500E 07	-45.0	45.0	2.500E 07	2.500E 07	-2.500E 07
4	1	22	5.000E 07	-4.160E 02	2.500E 07	-45.0	45.0	2.500E 07	2.500E 07	-2.500E 07
4	1	*	5.000E 07	2.400E 01	2.500E 07	-45.0	45.0	2.500E 07	2.500E 07	-2.500E 07
4	1	25	5.000E 07	-1.104E 03	2.500E 07	-45.0	45.0	2.500E 07	2.500E 07	-2.500E 07
4	1	13	5.000E 07	-4.080E 02	2.500E 07	-45.0	45.0	2.500E 07	2.500E 07	-2.500E 07
4	1	26	5.000E 07	-1.804E 03	2.500E 07	-45.0	45.0	2.500E 07	2.500E 07	-2.500E 07
4	1	9	5.000E 07	-4.780E 03	2.500E 07	-45.0	45.0	2.499E 07	2.500E 07	-2.500E 07
5	1	10	5.000E 07	-5.040E 02	2.500E 07	-45.0	45.0	2.500E 07	2.500E 07	-2.500E 07
5	1	27	5.000E 07	1.808E 03	2.500E 07	-45.0	45.0	2.500E 07	2.500E 07	-2.500E 07
5	1	7	5.000E 07	2.656E 03	2.500E 07	-45.0	45.0	2.500E 07	2.500E 07	-2.500E 07
5	1	25	5.000E 07	-3.000E 02	2.500E 07	-45.0	45.0	2.500E 07	2.500E 07	-2.500E 07
5	1	*	5.000E 07	1.240E 02	2.500E 07	-45.0	45.0	2.500E 07	2.500E 07	-2.500E 07
5	1	28	5.000E 07	-8.840E 02	2.500E 07	-45.0	45.0	2.500E 07	2.500E 07	-2.500E 07
5	1	9	5.000E 07	-8.520E 02	2.500E 07	-45.0	45.0	2.500E 07	2.500E 07	-2.500E 07
5	1	29	5.000E 07	-2.304E 03	2.500E 07	-45.0	45.0	2.500E 07	2.500E 07	-2.500E 07
5	1	11	4.999E 07	-5.188E 03	2.500E 07	-45.0	45.0	2.499E 07	2.500E 07	-2.500E 07

APPENDIX C2

Stress Analysis of a Generally Orthotropic Lamina in Tension

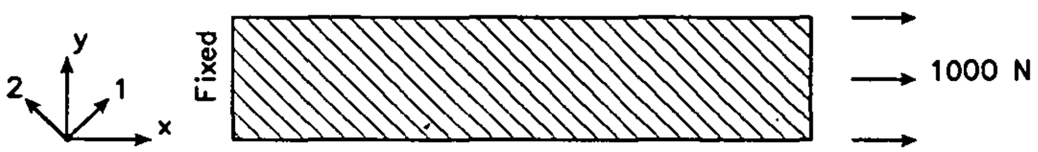

Considering the above 45° single lamina in tension used in Test 3.

From standard text, Reference 8, using a transformation matrix to obtain stresses in the material directions.

$$\begin{bmatrix}\sigma_x \\ \sigma_y \\ \tau_{xy}\end{bmatrix} = \begin{bmatrix}\cos^2 a & \sin^2 a & -2\sin a\cos a \\ \sin^2 a & \cos^2 a & -2\sin a\cos a \\ \sin a\cos a & \sin^2 a & \cos^2 a - \sin^2 a\end{bmatrix} \begin{bmatrix}\sigma_1 \\ \sigma_2 \\ \tau_{12}\end{bmatrix}$$

For a 45 ply , a=45, hence

$$\begin{bmatrix}\sigma_x \\ \sigma_y \\ \tau_{xy}\end{bmatrix} = \begin{bmatrix}0.5 & 0.5 & -1 \\ 0.5 & 0.5 & 1 \\ 0.5 & -0.5 & 0\end{bmatrix} \begin{bmatrix}\sigma_1 \\ \sigma_2 \\ \tau_{12}\end{bmatrix} \qquad \ldots(1)$$

In test 3 $\sigma_x = 1000 / 20 = 50\ \text{Nmm}^{-2}$, $\sigma_y = 0\ \text{Nmm}^{-2}$ and $\tau_{xy} = 0\ \text{Nmm}^{-2}$, substituting these values in in matrix (1) to give the following simultaneous equations.

$$50 = 0.5\,\sigma_1 + 0.5\,\sigma_2 - \tau_{12} \qquad \ldots(2)$$

$$0 = 0.5\,\sigma_1 + 0.5\sigma_2 + \tau_{12} \qquad \ldots(3)$$

$$0 = 0.5\,\sigma_1 - 0.5\,\sigma_2 \qquad \ldots(4)$$

Solving equations (2), (3) and (4) gives,

σ_1 **= 25 Nmm^{-2}**

σ_2 **= 25 Nmm^{-2}**

$\tau_{12} = -25\ \mathrm{Nmm}^{-2}$

These values agree with the results shown in figure 4.6.

APPENDIX C3

Calculation of Displacements for a Symmetric Laminate in Tension

i. Theoretical Verification

Considering the cross section of the symmetric laminate bar , $2[0/90]_s$ used in Test 1.

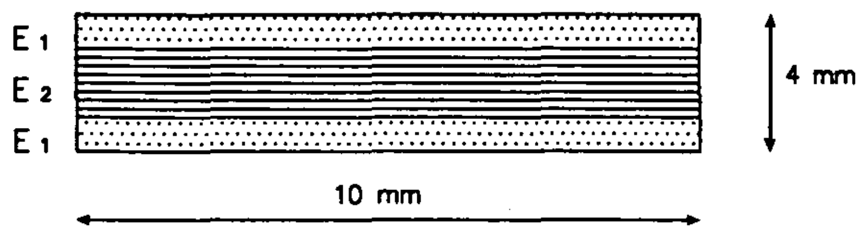

This is equivalent to,

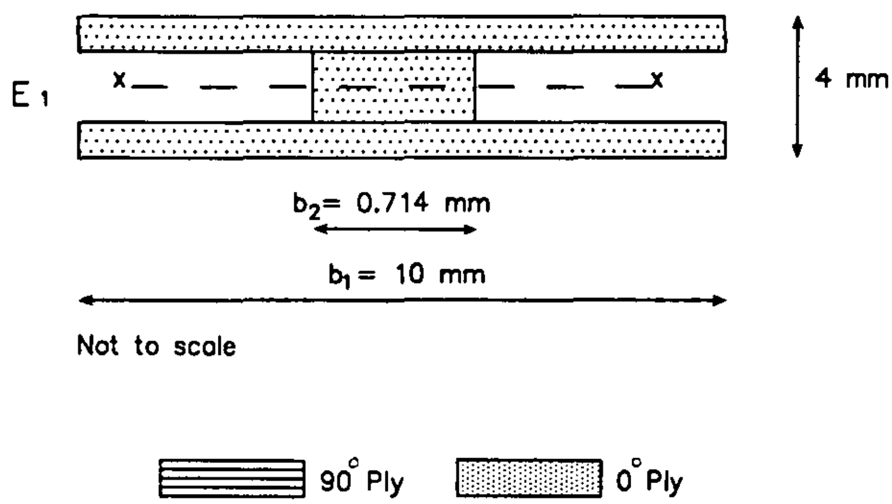

Where by proportions,

$$\frac{b_2}{b_1} = \frac{E_2}{E_1} \qquad \ldots (1)$$

As $E_1 = 140 \times 10^3$ Nmm^{-2}, $E_2 = 10 \times 10^3$ Nmm^{-2} and $b_1 = 10$ mm

$b_2 = 0.714$ mm

The cross section area of the bar analogy is,

Bar Analogy Cross Section = (2 x 1 x 10) + (2 x 0.714) = 21.43 mm^2

There are no shear coupling effects when the bar is subjected to tension, due to there being only specially orthotropic plies present in the laminate. Displacement occurs along the length of the beam only.

Displacement can be calculated from,

$$\text{Displacement} = \frac{\text{Load x Length of Bar}}{\text{Cross Sectional Area x E}} \quad \ldots (2)$$

As Load = 1000 N, Length of Bar = 50 mm, Cross Sectional Area = 21.43 mm^2

and E = 140 x 10^3 Nmm^{-2}

Displacement = 1.67 x 10^{-4} mm

ii. CoALA Verification

CoALA provides several equivalent engineering elastic constants for the laminate analysed, see Appendix C1.

Diff. case for Coala output.

According to CoALA the overall E for the laminate in tension is 0.7536 x 10^5 Nmm^{-2} ??

Which on substitution into (2), with Cross Sectional Area = 4 x 10 = 40 mm^2 gives,

Displacement = 1.67 x 10^{-4} mm

Hence CoALA agrees with the theoretical result derived above. PAFEC ? output not presented

APPENDIX C4

Stress Analysis of a Generally Orthotropic Lamina in Bending

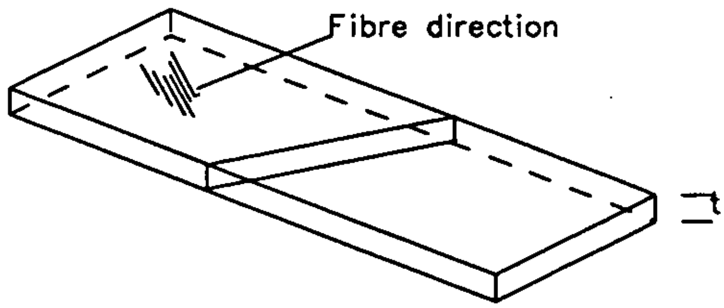

Considering a triangular element of the above bar, subjected to the following moments intensities (moments per unit width).

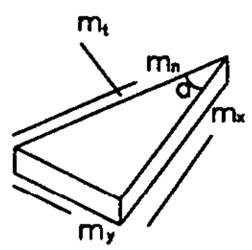

Resolving moments (m_x direction)

$$m_x = m_n \ (b / \cos a) \cos a \ + \ m_t \ (b / \cos a) \sin a$$

$$m_x = m_n \ + m_t \tan a \qquad \ldots (1)$$

Resolving moments (m_y direction)

$$m_y = m_n \ (b / \cos a) \sin a \ + \ m_t \ (b / \cos a) \cos a$$

As there is only m_x present in test 4, $m_y = 0$, hence

$$0 = m_n \tan a \ - m_t$$

$$m_t = m_n \tan a \qquad \ldots (2)$$

Hence substituting for (2) in (1),

$$m_x = m_n + m_n \tan^2 a$$

Hence,

$$m_n = m_x (1 + \tan^2 a) \qquad \ldots (3)$$

Considering a cross section of material in the fibre direction of unit width,

From the standard formula,

$$\frac{m}{I} = \frac{\sigma}{y}$$

Where $\sigma = \sigma_1$, $m = m_n$, $I = t^3/12$ and $y = t / 2$

Hence,

$$\sigma_1 = 6m_n / t^2$$

$$\sigma_1 = 6m_x / t^2 (1 + \tan^2 x)$$

In Test 4 $m_x = 10^2$ N (moment intensity), $t = 2$mm and $a = 45^\circ$,

Hence,

$$\sigma_1 = \mathbf{0.75 \times 10^2\ Nmm^{-2}}$$

This result agrees with the CoALA result as shown in figure 4.8.

APPENDIX C5

Calculation of Displacements and Stresses for a Symmetric Laminate in Bending

i. Theoretical Verification of Displacements

Considering the cross section of the symmetric laminate bar , $2[0/90]_s$ used in Test 2.

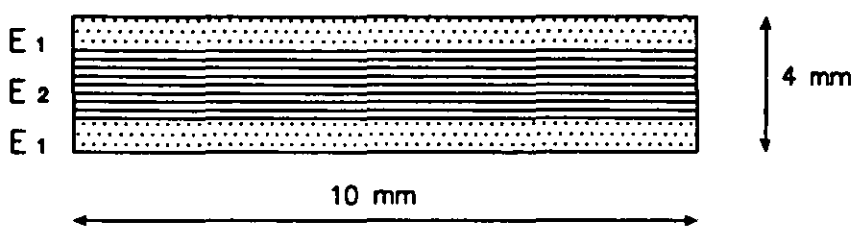

This is equivalent to,

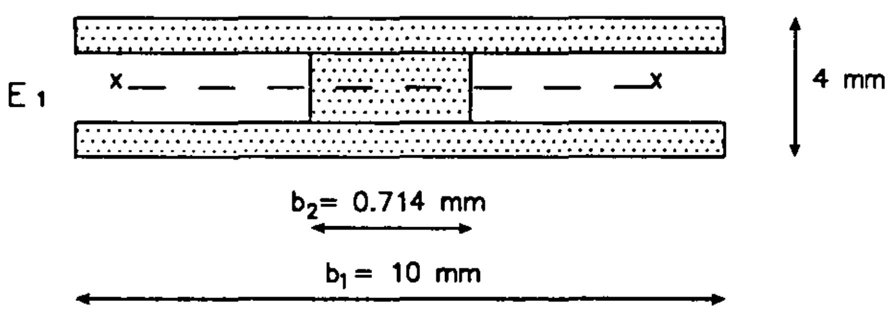

Not to scale

Where by proportions,

$$\frac{b_2}{b_1} = \frac{E_2}{E_1} \qquad \ldots (1)$$

As $E_1 = 140 \times 10^3 \ \text{Nmm}^{-2}$, $E_2 = 10 \times 10^3 \ \text{Nmm}^{-2}$ and $b_1 = 10$ mm

$b_2 = 0.714$ mm

Hence I_{XX} can be calculated from standard Second Moment of Area formula

$I_{XX} = 47.14 \text{ mm}^4$

There are no bend twist effects when the bar is subjected to a constant moment, due to there being only specially orthotropic plies present. Hence from the standard bending formula, Reference 8, for vertical displacements at the end of a cantilevered bar,subjected to constant moment.

$$\text{Displacement} = \frac{\text{Moment x (Length of Bar)}^2}{2\, E_1 I_{XX}} \qquad \ldots (2)$$

For, Moment = 10^4 Nmm, Length of Bar = 50 mm, $E_1 = 140 \times 10^3$ Nmm^{-2}, $I_{XX} = 47.14 \text{ mm}^4$,

Displacement = 1.89 mm

CoALA Verification

CoALA provides several equivalent engineering elastic constants for the laminate analysed, see Appendix C1.

According to CoALA the overall E for the laminate in bending mode is 0.12421×10^6 Nmm^{-2}

Which on substitution into (2), with $I_{XX} = 53.13 \text{ mm}^4$ (simply from $bd^3/12$)

Displacement = 1.89 mm

Hence CoALA agrees with the theoretical result derived above.

ii. Theoretical Verification of Stresses

Considering the upper ply, from

$$\sigma_1 = \frac{M\,y}{I_{xx}} \qquad \ldots (3)$$

Where $M = 10^7$ Nmm, $y = 1.5$ mm, $I_{xx} = 47.14 \text{ mm}^4$,

Hence , on substitution in (3)

$\boldsymbol{\sigma_1 = 0.318 \times 10^6 \text{ Nmm}^{-2}}$

This result agrees with the CoALA value shown in figure 4.7.

PLANS TAKEN FROM HERE

X1